An investigation into the genetic control of thalamocortical tract projection in the mouse using a fluorescent reporter transgene.

By

Thomas Pratt

Thesis submitted for the degree of doctor of philosophy at the University of Edinburgh

March 2001

'...sheer determination I walked those miles

pitiful, microscopic, nobody...'

Julian Cope

DISCLAIMER

I (Thomas Pratt) performed all of the experiments presented in this thesis unless otherwise clearly stated in the text. No part of this work has been, or is being submitted for any other degree of qualification.

Signed:

Date: 23.3.2001

ACKNOWLEDGEMENTS

I would like to thank my supervisors John Mason and David Price for the combined advice and support they gave me during the course of this work.

I am indebted to Linda Sharp and her confocal microscope and also to Andrew Sanderson for help with fluorescence activated cell sorting. Margaret Keighren, Gillian MacKay and Jenny Nichols kindly generated chimeras for germline transmission and for me to analyse. Thanks to Louise Anderson, Don Henderson, Andrew Jeske, Duncan M^{c}Neil, Vince Ranaldi, Sharon Rossiter and Dan Venner for taking care of the mice. I acknowledge that this work entailed the breeding of mice specifically for the purpose of sacrificing them and state that this was done humanely and as sparingly as possible. I am grateful to Vivian Alison, Dougie Colby, Katy Gillies, Derek Rout and Linda Sharp for showing me how to do things and tending the labs. I worked in.

Thanks to Julia Edgar, Tania Vitalis and Natasha Warren for their part in investigating the roles of Pax6 in formation of the thalamocortical tract, Jean Flockhart, Margaret Keighren and John West for compiling mouse growth and viability data and Price and Mason Lab. members past and present for many helpful acts and the occasional spark of inspiration. Ian Chambers, Meng Li, Jenny Nichols, and Austin Smith were instrumental in assisting my efforts with mammalian expression vectors, embryonic stem cells and the production of transgenic mice.

I also want to acknowledge Andrew, Ann, Collin, Craig, Drood, Francis, Julia, Katherine, Lawrence, Peter, Sally, Tony, Wendy, and others whose imprints are in here somewhere, and David Attenborough, and Diane without whom things would have been very different.

TABLE OF CONTENTS

ABBREVIATIONS

A-P – anterior to posterior

BMP – bone morphogenetic protein

bp- base pairs

ca - carotid artery

cb - cerebellum

cc - cerebral cortex

CNS - central nervous system

DMSO - dimethyl sulphoxide

DNA - deoxyribonucleic acid

dt - dorsal thalamus

E - embryonic age (E0.5 is defined here as the day of discovering vaginal plug)

e – eye

EB – embryoid body

ES - embryonic stem cell

FACS - fluorescence activated cell sorting

FCS - foetal calf serum

FGF – fibroblast growth factor

GFP - green fluorescent protein

ht – hypothalamus

ic- internal capsule (of the ventral forebrain)

iz – intermediate zone (of the cerebral cortex)

kb - kilobase pairs

LIF - leukaemia inhibitory factor

MTOC – microtubule organising centre

P - postnatal age (day of birth is P0)

p - prosomere

PBS - phosphate buffered saline.

PI – propidium iodide

RA - retinoic acid

Sey – small eye (null) mutant allele of *Pax6*

shh – sonic hedgehog

tau-GFP – tau tagged green fluorescent protein

TCA - thalamocortical axon

Tg - transgene

vt - ventral thalamus

vtel - ventral telencephalon

WT - wild-type

ABSTRACT

In the mature mammalian brain the thalamus relays sensory information from the periphery to the cerebral cortex via the thalamocortical axon tract. In the mouse, the thalamocortical tract is generated during embryogenesis as axons projecting from the dorsal thalamus navigate through the ventral thalamus and ventral telencephalon to reach the cerebral cortex where they form and refine connections with layer IV neurons during subsequent development. The mechanisms by which axons navigate the complex geometry of this route are largely unknown.

Studies of mutant mice whose thalamocortical tract is disrupted illustrate that genes involved in programming thalamocortical tract navigation are required by projecting cells of the dorsal thalamus and along its route to supply axon navigation cues. Small-eye homozygotes (*Pax6*$^{Sey/Sey}$) in which the transcription factor Pax6 is inactivated exhibit a range of defects throughout the developing central nervous system, including a failure in thalamocortical tract formation, and die at birth. The *Pax6*$^{Sey/Sey}$ phenotype describes disruption of both the dorsal thalamus and the tissues through which the thalamocortical tract navigates so does not reveal whether axons projected by the dorsal thalamus fail to navigate due to intrinsic mis-programming or due to a lack of important navigational cues along the route. To test the hypothesis that Pax6 is required within the dorsal thalamus for tract projection I developed a novel in vitro assay for thalamic axon navigation and cell surface properties.

First I generated lines of embryonic stem (ES) cells which ubiquitously express a tau tagged green fluorescent protein (tau-GFP) transgene. Germline transmission of ES lines produced two lines of transgenic mice designated TgTP6.3 and TgTP6.4. I show that the tau-GFP transgene is ubiquitously expressed in developing TgTP6.3 brain and that tau tagging anchors tau-GFP to the microtubule component of the cytoskeleton resulting in clear fluorescent marking of subcellular structures, including axons and the

mitotic machinery. The experimental potential of the TgTP6.3 mice is demonstrated in several cell mixing paradigms, including mouse chimeras and brain cell and tissue culture systems, where tau-GFP cells and axons can easily be detected against a background of unlabeled cells and tissues. The TgTP6.4 line exhibits very low levels of tau-GFP expression in the developing brain so is unsuitable for these experiments.

I next used a novel in vitro assay to show that *tau-GFP:Pax6*$^{+/+}$ dorsal thalamic axons are able to navigate through unlabelled *Pax6*$^{+/+}$ ventral telencephalon whereas *tau-GFP:Pax6*$^{Sey/Sey}$ axons are not. Seeding experiments show that *tau-GFP:Pax6*$^{+/+}$ dorsal thalamic cells adhere to slices of *Pax6*$^{+/+}$ ventral telencephalon at the point of thalamocortical tract entry (the internal capsule) whereas *tau-GFP:Pax6*$^{Sey/Sey}$ cells do not. I conclude that Pax6 is required autonomously within the dorsal thalamus to program successful axon navigation through the ventral telencephalon, presumably by controlling the transcription of genes which directly or indirectly modulate adhesive properties at the cell surface.

CHAPTER1: GENERAL INTRODUCTION.

The developing brain

The mammalian brain forms from a morphologically undifferentiated sheet of cells (the neural plate) during embryogenesis. The anatomical changes in the developing embryonic brain are shown in Fig. 1.1A. The development of the mature brain from the neural plate is moulded by processes of cell division, cell death, cell migration, cell-cell interaction, and the formation of connections between cells over long distances. The brain is then able to receive and interpret information from the periphery, and to refine its connections and structure in the light of experience.

Much study has gone into attempting to understand the mechanisms of brain development and recent advances in genetics have provided a clearer understanding of how genes control many of the processes involved.

The thalamocortical tract

The thalamus can be thought of as a 'relay station' for sensory information from the periphery (sight, touch, taste, smell, and hearing) passing through the thalamus en route to the cerebral cortex for processing and interpretation. This information pathway consists of axons, bundled together into fibre tracts, which connect different regions of the brain and transmit information in the form of nerve impulses which travel along axons from cell to cell.

The spatial organisation of sensory information is precisely maintained as it passes from the thalamus to the cortex. The layout of the cortex reflects its functions. Mapping which regions of the cortex respond to stimulation of areas of the body surface reveals that the body surface is 'represented' on the surface of the cortex

Figure 1.1

(A) Anatomy of brain development spanning the period of thalamocortical tract formation. Diagrams of developing mouse brain (rostral to left) at ages E9, E10, E12, and E14.5 showing the locations of major anatomical structures in sagittal section. Figure adapted from Altman and Bayer, (1995). (B) Topographical organisation of information is precisely maintained as it passes from the whisker pad on the face to the brain stem, thalamus and cerebral cortex. Figure adapted from Kandel et al., (2000). (C) Diagram of a mouse brain to show various cortical sensory areas determined by evoked potential techniques. Note that the body surface is precisely mapped onto the surface of the cortex. Figure adapted from Woolsey and Van der Loos, (1973).

Figure 1.1

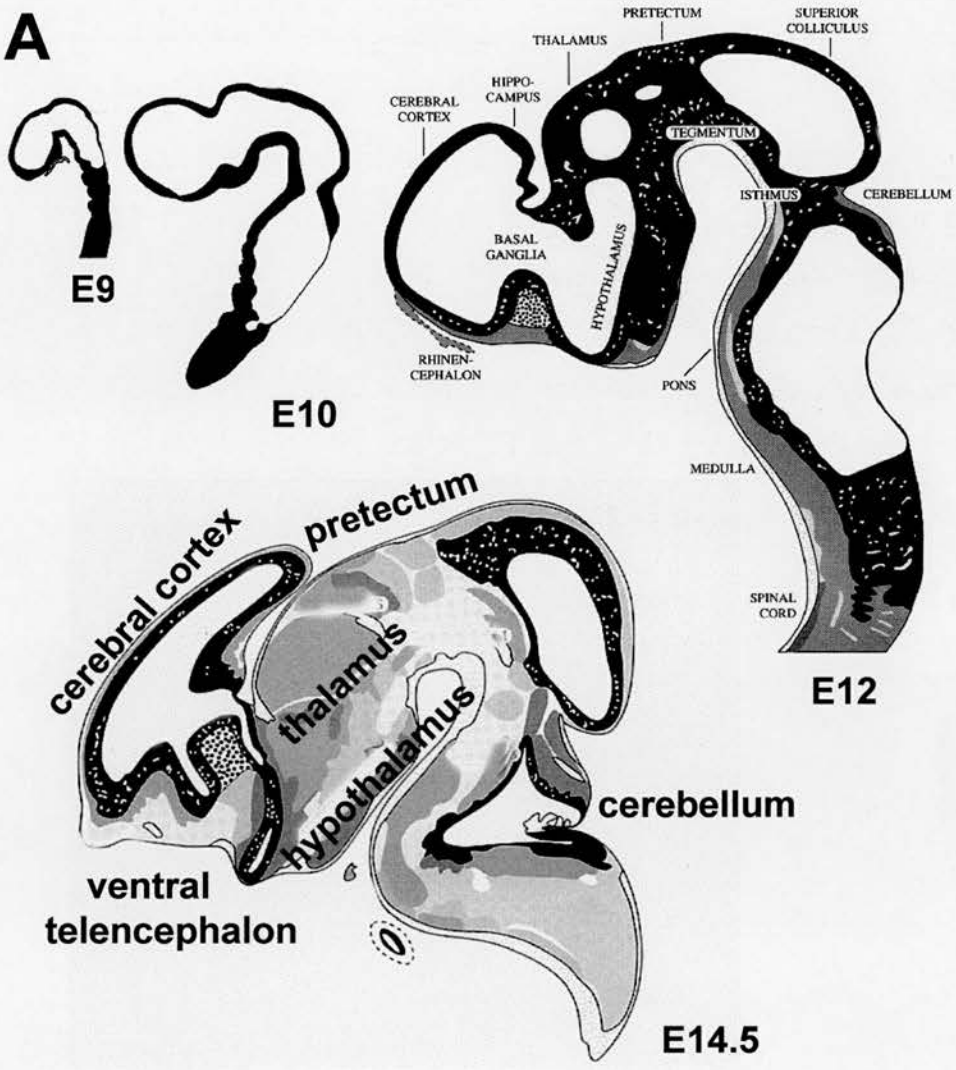
A
E9
E10
PRETECTUM
SUPERIOR COLLICULUS
THALAMUS
HIPPO-CAMPUS
CEREBRAL CORTEX
TEGMENTUM
ISTHMUS
CEREBELLUM
BASAL GANGLIA
HYPOTHALAMUS
RHINEN-CEPHALON
PONS
MEDULLA
SPINAL CORD
E12
cerebral cortex
pretectum
thalamus
hypothalamus
cerebellum
ventral telencephalon
E14.5

B

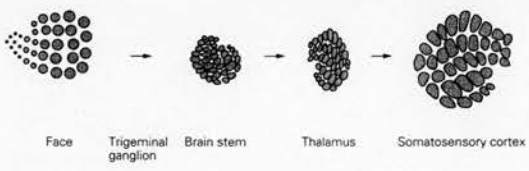
Face
Trigeminal ganglion
Brain stem
Thalamus
Somatosensory cortex

C

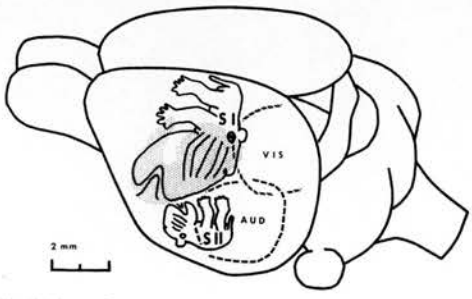
SI
VIS
AUD
SII
2 mm

(Woolsey and Van Der Loos, 1970 and Fig. 1.1C).

In the somatosensory system the pattern of whiskers on the rodent snout is precisely mapped onto the 'barrel fields' in the somatosensory cortex. This process involves the precise topographic organisation of axon projection from the whisker pad to the brainstem, brainstem to thalamus, and thalamus to cerebral cortex (for example Vanderhaeghen et al., 2000) as depicted in Fig. 1.1B. The identification of thalamocortical tract defects in animals carrying mutations in certain genes (see below) shows that genetic control is required for certain aspects of thalamocortical tract formation. This mapping is also dependent on experience since ablation of a whisker results in loss of the corresponding barrel in the cortex (Van der Loos and Woolsey, 1973). The formation of connections between cortex and thalamus therefore has a genetic component and an experience based component. Broadly, the establishment of the tract is genetically programmed but its refinement relies on sensory input. This thesis concentrates on the early aspects of thalamocortical tract projection which are primarily under genetic rather than epigenetic control.

Development of the thalamocortical tract

In the mouse, axons exit the dorsal thalamus at E12.5 and grow through the ventral thalamus. They make a sharp lateral turn at the hypothalamus and enter the ventral telencephalon through the internal capsule as illustrated in Fig 1.2A (Braisted et al., 1999, Tuttle et al., 1999, Auladell et al., 2000). The thalamic axons then grow into the cerebral cortex where they form synapses with layer 4 neurons. The basic thalamocortical circuitry is complete at this point. This timetable is illustrated in Fig. 1.2B but note that tract navigation is in reality more complex in space (as the tract

Figure 1.2

Thalamocortical tract formation during mouse embryogenesis. (A) Diagram showing the location of the thalamocortical tract in an E14.5 embryo (left panels) and the trajectory of the thalamocortical tract (red arrow on coronal tracing in right panel). Some images taken from Kaufman, (1995) and Altman and Bayer, (1995). The internal capsule is marked *. (B) The timetable of thalamocortical tract formation. Dorsal thalamus neurogenesis and key events in thalamocortical tract formation are related to embryonic age. (C) Mechanisms by which genetic control is exerted on thalamic axons navigating the thalamocortical route. 'Autonomous' implies that a particular gene is required only within the dorsal thalamus for axon navigation. 'Non-autonomous' implies that a particular gene is required only by cells along the pathway of the tract for thalamocortical axon navigation. 'Autonomous and non-autonomous' implies that a particular gene is required both within the dorsal thalamus and in cells along the pathway of the tract for axon navigation. The gene may have different functions within different cells. The blue arrows indicate whether the genetic instructions defining growth cone behaviour originate from the dorsal thalamus (autonomous) or from the route of the tract (non-autonomous).

Figure 1.2

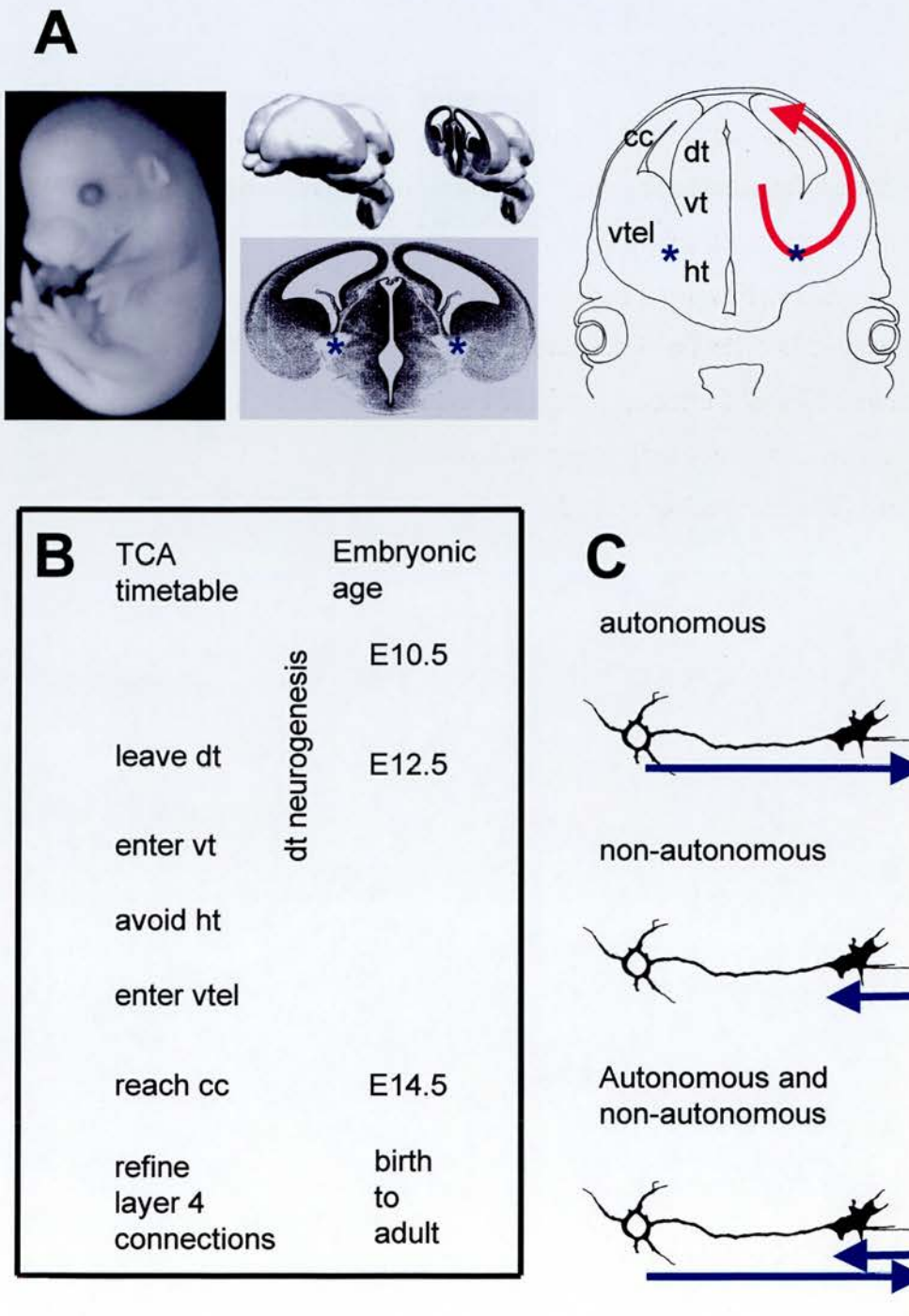
A
cc
dt
vt
vtel
ht
B
TCA timetable
Embryonic age
dt neurogenesis
E10.5
leave dt
E12.5
enter vt
avoid ht
enter vtel
reach cc
E14.5
refine layer 4 connections
birth to adult
C
autonomous
non-autonomous
Autonomous and non-autonomous

describes a three dimensional geometry) and time (as all thalamic axons do not navigate synchronously).

Autonomous and non-autonomous genetic control of axon navigation

How is genetic control of this complex journey achieved? There are several formal possibilities that are not mutually exclusive. These are depicted in figure 1.2C.

1. 'Autonomous': A particular gene is required within the dorsal thalamus to program axon navigation. If this gene is inactivated, thalamic growth cones will be incompetent to recognise navigation cues that are present along the tract and will become misrouted.
2. 'Non-autonomous': A particular gene is required along the pathway of the tract. If this gene is inactivated, navigation cues will not be supplied. The otherwise functional thalamic axon will become misrouted.
3. 'Autonomous and non-autonomous'. A particular gene is required both within the thalamic cell and along the pathway of the tract. The gene may have different roles in the different cell types involved. If this gene is inactivated the navigation cues along the pathway will be missing and the thalamic axon would not be able to recognise them in any case. The thalamic axon would become misrouted.

Different genes may participate in one or more aspects of thalamocortical tract formation. For example, genetic control may be required to regulate the proliferation of cells in one structure or to define the adhesive properties of those in another.

Motives for studying mechanisms of thalamocortical tract formation.

Apart from the intrinsic biological interest of understanding the mechanisms of tract formation, there are, albeit in the distant future, prospects for the application of this knowledge in medicine. If damaged brains are to be repaired, it is essential to understand how tracts form. For example, if a problem is caused by a defect in the tract,

there is unlikely to be much benefit gained from replacing the projecting structure without regenerating the tract. Attempts to replace the missing navigation landmarks may prove successful.

Key experiments in understanding thalamocortical tract formation

Much of the work on thalamocortical tract formation is focused on the termination of thalamic axons in the cerebral cortex and the formation of appropriate connections with layer 4 neurons. The focus of this thesis however is the mechanisms by which thalamic axons navigate to the cortex during embryogenesis. Some key experiments in understanding this process are listed below. The use of genetic approaches are discussed in following sections.

Tract labelling studies

1,1'-dioctadecyl-3,3,3',3'-tetramethylindocarbocyanine perchlorate (DiI) labelling experiments exploit diffusion of the red fluorescent dye DiI along axons. A crystal of DiI placed in the thalamus will label thalamic axons and allow their trajectory to be mapped. The technique can be refined using differently coloured dyes such as DiA (green) in double labelling experiments to label different subpopulations of axons. DiI experiments in rat (Molnar and Blakemore, 1998) and mouse (Auladell et al., 2000, Braisted et al., 1999, Tuttle et al., 1999) embryos in which labelling was performed at various ages has allowed the spatial and temporal route of thalamic axon growth to the cortex to be mapped. Interestingly, these studies also identified subpopulations of neurons in the ventral thalamus, hypothalamus, and ventral telencephalon that projected axons to the dorsal thalamus prompting the idea that thalamic axons might be guided by interaction with these axons. This idea resembles the 'handshake hypothesis' (Molnar and Blakemore, 1998) which suggested that corticothalamic axons project to the dorsal

thalamus and guide the thalamic axons. This hypothesis has been discredited by the observation that the thalamocortical and corticothalamic axons do not appear to come into contact, at least during the early stages of tract formation (Auladell et al., 2000). This issue remains controversial not least because it is hard to distinguish whether axons navigate along one another as opposed to both navigating along a common path simultaneously but independently. Another way of studying the thalamocortical tract is by immunostaining for molecules expressed on axons. This allows the staining of particular subpopulations of thalamocortical axons (Vitalis et al., 2000, Kawano et al., 1999, Vanderhaeghen et al., 2000, Pratt et al., 2000b, Tuttle et al., 1999, Braisted et al., 2000).

In vitro models of thalamocortical tract formation

Another approach has been to use organotypic culture systems in which thalamic explants are challenged in vitro with tissues which thalamic axons encounter during their journey to the cortex (ventral telencephalon, hypothalamus, and cerebral cortex). The use of such systems shows that thalamic axons are repelled by hypothalamus and attracted by ventral telencephalon (Braisted et al., 1999, Pratt et al., 2000b). This process presumably involves secreted factors as the attractive and repulsive behaviours are seen when the explants were separated in collagen gels (Braisted et al., 1999). The spatial organisation of these guidance cues is maintained in culture, perhaps anchored to the cell surface or extracellular matrix, in ventral telencephalic explants as labelled thalamic axons follow a trajectory within the explant similar to that seen in vivo (Pratt et al., 2000b). Co-cultures of thalamic explants with cortical explants (Molnar and Blakemore 1991, Molnar and Blakemore 1999, Goetz et al., 1992, Rennie et al., 1994, Pratt et al., 2000b) also showed that aspects of the in vivo innervation pattern were recapitulated. These studies show that the thalamic axons do not have to encounter

intervening tissues in order to respond correctly to tissues along the thalamocortical pathway.

In vitro models can also be used to test the function of molecules in thalamocortical tract formation. Netrin1 is a secreted protein originally isolated from chick for its ability to promote spinal cord axon growth (Tessier-Lavigne and Goodman, 1996). Netrin1 is expressed in the ventral telencephalon at the time thalamic axons penetrate so it is a candidate for the chemoattractive activity. However, although Netrin1 has a chemoattractive activity for thalamic axons in vitro, the chemoattractive effect of the ventral telencephalon for thalamic axons was not abolished by a Netrin1 blocking antibody so Netrin1 cannot be solely responsible for this effect (Braisted et al., 2000).

Seeding experiments in which fluorescently labelled thalamic cells are seeded onto tissues taken from the thalamocortical tract show that the adhesive properties of thalamic cells are matched to adhesive properties along the thalamocortical tract. Thalamic cells adhere selectively to the ventral telencephalon in the region where the thalamocortical tract penetrates (the internal capsule). Heparin-binding growth associated molecule (HB-GAM) and N-syndecan are extracellular matrix molecules expressed along the developing thalamocortical tract and their enzymatic removal abolishes this adhesion (Kinnunen et al., 1999). Similar experiments using slices of cortex (Emerling and Lander, 1994, Emerling and Lander, 1996) showed that the adhesion pattern and neurite outgrowth of the thalamic cells was reminiscent of the pattern of thalamic innervation. Thalamic cells adhere selectively to the intermediate zone rather than to the ventricular zone or cortical plate. This study implicated the extracellular matrix chondroitin sulphate proteoglycans (CSPGs) in axon navigation as enzymatic CSPG removal abolished the thalamic cell adhesion pattern (Emerling and Lander, 1996).

Genetic control of early brain development and tract formation

Tract formation in the forebrain mainly occurs after its basic functional units become discernible based on their morphology and patterns of gene expression. Recent advances in our understanding of the roles of transcription factors and secreted morphogens in establishing this basic structure are briefly outlined below. There are still large gaps in our knowledge as to how this original genetic patterning influences the mature cellular phenotype including cell surface and growth cone properties.

Forebrain

In the forebrain, secreted proteins Sonic Hedgehog (Shh), Bone Morphogenetic Proteins (BMPs), and Fibroblast Growth Factors (FGFs) modulate the expression of transcription factors implicated in subsequent development (Lumsden and Krumlauf, 1996). These interactions are suggested by the expression patterns of these genes and have been characterised in neural plate explants experiments. In vitro, ventrally Shh can induce expression of Nkx2.1, dorsally BMP7 induces Msx1, and FGF8 can induce either BF1 (forebrain marker) or En2 (midbrain marker) depending on the anterior-posterior positioning of the FGF8 source. These secreted proteins induce gradients of transcription factor expression which sometimes end in a sharp boundary, but no dose response data was presented (Shimamura et al., 1997). In vitro experiments have described antagonistic roles for Shh and BMP2 in forebrain cells with Shh promoting neuronal and oligodendroglial lineages and BMP2 promoting astroglial differentiation (Zhu et al., 1999). FGFs and Shh signals appear to cooperate in the specification of dopaminergic and serotonergic cell fate. Shh and FGF8 induce dopaminergic neurons in the midbrain and forebrain and Shh and FGF4 induce serotonergic neurons in the hindbrain (Ye et al., 1998). The transcription factor Otx2 is required for controlling expression of the cell adhesion molecule R-Cadherin and the secreted protein ephrinA2.

Otx2 mutant cells contribute poorly to the forebrain in $Otx2^{+/+} \leftrightarrow Otx2^{-/-}$ chimeras demonstrating the direct influence of this transcription factor on cell surface properties and cell sorting (Rhinn et al., 1999, Nguyen Ba-Charvet et al., 1998).

Midbrain

Expression gradients are important for tissue determination and axon navigation in the midbrain (Lumsden & Krumlauf, 1996). The transcription factor En1 is expressed strongly at the midbrain isthmus (the junction between the mid-brain and the hindbrain) with expression falling off in a gradient both anteriorly (into the midbrain) and posteriorly (into the hindbrain). Secreted proteins FGF8 and Wnt1, co-operate with En1 to maintain each other's expression gradients and influence axon navigation by controlling the expression of cell surface molecules. For example the expression of Eph-related receptor tyrosine kinases are induced by En-1 and ectopic expression of En1 and En2 results in misrouting of retinal axons (Friedman and O'Leary, 1996). Members of this receptor family interact with axon associated ligands (the ephrins) to regulate cell sorting (Cooke et al., 2001) and co-ordinate axon navigation (Friedman and O'Leary, 1996, Tessier-Lavigne and Goodman, 1996, Vanderhaeghen et al., 2000).

Hindbrain

In the hindbrain and spinal cord, expression of Shh ventrally in the notochord and the expression of BMPs dorsally set up opposing gradients of Shh and BMP concentration (Tanabe & Jessell, 1996). These secreted proteins influence the expression of the transcription factors with Shh repressing Pax6 expression and Pax3, Pax7, and Nkx2.2 being expressed ventrally (Briscoe et al., 2000, Ericson et al., 1997). Ultimately these interactions define the combination of LIM homeobox genes (LIM code) expressed by motor neurons and the path taken by their axons (Ericson et al., 1997, Osumi et al., 1997).

The prosomeric hypothesis of forebrain development

The regionalisation of the prosencephalic neural plate has been interpreted in terms of transverse and longitudinal domains of gene expression which relate to developing anatomical landmarks and functional units. These domains are defined by expression genes encoding transcription factors including *Nkx2.1*, *Nkx2.2*, *Dlx2*, *Gbx2*, *Otx2*, *Nkx2.1*, and *Pax6* and secreted proteins including *Shh* and *Wnt3*. The prosomeric model proposes that these domains correspond to segmental units of forebrain development called prosomeres (Puelles and Rubenstein, 1993, Bulfone et al., 1993, Rubenstein et al., 1994, Rubenstein et al., 1998). The diencephalon comprises prosomeres 1 to 3 (p1 posterior to p3 anterior) with p1 corresponding to the pretectum and epithalamus, p2 to the dorsal thalamus and p3 to the ventral thalamus. The secondary prosencephalon (p4 to p6) consists of the hypothalamus, ventral telencephalon, and cerebral cortex (dorsal telencephalon) and the nature of the segmental organisation is less clear than in the diencephalon. A simplified version of the prosomeric map at E12.5 showing genes relevant to this study is shown in Fig. 1.4. The term 'prosomere' is intentionally similar to the term 'rhombomere' used to define

segmental units in the hindbrain or rhomboncephalon (Tanabe and Jessell, 1996, Lumsden and Krumlauf, 1996) but it is by no means certain that the prosomeres fulfil the criteria of segmental identity.

For the purpose of this thesis, the prosomeric terminology is useful as it describes regions of the developing brain involved in thalamocortical tract formation in terms of gene expression patterns, which can be used to identify these regions. Whether, as was first thought (Fidgor and Stern, 1993, Shimumura et al., 1995) the boundaries of regulatory gene expression provide a scaffold for axon tract formation is less certain (Mastick and Easter, 1996, Nguyen Ba-Charvet et al., 1998). The sections below describe the emergence of these domains of gene expression and their relationship to the developing thalamocortical tract.

Regional gene expression defines developing thalamic territories

The prosomeric structure in the mouse becomes recognisable between E8.5 and E12.5 (Rubenstein et al., 1994, Rubenstein et al., 1998, illustrated in Fig 1.4A) and the first thalamocortical axons exit the dorsal thalamus at E12.5. The boundary between p2 (dorsal thalamus) and p3 (ventral thalamus) corresponds to the zona limitans intrathalamica (zli). Shh is expressed in the zli flanked by expression of the transcription factors Nkx2.2 and Otx2 (Pratt et al, 2000b, Nguyen Ba-Charvet et al, 1998). Prosomeres p2 and p3 can be identified by their expression of Wnt3, Pax6, and Dlx2. Wnt3 is expressed in p2 with a sharp ventral border of expression at the zli. Pax6 and Dlx2 are expressed in p3 with a sharp dorsal border of expression at the zli and this expression persists for several days (Bulfone et al., 1993, Stoykova et al., 1996, Warren and Price, 1997). This is an oversimplification as Pax6 is also expressed in the ventricular zone of the dorsal thalamus but not throughout it as is seen in the ventral thalamus (Warren and Price, 1997, Stoykova et al., 1996, Vitalis et al., 2000, Fig. 1.4A).

Segmental nature of the forebrain and thalamocortical tract formation

It has been proposed that forebrain axons use the same gene expression boundaries used to define the prosomeres as navigation cues (Rubenstein et al., 1994). This section examines restricted cell mixing and axon navigation (which is a special case of cell mixing) across those boundaries encountered by the thalamocortical tract.

Thalamocortical axons emanating from dorsal thalamus (p2) cross the p2/p3 boundary (Nguyen Ba-Charvet et al., 1998) and become highly fasiculated as they cross into the ventral thalamus (p3). This has been interpreted as evidence that the ventral thalamus is an unfavourable environment for these axons (Tuttle et al. 1999, Braisted et al, 1999). Short term (2 to 3 days) tracer labelling studies in chick diencephalon showed that cell mixing is restricted by borders of regulatory gene expression used to define prosomeres, and that fasiculated axons grow along these borders (Figdor and Stern, 1993). As retrovirally labelled thalamic cell clones allowed to develop for longer periods (16 days) can contribute to several prosomeres (Golden and Cepko, 1996), these boundaries are not absolutely respected by all thalamic cells throughout development.

The prosomeres p4, p5, and p6 comprising the hypothalamus and telencephalon are less defined than p1, p2, and p3 and have been interpreted differently by different authors (compare Rubenstein et al., 1994 to Vitalis et al., 2000). Borders of gene expression demarcating domains of the telencephalon and the hypothalamus have been described which the developing thalamocortical tract encounters as it navigates to the cerebral cortex. Thalamocortical axons do not cross the border between the ventral thalamus and the hypothalamus but do grow into the ventral telencephalon. The ventral

telencephalon and hypothalamus have been shown to be respectively attractive and repulsive to thalamocortical axons in vitro (Braisted et al., 1999, Pratt et al., 2000b).

Cell mixing is restricted at the boundary between the ventral (basal ganglia) and dorsal (cerebral cortex) telencephalon although there is significant migration of cells across this boundary (Fishell et al., 1993, Anderson et al., 1997, Inoue et al., 2001, Chapouton et al., 1999, Gotz et al., 1996). Thalamocortical axons become densely packed as they cross this boundary to enter the intermediate zone of the cerebral cortex (Auladell et al., 2000, Braisted et al 1999, Molnar and Blakemore, 1998).

If thalamic axons do not use segmental boundaries to navigate to the cerebral cortex, then how do they navigate this complex route (Molnar and Blakemore, 1995)? There is growing evidence from several points along the thalamocortical pathway that the growth cones of thalamic axons respond to gene products which are expressed in graded domains which bear no obvious relation to the sharp boundaries of gene expression defining prosomeric structure. Any segmented features described by prosomeres most likely represent a transient developmental point of restricted cell mixing corresponding to an evolutionary solution to brain development common to all vertebrates.

Secreted proteins, their receptors and thalamocortical navigation

Several secreted proteins have been shown to influence axon navigation in various regions of the brain by interacting with cell surface receptors expressed by axon projecting cells. The secreted proteins include Netrin1, and members of the semaphorin, ephrin and slit families. These bind to their respective cell surface receptors DCC, neogenin, Unc5 (receptors for Netrin1), plexin and neuropillin (receptors for the semaphorins), Eph receptors (receptors for the ephrins), and Robo1 and Robo2 (receptors for Slit1 and Slit2). To date it has been shown that Netrin1, LAMP, Sema6A,

and Eph4A mediate aspects of thalamocortical axon growth (Vanderhaeghen et al., 2000, Mann et al., 1998, Braisted et al., 2000, Leighton et al., 2001). Other secreted proteins such as the Slits, semaphorins, and molecules yet to be identified, are likely to be involved in thalamocortical tract development. The sections below examine molecules known to have roles in thalamocortical tract development.

Axons in other systems have been shown to respond to gradients of the secreted protein Netrin1 (Tessier-Lavigne and Goodman, 1996) and Netrin1 is expressed by cells along the thalamocortical tract (Braisted et al., 2000). The attractive Netrin1 receptor DCC is expressed in the dorsal thalamus suggesting a mechanism for thalamocortical axon response to this secreted protein (Braisted et al., 2000). The roles of Netrin1 in thalamocortical tract formation are discussed in more detail elsewhere in this Chapter.

The limbic associated membrane protein (LAMP) has been shown to mediate thalamocortical tract projection. LAMP is expressed in the limbic cortex and in the limbic thalamus (but not in the non-limbic cortex or non-limbic thalamus). In vivo axons project from the limbic thalamus to the limbic cortex and in vitro LAMP is permissive for limbic axon outgrowth but not for non-limbic axon outgrowth (Mann et al., 1998).

The secreted ephrin proteins and their Eph receptors are implicated in axon navigation (Marcus et al., 2000, Tessier-Lavigne and Goodman, 1996). EphrinA5 has been shown to repel thalamic axons and is expressed in a gradient in the developing cerebral cortex. Its receptors. EphA3, EphA4, and EphA5 are expressed in the dorsal thalamus (Mackarehtschian et al., 1999). EphrinA5 protein is expressed as a gradient in the cerebral cortex and expression of the corresponding Eph receptor, EphA4, is graded in a matching way in the dorsal thalamic cells, which will project axons to this region. In vitro these axons are repelled by EphrinA5 and the normal projection pattern of these thalamic axons on arriving in the cerebral cortex is disrupted in EphrinA5 knockout

mice (Vanderhaeghen et al., 2000). As the thalamocortical tract reaches the cerebral cortex in these mutant mice ephrinA5 is not essential for tract projection. The Eph receptors show promiscuity in ephrin binding and expression of several ligands (ephrinA5 and ephrinA4) and receptors (EphA3, EphA4, and EphA5) in overlapping gradients in thalamocortical territory may allow some redundancy. This might ameliorate the severity of phenotype seen when one of these genes is inactivated (Mackarehtschian et al., 1999, Vanderhaeghen et al., 2000). Contrary to the repulsive interaction in the thalamocortical system, an attractive interaction has been reported between the EphA family receptors and their ligands in the vomeronasal axon system (Knoll et al., 2001).

In mouse, Slit family proteins are secreted ligands for the Robo receptors. Analysis of their expression patterns show that they are expressed at positions along the thalamocortical tract consistent with a role in thalamocortical axon guidance (Nguyen Ba-Charvet et al., 1999, Yuan et al., 1999, Ringstedt et al., 1999). In other developing brain systems Robos and Slits play critical roles in axon navigation. Slit2 acts as a repellent for retinal, olfactory and hippocampal axons and treatment with Slit2 in vitro collapses their growth cones (Nguyen Ba-Charvet et al., 1999, Erskine et al., 2000). Slit2 is secreted by the choroid plexus and repels neuronal migration by cortical and olfactory neurons (Hu, 1999). Retinal ganglion cells express Robo2 at the time their axons are navigating through territory expressing Slit1 and Slit2 (Erskine et al., 2000).

The semaphorins are secreted proteins implicated in axon navigation (Tessier-Lavigne and Goodman, 1996). It has recently been shown that Semaphorin6A (Sema6A) is required for caudal thalamocortical tract projection (Leighton et al., 2001). Although Sema6A is expressed in several fibre tract systems including the thalamocortical tract, only the caudal thalamocortical tract is severely disrupted when *Sema6A* is mutated (Leighton et al., 2001). Another example of system-specific

Semaphorin action is seen in cortical neurons. Cortical axons are repelled by Semaphorin3A (Sema3A) whereas dendrites from the same cortical cell are attracted towards Sema3A (Polleux et al., 1998, Polleux et al., 2000). Both axons and dendrites express the Sema3A receptor Neuropilin1 and it is the asymmetric subcellular distribution of a soluble guanylate cyclase that is responsible for mediating these opposite cellular responses to the Sema3A/ Neuropilin1 interaction (Polleux et al., 2000). These are clear illustrations that a particular cell surface molecule (Sema3A, Sema6A, or Neuropilin1) can have different roles in different systems, presumably reflecting system-specific differences in local genetic and biochemical environment.

Transcription factors regulate expression of cell surface molecules involved in cell adhesion and axon navigation (see above). In the developing cerebral cortex there are opposing gradients of transcription factors Pax6 and Emx2 and alterations in these gradients in *Pax6* and *Emx2* mutants result in corresponding alterations to the expression gradients of Cadherins (cell adhesion molecules) and disruption to area specific thalamocortical projections (Bishop et al., 2000). In the ventral thalamus gradients of Pax6 and RPTPδ (a transmembrane phosphotyrosine phosphatase) are formed and their disruption coincides with thalamic axons failing to navigate these territories (Tuttle et al., 1999).

Mutants illustrate genetic control of thalamocortical tract formation.

The study of mutant animals in which thalamocortical tract formation is disrupted has provided several important insights into the genetic control of this process. Much of this work has been carried out in mice due to their amenability to genetic manipulation. The sections below describe mutant animals which illustrate that thalamocortical axon navigation requires autonomous genetic input in the dorsal thalamus (*Gbx2*) and non-autonomous input along the thalamocortical pathway (*Mash1*) as illustrated in Fig. 1.3.

Gbx2 is required within the dorsal thalamus only

Gbx2 is a homeobox containing transcription factor, which is expressed by cells of the developing dorsal thalamus. The *Gbx2* gene is not expressed in other domains of the thalamocortical axon tract. In mice lacking *Gbx2* gene function, the dorsal thalamus differentiates abnormally and analysis of regional markers *Id4* and *Lef1* suggests that normal dorsal thalamic post-mitotic cells are not produced in the absence of *Gbx2* function (Miyashita-Lin et al., 1999). DiI labelling experiments show that the thalamocortical tract does not form in the *Gbx2* mutants and that thalamic axons stop in the internal capsule. These findings are confirmed by immunostaining for serotonin and calretinin which specifically label subsets of thalamic axons. Since Gbx2 is expressed in the dorsal thalamus itself but not along the thalamocortical pathway, this study shows that Gbx2 is an example of a gene whose function is required only within the dorsal thalamus (and not within cells along the tract) for thalamocortical tract projection (see Fig. 1.3B)

Figure 1.3

Mouse mutants illustrating genetic control of thalamocortical tract formation. A tracing of a coronal section of E14.5 brain is shown with the dorsal thalamus, ventral thalamus, hypothalamus, ventral telencephalon, and cerebral cortex marked in the left panel in (A). Blue Xs in the left half mark the position of wild-type gene expression in (B to D). Red arrow in the right half indicates the trajectory of the thalamocortical tract in (A) the wild-type and (B,C,D) the mutant. Red X indicates tract termination. (B) in *Gbx2* mutants the tract becomes stalled as it leaves the thalamus. The transcription factor Gbx2 is expressed only in the dorsal thalamus. (C) in *Mash1* mutants the tract becomes stalled within the thalamus. The transcription factor Mash1 is expressed in the ventral thalamus, hypothalamus, and ventral telencephalon (but not in the dorsal thalamus). (D) in *Netrin1* mutants a reduced tract (indicated by thin red arrow) reaches the cerebral cortex. The secreted protein Netrin1 is expressed in the dorsal thalamus and along the thalamocortical tract route.

Figure 1.3

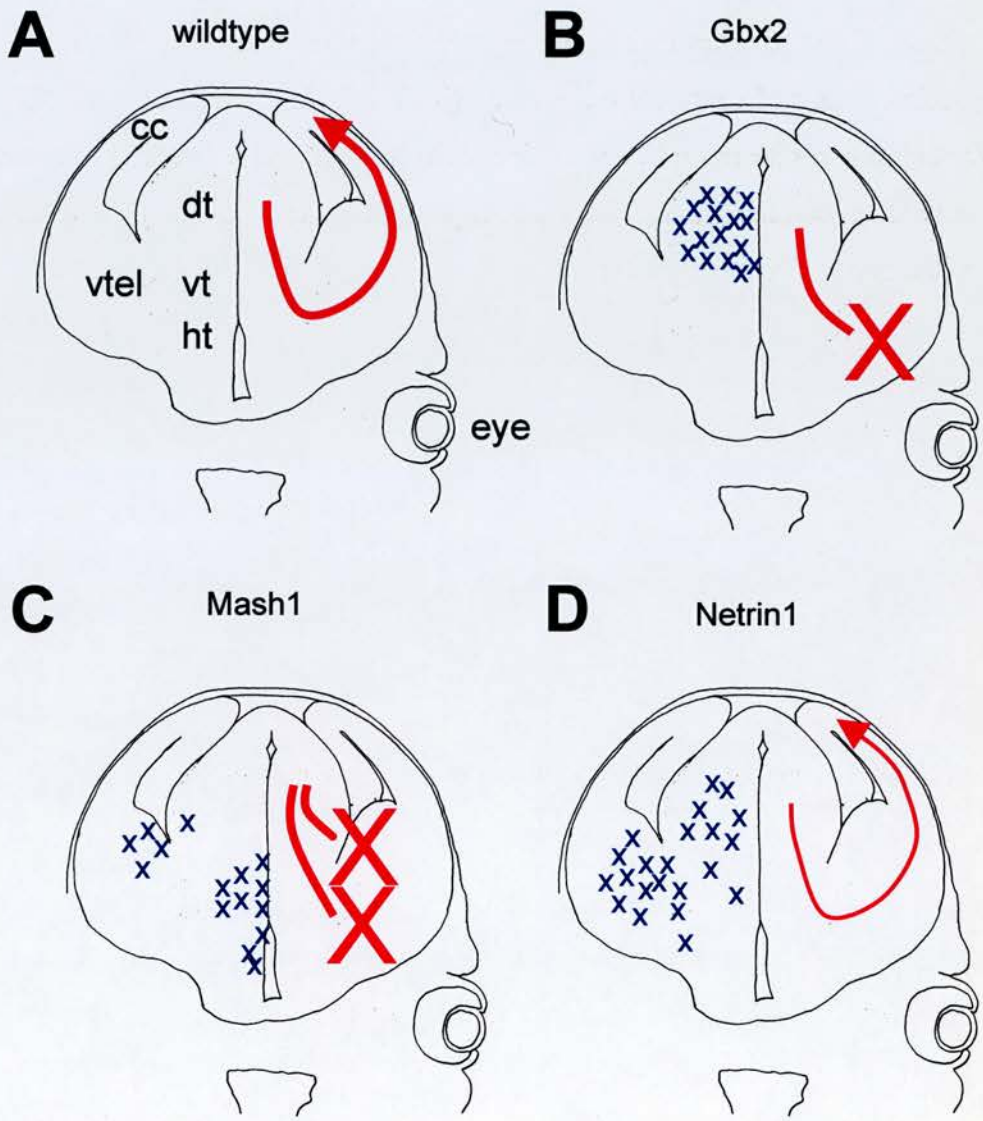

Mash1 is required along the thalamocortical tract only

Mash1 a basic helix-loop-helix transcription factor which is highly expressed in the proliferative zones of the forebrain that give rise to the domains along the thalamocortical tract. Mash1 is a mammalian homologue of the *Drosophila* achaete-scute complex genes which are involved in neuroblast specification. During embryogenesis Mash1 is expressed in the ventricular zone of the ventral thalamus, hypothalamus, zona limitans intrathalamica, and the lateral, medial, and caudal ganglionic eminencies of the ventral telencephalon. Mash1 is not expressed in the dorsal thalamus itself. DiI labelling experiments showed that the thalamic axons projecting from the *Mash1* mutant dorsal thalamus fail to reach the cerebral cortex with many becoming stalled in the ventral thalamus and the remaining axons becoming stalled in the ventral telencephalon (see Fig. 1.3C). The failure of tract formation in mutants coincided with the disappearance of Mash1 expressing cell domains in the thalamus and ventral telencephalon which project to the dorsal thalamus in the wild type during tract formation (these cells were retrogradely labelled after DiI placement in the dorsal thalamus). The loss of Mash1 also resulted in alterations in the expression patterns of genes implicated in axon pathfinding including a steepening of the gradient of RPTPδ expression in the ventral thalamus and loss of Netrin1 in populations of cells in the ventral telencephalon. These observations prompt the speculation that the thalamocortical tract is guided by the axons of cells along the thalamocortical tract projecting back into the dorsal thalamus and by gradients of cell surface and secreted molecules such as RPTPδ and Netrin1. Mash1 is required to regulate the paving of this pathway for thalamic axons to navigate along (Tuttle et al., 1999).

Netrin 1 is required along the thalamocortical tract

Netrin1 is a secreted protein which has been implicated in axon guidance and shown to be chemoattractive for some axons and chemorepellent for others (Tessier-Lavigne and Goodman, 1996). These dual roles are thought to be mediated by different axon cell surface receptors for Netrin1 with DCC and neogenin mediating attractant effects and unc5h2 and unc5h3 mediating repulsive effects. Netrin-1 is expressed in the dorsal thalamus itself and in close association with the thalamocortical tract as it passes through the internal capsule and into the ventral telencephalon. *Netrin1* has been disrupted in transgenic mice, these mice do not have a total loss of Netrin1 function (Serafini et al., 1996) and the thalamocortical phenotype in these animals is variable. In any case, disruption of Netrin-1 function does appear to correlate with a defect in thalamocortical tract formation and this fits nicely with the notion that Netrin-1 expressing cells guide DCC and neogenin expressing thalamic axons along sections of the thalamocortical route. This model does not explain why many axons do successfully navigate to the cerebral cortex in these mutant animals. This observation, taken together with the failure of blocking Netrin1 in vitro to abolish the attraction of thalamic axons for internal capsule, suggests that Netrin1 is not the only molecule involved and may be at least partially redundant (Braisted et al. 2000). It would be interesting to know the thalamocortical phenotype in animals lacking DCC and neogenin function (Deiner et al., 1999). As Netrin1 is expressed in the dorsal thalamus and along the thalamocortical tract it is not possible to determine whether the defect reflects a requirement for Netrin1 in the dorsal thalamus (source defect) or along the tract (pathway defect) based on its expression pattern and analysis of mutant animals. This type of situation is also encountered in *Pax6* mutants (see below). Tissue culture experiments described above in which Netrin1 activity was blocked using antibodies (Braisted et al., 2000) were

interpreted as evidence for a pathway defect but did not test the capacity of *Netrin1* mutant dorsal thalamus to project a tract into a wild-type tract environment.

Pax6 is a transcription factor with many developmental roles

Pax6 is a transcription factor containing a paired DNA binding domain and a homeobox DNA binding domain (Walther & Gruss, 1991, Hill et al., 1991). Pax6 is widely expressed throughout the central nervous system during development and expression persists into adulthood in some cells. Pax6 is also expressed in the pancreas (Stoykova et al 1996, Stoykova et al., 1997, Warren and Price 1997, Grindley et al., 1997, Mansouri et al., 1994). Mutant mice lacking functional Pax6 exhibit a wide range of defects from early in development and die at birth. Defects in homozygous mutant embryos (*Pax6*$^{-/-}$) have been detected in all Pax6 expressing structures examined to date arguing that Pax6 plays a fundamental role in the development of these diverse structures in the wild-type, some of which are listed below.

Pax6 and the eye

Pax6 is expressed in several eye tissues throughout development. Mutants lacking functional Pax6 fail to develop eyes. Ectopic expression of Pax6 in Drosophila (Halder et al., 1995) and Xenopus (Chow et al., 1999) has been shown to induce eye formation, suggesting that Pax6 can orchestrate the genetic program required for eye formation. Pax6 has been shown to directly regulate the transcription of many genes involved in eye formation by binding to their promoters. The downstream target genes identified to date include transcription factors *Pax6* and *Pax2*, and structural proteins *αB-* , *αA* , *βB1-* , *β-* , *δ-* , and *ζ-crystallins* (Duncan et al., 1998, Richardson et al., 1995, Cvekl et al., 1995, Schwarz et al., 2000). Pax6 appears to be able to positively

Figure 1.4

Pax6 and thalamocortical tract formation. (A) (top panel) Mapping of the expression pattern of transcription factors *Pax6* (red) and *Dlx1* (yellow) at E12.5 on the prosomeric model of Puelles and Rubenstein (1993). (lower panels) Mapping of the expression pattern of *Pax6* (red) and *Dlx1* (yellow) onto coronal sections of $Pax6^{+/+}$ (middle panel) and $Pax6^{Sey/Sey}$ (bottom panel) at E12.5, E14.5, and E18.5 during the period of thalamocortical tract formation. Figure adapted from Stoykova et al., 1996. Abbreviations: AA, Amydala; ACX, Archicortex, AD, Hypothalamic nucleus, anterodorsal; AEP, Anterior entopeduncular area; AH, Anterior hypothalamus; CGE, Caudal ganglionic eminence; DB, Diagonal band; DT, Dorsal thalamus; EMT, Eminentia thalami; EP, Entopeduncular nucleus; ET, Epithalamus; HCC, Hypothalamic cell cord; HT, hypothalamus; LGE, Lateral ganglionic eminence; LV, Lateral ventricle; M, Mesencephalon; MGE, Medial ganglionic eminence; NCX, Neocortex; OB, Olfactory bulb; P1 to P6, Prosomeres 1 to 6; POA, Anterior preoptic area; POP, Posterior preoptic area; PT, Pretectum; r1 to r7, Rhombomeres 1 to 7; SE, Septum; SCH, Suprachiasmatic area; SPV, Supraoptic/paraventricular area; STM, Stria medullaris; VLG, Ventral lateral geniculate body; VT, Ventral thalamus; ZI, Zona incerta; 3V, Third ventricle. (B) Thalamocortical axon trajectory (brown) and Pax6 protein expression (green) in camera lucida drawings of serial sections (rostral-most at front) taken from E16 rat embryos (equivalent to mouse E14.5). Left panel shows $Pax6^{+/+}$ embryonic brain, right panel shows $Pax6^{rSey/rSey}$ embryonic brain (which does not express Pax6 protein). In the mutant, thalamocortical axons become stalled in the ventral telencephalon forming a characteristic mushroom shaped structure rostrally. This figure was taken from Kawano et al., 1999. (C) Comparison of the timetables of thalamocortical tract projection (left) and Pax6 gene expression (right) in tissues neighbouring the thalamocortical tract at mouse embryonic ages shown in the middle. Black arrows on the right indicate that Pax6 is expressed within a particular structure (although not necessarily throughout it), dotted lines indicate diminishing expression.

Figure 1.4

A

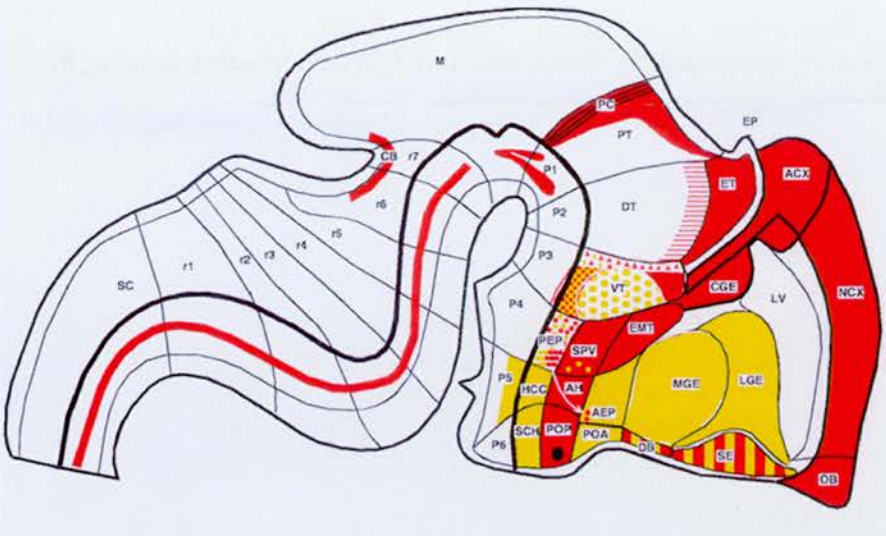

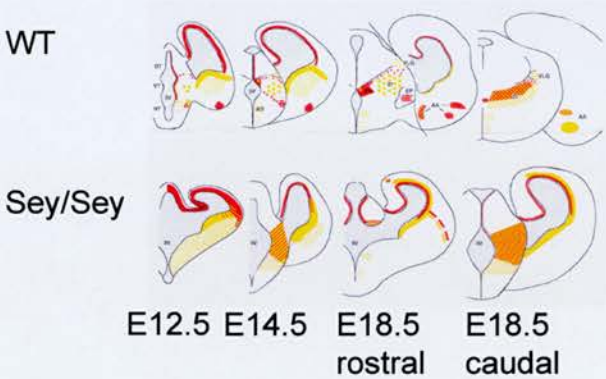

B

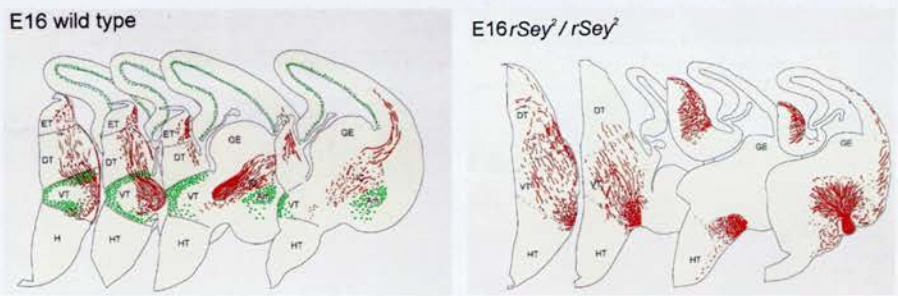

C

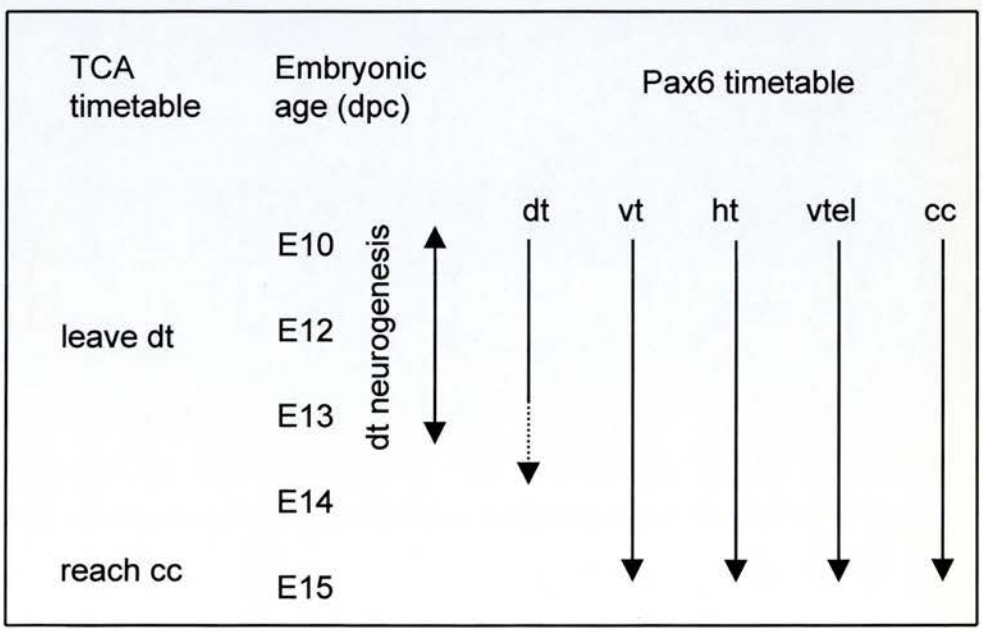

regulate expression of some genes (*Pax6*, *αB-* , *αA-* , *β-* , *δ-* , and *ζ-crystallins*) and negatively regulate the transcription of others (*Pax2*, *βB1-crystallin*).

Examination of mouse. $Pax6^{+/+} \leftrightarrow Pax6^{-/-}$ chimeras has shown that Pax6 is required in the optic vesicle for maintenance of contact with the overlying lens epithelium, a necessary event in eye formation, and a clue that Pax6 may be involved in defining the adhesive properties of these cells. Pax6 appears to act in a cell autonomous manner in these aspects of eye development (Collinson et al., 2000, Quinn et al., 1996). The dosage of Pax6 expression also appears to be important (Schedl et al., 1996) as increasing *Pax6* gene dosage in the eye results in aberrant eye development although unlike $Pax6^{-/-}$ animals these mice are viable beyond birth.

Pax6 and the thalamus

Pax6 is expressed in the proliferating ventricular neuroepithelium of the thalamus. Mutants lacking functional Pax6 do produce a dorsal thalamus (prosomere p2) and ventral thalamus (prosomere p3) as judged by anatomical features and Pax6, Dlx2 and Wnt3a expression (Warren & Price 1997, Grindley et al., 1997, Stoykova et al, 1996, Pratt et al., 2000b, Fig. 1.4A). Thalamic morphology is severely disrupted however and axons projecting from the dorsal thalamus fail to reach the cortex (Warren and Price, 1997, Kawano et al., 1999, Vitalis et al., 2000, Pratt et al., 2000b, Fig. 1.4B). The rates of thalamic cell proliferation are abnormally low, and this may explain the reduced size of the mutant thalamus during subsequent development (Warren and Price, 1997).

Pax6 and the cerebral cortex

Pax6 is expressed mainly in the proliferative ventricular zone of the cerebral cortex. Mutants lacking functional Pax6 do develop a cerebral cortex but its morphology is severely disrupted (Stoykova et al., 1996, Schmahl et al., 1993, Caric et al., 1997, Warren et al., 1999). Pax6 is expressed in radial glial cells and radial glial morphology and *tenascin-C* gene expression is altered in developing Pax6 mutant cortex. Pax6 acts through both cell autonomous and non-autonomous mechanisms in influencing glial cell morphology and glial cell number respectively (Gotz et al., 1998). The adhesive properties of cortical cells are also altered in Pax6 mutants. An in vitro segregation assay shows that the segregation (failure to mix) seen between cortical and striatal cells from wild type embryos (Gotz et al., 1996) was lost when cortical and striatal cells from mutants were mixed (Stoykova et al., 1997). Mutant and wild type cortical cells also appeared to segregate from one another in this in vitro assay. This alteration in adhesive properties may reflect a loss of R-Cadherin observed in the mutant cortex (Stoykova et al., 1997). Comparisons between the expression patterns of several genes including transcription factors *Dlx1*, *Ngn1*, *Ngn2*, *Mash1*, *Emx2* and cell surface molecules *TrkB*, *R-Cadherin*, *tenascin-C* certainly show differences which can be attributed to the loss of Pax6 function (Warren et al., 1999, Gotz et al., 1998, Stoykova et al., 1997, Bishop et al., 2000, Toresson et al., 2000) but it is not certain which if any of these genes are directly under Pax6 transcriptional control. Pax6 mutant cortical cells also exhibit increased rates of proliferation and disrupted interkinetic nuclear movement during cell division in the ventricular zone (Gotz et al., 1998, Warren et al., 1999). Cortical cells show defective migration from the ventricular zone to the cortical plate in Pax6 mutants (Caric et al., 1997). The migratory defect appears to require non-cell autonomous Pax6 function as mutant cells transplanted into a wild-type cortex migrate to their normal positions (Caric et al., 1997) although the mutant cells do not mix with cells in the wild

type cortex and aggregate into clumps (David J. Price, unpublished observation) arguing that Pax6 also has cell autonomous roles. As cortical neurons migrate along radial glia, which are themselves disrupted in the Pax6 mutant (Gotz et al., 1998), it is possible that these transplant experiments highlight a separation of the roles of Pax6 in neuronal and glial development.

Pax6 and the cerebellum

Pax6 is strongly expressed in the rhombic lip of the cerebellar system and in cells migrating away from it. In *Pax6* mutants, some precerebellar nuclei fail to form and migratory streams from the precerebellar neuroepithelium are absent. There are no proliferative defects in the cerebellar granule cell population. In vitro assays show that cerebellar explants from wild-type embryos form long neurites along which cells from the explant migrate but comparable explants isolated from Pax6 mutants do not (Engelkamp et al., 1999).

Pax6 and the hindbrain

Pax6 is expressed in the ventral part of the developing spinal cord in undifferentiated motor neuron progenitor cells destined to form the hypoglossal nucleus which projects the hypoglossal motor nerve to the periphery. Other motor neuron progenitors contribute to other nuclei including the vagal nucleus. In Pax6 mutants, the hypoglossal motor nerve is missing but the number of motor neuron progenitors is not reduced. This implies that Pax6 is required to program the projection pattern of these motor neurons (Osumi et al., 1997, Ericson et al., 1997). Further experiments have investigated the molecules involved in the specification of motor neuron subtype by Pax6. The secreted protein Sonic Hedgehog (Shh) is a key regulator of brain and spinal cord development and mutants lacking Shh fail to develop a brain (Chiang et al., 1996).

In vivo Pax6 and Shh are expressed in complementary dorsal to ventral gradients (Pax6 levels are high dorsally and Shh levels are high ventrally). Exogenously applied Shh represses Pax6 expression in vitro in a dose dependent manner and immunodepletion of Shh in explant cultures results in an increase in the number of Pax6 expressing cells (Ericson et al., 1997). Different motor neurons express characteristic combinations of LIM homeodomain proteins (the LIM code). Hypoglossal motor neurons express Isl1, Isl2, Gsh4, and Lim3 whereas vagal motor neurons express only Isl1 and Gsh4. In Pax6 mutants, Lim3 and Isl2 are not expressed in cells which would normally express Pax6 indicating a transition from a 'hypoglossal LIM code' to a 'vagal LIM code'(Ericson et al., 1997). The transcription factor Nkx2.2 is not expressed in Pax6 expressing motor neuron progenitors (Ericson et al., 1997) and the expression domain of the secreted protein Wnt7b overlaps with that of Pax6 (Osumi et al., 1997). Another Wnt gene, Wnt7a, has been shown to induce axon remodelling (Lucas & Salinas, 1997, Hall et al., 2000). Loss of Pax6 function results in an increase in the number of motor neuron progenitor cells expressing Nkx2.2 (Ericson et al., 1997) and a loss of Wnt7b expression in these cells (Osumi et al., 1997). A model emerges in which Pax6 interprets the gradient of Shh signalling and transduces this signal by regulating the expression of several transcription factors and at least one secreted protein (Ericson et al., 1997, Osumi et al., 1997). How this signalling cascade influences axon navigation is yet to be determined.

Pax6 and the pancreas

Pax6 is expressed in the developing pancreas. In Pax6 mutants pancreatic morphology is abnormal, numbers of all four types of endocrine cells in the pancreas (α, β, δ, and PP cells) are decreased, and production of the hormones glucagon, insulin, and somatostatin (particularly glucagon) are reduced (Sander et al., 1997). The reduction in hormone production is greater than can be accounted for by the reduced number of hormone secreting cells implying that Pax6 is required both for the generation of pancreatic cells and for the induction of hormone production. In vitro studies showed that Pax6 protein binds to DNA sequence elements in the promoters of glucagon, insulin, and somatostatin and that Pax6 can activate transcription from the glucagon and insulin promoters (Sander et al., 1997). Interestingly, a slightly different pancreatic phenotype was reported in a line of mice in which a null allele of Pax6 had been generated by gene targeting (St-Onge et al., 1997). In this line it appeared that no α-cells were generated leading to the suggestion that Pax6 was specifically required for their specification although it was subsequently revealed that insulin levels were also reduced (see Sander et al., 1997 for a full discussion of this discrepancy). Methodological differences between these two studies make it hard to see whether there is a fundamental conflict between the pancreatic phenotypes which both describe loss of cells and reduction in hormone production.

Extrapolating the role of Pax6 from other systems

As described above, the roles of Pax6 have been studied in a range of developing systems other than the thalamocortical tract which is the main focus of this thesis. These studies do not however reveal a unified picture of Pax6 function. For example loss of Pax6 results in reduced proliferation in the thalamus and increased proliferation in the cerebral cortex, while having no effect on proliferation in the cerebellum or spinal cord.

That a human Pax6 protein can orchestrate eye development in the leg of a fruitfly (Halder et al., 1995) or toad (Chow et al., 1999) provides a clear demonstration of a gene specifying a structure but does not explain why a pancreas or thalamus does not emerge along with the ectopic eye. In this context it is useful to remember that a gene is not a protein. The level timing and position of protein expression are also critical. Protein function is also dependent on the availability of the various cofactors with which the protein interacts. The *Drosophila* transcription factor *orthodenticles* (*Otd*) gene has two mouse homologues, *Otx1* and *Otx2* which are expressed in the developing forebrain. 'Knock-in' experiments in which the *Otx1* coding sequence was replaced with either *Otx2* or *Otd* showed a rescue of the *Otx1* mouse mutant phenotype indicating that the proteins themselves were equivalent (Acampora et al., 1999). Similarly *En1* and *En2* mouse mutants have distinct midbrain phenotypes but En2 under the control of the *En1* gene promoter could rescue the *En1* mutant phenotype showing that functionally equivalent proteins can have different roles in development of the mouse (Hanks et al., 1995).

This highlights the fundamental difference in the ways different systems exploit similar genes. As a particular transcription factor can program different phenotypes depending on the context of its expression, the genetic cascades initiated by these genes in different species or tissues are certain to have diverged from one another. Extrapolating the role of Pax6 from other systems to thalamocortical tract formation is therefore a hazardous undertaking.

Untangling potential roles for Pax6 in thalamocortical tract

Because Pax6 is so widely expressed in the central nervous system, it is often difficult to determine from observation of mutants lacking Pax6 function alone where the primary defect lies. The scope for both cell autonomous and non cell autonomous roles for Pax6 in the development of the thalamocortical tract exemplifies this problem. A comparison of the timetables of Pax6 expression and thalamocortical tract formation show several points at which Pax6 expressing cells could influence the developing tract (see Fig. 1.4C). It is conceivable that the failure of tract formation resides in a defective dorsal thalamus (as seen in *Gbx2* mutants) or in a defect in the structures through which the tract navigates (as seen in *Mash1* mutants) or both. The situation is analogous to the discovery of a broken wing and a broken propeller amongst the wreckage of a crashed aeroplane not establishing which (if either) caused the crash as both were intimately associated with the aeroplanes' ability to fly and its subsequent destruction.

One way to establish whether Pax6 has an autonomous role in programming thalamic axons to respond appropriately to navigational cues would be to replace the route present in the mutant with one from the wild-type. If the mutant dorsal thalamus still cannot project a tract then this shows a defect within the dorsal thalamus itself. This experiment requires that thalamic axons can be visualised clearly. Given the importance of the extracellualar matrix in thalamocortical tract formation (see above), I deemed it important to see the axons as they navigated through intact tissue. A tractable way to achieve this is to generate a transgenic mouse ubiquitously expressing a tau tagged green fluorescent protein (tau-GFP). Tracts projected by dorsal thalamic explants from tau-GFP embryos would be expected to be clearly visible against a background of unlabelled tissue (see below).

The sections below discuss the considerations involved in making a transgenic mouse ubiquitously expressing tau-GFP. The experiment described above was the

primary motive behind the production of these animals. The decision to generate a ubiquitously expressing mouse (rather than one expressing solely in the dorsal thalamus) allows for the use of cells and tissues from this animal with a wide variety of applications in cell mixing experiments. The decision to exploit germline transmission via embryonic stem (ES) cells supplies the extra benefit of tau-GFP labelled ES cells.

The need to mark cells

The processes involved in the development of neuronal circuitry are extremely dynamic. Axons navigate through complex cellular environments and follow complex trajectories in space and time. Any study of axon behaviour demands that the experimenter is able to record the events involved in axon extension. In some cases this can be achieved in vitro by culturing an isolated neuron on a microscope slide and watching the process form or recording its responses to gradients of applied factors (Tessier Lavigne and Goodman, 1996) or substrate molecules (Mann et al., 1998, Braisted et al., 2000, Vanderhaeghen et al., 2000). This approach is generally not feasible in vitro if the cell of interest is interacting with other cells or tissues which make identification of the cell of interest difficult and is completely impossible in vivo, at least for the mammalian brain. In these cases it becomes necessary to mark the cell of interest in some way so that it and its extensions can be distinguished from the cells and tissues with which it is interacting.

Reporter genes

Several genes have been identified which have proved useful as reporter genes. The two most widely used in transgenic mice are LacZ and GFP.

LacZ

Exploitation of the *LacZ* gene dates back to the middle of the last century and the foundation of molecular biology (Judson, 1979). *LacZ* forms part of the *E. coli* Lac Operon and encodes the hydrolytic enzyme β-Galactosidase (LacZ). The active enzyme functions as a tetramer. Over the years, synthetic substrates for β-Galactosidase have been developed. The most commonly used is X-gal which is converted to an insoluble blue precipitate by β-Galactosidase. Cells expressing LacZ can be identified because they turn blue when incubated with X-gal. More recently, substrates have been developed which fluoresce when processed by β-Galactosidase and this has permitted the option of viewing living LacZ expressing cells (although initially marking was not efficient because the fluorescent product tended to diffuse out of the cell). Increasingly sophisticated LacZ substrates which can freely diffuse into the cell, but are converted into fluorescent products which cannot leave the cell, have permitted the staining of living cells expressing a *LacZ* transgene. These have provided a means for identifying LacZ expressing targets for injection of fluorescent dyes (Studer et al., 1996) or for electrophysiological recordings from single cells (Pettit et al., 1994). The sensitivity of fluorescent detection of β-Galactosidase using these fluorescent products appears to be lower than that of detection by the more conventional X-Gal assay (Westerfield et al., 1992) and the main application of *LacZ* as a reporter gene remains its detection in fixed tissues.

Green fluorescent protein

Green fluorescent protein (GFP) was isolated from the jellyfish *Aequorea victoria.* In its natural context GFP is a companion protein to aequorin. GFP converts the blue light emitted by the chemiluminesent aequorin to the green glow seen in the intact jellyfish cells. Although it remains unclear exactly what ecological function is served by bioluminescence, related fluorescent proteins exist in a variety of coelenterates (jelly fish and corals) where they partner and modulate the emission of chemiluminescent proteins (Tsien et al., 1998). Importantly, the GFP gene encodes all the information necessary for the post-translational synthesis of its chromophore, and no jellyfish-specific proteins are needed. This has been demonstrated by the expression of GFP as a transgene in other organisms (Chalfie et al, 1994).

GFP protein structure

Wild-type GFP is a 238 amino acid protein with a calculated molecular mass of 26888 Da (Prasher et al., 1996). The chromophore is a p-hydroxy-benzylideneimidazolinone formed by oxidative cyclization of the Ser-Tyr-Gly tripeptide (residues 65, 66, and 67 in the native protein). The crystal structure of GFP has been solved to atomic resolution (Ormo et al., 1996, Yang et al., 1996) and shows that the GFP folds into an hollow cylinder composed of 11 β-strands through which is threaded an α-helix bearing the chromophore (Fig. 1.5). Residue 1 at the N terminal end and residues 230 to 238 at the C-terminal end appear to be disorganised. Deletion analysis of GFP has shown that residues 2 to 232 are necessary for fluorescence (Dopf and Horiagon, 1996). A fluorescence spectrum for wild-type GFP is shown in Fig. 1.6A along with the spectra of the thermostable GFP variant GFP5 (Siemmering et al., 1996).

Figure 1.5

Structure of green fluorescent protein. A ribbon model of green fluorescent protein is shown from two perspectives. Eleven strands of β-sheet (green arrows, numbered in red on left) form the walls of a cylinder. Short segments of α-helices (blue) cap the top and bottom of the 'β-can' and also provide a scaffold for the fluorophore (yellow ball-and-stick) which is near the geometric centre of the can. This folding motif, with β-sheet outside and helix inside, represents a new class of proteins. This figure is taken from Yang et al., (1996).

Figure 1.6

Spectra of green fluorescent protein and variants. (A) Alterations to GFP sequence results in altered spectral properties. Excitation (ex) and emission (em) spectra of wild type GFP and the thermotolerant GFP variant GFP5 generated by the substitutions V163A and S175G. The GFP variant MGFP6 used in this study (see Chapter 2) was generated from GFP5 by additional substitutions I167T to increase absorption in blue part of spectrum, S65T to enhance the second absorption peak, and F64L to improve solubility (Zernika-Goetz et al., 1996, 1997). This figure is adapted from Siemering et al., (1996). (B) Excitation and emission spectra of GFP spectral variants commercially available from Clontech. This figure was taken from the Clontech 2001 on-line catalogue.

Figure 1.5

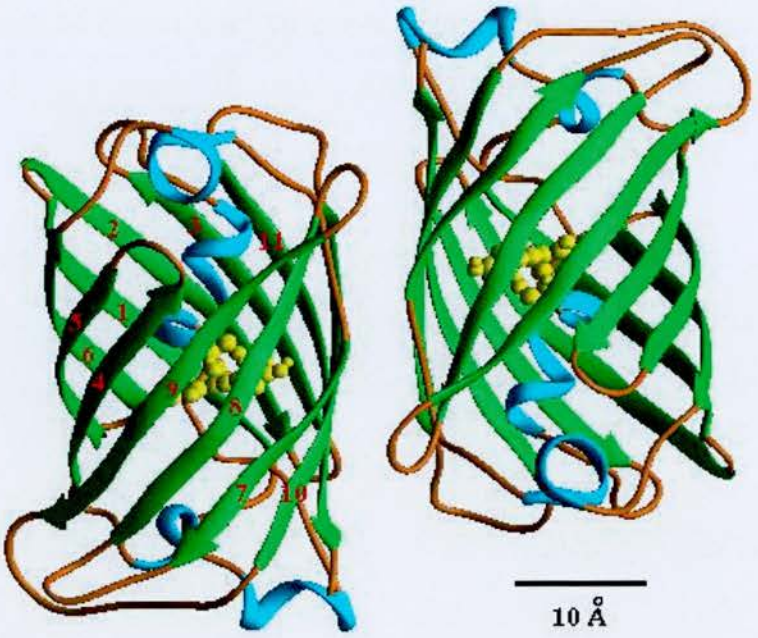

Figure 1.6

A

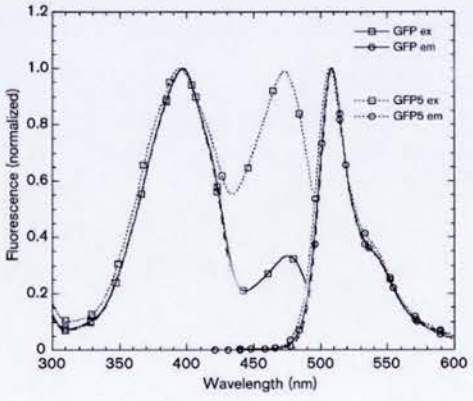

B

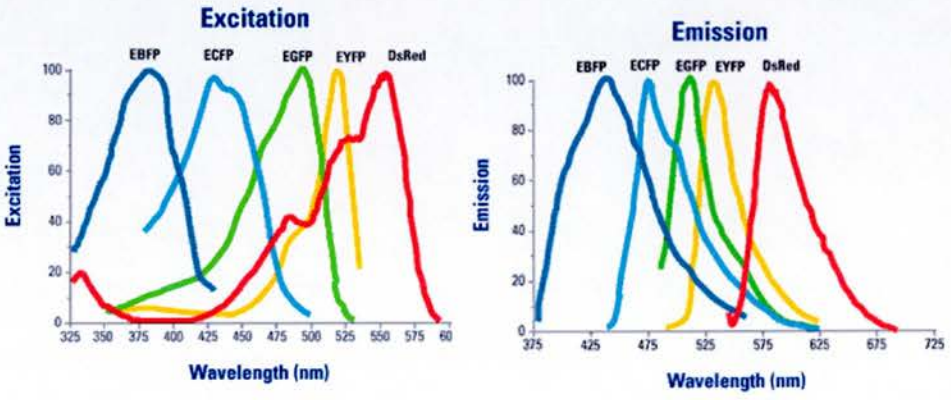

Figure 1.7

Spectral characteristics of the major classes of green fluorescent proteins (GFPs).

[a] Substitutions from the primary sequence of GFP are given as the single-letter code for the amino acid being replaced, its numerical position in the sequence and the single letter code for its replacement. Phenotypically neutral mutations are omitted.

[b] λ_{exc} is the peak of the excitation spectrum (nm). ε in parentheses is the absorbance extinction coefficient ($10^{-3}M^{-1}cm^{-1}$). Two numbers separated by a dash indicate a range of reported values, two numbers on separate lines indicate two distinct peaks in the excitation spectrum.

[c] λ_{em} is the peak of the emission spectrum (nm). QY in parentheses is the fluorescence quantum yield. The product of ε and QY gives the overall brightness of GFP.

[d]Relative fluorescence intensities for proteins expressed in *E. coli* at 37°C under similar conditions. These have been arbitrarily normalised to 100 for the brightest member of each class and cannot be used to compare classes. This figure is modified from Tsien, (1998).

Figure 1.7

Mutation[a]	Common name	λ_{exc} (ϵ)[b]	λ_{em} (QY)[c]	Rel. fl.[d] @ 37°C
Class 1, wild-type				
None or Q80R	Wild type	395–397 (25–30) 470–475 (9.5–14)	504 (0.79)	6
F99S, M153T, V163A	Cycle 3	397 (30) 475 (6.5–8.5)	506 (0.79)	100
Class 2, phenolate anion				
S65T		489 (52–58)	509–511 (0.64)	12
F64L, S65T	EGFP	488 (55–57)	507–509 (0.60)	20
F64L, S65T, V163A		488 (42)	511 (0.58)	54
S65T, S72A, N149K, M153T, I167T	Emerald	487 (57.5)	509 (0.68)	100
Class 3, neutral phenol				
S202F, T203I	H9	399 (20)	511 (0.60)	13
T203I, S72A, Y145F	H9–40	399 (29)	511 (0.64)	100
Class 4, phenolate anion with stacked π-electron system (yellow fluorescent proteins)				
S65G, S72A, T203F		512 (65.5)	522 (0.70)	6
S65G, S72A, T203H		508 (48.5)	518 (0.78)	12
S65G, V68L, Q69K S72A, T203Y	10C Q69K	516 (62)	529 (0.71)	50
S65G, V68L, S72A, T203Y	10C	514 (83.4)	527 (0.61)	58
S65G, S72A, K79R, T203Y	Topaz	514 (94.5)	527 (0.60)	100
Class 5, indole in chromophore (cyan fluorescent proteins)				
Y66W		436	485	—
Y66W, N146I, M153T, V163A	W7	434 (23.9) 452	476 (0.42) 505	61
F64L, S65T, Y66W, N146I, M153T, V163A	W1B or ECFP	434 (32.5) 452	476 (0.4) 505	80
S65A, Y66W, S72A, N146I, M153T, V163A	W1C	435 (21.2)	495 (0.39)	100
Class 6, imidazole in chromophore (blue fluorescent proteins)				
Y66H	BFP	384 (21)	448 (0.24)	18
Y66H, Y145F	P4–3	382 (22.3)	446 (0.3)	52
F64L, Y66H, Y145F	EBFP	380–383 (26.3–31)	440–447 (0.17–0.26)	100
Class 7, phenyl in chromophore				
Y66F		360	442	—

Directed evolution of GFP for use in transgenic mice

Despite its potential as a reporter gene, the wild type GFP protein is unsuitable as a reporter in transgenic mice. The most extreme problem is the failure of wild-type GFP to fluoresce at 37°C, although this problem would not arise in its natural context of a jellyfish living in cooler seas. Mutations in GFP which suppress this thermosensitivity were isolated by screening a panel of randomly mutagenised GFP variants for ability to fluoresce at 37°C (Siemering et al., 1996). This improvement in fluorescence was attributed to the amino acid substitutions Val to Ala at position 163 (V163A) and Ser to Gly at position 175 (S175G) and resulted in a 35-fold increase in fluorescence at 37°C. The substitution Phe to Leu at position 64 (F64L) improves the solubility of GFP and may assist its folding properties (Cormack et al., 1996). Substitutions within the chromophore itself have been identified which alter the fluorescence properties of GFP. The substitution Ser to Thr at position 65 (S65T) improves chromophore ionisation and so enhances fluorescence (Heim and Tsien, 1996). These advantageous mutations have been combined in the GFP variants mgfp6 and MmGFP (Zericka-Goetz et al., 1996, Zericka-Goetz et al., 1997) and EGFP (Zhang et al., 1996). A number of these mutations and their properties are listed in Fig. 1.7.

Spectral variants of GFP

Other mutations have been exploited to alter the excitation and emission spectra generating different 'colours' of GFP for double labelling and fluorescence resonance energy transfer (FRET) experiments (Heim and Tsien, 1996). These versions are marketed by Clontech as the 'Living colours series' and currently include Yellow, Cyan, and Blue Fluorescent proteins (Fig. 1.6B). The green, cyan, and yellow variants have been used successfully in transgenic mice (Feng et al., 2000, Hadjantonakis et al., 1998, Kawamoto et al., 2000) although detection problems were encountered with the blue

variant (Feng et al., 2000). A number of these GFP spectral variants are listed in Fig. 1.7.

Other Fluorescent Proteins

Although spectral variants of GFP have been generated, the green fluorescent variants exhibit the strongest fluorescence and are the most widely used. This prompted the search for other fluorescent proteins to increase the palette available for double labelling experiments. The isolation of fluorescent proteins from nonbioluminescent Anthozoa species (Matz et al., 1999) on the basis of sequence homology to the *Aequorea victoria* GFP offers this potential. The red fluorescent protein DsRed (originally named drFP583) from the coral Discosoma sp. is responsible for the red coloration around the coral's oral disc. DsRed adsorbs maximally at 558nm (green) and emits at 583nm (red) as shown in Fig. 1.6C, and can be detected using an epifluorescence microscope equipped with a rhodamine filter. The DsRed protein is predicted to have a similar 11-stranded β-barrel structure to GFP (Fig. 1.5) and exhibits similarities at other residues known to be critical for GFP fluorescence including the chromophore residues Tyr-66 and Gly-67 and some of the important polar residues contacting the chromophore such as Arg-96 and Glu-222.

Apart form the advantages of being red, DsRed is highly fluorescent and its fluorescence may be more long lived than that for GFP. However, there are some features of DsRed which may diminish its usefulness as a reporter molecule. DsRed appears to take a long time (days) to mature which may be an unacceptable lag in reporting on gene expression or for use in transient transfection experiments (Matz et al., 1999, Baird et al., 2000). DsRed also appears to form a tetramer, which may limit its use as a fusion tag as the tagged protein would also be forced into a tetramer conformation which might have functional implications (Baird et al., 2000). Trangenic mice

expressing DsRed have been generated and it was reported that the DsRed did not freely diffuse throughout the cell (Feng et al., 2000). It may be that these problems can be resolved, as has been seen for the original GFP (Heim and Tsien, 1996, Siemmering et al., 1996), and that these drawbacks can be engineered out of DsRed.

Problems with GFP

Despite its many appealing features, there are several drawbacks to working with GFP molecules. A major advantage of GFP is that cells can be imaged in real time. The corresponding drawback is the problem of phototoxicity. During fluorescence imaging, the cell may be damaged by the light source used to excite the chromophore. This is a particular problem for ultra-violet excitation and the problem is reduced for GFP excited at longer, lower energy, wavelengths. The cell may also be damaged by fluorophore-mediated generation of free radicals. In practice, however, continuous imaging of GFP fluorescence has been reported in systems as sensitive as the developing mouse embryo (Zernika-Goetz et al., 1997) which continued to develop despite continuous imaging using a confocal microscope. GFP expressing morulae developed into normal mice after observation using a microscope equipped for epifluorescence (Ikawa et al., 1995) although many eggs did fail to form blastocysts if they were observed for longer than a few minutes. Technological advances in the sensitivity of epifluorescence and confocal microscopes may serve to alleviate this problem by reducing the doses of radiation the cells must be exposed to generate a detectable fluorescent signal.

Fusion proteins (tagging)

Modifications to the sequence of the reporter protein can be made so as to alter the properties of the reporter (other than its fluorescence properties as described above). Expression of LacZ or GFP results in labelling of the cell. The reporter molecule is in principle free to diffuse throughout the cell. In the case of LacZ, labelling is not uniform and this is a particular problem for visualisation of cellular processes and axons which are not efficiently labelled with LacZ. GFP, perhaps because it is a smaller molecule which functions as a monomer, diffuses throughout the cell more freely than LacZ.

In many cases it is useful to modify GFP so that its subcellular localisation or other properties can be tailored for a particular experiment. GFP can be fused to an intact protein, isolated protein domains, or peptide sequences for the dual purposes of investigating their function and modifying the properties of GFP. If the properties of the fusion tag are of interest then the reporter component of the fusion protein will report on these properties. This could also be achieved by immunohistochemistry but this provides a static view. By fusing to a vital reporter such as GFP the subcellular localisation and dynamics of the protein can be detected in living cells and its response to experimental manipulations monitored. This yields time lapse footage which is much easier to interpret than a series of snap-shots each acquired from a different cell, albeit grown under equivalent conditions. Since the start of this study, the generation of GFP fusion proteins has become a standard technique in the study of protein function. Having characterised the localisation of the fusion protein, presence of the reporter molecule can be used as a marker for the protein so obviating the need for detection by other means such as immunohistochemistry.

A concern in using GFP as a fusion tag is that the GFP may disrupt protein function and provide a misleading account of protein behaviour. This problem is generally applicable to all fusion tags. Given the globular structure of many proteins in

which many domains function as semi-autonomous units and the compact globular structure of GFP itself, the addition of an extra GFP domain may in many cases not have a great effect. This appears to be the case with many GFP fusion proteins which retain properties seen in the untagged protein (see below). The more that is known about the structure and function of a protein, the easier it should be to design a fusion protein in which the GFP tag does not interfere with functional domains, although this will remain more of a problem for novel proteins. One way to ameliorate this problem is to compare the behaviour of several positions of GFP fusion tag, for example N-, C- terminal and internal fusions. Since different GFP tag positions are unlikely to influence protein behaviour in the same way, similar behaviour seen for a variety of fusion tags will suggest that the GFP is not interfering with protein function.

Some GFP fusion proteins

The usefulness of GFP tagging is attested to by the sheer number which have been generated in the five years since GFP was isolated. It should be remembered that published work is likely to emphasise 'positive' aspects of GFP as a fusion tag. Failed GFP fusion proteins may not be reported and it may take longer for 'negative' aspects of GFP to emerge. The examples below serve to indicate the versatility of GFP as a reporter molecule and illustrates some considerations when using GFP as a fusion tag. This list is not intended to be comprehensive.

The stability of GFP is a variable that can be manipulated experimentally. Proteins containing the proline rich PEST motif domains are known to be targeted for ubiquitination and degradation by the proteosome. Fusion of such motifs to the carboxyl terminus of GFP dramatically reduced the half-life of the GFP from 26 hours to between 2 and 6 hours (Li et al., 1998, Corish and Tyler-Smith, 1999). These unstable GFPs should prove useful as reporters for the cessation of gene expression as once GFP

synthesis stops they will be cleared from the cell more rapidly than the more stable GFP versions.

Fusion of GFP to cytoskeletal proteins has allowed new insights into cytoskeletal dynamics (Olson et al., 1995, Ludin and Matus, 1998) and this list is increasing all the time. Fusion of GFP to cytoskeletal proteins allows direct visualisation of the protein and functional analysis by site directed mutagenesis and deletion mapping as exemplified for the microtubule associated protein MAP4 (Olson et al., 1995). The availability of different GFP spectral variants allows for double labelling experiments in which the interactions between cytoskeletal proteins can be monitored.

GFP tagging has proved generally useful for watching protein trafficking and secretion (Stephens and Pepperkok, 2001). Fusion of GFP to the γ-Subspecies of Protein Kinase C (γ-PKC-GFP) produced a fusion protein which retained kinase activity and exhibited translocation to the plasma membrane in response to phorbol ester treatment, K^+ depolarisation, NMDA treatment, and mGluR1 activation status. This showed that γ-PKC-GFP retained many aspects of its function despite the addition of a GFP tag (Sakai et al., 1997). Similarly, fusion of GFP to secreted peptides chromogranin B or neuropeptide Y allowed the dynamics of secretion to be monitored. These fusions localised correctly to immunohistochemically identified granules within neurites (although some did appear in unexpected locations) and Ca^{2+} treatment induced appropriate secretion of the GFP fusion peptides (Lang et al., 1997) showing that the GFP tag did not prevent correct processing and export.

A fusion between GFP and the shaker voltage-sensitive K^+ channel (GFP-Shaker) has been shown to provide a genetically encoded optical probe for membrane voltage. Conformational changes in the shaker molecule associated with changes in the voltage across the plasma membrane resulted in conformational changes to the GFP structure resulting in a 5% alteration in fluorescence. This was sufficient to be detectable

and the authors estimated a 30-fold increase in ease of detection over existing voltage-sensitive dyes. This report was also interesting because the GFP was not fused as a C- or N- terminal fusion but was fused internally to the shaker molecule (Siegel and Isacoff, 1997). This approach could potentially be used to detect conformational shifts in a wide range of proteins although care must be taken to introduce the GFP so that protein folding and function are maintained and this will require detailed characterisation of the target molecule.

Transcription factors such as NFκB and members of the Gli gene family are functionally restricted by intracellular compartmentalisation with translocation to the nucleus being a prerequisite for transcription control. GFP fusions have allowed the identification of the nuclear localisation sequences (NLS) required for nuclear translocation in the *Dlx3* gene (Bryan and Morasso, 2000) and several *Kruppel* gene family members (Shields and Yang, 1997). This type of fusion is anticipated to be useful in dissecting the relationship between subcellular localisation, function of transcription factors, and nuclear dynamics.

Driving reporter transgene expression in transgenic mice

There are several methodological approaches which can be used to introduce a reporter transgene into the germline of transgenic mice. The choice of which method to use depends on the reporter gene expression pattern desired. The section below briefly summarises the methods available and comments on their applicability to generating a transgenic mouse in which reporter gene expression is ubiquitous.

Random DNA integration and position effects

The transgene can be introduced as a random integration event. This can be achieved by microinjection of DNA into a pronucleus of a fertilised mouse egg (Jaenisch, 1988, Okabe et al., 1997) which is implanted and allowed to develop (Hogan et al., 1994) or by introduction into embryonic stem cells by electroporation (Hadjantonakis et al., 1998, Pratt et al., 2000a, Kawamoto et al., 2000, Hogan et al., 1994) and the establishment of transgenic lines by germline transmission (Hogan et al., 1994). In this approach the experimenter has no control of the genomic locus into which the DNA will integrate. The transgene is therefore subject to position effects (Al-Shawi et al., 1990) caused by the influence of genomic sequence at the integration site on transcription of the transgene. The result of this is that different transgenic lines generated using the same transgene will exhibit different patterns of transgene expression.

The spectrum of position effects obtained largely depends on the transgene construct. This has been exploited in 'enhancer trap' (Korn et al., 1992) and 'gene trap' (Forrester et al., 1996, Takeuchi et al., 1995, Serafini et al., 1996, Cecconi et al., 2000, Gossler et al., 1989, Leighton et al., 2001) experiments where the intention is to use the cis-acting genomic elements at the integration site to drive expression of a transgene with minimal cis-acting transcriptional elements of its own. At the other extreme, the

introduction of large yeast artificial chromosome (YAC) genomic clones comprising genes with large amounts of their own cis acting elements frequently results in transgene expression patterns largely free of position effects (Peterson et al., 1993, Schedl et al., 1996).

Cell type specific expression accidental and intentional

The majority of transgenic mice which have been generated by random integration have used relatively compact promoter elements 'designed' to drive a particular pattern of gene expression. Transgenic mice generated by pronuclear injection using a neuron specific enolase (NSE) promoter fragment to drive LacZ expression exhibited LacZ expression which recapitulated the endogenous NSE expression in 2 out of 7 transgenic lines (Forss-Petter et al., 1990). In 2 out of 9 lines in which GFP expression was driven by a glial fibrillary acidic protein (GFAP) promoter, GFP recapitulated GFAP expression (Zhuo et al., 1997). In some cases unexpected but useful expression patterns are obtained by position effects. The HZ1 line in which somatosensory cortical barrels express LacZ (Cohen-Tandoui, 1994), a panel of transgenic lines in which GFP spectral variants are expressed in different subsets of cells in different lines despite the use of the same basic construct in all cases (Feng et al., 2000). A recent gene trap screen has generated transgenic lines in which placental alkaline phosphatase (PLAP) labels subpopulations of axons including those of the thalamocortical tract (*Sema6A* gene trap) and cortical barrels (LST16 gene trap) (Leighton et al., 2001). A drawback of this approach is that large numbers of transgenic lines often have to be screened in a to find one suitable for a particular experiment.

Ubiquitous expression accidental and intentional

For some experiments, the aim is to drive expression of the reporter in all the cells in an animal. The CAG promoter combines the cytomegalovirus immediate early enhancer and β-actin promoter and first intron (Niwa et al., 1991) and has been used successfully to drive apparently ubiquitous reporter gene expression including GFP (Hadjanonakis et al., 1998, Kawamoto et al., 2000, Pratt et al., 2000a). The CAG promoter is not immune from position effects and lines in which transgene expression is clearly not ubiquitous are also obtained using this promoter. Ubiquitous expression can also be achieved without the use of a strong transgene promoter. The ROSA26 line, which ubiquitously expresses LacZ (Zambrowicz et al 1997) contains a randomly integrated retroviral *LacZ* transgene (Friedrich and Soriano, 1991).

Targeted DNA integration

Reporter genes can also be integrated into a particular genomic locus by exploiting the process of homologous recombination. Targeting constructs have been devised that allow the expression of the reporter gene to come under the transcriptional control of the targeted gene (Mountford et al., 1994, St-Onge et al., 1997, Godwin et al., 1998). These include placing a *tau-LacZ* or *tau-GFP* transgene in the *OMP* locus resulting in faithful reporter expression in OMP expressing olfactory neurons (Mombaerts et al., 1996, Rodriguez et al., 1999) and the targeting of a GFP transgene to the *Hoxa1* and *Hoxc13* loci resulting in fluorescent labelling of Hoxa1 and Hoxc13 expressing cells respectively (Godwin et al., 1998). This approach can deliver accurate reporter gene expression without the uncertainties introduced when relying on random integration events. So long as a gene is known which has the expression pattern required for the reporter gene expression, targeting is the method of choice. The main drawbacks are that the production of a targeting construct requires detailed characterisation of the

target locus which is time consuming, and the targeting event may disrupt or inactivate the target gene.

Tau Biology

Tau proteins (particularly the human forms) have been the subject of intensive research, largely prompted by their appearance in the neurofibrillar protein aggregates which are one of the major diagnostic features of Alzheimer's Disease. In spite of this, the exact biological function of tau remains largely unknown (Buee et al., 2000, Mandelkow & Mandelkow, 1998, Spillantini & Goedert, 1998). The tau gene is highly conserved between mammalian species including rodents, cows, and humans. The discussion below focuses on the features of tau likely to be important when using a tau tagged green fluorescent protein as a reporter gene in transgenic mice.

Tau gene and protein structure

In humans, there is a single tau gene located on chromosome 17 and spanning 100kb. Alternative splicing yields six transcripts which are translated to produce the six human tau isoforms. These differ in having three (3R tau) or four (4R tau) 31 or 32 amino acid repeats at the carboxyl terminus and in the 0, 29 or 58 amino acid inserts found at the amino terminus. In humans the three repeat isoform is found in foetal brains whereas adult brains contain the four repeat isoforms. Further heterogeneity is introduced by post-translational modifications including phosphorylation (Buee et al., 2000, Mandelkow and Mandelkow, 1998, Spillantini and Goedert, 1998, Fig. 1.9).

Figure 1.8

Schematic representation of the functional domains of the 4-repeat tau isoform. The projection domain, including an acidic and a proline rich region, interacts with cytoskeletal elements to determine the spacing between microtubules in axons. The N-terminal part is also involved in signal transduction pathways by interacting with proteins such as PLC-γ and Src-kinases. The C-terminal part, referred to as microtubules binding domain, regulates the rate of microtubule polymerisation. It is also involved in binding with functional proteins such as protein phosphatase 2A (PP2A) or presenilin-1 (PS1). This figure is adapted from Buee et al., (2000).

Figure 1.9.

Phosphorylation control of tau. (A) Diagram of tau protein, its functional domains, and sites of phosphorylation. The near-N-terminal inserts (exons 2 and 3, grey) and the second of the four microtubules binding repeats (exon 10, grey) can be absent owing to alternative splicing. The microtubule binding repeats are numbered 1 to 4. SP and TP motif proline (P) resides can be phosphorylated by proline directed kinases including MAPK, GSK-3β, and Cdk5 and dephosphorylated by protein phosphatases including PP2A and PP2B. KXGS motifs can be phosphorylated at the serine (S) residue by kinases including protein kinase A (PKA) and microtubule affinity regulating kinase (MARK). (B) Model showing the link between the phosphorylation status of tau and its affinity for and stabilisation of microtubules. Phosphorylation (P) of tau at crucial sites detaches tau from microtubules (shown inn red and yellow). This figure is adapted from Mandelkow and Mandelkow, (1998).

Figure 1.8

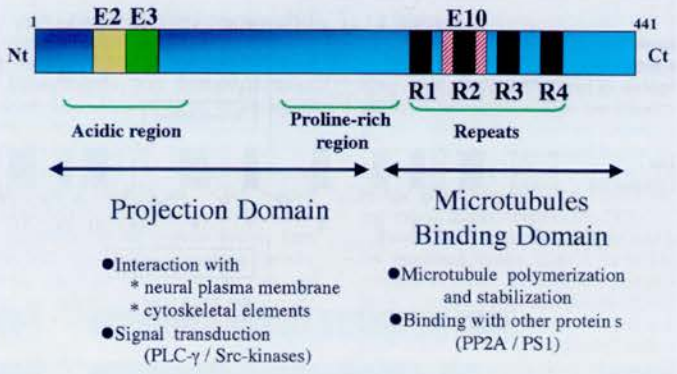

Figure 1.9

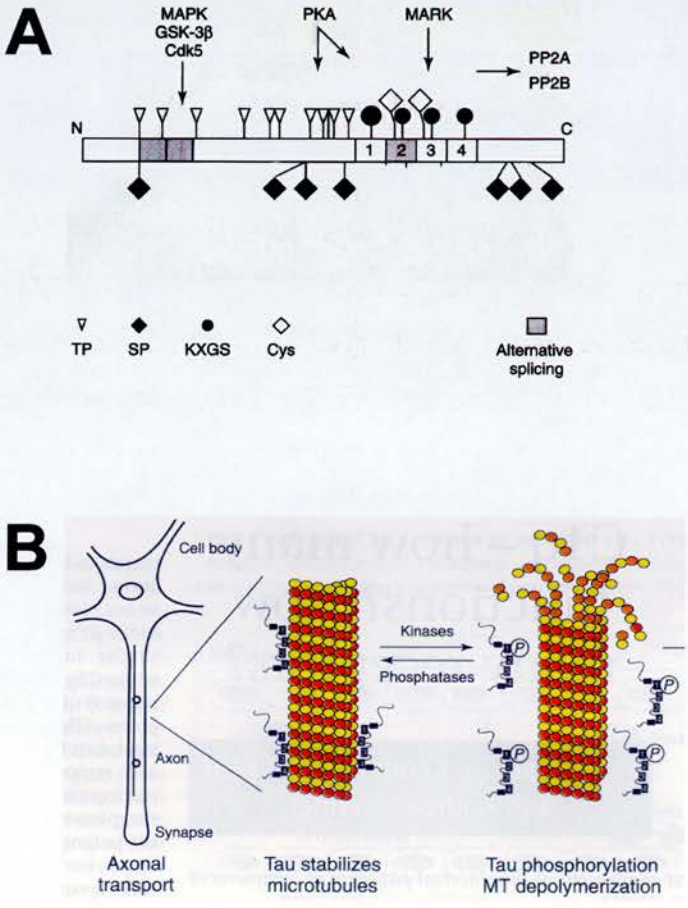

Subcellular localisation of tau protein

Tau protein has been described as an 'axonal' protein. The tau mRNA contains sequence elements which result in trafficking to the axon where translation takes place and tau protein is preferentially sorted into axons (Litman et al., 1994, Litman et al., 1996, Kanai and Hirokawa, 1995, Hirokawa et al., 1996). Tau is however found in other cellular compartments and the assignment 'axonal protein' may partly be attributed to use of the antibody 'Tau-1' which recognises a dephosphorylated tau site and which does predominantly label axons. Antibodies recognising other forms of tau label non-axonal parts of the cell and ectopically expressed tau is found in the somatodendritic as well as the axonal compartment (Buee et al., 2000, Brion et al., 1999, Ishihara et al., 1999, Spittaels et al., 1999, and Gotz et al., 1995, Pratt et al., 2000a).

Tau and microtubules

One function of tau is as a microtubule associated protein (MAP) which binds to microtubules and stabilises and promotes microtubule assembly. Protein structure and function studies have mapped these activities to the carboxyl terminal 'Microtubule Binding Domain' (Fig. 1.8). The highly conserved 18-amino acid sequence within the 31 or 32 amino acid repeat binds to the microtubules through a flexible array of distributed weak sites (Butner and Kirschner, 1991). The KKVAVVR sequence found in the proline rich region also contributes to microtubule binding. Tau also has been implicated in assembly and stabilisation of microtubules. The 4R isoform is more efficient at promoting microtubule assembly than the 3R isoform in vitro and this has been attributed to the 4R specific KVQIINKK sequence between repeats 1 and 2. Overall the 4R isoform binds to microtubules 40-fold more strongly than the 3R isoform. The N-terminal region of tau, the 'Projection Domain' comprises an 'Acidic Region' and a 'Proline rich' region (Fig. 1.8). Different isoforms contain an insert of 0,

29 or 58 amino acids. The projection domain is involved in determining the properties of the microtubules themselves by determining the spacing between microtubules which in turn will influence process properties such as diameter (Chen et al., 1992). This notion is supported by the observation that a tau isoform called 'big-tau', which has a large projection domain, is expressed in peripheral neurons with long axons of large diameter.

Tau phosphorylation control

The tau protein contains numerous targets for a variety of kinases and phosphatases (Fig. 1.9A) and one role of phosphorylation is to modulate the affinity of tau for microtubules (Fig. 1.9B). This control is complex with some of the phosphorylation sites having a greater impact on microtubule binding than others. Phosphorylation is subject to developmental regulation and to cell-cycle regulation. Phosphorylation is likely to be involved in regulating roles of tau not directly involved in microtubule binding (Buee et al., 2000, Mandelkow and Mandelkow, 1998, Spillantini and Goedert, 1998).

Phosphorylation is a developmentally regulated process with phosphorylation levels being higher during foetal development than at later stages. Tau phosphorylation also varies with the cell cycle (Preuss and Mandelkow, 1998, Mills et al., 1998). Tau remains in a low state of phosphorylation in interphase cells but becoming highly phosphorylated during mitosis leading to the suggestion that Alzheimer's Disease tau hyperphosphorylation pathology may reflect inappropriate activation of regeneration machinery in affected neurons (Preuss and Mandelkow, 1998).

Tau phosphorylation: sites and enzymes

Proline directed protein kinases (PDPK) phosphorylate serine or threonine residues at Ser-Pro (SP) or Thr-Pro (TP) motifs. The majority (but not all) of the tau phosphorylation sites fall into this category including phosphorylation by mitogen activated protein kinase (MAPK), glycogen synthase kinase 3 (GSK3), tau-tubulin kinase, and cyclin dependent kinases including cdc2 and cdc5. Non ser/Thr-Pro sites can be phosphorylated by kinases including microtubule affinity regulating kinase (MARK), Ca^{2+} /Calmodulin dependent protein kinase II (CaMPK II), cyclic-AMP-dependent kinase (PKA), and casein kinase II. Tau phosphorylation by the above kinases is modulated by the activity of phosphatases including Ser/Thr phosphatase proteins 1, 2A and 2B. The greater the phosphorylation of tau, the lower its affinity for microtubules (with a corresponding reduction in its microtubule stabilising activity) although GSK3, Cdk5, and MAP kinase phosphorylation have a smaller influence on microtubule binding than MARK phosphorylation which causes tau to dissociate completely (Buee et al., 2000, Mandelkow & Mandelkow, 1998, Spillantini and Goedert, 1998, Fig. 1.9).

Interactions between tau and proteins other than microtubules

Tau binds to microtubules with its C-terminal 'Microtubule Binding Domain' portion leaving the N-terminus 'Projection Domain' to project and potentially interact with other proteins (Fig. 1.8). A number of other roles have been proposed for the projection domain including binding to cytoskeletal proteins such as spectrin and actin filaments and interaction with the plasma membrane and cytoplasmic organelles. The interaction with the plasma membrane may be mediated by a PXXP motif located within the proline rich region which has SH3 domain binding activity, this may interact with the SH3 domains of proteins such as fyn (a src-family non-receptor tyrosine kinase) and phospholipase-C γ (PLC- γ). Colocalisation experiments have suggested that this is the

case and this would allow for a role for tau in signal transduction pathways. The tau-fyn complexes might modulate the actin cytoskeleton via the src-family tyrosine kinase signalling pathway and the tau- PLC- γ interaction would allow a role for tau in the PLC- γ signalling pathway (Buee et al., 2000).

Implications of manipulating tau protein expression in transgenic mice

Tau protein is implicated in major human neuropathological disorders including Alzheimers disease, in which hyperphosphorylated tau forms tangles. Mutations in the human tau gene have been linked to neuropathological disorders. The precise mechanism, if any, by which wild-type tau can precipitate neurodegeneration remains unknown and it may be that mutant rather than wild-type isoforms of tau have this activity. Tau protein is a target for protein kinases and phosphatases involved in a range of signal transduction pathways, and has a key role in defining the properties of axons (Lee and Trojanowski, 1999, Buee et al., 2000, Mandelkow and Mandelkow, 1998, Spillantini and Goedert, 1998). The balance of tau may therefore be delicately poised and interference with tau might be expected to have catastrophic consequences. The viability of several lines of transgenic mice in which tau levels have been manipulated suggest this is not the case (below).

Tau knockout mice

Mice in which the tau gene has been knocked out by homologous recombination appear to be relatively normal with only a minor defect in a subset of axons (Harada et al., 1994) although delayed maturation of hippocampal neurons was recently demonstrated in another tau knockout line (Dawson et al., 2001). The survival of the knockout animals could be explained by redundancy or compensation, and it has been suggested that increased levels of another microtubule associated protein, MAP1A, in tau knockout mice may compensate for loss of tau function (Harada et al., 1994).

Tau overexpressing mice

Transgenic mice ectopically expressing tau do not necessarily suffer any ill effects. It might be that the level of tau protein is relatively unimportant. Tight post-translational control (for example by phosphorylation or degradation) of tau might maintain the pool of 'active' tau at the same level regardless of how much tau the cell is producing. It appears from these reports that the ratio of transgenic to endogenous tau protein is less than that for tau mRNA (Gotz et al., 1995, Brion et al., 1999). Although this could conceivably be a artefact of differential detection of endogenous and transgenic tau mRNA and protein it might reflect a cellular mechanism for controlling levels of tau protein.

Interpretation of the reports of transgenic mouse lines overexpressing tau is complicated because of differences in experimental method and interpretation. There are, however, some features which are consistent between the studies reported so far (Probst et al., 2000, Brion et al., 1999, Ishihara et al., 1999, Spittaels et al., 1999, and Gotz et al., 1995). The aim of these was to generate animal models which would recapitulate the pathology seen in neurological disorders such as Alzheimer's disease by overexpressing tau protein in transgenic mice (Lee and Trojanowski et al., 1999). The

studies differed in whether the four repeat (Probst et al., 2000, Gotz et al., 1995, Spittaels et al., 1999) or three repeat (Brion et al., 1999, Ishihara et al., 1999) isoform of tau was used. The subset of neurons in which transgenic tau was expressed also differ reflecting the use of different promoters including the Thy-1 promoter (Probst et al., 2000, Gotz et al., 1995, Spittaels et al., 1999), the PrP promoter (Ishihara et al., 1999), and the HMGCR promoter (Brion et al., 1999) and position effects associated with the site of transgene insertion. In all cases subsets of neurons expressed transgenic tau protein showed some features of tau pathology (notably somatodendritic localisation and phosphorylation status) but this did not necessarily appear to adversely affect the transgenic animals (Gotz et al., 1995, Brion et al., 1999). In the lines where adverse effects were reported (Spittaels et al., 1999, Ishihara et al., 1999, Probst et al., 2000) it appeared that these effects were of increasing severity with increased doses of tau protein. The adverse effects included death in utero (observed for animals homozygous for a high level expression tau transgene), and a panel of sensorimotor defects, and axon degeneration. These effects were progressive in nature and the consequences became more pronounced in aged mice.

The relationship between tau protein and neurodegeneration is yet to be resolved and is not the main focus for this thesis. It does however appear that transgenic mice are reasonably robust to experimental manipulation of the levels of tau protein.

Ectopically expressed tau efficiently labels axons

Tau is a good candidate for tagging reporter molecules and causing them to be localised to axons. As discussed above, LacZ does not freely diffuse throughout the cell and so does not label axons well. This is a problem if the aim of an experiment is to visualise the axons of a LacZ labelled cell. Fusion of LacZ to tau generates a molecule which efficiently labels axons in flies (Callahan & Thomas, 1994) and transgenic mice

(Mombaerts et al., 1996) and the same is also true for tau-GFP fusions (Rodriguez et al., 1999, Pratt et al., 2000a,b). This labelling does not appear to disrupt the trajectory of axons formed by expressing cells as demonstrated by expressing tau fusion proteins in neurons of the highly characterised olfactory (Mombaerts et al., 1996, Rodriguez et al., 1999) and thalamocortical (Pratt et al., 2000b) fibre tract systems.

Although GFP is more diffusable than LacZ and does appear to be able to label axons to some extent (Feng et al., 2000), tau tagging of GFP improves the quality of axonal labelling (Rohm et al., 2000, Chapter 2).

Summary of following chapters

In Chapter 1 I have explained that one way to obtain a deeper understanding of the mechanisms by which the transcription factor Pax6 influences the development of the thalamocortical tract is to isolate *Pax6*$^{+/+}$ and *Pax6*$^{-/-}$ structures and test their participation in thalamocortical tract projection individually. This type of experiment demands that thalamic axons can be detected as they navigate through target tissues. I discuss using a tau tagged green fluorescent protein (tau-GFP) reporter transgene as an axonal label and considerations involved in generating transgenic mice ubiquitously expressing this reporter. These mice can then be used as a source of tau-GFP labelled cells and tissues, including dorsal thalamus.

Chapter 2

I describe the generation of tau-GFP expressing embryonic stem cells and two lines of transgenic mice. The consequences of transgene dosage on growth and viability are also examined.

Chapter 3

I describe the characterisation of tau-GFP expression in these transgenic lines and establish that all cells in the developing brain, including the dorsal thalamus, express tau-GFP at the time of thalamocortical tract formation in one line (TgTP6.3) but not in the other line (TgTP6.4). I show that tau-GFP efficiently labels microtubule containing structures including.axons and the mitotic machinery.

Chapter 4

I describe 'proof of concept' experiments in which TgTP6.3 embryos are used as a source of cells for cell mixing experiments. These demonstrate that tau-GFP labelled cells and axons can readily be distinguished against a background of unlabelled cells and axons in chimeras and in several neural culture paradigms.

Chapter 5

I investigate the requirement for the transcription factor Pax6 in the dorsal thalamus for the development of the thalamocortical tract. I show that in vitro, explants of tau-GFP labelled dorsal thalamus project axons that respond appropriately to target tissues encountered by the thalamocortical tract but that dorsal thalamus isolated from $Pax6^{Sey/Sey}$ embryos which lack Pax6 function do not. These experiments demonstrate an autonomous requirement for Pax6 in the dorsal thalamus for thalamocortical tract projection. Finally, I propose further experiments to address some of the questions raised by this work.

CHAPTER 2

GENERATION OF EMBRYONIC STEM CELLS AND TRANSGENIC MICE EXPRESSING A TAU TAGGED GREEN FLUORESCENT PROTEIN

SUMMARY

Chapter 2 describes the generation of lines of transgenic ES cells and mice expressing a tau tagged GFP transgene and observations on the consequences of transgene expression.

First I wanted to assess the properties of tau-GFP fusion proteins as fluorescent markers when inserted into the mammalian expression vector pCAGiP. Fusion cDNAs comprising tau cDNA coding sequences fused in frame at their 5' or 3' ends to GFP cDNA coding sequences were inserted into pCAGiP to generate pTP3 and pTP6 respectively. These constructs expressed fusion proteins in which tau was tagged at its amino terminus (GFP-tau expressed from pTP3) or its carboxyl terminus (tau-GFP expressed from pTP6) with GFP when introduced into mammalian cells. The properties of these fusion proteins were compared to each other and to untagged GFP (plasmid pTP5). This showed that tau-GFP and GFP-tau exhibited similar labelling properties in HEK293 cells and in ES cells before and after differentiation into neurons with processes being well labelled and with the label being excluded from the interphase nucleus. Neither tau-GFP fusion showed decreased fluorescence compared to untagged GFP and although untagged GFP did label processes in neurons derived from ES cells, it was less easy to detect these processes than when they were labelled with either tau tagged GFP. I concluded that both fusions offered sufficient advantages over untagged GFP to merit their use as a marker in the transgenic mice for use in the experiments described in Chapter 5.

The expression construct pTP6 was then introduced into ES cells and transgenic lines assessed for their suitability in generating transgenic mice according to their tau-GFP fluorescence in ES cells before and after differentiation into neurons. No major differences were observed between the lines tested. Three tau-GFP expressing ES lines were selected for the generation of transgenic mice resulting in two lines of transgenic mice (TgTP6.3 and TgTP6.4) and the consequences of transgene expression in these two lines was evaluated. Characterisation of the expression of tau-GFP in these lines and their application in a variety of experiments is described in the following chapters.

INTRODUCTION

As described in Chapter 1, there are several methodologies for the production of transgenic animals. My aim was to generate transgenic mice expressing a tau-GFP transgene ubiquitously for use in experiments such as those described in Chapters 4 and 5. Using gene targeting was an unattractive option as this approach would involve detailed and time consuming identification and characterisation of a ubiquitously expressed gene (see Chapter 1). A more attractive approach was to use a promoter that conferred ubiquitous expression in transgenic mice. The CAG promoter is constructed from the human cytomegalovirus immediate early enhancer (HCMVIEE) coupled to the chicken β-actin promoter and first intron (CBA) to drive transgene expression. This promoter was designed to be active in a wide variety of mammalian cell types when introduced as a random integration event (Niwa et al., 1991) and has subsequently proved to be able to drive widespread transgene expression in transgenic mice (Okabe et al., 1997, Hadjantonakis et al., 1998, Pratt et al., 2000a, Kawamoto et al., 2000). The generation of an expression construct in which tau-GFP transgene expression is driven by the CAG promoter is more straightforward than the generation of gene targeting constructs. This approach does however suffer from the potential drawback that, as the

transgene is introduced into the genome as a random integration event, transgene expression will be influenced by unpredictable position effects.

The GFP variant I chose to use was 'mgfp6' (Siemerring et al., 1996, Zernicka-Goetz et al., 1996, Zernicka-Goetz et al., 1997). This GFP comprises several amino acid substitutions into the wild-type amino acid sequence which confer thermostability at 37°C and enhanced fluorescence as described in Chapter 1. I was primarily concerned with tau-GFP expression in neural structures (see Chapter 1). Tagging the GFP with tau protein was anticipated to improve the quality of labelling, particularly of axons, by anchoring GFP to the microtubule containing cytoskeleton as described in Chapter 1. A preliminary description of the labelling properties of tau-GFP is presented in this Chapter with a more detailed description in Chapter 3. The generation of transgenic mice via germline transmission of embryonic stem cells allows for the evaluation of transgenic ES cell lines before transgenic mice are generated. ES cells can be induced to differentiate into neurons in vitro allowing an assessment of neuronal labelling properties of tau-GFP fusions for various transgenic ES cell lines. For this reason the expression vector I used (pCAGiP) contained an internal ribosome entry site (IRES) (Mountford and Smith, 1995) coupling transgene expression to a puromycin resistance gene to facilitate isolation of ES clones stably transfected with the tau-GFP expression construct by virtue of their puromycin resistance

MATERIALS AND METHODS

Molecular biology materials and ES cell culture materials used in this Chapter are listed in Appendix A and B respectively. Chimeras for germline transmission were generated by Jenny Nichols. Data on growth and viability of transgenic mice gathered by Margaret Keighren and John West are presented in Appendix C. Confocal imaging was performed as described in Chapter 3.

Preparation of competent *E. coli*

Competent *E. coli* cells, strain DH5α were prepared by harvesting an exponentially proliferating DH5α culture grown in 500ml LB medium (absorption at 600nm (A_{600}) of 0.4-0.6 measured using a Jenway spectrophotometer). The cells were chilled on ice and washed twice by centrifugation at 2000g for 10 minutes at 4°C followed by resuspension in ice cold 50mM $CaCl_2$ and finally resuspended in 50ml of ice cold competent cell freezing mix (CCFM). Competent DH5α cells were stored as 0.5ml aliquots at -70^0C until use.

Transformation of *E. coli* with plasmid DNA

Competent DH5α cells were thawed on ice and an 100µl aliquot mixed with DNA (10 to 100 ng) in a 15ml vented universal tube on ice. After a further 30 minutes on ice the cells were heat shocked in a 42°C water bath for exactly 2 minutes. 2 volumes (100l) of LB medium was then added to the mixture which was then incubated at 37°C in a shaking incubator for 30 minutes to 1 hour. The cells were then plated on LB agar plates containing 50g/ml ampicillin and incubated overnight at 37°C until colonies were visible to the naked eye. Clones were then streaked onto fresh LB-agar plates and the resulting colonies expanded in liquid culture for plasmid DNA extraction. These volumes were adjusted as required to scale up or down the transformation.

Plasmid DNA

All plasmid DNA was propagated in the *E. coli* strain DH5α. Liquid cultures of DH5α were grown in LB medium and colonies were grown on LB-agar plates. Plasmids were characterised by restriction digest using appropriate restriction enzymes and the products visualised on ethidium bromide stained agarose gels (generally 1% agarose) following electrophoresis. Tau and GFP fusion sequences were confirmed by DNA sequencing. Unless otherwise stated, standard procedures (Sambrook et al., 1989) were used throughout for handling bacteria and plasmids and manufacturer's guidelines were followed for the use of kits and enzymes.

Glycerol stocks for cryopreservation of *E. coli*

For long term storage of bacterial clones, glycerol was added to liquid bacterial cultures to a final concentration of 15% and 0.5ml aliquots were stored at –70°C. Clones were recovered by streaking out onto fresh LB-agar plates containing 50μg/ml ampicillin.

DNA ligation

DNA fragments were ligated together using T4 DNA ligase according to the manufacturer's guidelines. Competent DH5α were transformed with the ligation reaction and recombinant plasmids recovered. In some cases DNA was modified by phosphorylation, dephosphorylation or blunt-ending prior to ligation. If required: oligonucleotides were phosphorylated in the presence of polynucleotide kinase; plasmid DNA was dephosphorylated using calf intestinal alkaline phosphatase; DNA fragments with 5' overhangs were blunt ended using Sequenase.

DNA site directed mutagenesis

Site directed mutagenesis was performed essentially as described for the QuikChange™ site directed Mutagenesis kit (Stratagene, 200518) to introduce a BspH1 site into pMGFP6. *Pfu* polymerase (2.5 units) was used to amplify pMGFP6 (50ng) using oligonucleotides GFPBSPH1.1 and GFPBSPH1.2 (125ng) in a reaction volume of 50µl. Following 30 seconds at 95°C the reaction was subjected to 14 cycles of 95°C for 30 seconds, 50°C for 1 minute and 68°C for 8 minutes in a thermal cycler. The reaction was then digested with the methylation sensitive restriction enzyme *Dpn1* to destroy the original DNA which was methylated at *Dpn1* sites by propagation in DH5α but not unmethylated DNA synthesised by *Pfu* polymerase. Competent DH5α were transformed with the reaction and resultant plasmids extracted and analysed.

DNA sequencing

Manual DNA sequencing was performed using the Sequenase 2.0 kit. A list of the sequencing primers used for sequencing tau GFP fusion constructs are listed in Appendix A. In some cases, plasmid DNA was sequenced commercially by MWG Biotech.

Mouse Genomic DNA extraction

Mouse tail tips (approx 0.5cm long) were digested overnight in 500µl tail tip lysis buffer (TTLB) containing 100µg/ml Proteinase K and then mixed with 500µl PCIA (phenol: chloroform: isoamyl alcohol 50:49:1) for 20 minutes, centrifuged at 16000g for 5 minutes and the upper aqueous layer removed to a fresh tube. A further 500µl PCIA was added to the recovered aqueous layer and the process repeated resulting in two rounds of PCIA extraction. DNA was precipitated by the addition of 1/10 volumes of sodium acetate pH5.5 and 2 volumes of 96% ethanol to the recovered

aqueous portion. The DNA was recovered, dried, and dissolved in 100l TE with shaking overnight at 37°C.

Southern blotting DNA

Blot preparation

Mouse tail tip DNA was digested with the appropriate restriction enzyme and separated on an 0.8% SeaKem LE agarose gel. Following staining with ethidium bromide and imaging on a transilluminator, the gel was treated with 0.25M HCl for 30 minutes, denatured in Southern denaturing solution for 1 hour and neutralised in Southern neutralising solution for 1 hour. The DNA was transferred to a positively charged nylon membrane by capillary action in 20xSSC overnight, rinsed in 3xSSC, crosslinked with ultraviolet light (1200mJ) and baked at 120°C for 30 minutes.

^{32}P labelled probe preparation and hybridisation

Plasmid DNA was digested with the appropriate restriction enzyme, subjected to agarose gel electrophoresis, and the desired fragment identified and extracted from the gel. The HiPrime Kit (Roche) was used to produce ^{32}P labelled probe from this DNA fragment using random hexanucleotide priming. The probe was hybridised to the nylon filter in Church solution at 65°C overnight. After washing twice in Church wash at 65°C the filter was exposed to X-ray film at –70°C which was developed after an appropriate time using an automatic X-ray developer (Amersham).

Expression vector construction

pTP5 (untagged GFP)

pMGFP6 (a gift from J. Haseloff, Fig. 2.1A) was digested with *Kpn1* and *Sac1* and the 0.8kb fragment containing mgfp6 sequence extracted after agarose gel electrophoresis and the ends blunted using Sequenase2.0. *BstX1* oligonucleotide linkers BST-P1 and BST-P2 were phosphorylated using polynucleotide kinase, annealed, and ligated to the blunt-ends of mgfp6 prior to ligation into *BstX1* digested pCAGGS-BstX1(+SVori) (Fig. 2.1D) as described by Aruffo et al., 1987. This plasmid was digested with *EcoR1* and the 0.8kb fragment containing mgfp6 sequence was ligated to *EcoR1* digested pCAGiP (a gift from I Chambers, Fig. 2.1E) to generate pTP5 (Fig. 2.2A).

pTP3 (GFP-tau fusion)

The *Sac1* site in pMGFP6 (a gift from J. Haseloff, Fig. 2.1A) 3' to mgfp6 sequence was converted to an *EcoR1* site by digestion with *Sac1*, dephosphorylation with calf intestinal alkaline phosphatase, and ligation to annealed SAC1/ECOR1 oligonucleotides which had been phosphorylated using polynucleotide kinase. A *BspH1* site was introduced into the 3' end of the MGFP6 sequence using the oligonucleotides GFPBSPH1.1 and GFPBSPH1.2 for *Pfu* polymerase PCR site directed mutagenesis. The resulting plasmid, pMGFP6.BSPH1 (which contains two *BspH1* sites in the pBluescript SK backbone in addition to the one I introduced into the mgfp6 sequence), was digested to completion with *EcoR1*, purified, subjected to partial digestion with *BspH1*, and the 3.5kb product recovered. A 1.3kb *Nco1/EcoR1* fragment of pEn2^{+}3^{+}1234 (a gift from G. Lee, Fig. 2.1C) containing human tau sequence htau40 was ligated into the 3.5kb *EcoR1/BspH1*(partial) pMGFP6.BSPH1 backbone to generate a 2.1kb in frame GFP-tau fusion sequence in pMGFP6CHTAU. Oligonucleotides

KPN1CAG and BSTX1CAG were phosphorylated with polynucleotide kinase and annealed to the 2.1kb *Kpn1* fragment of pMGFP6CHTAU containing the GFP-tau fusion sequence. Unbound oligonucleotide were removed using a Chromaspin-400 column (Clontech K1303-1) according to the manufacturers instructions and the 2.1kb fragment ligated into *BstX1* digested pCAGGS-BstX1(+SVori) (Fig. 2.1D) as above. This plasmid was digested with *EcoR1* and the 2.1kb fragment containing mgfp6chtau fusion sequence was ligated into *EcoR1* digested pCAGiP (a gift from I. Chambers, Fig. 2.1E) to generate pTP3 (Fig. 2.2B). The GFP-tau fusion cDNA sequence is shown in Fig. 2.3 A,B.

pTP6 (tau-GFP fusion)

The *Asp718* site in pMGFP6 (a gift from J. Haseloff, Fig. 2.1A) 5' to mgfp6 sequence was converted to a *BglII* site by digestion with *Asp718*, dephosphorylation with calf intestinal alkaline phosphatase, and ligation to annealed ASP718/BGL2 oligonucleotides which had been phosphorylated using polynucleotide kinase to generate pMGFP6.BGL2. The 0.7kb *Bgl2/Sac1* fragment of pMGFP6.BGL2 containing mgfp6 sequence was then inserted into the 4.2kb *BamH1/Sac1* fragment of ptauLacZ (Callahan and Thomas, 1994, Fig. 2.1B) to generate an in frame fusion between bovine tau and mgfp6 sequences in pBTAUNMGFP6. Oligonucleotides KPN1CAG, SAC1CAG, and BSTX1CAG were phosphorylated with polynucleotide kinase and annealed to the 2.1kb *Kpn1/Sac1* fragment of pBTAUNMGFP6 containing the tau-GFP fusion sequence. Unbound oligonucleotide were removed using a chromaspin-400 column (Clontech K1303-1) according to the manufacturers instructions and the 2.1kb fragment ligated into *BstX1* digested pCAGGS-BstX1(+SVori) (Fig. 2.1D) as above. This plasmid was digested with *EcoR1* and the 2.1kb fragment containing btaunmgfp6 fusion sequence was ligated into *EcoR1* digested pCAGiP (a gift from I. Chambers, Fig.

2.1E) to generate pTP6 (Fig. 2.2C). The tau-GFP fusion cDNA sequence is shown in Fig. 2.3 C,D.

Embryonic stem cell culture

Routine culturing of ES cells

All procedures were performed using sterile technique in a tissue culture area dedicated solely to the handling of germline competent ES cells. ES cells were cultured without a feeder layer as described by Smith (1991) without antibiotic in 10ml GMEM medium containing -mercaptoethanol and 10% foetal calf serum (GMEM+FCS) plus Leukemia Inhibitory Factor (LIF). Tissue culture flasks and plates were gelatinised by rinsing with a 0.1% solution of swine skin gelatin dissolved in PBS.

The ES cells were passaged every two to three days as they approached confluence. The protocol below describes passaging ES cells growing in a tissue culture flask with a $25cm^2$ growing area (T25 flask). These volumes and cell numbers were adjusted accordingly for larger or smaller cultures. Passage was accomplished by aspirating the medium, rinsing the cells with phosphate buffered saline (PBS), and adding 1ml of TVP (a 0.025% trypsin solution). The cells were incubated at 37°C until they started to detach from the substrate and the flask was tapped sharply on the bench to dislodge the cells. The trypsinisation was stopped by the addition of 5ml GMEMβ+FCS. The cells were further dissociated by triturating using a 5ml plastic pipette before centrifugation at 2000g for 3 minutes and resuspension of the cell pellet in 10ml GMEMβ+FCS+LIF. Cells were counted using a hemocytometer. A confluent T25 flask typically yielded $1x10^7$ cells. Approximately $1x10^6$ cells in 10 ml GMEMβ+FCS+LIF were returned to a fresh gelatinised T25 flask. Cells were cultured in a humidified incubator at 37°C with 5% CO_2 and all solutions and media were prewarmed to 37°C before use.

Freezing and Thawing ES cell clones

ES cells grown to confluence in a T25 were trypsinized as described above and resuspended in 8.5ml of GMEMβ+FCS+LIF to which 1ml dimethyl sulphoxide (DMSO) was slowly added. The cells were pelleted by centrifugation at 2000g for 3 minutes and gently resuspended in 1ml freezing mixture consisting of GMEMβ+FCS+LIF+10% DMSO (final concentration of $1x10^7$ cells/ml). Aliquots of 0.5ml were placed in cryo-tubes which were inserted into a polystyrene rack at -70°C overnight. The polystyrene packing ensured that the vials were cooled slowly enough to ensure good cryopreservation. The vials could then be stored indefinitely in the vapour phase of liquid nitrogen (-180°C) in a cryo-bank. These volumes were adjusted accordingly when freezing larger or smaller cultures.

ES cells were recovered by rapidly thawing the vials in a 37°C water bath and quickly transferring their contents to 9.5ml of warm GMEMβ+FCS+LIF. The cells were pelleted by centrifugation at 2000g, resuspended in 10ml GMEMβ+FCS+LIF to remove traces of DMSO, pelleted again, and resuspended in 4ml growth medium for culture in 6 well plates. In some cases thawing the cells into a smaller culture (for example a 12-well plate) facilitated recovery of clones. Clones were expanded by passage into successively larger cultures.

Retinoic acid induced neuronal differentiation of ES cells

The protocol used was a combination of the '-4/+4' protocols described by Bain et al., (1997) and Li et al., (1998) with minor modifications. Confluent ES cells growing in a T25 flask (approximately $1x10^7$ cells) were dissociated gently to generate small cell clumps rather than fully dissociated cells. This was achieved by reducing time of TVP treatment and the amount of triturating the cells were subjected to during resuspension.

The cells were then washed twice in 10ml GMEMβ+FCS to remove traces of LIF which would otherwise inhibit differentiation. The washed cells were resuspended in 10ml GMEMβ+FCS and transferred to a 9cm bacterial grade sterile dish (not tissue culture treated plastic). Under these conditions the ES cells aggregated to one another to form embryoid bodies (EBs). The EBs were agitated daily to discourage them from aggregating together or adhering to the bottom of the dish. Fresh medium was supplied every second day using a method that selectively enriched the culture for EBs while depleting un-aggregated cells and debris. This was accomplished by swirling the dish to concentrate the EBs in the centre and transferring them to a 30ml universal which was allowed to stand for 5 minutes allowing the EBs to settled to the bottom. The medium (mainly containing single cells and debris that had not sunk to the bottom) was then carefully aspirated off the EB pellet and replaced with fresh GMEMβ+FCS and the EBs transferred to a fresh 10cm dish. All trans retinoic acid (RA) was included in the medium from the fourth day in culture until the eighth day. The RA stock was diluted into growth medium to give a final concentration of 10^{-6}M.

After eight days the EBs were collected, rinsed twice in PBS and incubated with TVP at 37°C until cells could be seen detaching from the EBs. The digestion was stopped by addition of 5ml GMEMβ+FCS and the EBs further dissociated by pipetting up and down ten times with a 5ml plastic pipette. The partly dissociated EBs were allowed to stand for 5 minutes to allow undissociated clumps to fall to the bottom. The supernatant (containing dissociated cells) was carefully removed and the cells counted with a hemocytometer. The cells were pelleted and resuspended in DMEM/F12 medium containing N2 and B27 supplements to a final concentration of $3x10^5$ cells/ml.

The 'ES neurons' were cultured in Nunc 4 well dishes that had been treated with poly-D-Lysine (PDL) and Laminin. PDL in PBS (0.001%) was added to tissue culture plates for 15 minutes at room temperature and aspirated before washing three times with

PBS. Laminin in cold PBS (2g/ml) was then added to the tissue culture plates for 20 minutes and removed just prior to plating cells. Approximately $3x10^5$ cells were plated in each well in a volume of 1 ml. The dishes were returned to the incubator and cultured for 1 to 3 days until recognisable neuronal morphology became apparent.

Electroporation of ES cells

Preparation of DNA for electroporation

For each electroporation, 100g of $CsCl_2$ gradient purified plasmid DNA was linearised with an appropriate restriction enzyme in a 500µl volume. An aliquot was electrophoresed on an agarose gel to confirm that the digest had reached completion. The linearised plasmid was precipitated by addition of 50µl 3M Sodium Acetate pH5.5 and 1ml ethanol at –20°C followed by centrifugation at 16000g for 5 minutes to pellet the DNA. The DNA pellet was washed twice in 70% ethanol and transported to the ES cell culture area in 100% ethanol. Inside the tissue culture hood most of the ethanol was removed by aspiration and the remainder allowed to evaporate. These steps ensured the sterility of plasmid DNA solution prior to its introduction into ES cells. Once dry, the DNA was dissolved in 100µl PBS overnight at 4°C in a sealed tube (final concentration 1mg/ml). This step was necessary as the DNA dissolved slowly in PBS.

Preparation of ES cells for electroporation

ES cells were grown to near confluence in a $175cm^2$ (T175) gelatinised tissue culture flask in GMEMβ+FCS+LIF. The cells were fed by replacing the culture medium with fresh medium 3-4 hours before electroporation. The ES cells were then trypsinized, resuspended in growth medium, counted using a hemocytometer (a single T175 flask typically yielded $5x10^7$ cells), washed twice with PBS to remove traces of growth medium, and resuspended in ice cold PBS at a final density of $1.43x10^7$ cells/ml.

Selection of stable transfectants

DNA (100l at 1mg/ml) and ES cells (700μl containing $1x10^7$ cells) were transferred to a sterile ice cold electroporation cuvette with a plugged glass Pasteur pipette and mixed by gently pipetting up and down. The cuvette was placed in a Gene-Pulser II and electroporated at 0.8kV, 3μF with a time constant of 0.1s. The cells were then added to 20ml GMEMβ+FCS+LIF ($5x10^5$ cells/ml). Volumes of 1ml ($5x10^5$ cells) or 2ml ($1x10^6$ cells) were added to the required number of gelatinised 10cm diameter tissue culture dishes containing 10ml of prewarmed GMEMβ+FCS+LIF which had been prepared the previous day and stored in the incubator. Control plates containing the same numbers of cells which had not undergone electroporation were also set up. The plates were then returned to the incubator overnight. The medium was replaced with selection medium (GMEMβ+FCS+LIF containing 2μg/ml puromycin) about 40 hours after the electroporation. This was to allow time for expression of antibiotic resistance by transfected cells. Selection medium was replaced every two days until stably transfected puromycin resistant ES clones appeared.

Picking and expanding ES cell clones

Once ES cells were visible to the naked eye (typically after 10 to 12 days) their positions were marked on the underside of the dish. The medium was aspirated off, the cells rinsed twice with PBS and the clones left just covered with PBS. Individual clones were dislodged from the plate using a yellow pipette tip and transferred into 50µl TVP in a 96-well plate. After incubation at 37°C for 5 minutes the cells were dissociated by pipetting up and down six times and transferred to 2ml GMEMβ+FCS+LIF+Puromycin in a 24-well (ungelatinised) plate. As ES cells became confluent they were expanded by passaging into larger cultures.

Germline transmission of ES cells

ES cells were injected into C57BL/6 blastocysts and reintroduced into pseudo-pregnant females by Jenny Nichols (Edinburgh University) using standard procedures (Hogan et al., 1994). Chimeric offspring were identified by coat colour and test-crossed to wild type animals to establish germline transmission.

Mouse genetics

The E14Tg2a ES cell line used for germline transmission were derived from 129/Ola strain (Hooper et al., 1987) so the initial genotype of the TgTP6.3 and TgTP6.4 transgenic mice was 129/Ola. Animals used throughout this study were derived by backcross breeding onto outbred CD1 background (Banton and Kingman, UK) and inbred C57BL/6 background (Banton and Kingman, UK). The results reported here used animals which had been back-crossed for four or less generations so represent TgTP6.3 and TgTP6.4 alleles on mixed 129/Ola, C57BL/6, and CD1 background.

Quantifying GFP fluorescence by FACS

ES cells were dissociated as for passage, resuspended in PBS containing 1% Bovine Serum Albumin (BSA), and green fluorescence profiles obtained using fluorescence activated cell sorter (Becton Dickinson, Rutherford, NJ) operated by Andrew Sanderson (Edinburgh University)

RESULTS

Construction of expression vectors

The expression constructs pTP3 (Fig. 2.2B), pTP5 (Fig. 2.2A) and pTP6 (Fig. 2.2C) consisted of a GFP-tau (Fig 2.3 A,B), untagged GFP, or tau-GFP (Fig. 2.3 C,D) cDNA sequences inserted between the *EcoR1* sites of pCAGiP (Fig. 2.1 E) respectively. The GFP variant used for all these experiments was mgfp6 (Siemering et al., 1996, Zernika-Goetz et al., 1996, Zernika-Goetz et al., 1997) as this version has enhanced fluorescence and thermostability at 37°C compared to wild-type GFP (see Chapter 1).

The tau-GFP fusion in pTP6 was made using a bovine tau clone extracted from a tau-LacZ fusion plasmid ptau-LacZ which successfully labelled axons in fruitfly (Callahan & Thomas, 1994) and transgenic mice (Mombaerts et al., 1996) using a *BamH1* site at the junction between tau and LacZ sequences. This *BamH1* site was ligated to a *Bgl2* site which I introduced into the 5' end of the mmgfp6 clone by ligating an oligonucleotide containing a *Bgl2* site into the *Asp718* site of the mgfp6 plasmid. This generated an in frame fusion.

The GFP-tau fusion in pTP3 was made using a human tau clone (htau40) which had an *Nco1* site engineered into its start ATG codon (a kind gift from G. Lee). This

Figure 2.1

Plasmids used in this study. (A to D) Simplified plasmid maps showing the plasmids used as starting materials. GFP, tau, and LacZ coding sequences are indicated by green, red, and blue arrows respectively. (A) pMGFP6 from which MGFP6 coding sequence was obtained, (B) ptauLacZ from which bovine tau coding sequence was obtained, (C) pEn2+3+1234 from which human tau coding sequences were obtained, (D) pPHCAGGS-BstX1(+Svori) and (E) Mammalian 'CAG promoter' expression vector pCAGiPuro. 'CAG promoter' expression is driven by human cytomegalovirus immediate early enhancer (HMVCIEE) coupled to chick β-actin promoter and first intron (CBA promoter) with bovine growth hormone polyadenylation signal (bGHpA). The cDNA to be expressed is inserted between *EcoR1* sites. The internal ribosome entry site (IRES) between the inserted cDNA and the puromycin resistance gene (Puro) allows expression of both from the same bicistronic transcript. pMGFP6, ptauLacZ, pPHCAGGS-BstX1(+Svori) and pCAGiPuro are pBluescript SK (Stratagene) derivatives and pEn2+3+1234 is a pECE derivative. All plasmids confer ampicillin resistance to bacteria.

Figure 2.1

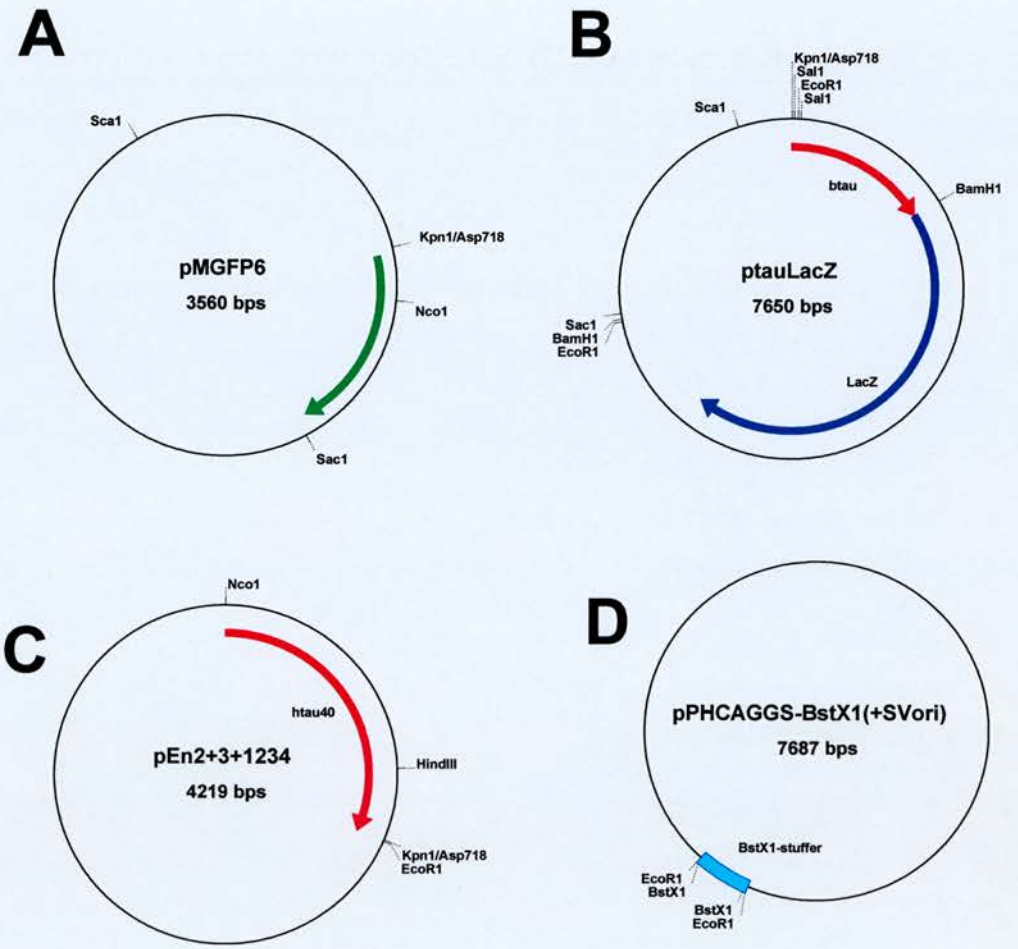
A
Sca1
Kpn1/Asp718
pMGFP6
3560 bps
Nco1
Sac1
B
Kpn1/Asp718
Sal1
EcoR1
Sal1
Sca1
btau
BamH1
ptauLacZ
7650 bps
Sac1
BamH1
EcoR1
LacZ
C
Nco1
htau40
pEn2+3+1234
4219 bps
HindIII
Kpn1/Asp718
EcoR1
D
pPHCAGGS-BstX1(+SVori)
7687 bps
BstX1-stuffer
EcoR1
BstX1
BstX1
EcoR1

E

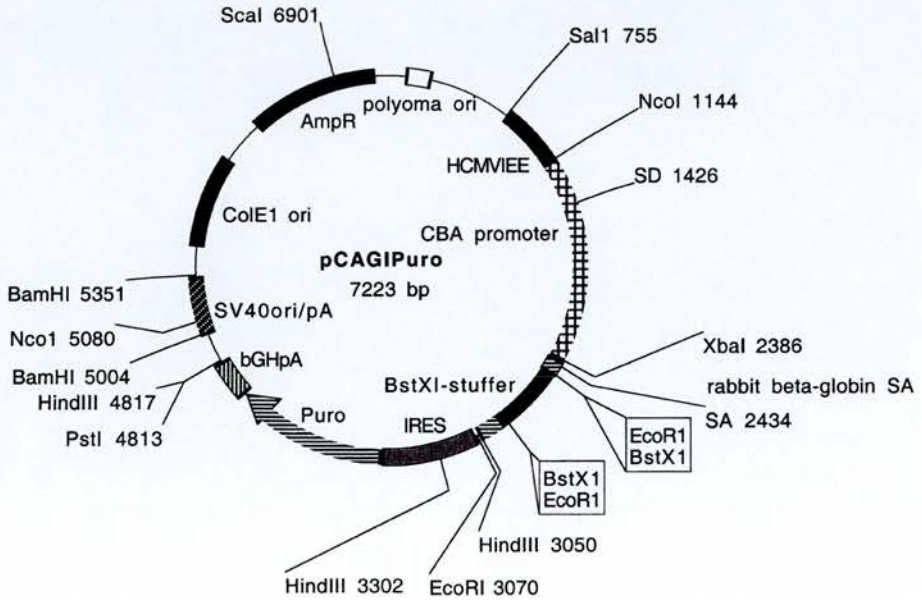
ScaI 6901
SalI 755
NcoI 1144
polyoma ori
AmpR
HCMVIEE
SD 1426
ColE1 ori
CBA promoter
pCAGIPuro
7223 bp
BamHI 5351
SV40ori/pA
Nco1 5080
XbaI 2386
bGHpA
BamHI 5004
BstXI-stuffer
rabbit beta-globin SA
HindIII 4817
Puro
IRES
SA 2434
PstI 4813
EcoR1
BstX1
BstX1
EcoR1
HindIII 3050
HindIII 3302
EcoRI 3070

Figure 2.2

Plasmid maps of GFP and tau tagged GFP expression vectors generated during this study. (A) pTP5 in which mgfp6 cDNA is inserted into pCAGiP. (B) pTP3 in which mgfp6-htau40 fusion cDNA is inserted into pCAGiP. (C) pTP6 in which btau-mgfp6 fusion cDNA is inserted into pCAGiP.

Figure 2.2

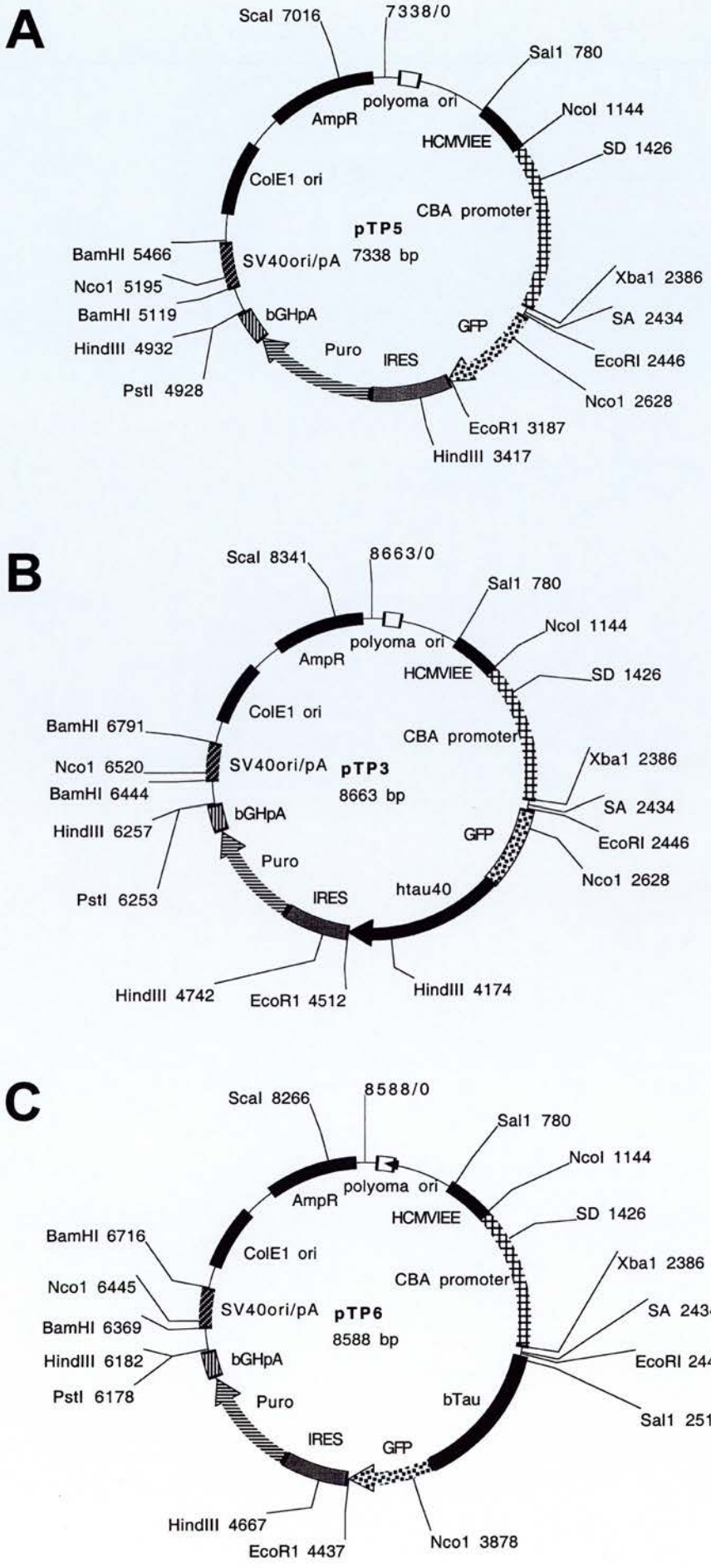
A
ScaI 7016
7338/0
SalI 780
polyoma ori
AmpR
NcoI 1144
HCMVIEE
SD 1426
ColE1 ori
CBA promoter
pTP5
7338 bp
BamHI 5466
SV40ori/pA
Nco1 5195
BamHI 5119
bGHpA
Xba1 2386
SA 2434
GFP
HindIII 4932
Puro
IRES
EcoRI 2446
PstI 4928
Nco1 2628
EcoR1 3187
HindIII 3417
B
ScaI 8341
8663/0
SalI 780
polyoma ori
NcoI 1144
AmpR
HCMVIEE
SD 1426
ColE1 ori
BamHI 6791
CBA promoter
Nco1 6520
SV40ori/pA
pTP3
Xba1 2386
BamHI 6444
8663 bp
SA 2434
bGHpA
HindIII 6257
GFP
EcoRI 2446
Puro
Nco1 2628
PstI 6253
IRES
htau40
HindIII 4742
EcoR1 4512
HindIII 4174
C
ScaI 8266
8588/0
SalI 780
polyoma ori
NcoI 1144
AmpR
HCMVIEE
SD 1426
BamHI 6716
ColE1 ori
Xba1 2386
CBA promoter
Nco1 6445
SV40ori/pA
pTP6
SA 2434
BamHI 6369
8588 bp
HindIII 6182
bGHpA
EcoRI 2446
PstI 6178
Puro
bTau
SalI 2516
IRES
GFP
HindIII 4667
EcoR1 4437
Nco1 3878

Figure 2.3

Tau tagged GFP fusion genes generated during this study. (A,C) show schematics of (A) GFP-tau and (C) tau-GFP fusion cDNAs with restriction sites used for mapping marked (mgfp6 sequence coloured green and tau sequence coloured red). Scale in base pairs (bp). (B,D) Nucleotide and amino acid sequences of (B) GFP-tau and (D) tau-GFP fusion proteins. Nucleotide sequences (upper) are numbered and amino acid sequences (lower) are shown using single letter code. MGFP6 amino acids are coloured green with substitutions to wild-type GFP sequence resulting in improved thermostability and fluorescence bold and underlined. (B) human and (D) bovine tau amino acid sequences are coloured red with the four microtubules binding repeats bold and underlined.

Figure 2.3

A

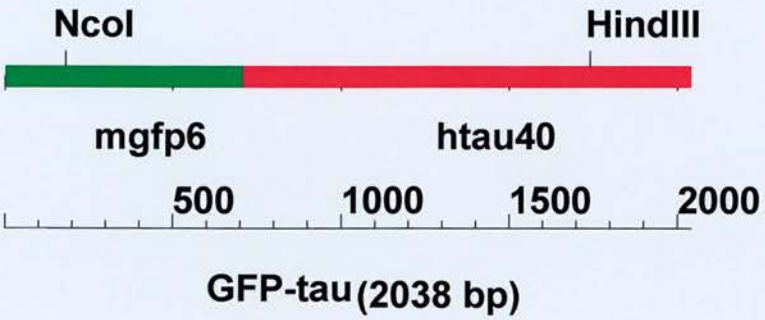

B

GFPtau

```
      GGTACCGGTAGAAAAAATGAGTAAAGGAGAAGAACTTTTCACTGGAGTTGTCCCAATTCT
    1 ---------+---------+---------+---------+---------+---------+ 60
                       M  S  K  G  E  E  L  F  T  G  V  V  P  I  L
      TGTTGAATTAGATGGTGATGTTAATGGGCACAAATTTTCTGTCAGTGGAGAGGGTGAAGG
   61 ---------+---------+---------+---------+---------+---------+ 120
        V  E  L  D  G  D  V  N  G  H  K  F  S  V  S  G  E  G  E  G
      TGATGCAACATACGGAAAACTTACCCTTAAATTTATTTGCACTACTGGAAAACTACCTGT
  121 ---------+---------+---------+---------+---------+---------+ 180
        D  A  T  Y  G  K  L  T  L  K  F  I  C  T  T  G  K  L  P  V
      TCCATGGCCAACCCTGGTCACCACCCTGACCTACGGCGTGCAGTGCTTCTCCCGTTACCC
  181 ---------+---------+---------+---------+---------+---------+ 240
        P  W  P  T  L  V  T  T  L  T  Y  G  V  Q  C  F  S  R  Y  P
      TGATCATATGAAGCGGCACGACTTCTTCAAGAGCGCCATGCCTGAGGGATACGTGCAGGA
  241 ---------+---------+---------+---------+---------+---------+ 300
        D  H  M  K  R  H  D  F  F  K  S  A  M  P  E  G  Y  V  Q  E
      GAGGACCATCTTCTTCAAGGACGACGGGAACTACAAGACACGTGCTGAAGTCAAGTTTGA
  301 ---------+---------+---------+---------+---------+---------+ 360
        R  T  I  F  F  K  D  D  G  N  Y  K  T  R  A  E  V  K  F  E
      GGGAGACACCCTCGTCAACAGGATCGAGCTTAAGGGAATCGATTTCAAGGAGGACGGAAA
  361 ---------+---------+---------+---------+---------+---------+ 420
        G  D  T  L  V  N  R  I  E  L  K  G  I  D  F  K  E  D  G  N
      CATCCTCGGCCACAAGTTGGAATACAACTACAACTCCCACAACGTATACATCATGGCCGA
  421 ---------+---------+---------+---------+---------+---------+ 480
        I  L  G  H  K  L  E  Y  N  Y  N  S  H  N  V  Y  I  M  A  D
      CAAGCAAAAGAACGGCATCAAAGCCAACTTCAAGACCCGCCACAACATCGAAGACGGCGG
  481 ---------+---------+---------+---------+---------+---------+ 540
        K  Q  K  N  G  I  K  A  N  F  K  T  R  H  N  I  E  D  G  G
      CGTGCAACTCGCTGATCATTATCAACAAAATACTCCAATTGGCGATGGCCCTGTCCTTTT
  541 ---------+---------+---------+---------+---------+---------+ 600
        V  Q  L  A  D  H  Y  Q  Q  N  T  P  I  G  D  G  P  V  L  L
      ACCAGACAACCATTACCTGTCCACACAATCTGCCCTTTCGAAAGATCCCAACGAAAAGAG
  601 ---------+---------+---------+---------+---------+---------+ 660
        P  D  N  H  Y  L  S  T  Q  S  A  L  S  K  D  P  N  E  K  R
      AGACCACATGGTCCTTCTTGAGTTTGTAACAGCTGCTGGGATTACACATGTCATGGCTGA
  661 ---------+---------+---------+---------+---------+---------+ 720
           D  H  M  V  L  L  E  F  V  T  A  A  G  I  T  H  V  M  A  E
      GCCCCGCCAGGAGTTCGAAGTGATGGAAGATCACGTCGGGACGTACGGGTTGGGGGACAG
  721 ---------+---------+---------+---------+---------+---------+ 780
        P  R  Q  E  F  E  V  M  E  D  H  V  G  T  Y  G  L  G  D  R
      GAAAGATCAGGGGGGCTACACCATGCACCAAGACCAAGAGGGTGACACGGACGCTGGCCT
  781 ---------+---------+---------+---------+---------+---------+ 840
        K  D  Q  G  G  Y  T  M  H  Q  D  Q  E  G  D  T  D  A  G  L
      GAAAGAATCTCCCCTGCAGACCCCCACTGAGGACGGATCTGAGGAACCGGGCTCTGAAAC
  841 ---------+---------+---------+---------+---------+---------+ 900
        K  E  S  P  L  Q  T  P  T  E  D  G  S  E  E  P  G  S  E  T
      CTCTGATGCTAAGAGCACTCCAACAGCGGAAGATGTGACAGCACCCTTAGTGGATGAGGG
  901 ---------+---------+---------+---------+---------+---------+ 960
        S  D  A  K  S  T  P  T  A  E  D  V  T  A  P  L  V  D  E  G
      AGTCCCCGGCAAGCAGGCTGCCGCGCAGCCCCACACGGAGATCCCAGAAGGAACCACAGC
  961 ---------+---------+---------+---------+---------+---------+ 1020
        V  P  G  K  Q  A  A  A  Q  P  H  T  E  I  P  E  G  T  T  A
```

Figure 2.3...

B...


TGAAGAAGCAGGCATTGGAGACACCCCCAGCCTGGAAGACGAAGCTGCTGGTCACGTGAC
1021 1080
E E A G I G D T P S L E D E A A G H V T
CCAAGCTCGCATGGTCAGTAAAAGCAAAGACGGGACTGGAAGCGATGACAAAAAAGCCAA
1081 1140
Q A R M V S K S K D G T G S D D K K A K
GGGGGCTGATGGTAAAACGAAGATCGCCACACCGCGGGGAGCAGCCCCTCCAGGCCAGAA
1141 1200
G A D G K T K I A T P R G A A P P G Q K
GGGCCAGGCCAACGCCACCAGGATTCCAGCAAAAACCCCGCCCGCTCCAAAGACACCACC
1201 1260
G Q A N A T R I P A K T P P A P K T P P
CAGCTCTGGTGAACCTCCAAAATCAGGGGATCGCAGCGGCTACAGCAGCCCCGGCTCCCC
1261 1320
S S G E P P K S G D R S G Y S S P G S P
AGGCACTCCCGGCAGCCGCTCCCGCACCCCGTCCCTTCCAACCCCACCCACCCGGGAGCC
1321 1380
G T P G S R S R T P S L P T P P T R E P
CAAGAAGGTGGCAGTGGTCCGTACTCCACCCAAGTCGCCGTCTTCCGCCAAGAGCCGCCT
1381 1440
K K V A V V R T P P K S P S S A K S R L
GCAGACAGCCCCCGTGCCCATGCCAGACCTGAAGAATGTCAAGTCCAAGATCGGCTCCAC
1441 1500
Q T A P V P M P D L K N V K S K I G S T
TGAGAACCTGAAGCACCAGCCGGGAGGCGGGAAGGTGCAGATAATTAATAAGAAGCTGGA
1501 1560
E N L K H Q P G G G K V Q I I N K K L D
TCTTAGCAACGTCCAGTCCAAGTGTGGCTCAAAGGATAATATCAAACACGTCCCGGGAGG
1561 1620
L S N V Q S K C G S K D N I K H V P G G
CGGCAGTGTGCAAATAGTCTACAAACCAGTTGACCTGAGCAAGGTGACCTCCAAGTGTGG
1621 1680
G S V Q I V Y K P V D L S K V T S K C G
CTCATTAGGCAACATCCATCATAAACCAGGAGGTGGCCAGGTGGAAGTAAAATCTGAGAA
1681 1740
S L G N I H H K P G G G Q V E V K S E K
GCTTGACTTCAAGGACAGAGTCCAGTCGAAGATTGGGTCCCTGGACAATATCACCCACGT
1741 1800
L D F K D R V Q S K I G S L D N I T H V
CCCTGGCGGAGGAAATAAAAAGATTGAAACCCACAAGCTGACCTTCCGCGAGAACGCCAA
1801 1860
P G G G N K K I E T H K L T F R E N A K
AGCCAAGACAGACCACGGGGCGGAGATCGTGTACAAGTCGCCAGTGGTGTCTGGGGACAC
1861 1920
A K T D H G A E I V Y K S P V V S G D T
GTCTCCACGGCATCTCAGCAATGTCTCCTCCACCGGCAGCATCGACATGGTAGACTCGCC
1921 1980
S P R H L S N V S S T G S I D M V D S P
CCAGCTCGCCACGCTAGCTGACGAGGTGTCTGCCTCCCTGGCCAAGCAGGGTTTGTGA
1981 2038
Q L A T L A D E V S A S L A K Q G L *

Figure 2.3...

C

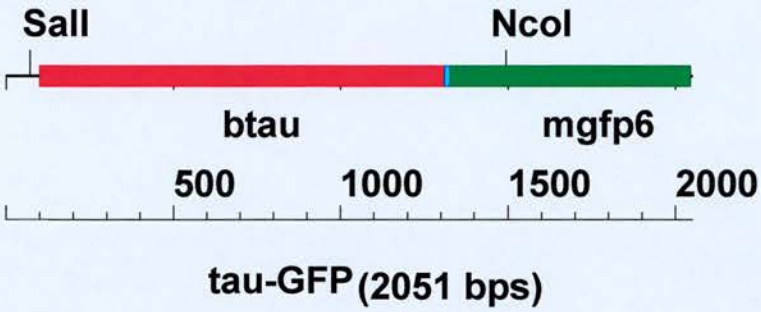

D

```
tau-GFP
       CGGCGCCCACCTTCTGCCGCCGCCACCACAGCCACTTTCTCCTCTGCCTCCCTCTACTGT
     1 ---------+---------+---------+---------+---------+---------+ 60

       CCTCGGCCCTCTGTCGACTATCAGGTGGGCCTTGAACCAGGATGGCTGAGCCCCGCCAGG
    61 ---------+---------+---------+---------+---------+---------+ 120
                                                 M  A  E  P  R  Q  E
       AGTTCGACGTGATGGAAGATCATGCTCAGGGGGACTACACCCTGCAAGACCAGGAGGGTG
   121 ---------+---------+---------+---------+---------+---------+ 180
         F  D  V  M  E  D  H  A  Q  G  D  Y  T  L  Q  D  Q  E  G  D
       ACATGGACCCCGGCCTGAAAGAGTCTCCCCTGCAGACCCCGGCCGATGATGGATCTGAGG
   181 ---------+---------+---------+---------+---------+---------+ 240
         M  D  P  G  L  K  E  S  P  L  Q  T  P  A  D  D  G  S  E  E

       AACCAGGCTCTGAAACCTCTGATGCTAAGAGCACTCCGACGGCGGAAGATGCGACAGCAC
   241 ---------+---------+---------+---------+---------+---------+ 300
         P  G  S  E  T  S  D  A  K  S  T  P  T  A  E  D  A  T  A  P
       CCTTAGTGGATGAGGGAGCCCCCGGTGAGCAGGCGGCCGCTCAGGCCCCCGCGGAGATCC
   301 ---------+---------+---------+---------+---------+---------+ 360
         L  V  D  E  G  A  P  G  E  Q  A  A  A  Q  A  P  A  E  I  P
       CAGAAGGAACCGCAGCTGAAGAAGCAGGCATTGGCGACACGTCCAACCTGGAAGACCAAG
   361 ---------+---------+---------+---------+---------+---------+ 420
         E  G  T  A  A  E  E  A  G  I  G  D  T  S  N  L  E  D  Q  A
       CTGCCGGACACGTGACCCAAGCTCGCATGGTCAGTAAAGGCAAAGATGGGACTGGACCCG
   421 ---------+---------+---------+---------+---------+---------+ 480
         A  G  H  V  T  Q  A  R  M  V  S  K  G  K  D  G  T  G  P  D
       ATGACAAAAAAACCAAGGGGGCGGATGGTAAGCCTGGAACGAAGATTGCCACACCCCGGG
   481 ---------+---------+---------+---------+---------+---------+ 540
         D  K  K  T  K  G  A  D  G  K  P  G  T  K  I  A  T  P  R  G
       GAGCAGCCCCTCCAGGCCAGAAAGGCCAGGCCAACGCCACCCGGATTCCAGCAAAAACCA
   541 ---------+---------+---------+---------+---------+---------+ 600
         A  A  P  P  G  Q  K  G  Q  A  N  A  T  R  I  P  A  K  T  T

       CTCCCACCCCGAAGACCTCGCCAGCAACCATGCAAGTGCAGAAAAAACCACCCCCTGCAG
   601 ---------+---------+---------+---------+---------+---------+ 660
         P  T  P  K  T  S  P  A  T  M  Q  V  Q  K  K  P  P  P  A  G
       GGGCAAAATCTGAGAGAGGTGAATCTGGGAAATCCGGGGACCGCAGCGGCTACAGCAGCC
   661 ---------+---------+---------+---------+---------+---------+ 720
         A  K  S  E  R  G  E  S  G  K  S  G  D  R  S  G  Y  S  S  P
       CCGGCTCCCCAGGCACTCCGGGCAGCCGCTCCCGCACACCCTCCCTGCCGACCCCGCCCA
   721 ---------+---------+---------+---------+---------+---------+ 780
         G  S  P  G  T  P  G  S  R  S  R  T  P  S  L  P  T  P  P  T
       CCCGGGAGCCCAAGAAGGTGGCGGTGGTCCGCACTCCCCCCAAGTCGCCGTCTGCAGCCA
   781 ---------+---------+---------+---------+---------+---------+ 840
         R  E  P  K  K  V  A  V  V  R  T  P  P  K  S  P  S  A  A  K
       AGAGCCGCCTGCAGGCCGCTCCCGGGCCCATGCCAGACCTGAAGAACGTCAAGTCCAAAA
   841 ---------+---------+---------+---------+---------+---------+ 900
         S  R  L  Q  A  A  P  G  P  M  P  D  L  K  N  V  K  S  K  I
       TCGGCTCCACGGAAAACCTGAAGCACCAGCCAGGAGGTGGCAAGGTGCAGATAATTAATA
   901 ---------+---------+---------+---------+---------+---------+ 960
         G  S  T  E  N  L  K  H  Q  P  G  G  G  K  V  Q  I  I  N  K
       AGAAGCTGGATCTTAGCAACGTCCAGTCCAAGTGTGGCTCAAAGGATAATATCAAACACG
   961 ---------+---------+---------+---------+---------+---------+ 1020
         K  L  D  L  S  N  V  Q  S  K  C  G  S  K  D  N  I  K  H  V
       TGCCAGGAGGCGGCAGTGTGCAAATAGTCTACAAACCAGTGGATCTGAGCAAGGTGACCT
  1021 ---------+---------+---------+---------+---------+---------+ 1080
         P  G  G  G  S  V  Q  I  V  Y  K  P  V  D  L  S  K  V  T  S
```

Figure 2.3...

D...

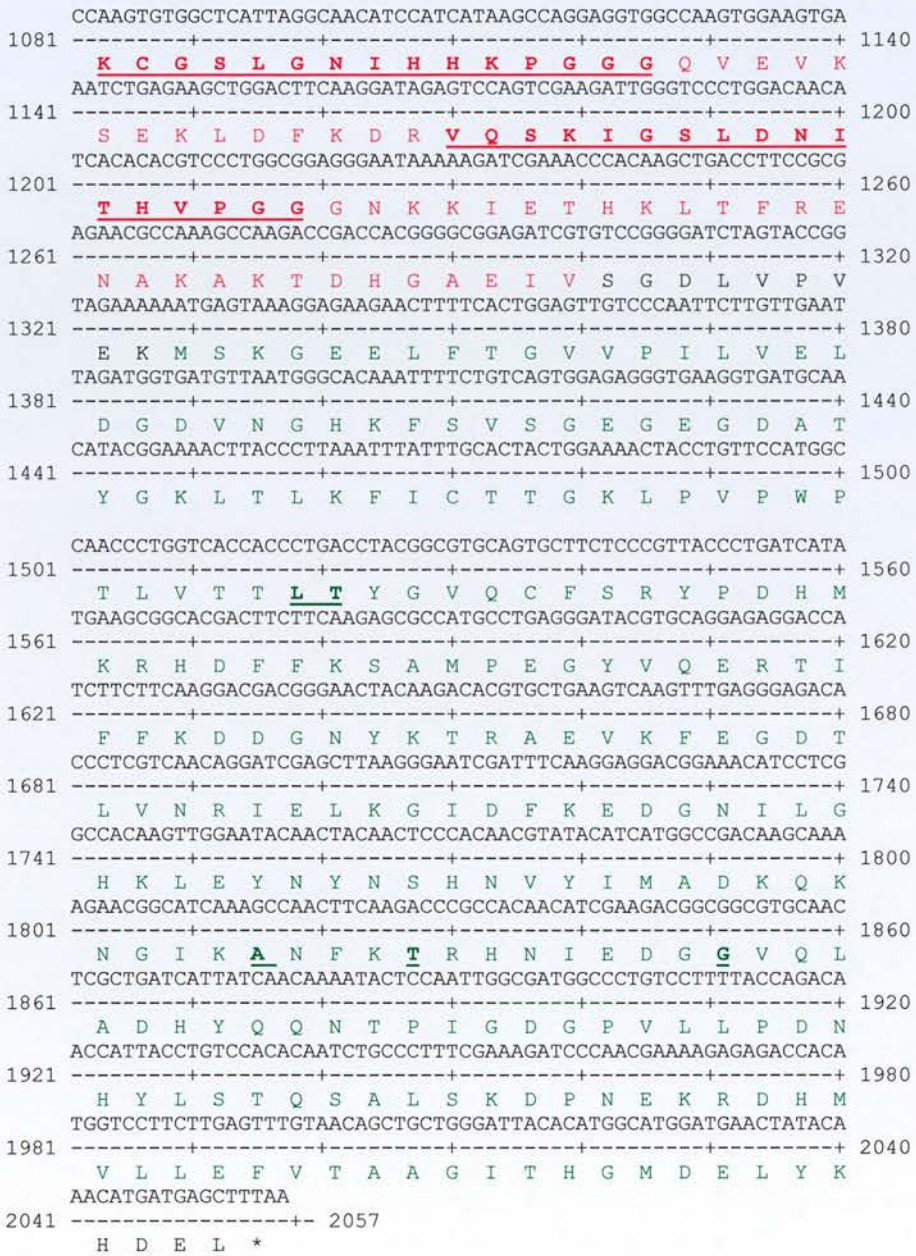
CCAAGTGTGGCTCATTAGGCAACATCCATCATAAGCCAGGAGGTGGCCAAGTGGAAGTGA
1081 1140
K C G S L G N I H H K P G G G Q V E V K
AATCTGAGAAGCTGGACTTCAAGGATAGAGTCCAGTCGAAGATTGGGTCCCTGGACAACA
1141 1200
S E K L D F K D R V Q S K I G S L D N I
TCACACACGTCCCTGGCGGAGGGAATAAAAAGATCGAAACCCACAAGCTGACCTTCCGCG
1201 1260
T H V P G G G N K K I E T H K L T F R E
AGAACGCCAAAGCCAAGACCGACCACGGGGCGGAGATCGTGTCCGGGGATCTAGTACCGG
1261 1320
N A K A K T D H G A E I V S G D L V P V
TAGAAAAAATGAGTAAAGGAGAAGAACTTTTCACTGGAGTTGTCCCAATTCTTGTTGAAT
1321 1380
E K M S K G E E L F T G V V P I L V E L
TAGATGGTGATGTTAATGGGCACAAATTTTCTGTCAGTGGAGAGGGTGAAGGTGATGCAA
1381 1440
D G D V N G H K F S V S G E G E G D A T
CATACGGAAAACTTACCCTTAAATTTATTTGCACTACTGGAAAACTACCTGTTCCATGGC
1441 1500
Y G K L T L K F I C T T G K L P V P W P
CAACCCTGGTCACCACCCTGACCTACGGCGTGCAGTGCTTCTCCCGTTACCCTGATCATA
1501 1560
T L V T T L T Y G V Q C F S R Y P D H M
TGAAGCGGCACGACTTCTTCAAGAGCGCCATGCCTGAGGGATACGTGCAGGAGAGGACCA
1561 1620
K R H D F F K S A M P E G Y V Q E R T I
TCTTCTTCAAGGACGACGGGAACTACAAGACACGTGCTGAAGTCAAGTTTGAGGGAGACA
1621 1680
F F K D D G N Y K T R A E V K F E G D T
CCCTCGTCAACAGGATCGAGCTTAAGGGAATCGATTTCAAGGAGGACGGAAACATCCTCG
1681 1740
L V N R I E L K G I D F K E D G N I L G
GCCACAAGTTGGAATACAACTACAACTCCCACAACGTATACATCATGGCCGACAAGCAAA
1741 1800
H K L E Y N Y N S H N V Y I M A D K Q K
AGAACGGCATCAAAGCCAACTTCAAGACCCGCCACAACATCGAAGACGGCGGCGTGCAAC
1801 1860
N G I K A N F K T R H N I E D G G V Q L
TCGCTGATCATTATCAACAAAATACTCCAATTGGCGATGGCCCTGTCCTTTACCAGACA
1861 1920
A D H Y Q Q N T P I G D G P V L L P D N
ACCATTACCTGTCCACACAATCTGCCCTTTCGAAAGATCCCAACGAAAAGAGAGACCACA
1921 1980
H Y L S T Q S A L S K D P N E K R D H M
TGGTCCTTCTTGAGTTTGTAACAGCTGCTGGGATTACACATGGCATGGATGAACTATACA
1981 2040
V L L E F V T A A G I T H G M D E L Y K
AACATGATGAGCTTTAA
2041 2057
H D E L *

Figure 2.4

Ethidium bromide stained agarose gels showing restriction digests of (A) pCAGiP, (B) pTP5, (C) pTP3 and (D) pTP6: *EcoR1* (lane 1), *Nco1* (lane 2), *HindIII* (lane 3), *Sal1* (lane 4), *EcoR1* and *Nco1* (lane 5), *EcoR1* and *HindIII* (lane 6), *EcoR1* and *Sal1* (lane 7) and *Nco1* and *Sal1* (lane 8). *EcoR1* excises cDNAs inserted into pCAGiPuro (faint 0.8kb *EcoR1* fragment in (B) lane 1, 2.1kb *EcoR1* fragments in (C) lane 1 and (D) lane 1). The marker lane (M) contains 1kb ladder molecular weight marker (Gibco BRL: 10787-018) with fragment sizes in kb shown in A. Images are shown as inverse.

Figure 2.4

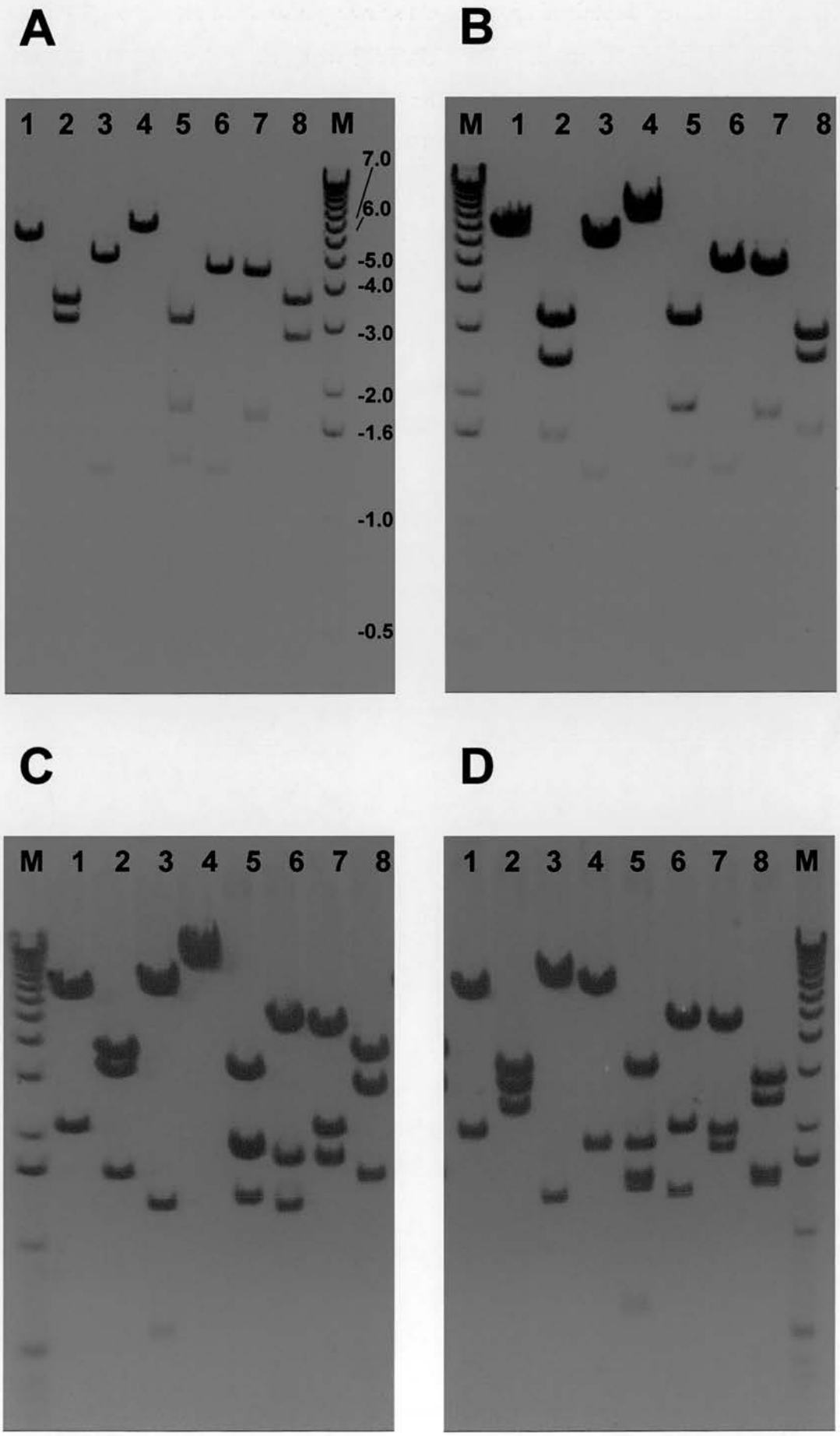
A
1 2 3 4 5 6 7 8 M
7.0
6.0
-5.0
-4.0
-3.0
-2.0
-1.6
-1.0
-0.5
B
M 1 2 3 4 5 6 7 8
C
M 1 2 3 4 5 6 7 8
D
1 2 3 4 5 6 7 8 M

was fused to a *BspH1* site which I introduced into the 3' end of the mgfp6 clone by site directed mutagenesis to generate an in frame fusion. Restriction digests of pCAGiP, pTP3, pTP5, and pTP6 are shown in Fig. 2.4.

Comparison of different tau-GFP fusions

Transient transfection of HEK293 cells with these constructs established that whereas the untagged GFP was distributed throughout the cell, the tau-GFP and GFP-tau fusions were excluded from the nucleus. These results are shown in Fig. 2.5. These experiments confirmed that the expression constructs were functional.

ES cells (Sox2 line, Li et al., 1998) were electroporated with pTP3, pTP5, and pTP6 which had been linearised with *Sca1* which cuts within the ampicillin resistance gene and puromycin resistant stably transfected clones were isolated and expanded for analysis. FACS profiles of proliferating ES cells grown in the presence of LIF were obtained for two independent clones for each plasmid (Fig. 2.5). These showed that clones transfected with all three constructs exhibited similar levels of GFP fluorescence. These ES cells were induced to differentiate into neurons by aggregating them into embryoid bodies (EBs) and exposure to retinoic acid (Bain et al., 1995, Li et al., 1998). The EBs were dissociated and cultured for 2 days until cellular processes were visible. These were then assessed by eye using epifluorescence microscopy (FITC filter set) and imaged on an inverted confocal microscope while the cultures were still alive to assess the quality of process labelling. This showed that processes were labelled by both tagged and untagged GFP but that processes expressing either tau tagged GFP version were easier to detect than those expressing untagged GFP. The images presented in Fig. 2.5 demonstrate this. It should be noted that for unknown reasons, the neural

Figure 2.5.

Comparing labelling properties of various tau tagged GFP proteins. (A to G) FACS profiles collected in the FITC (green) channel of (A) untransfected ES cells and ES cells stably transfected with (B,C) pTP3, (D,E) pTP5, or (F,G) pTP6. Note broadly similar profiles for tau tagged and untagged GFP. (H,I) show bright field and green fluorescence confocal images of untransfected cells respectively. (J to U) Fluorescence images and confocal micrographs of (J,N,R) HEK293 cells and (K to M, O to Q and S to U) ES cells after differentiation into neurons expressing (J to M) untagged GFP from pTP5, (N to Q) GFP-tau from pTP3 and (R to U) tau-GFP from pTP6. In HEK293 cells, GFP labels the whole extent of the cell whereas tau-GFP and GFP-tau are excluded from the nucleus. In ES cell neurons, tau-GFP and GFP-tau label neural processes more clearly than untagged GFP (compare fine filaments seen in O and S to more diffuse label in K). When examined under bright field the ES neurons shown in O, S, and K all contained bundles of processes of similar appearance. Comparison of bright field and fluorescence images of individual processes show that tau tagged GFP labelled processes (compare P to Q and T to U) are easier to detect than those labelled with untagged GFP (compare L to M). All bars 10μm.

Figure 2.5

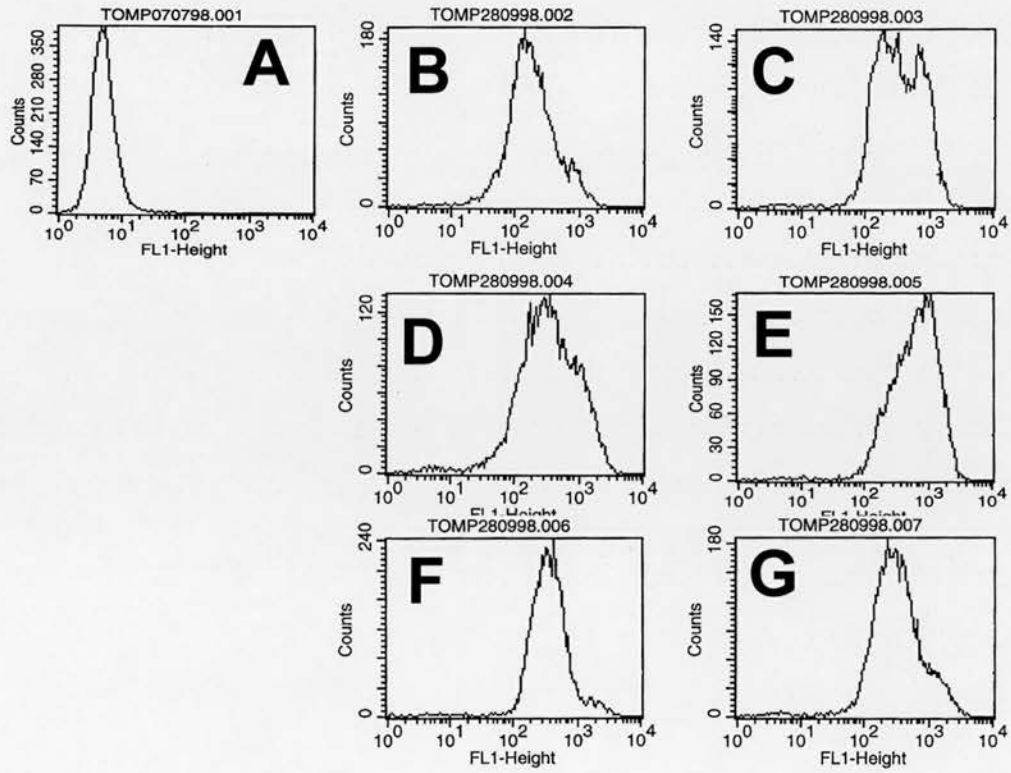
TOMP070798.001
A
Counts
FL1-Height
TOMP280998.002
B
Counts
FL1-Height
TOMP280998.003
C
Counts
FL1-Height
TOMP280998.004
D
Counts
TOMP280998.005
E
Counts
TOMP280998.006
F
Counts
FL1-Height
TOMP280998.007
G
Counts
FL1-Height

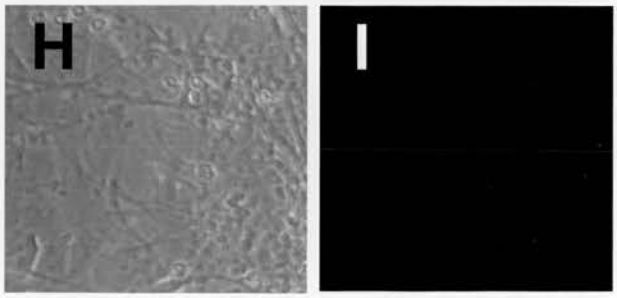
H
I

Figure 2.5...

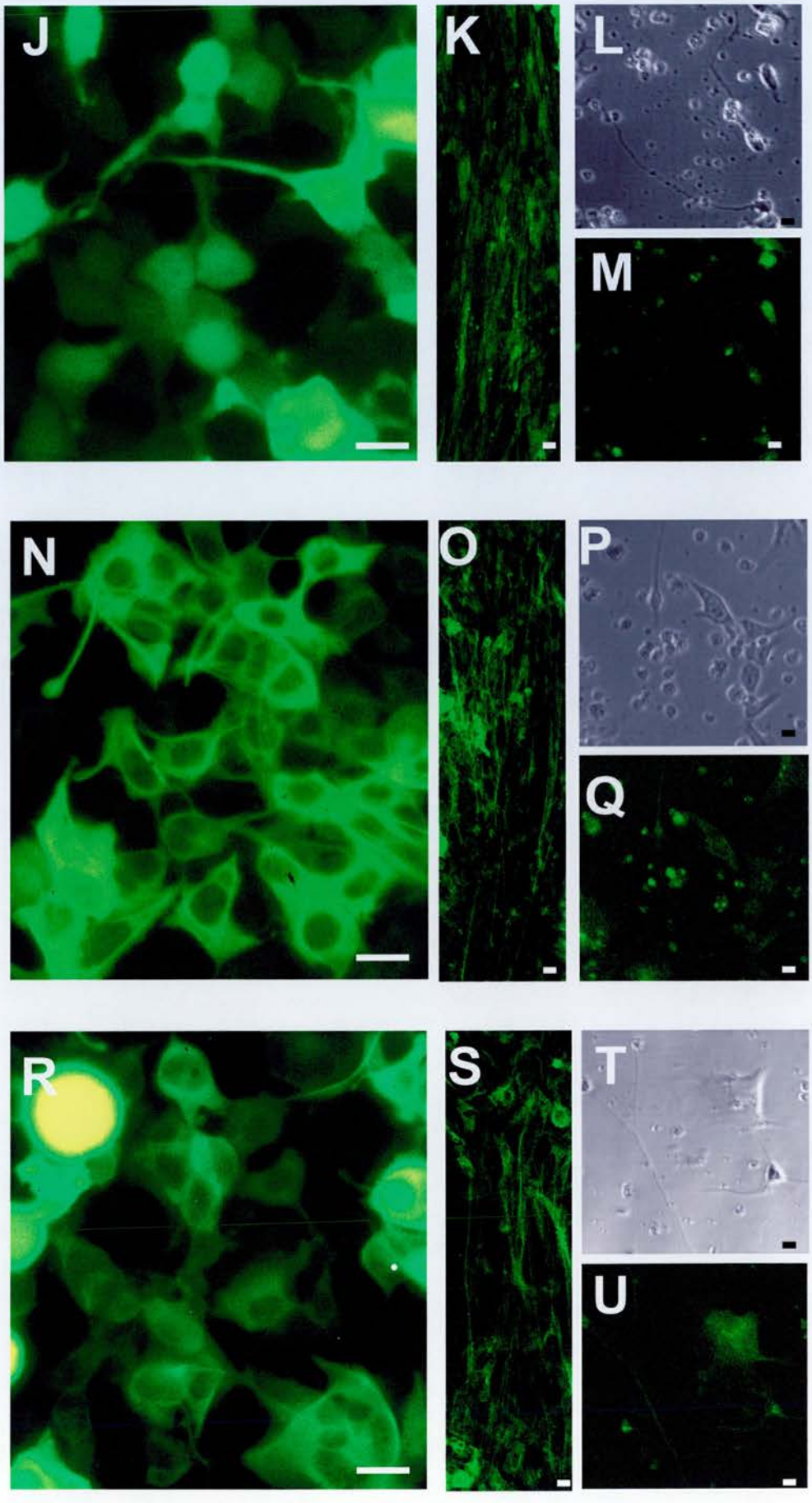

differentiation protocol was less successful with the Sox2 ES cells (Li et al., 1998) used in these experiments than for the E14Tg2a ES cell line (Hooper et al., 1987) subsequently used for generation of transgenic mice (see below and compare Fig. 2.5H to Fig. 2.5 L,P, and T) even when the two lines were subjected to the differentiation protocol in parallel. Viewing the cells through tissue culture plastic also adversely affected the fluorescent signal (compare Figs 2.5 and 2.6 in this chapter to Fig. 3.5 in Chapter 3 for ES cells exhibiting similar levels of fluorescence but imaged through a plastic culture well or through a glass coverslip respectively). These factors combine to reduce the quality of the images presented in this Chapter but the conclusion is clear as both tagged and untagged GFP versions were assessed under the same conditions.

These results show that the tau-GFP labelling generated by stable transfection with pTP6 successfully labelled cell processes and was not obviously disadvantageous to the cell. The pTP6 construct linearised by *Sca1* was introduced into the germline competent ES cell line E14Tg2aSc4 (a subclone of the E14Tg2a ES cell line (Hooper et al., 1987)). Ten puromycin resistant clones were selected at random without checking their fluorescent properties and expanded for analysis.

FACS profiles of proliferating ES cells grown in the presence of LIF were obtained for nine of these ten independent clones (Fig. 2.6). This showed that all clones exhibited similar levels of GFP fluorescence.

Seven of these ES clones were induced to differentiate into neurons by aggregating them into embryoid bodies (EBs) and exposure to retinoic acid (Bain et al., 1995, Li et al., 1998). The EBs were dissociated and cultured for 2 to 3 days until long cellular processes were visible. These were then assessed by eye using epifluorescence microscopy (FITC filter set) and imaged on an inverted confocal microscope while the cultures were still alive to assess the quality of process labelling (Fig. 2.7). These experiments established that all clones exhibited similar levels of fluorescence and, after

differentiation into neurons, their processes were clearly fluorescent. There appeared to be no non-expressing cells in either the Sox2 ES cells stably expressing pTP3, pTP5 or pTP6 or in the E14Tg2aSc4 ES cells stably expressing pTP6 either before or after neural differentiation indicating that the CAG promoter was able to drive ubiquitous transgene expression at least in ES cells and in neurons derived from these ES cells.

Generation of tau-GFP expressing transgenic mice

According to the assays described above, all tau-GFP expressing E14Tg2aSc4 clones stably transfected with pTP6 appear equally suitable for generation of transgenic mice. Three (E14Tg2aSc4TP6.3, E14Tg2aSc4TP6.4 and E14Tg2aSc4TP6.6) were chosen for injection into blastocysts, transfer to pseudopregnant females and production of chimeras. Two of the ES lines (E14Tg2aSc4TP6.3 and E14Tg2aSc4TP6.4) generated chimeras as judged by coat colour and these were test crossed to determine whether germline transmission had been accomplished. Examination of coat colour of these test cross offspring showed that ES lines E14Tg2aSc4TP6.3 and E14Tg2aSc4TP6.4 had successfully contributed to the germline and I named these lines 'TgTP6.3' and 'TgTP6.4' respectively. Examination of ear punches under epifluorescence microscopy (FITC filter set) confirmed that some of the offspring did possess green fluorescent ears indicating that the tau-GFP transgene had been successfully transmitted and was expressed in these transgenic lines.

The fluorescent (transgenic) offspring were test-crossed to wild-type mice and the progeny were tail tipped. Tail tips were assessed for fluorescence prior to extraction

Figure 2.6

Comparing tau-GFP labelling in undifferentiated ES cells stably transfected with pTP6. FACS profiles collected in the FITC (green) channel of (A) untransfected ES cells and (B to J) nine ES lines (B to J show profiles for clones E14Tg2aSc4TP6.1 to E14Tg2aSc4TP6.9 respectively) stably expressing tau-GFP. All nine clones exhibit similar fluorescence properties with the vast majority of cells being green. Note that the exact shape of the FACS profile was not constant for a particular ES clone (compare G to G' profiles which were collected from different passages of the ES clone E14Tg2aSc4PT6.6).

Figure 2.6

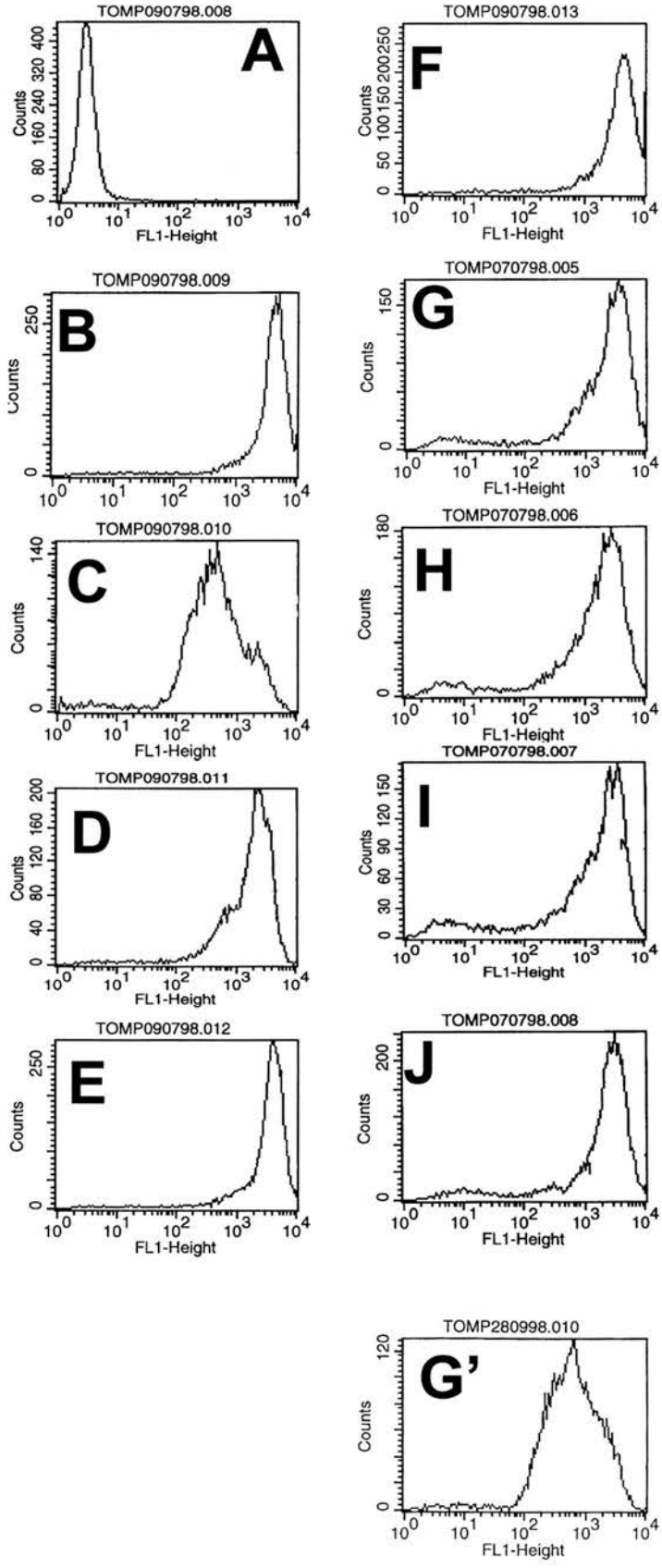
TOMP090798.008
A
Counts
FL1-Height
TOMP090798.009
B
Counts
FL1-Height
TOMP090798.010
C
Counts
FL1-Height
TOMP090798.011
D
Counts
FL1-Height
TOMP090798.012
E
Counts
FL1-Height
TOMP090798.013
F
Counts
FL1-Height
TOMP070798.005
G
Counts
FL1-Height
TOMP070798.006
H
Counts
FL1-Height
TOMP070798.007
I
Counts
FL1-Height
TOMP070798.008
J
Counts
FL1-Height
TOMP280998.010
G'
Counts
FL1-Height

Figure 2.7.

Comparing tau-GFP labelling in ES cells stably expressing pTP6 which have been differentiated to generate 'ES neurons' and cultured to allow neural processes to develop. Bright field and green fluorescence confocal images show (A,B) untransfected ES neurons and (C to W) tau-GFP expressing ES neurons. Comparison of bright field and fluorescence images showed that in all clones examined, all ES neurons expressed tau-GFP in their processes (compare C to D, F to G, I to J, L to M, O to P, R to S, U to V). A high power view of each culture is shown in the right hand column (E, H, K, N, Q, T, and W). The ES cell lines were as follows (A,B) E14Tg2aSc4, (C to E) E14Tg2aSc4TP6.1, (F to H) E14Tg2aSc4TP6.2, (I to K) E14Tg2aSc4TP6.3, (L to N) E14Tg2aSc4TP6.4, (O to Q) E14Tg2aSc4TP6.5, (R to T) E14Tg2aSc4TP6.6, (U to W) E14Tg2aSc4TP6.7. Red boxed areas in D, G, J, M, P, S, and V are enlarged in E, H, K, N, Q, T, and W. Bars 50μm.

Figure 2.7

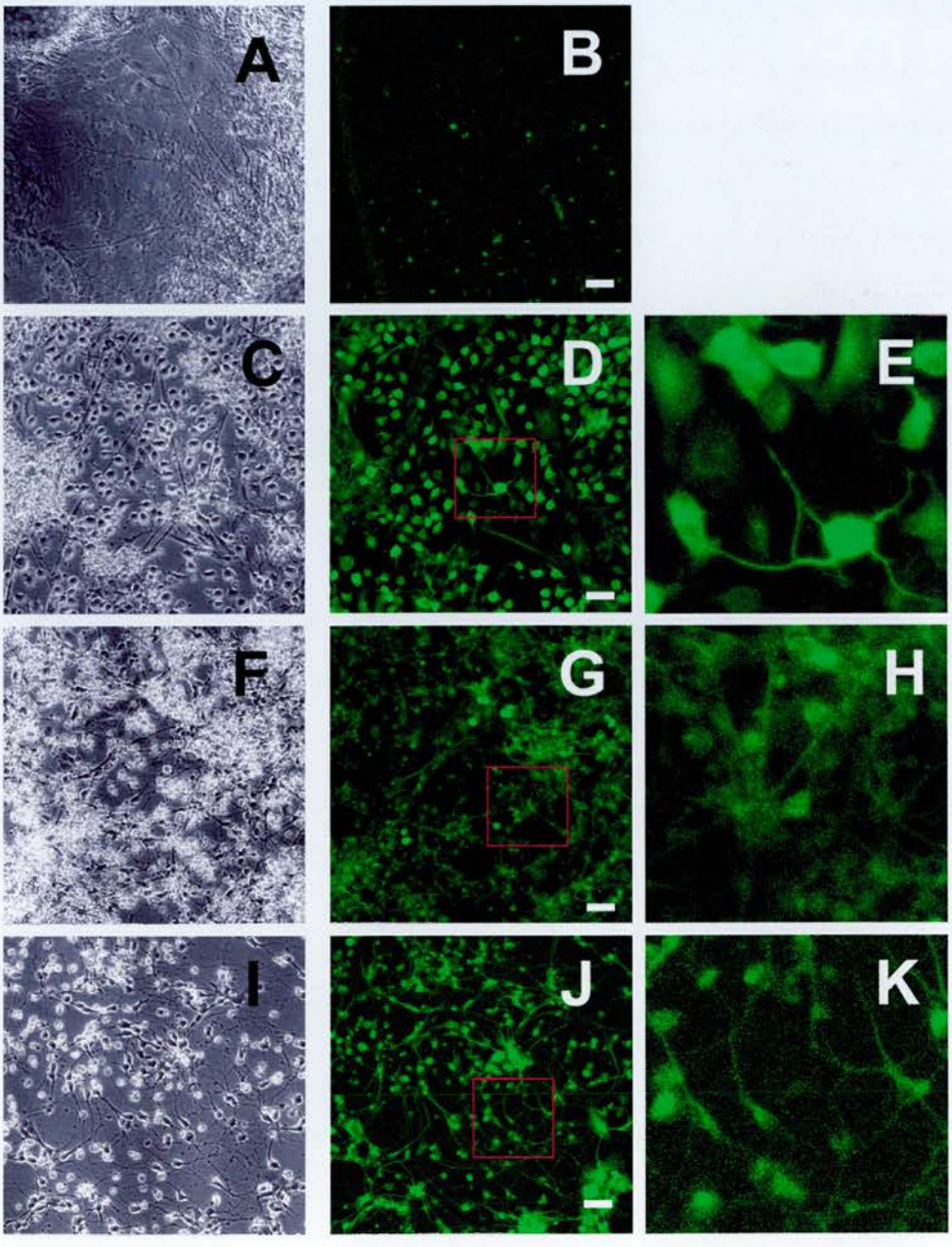

Figure 2.7...

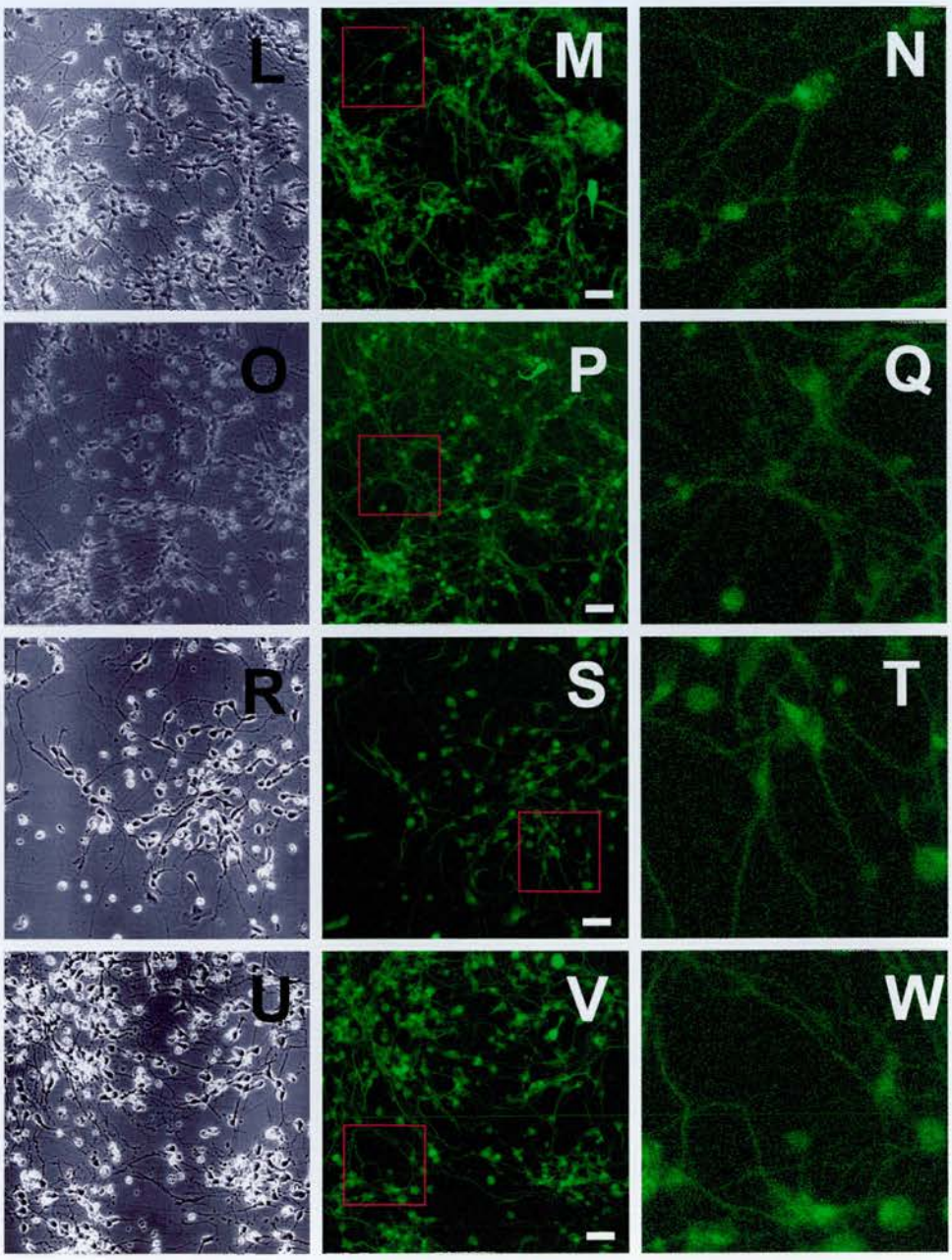

of DNA. The DNA was digested with *EcoR1* (which should release a 2.1kb fragment containing the tau-GFP fusion cDNA from pTP6, see Fig2.4 D) and subjected to agarose gel electrophoresis and southern blotting onto a nylon membrane. The blots were then hybridised to a ^{32}P labelled 738bp pMGFP6 *EcoR1* fragment (see Fig. 2.4 B) and hybridising bands detected by autoradiography. For both TgTP6.3 and TgTP6.4 lines, all animals which exhibited green fluorescent tails and ears also exhibited a 2.1kb *EcoR1* fragment hybridising to the mgfp6 probe (Fig. 2.8). This experiment showed that the transgene was expressed in all animals carrying a copy of the transgene and that there was no evidence for position effects silencing the transgene (see Chapter 1), at least in the ears and tail.

Deleterious effects of TgTP6.3 and TgTP6.4 transgenes

TgTP6.3 Heterozygotes

In the course of breeding the TgTP6.3 line it was observed that transgenic animals were frequently smaller than their non-transgenic littermates and that from the time of weaning until reaching maturity (3-6 weeks of age) transgenic TgTP6.3 animals appeared to be under-represented in litters. This prompted an examination of whether the TgTP6.3 or TgTP6.4 transgenic alleles adversely affected growth and survival. The embryos and adults used for these counts were obtained by crossing TgTP6.3 heterozygote mice to non-transgenic mice. This cross should result in transmission of the transgene to half the progeny (Mendelian ratio Tg/-: -/- of 1:1 for a Tg/- x -/- cross). Any viability disadvantage (or advantage) conferred by the transgene results in deviation from this 1:1 ratio. The comparison of littermates controls for variation in viability or weight reflecting epigenetic factors such as nursing and animal husbandry. These results are depicted graphically in Fig. 2..9.

Figure 2.8

Southern blots showing that TgTP6.3 and TgTP6.4 transgene is present in green fluorescent animals from each line. Each blot represents southern blot results for a litter of (A) TgTP6.3 or (B) TgTP6.4 animals generated by mating a heterozygous transgenic animal to a wild-type animal. The numbers above the gel represent the lane number. Below is indicated if examination of tail tips before DNA extraction for southern blot revealed that the animal was 'g' fluorescent or 'ng' not fluorescent. This showed that all animals containing the 2.1kb EcoR1 fragment hybridising the GFP probe were fluorescent for both TgTP6.3 (lanes 2, 3 and 4 in (A)) and TgTP6.4 lines (lanes 2, 4 and 6 in (B)). These results are typical of those for several litters analysed.

Figure 2.8

A

TgTP6.3

M 1 2 3 4 5 6

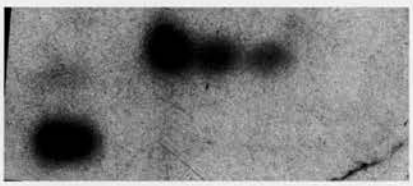

n g g g n n

B

TgTP6.4

1 2 3 4 5 6 7M

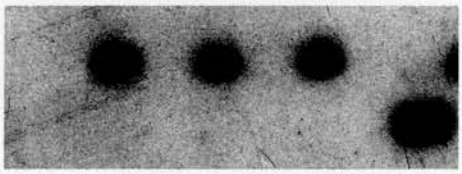

n g n g n g n

For animals aged between 3 and 6 weeks (P21 to P42), the mean number of transgenic animals (2.3 animals per litter) was less than the mean number of non-transgenic animals (4.1 animals per litter) for 42 litters counted. This difference in average number of animals per litter was statistically significant (Mann-Whitney Rank Sum Test, $P<0.001$). To see whether this reduced viability could be traced to before birth, litters of mid to late gestation embryos (E13.5-E16.5) were examined. This showed that there was no significant difference (Mann-Whitney Rank Sum Test) between the mean number of transgenic (5.7 embryos per litter) and non-transgenic (4.9 embryos per litter) at this stage of development for 34 litters counted. A χ^2 test confirmed that there were significantly fewer TgTP6.3 tau-GFP$^+$ animals surviving to between three and six weeks than their tau-GFP$^-$ littermates (95 versus 172, $\chi^2=21.5$, $P<0.05$) but that there was no survival difference at E15 (193 versus 168, $\chi^2=1.9$, $P>005$). The χ^2 was used to test the null hypothesis that equal numbers of tau-GFP$^+$ and tau-GFP$^-$ animals survived to each time-point. Although showing no reduction in viability, TgTP6.3 transgenic embryos were on average 10% lighter than non-transgenic embryos at this stage of development. Weighing E14.5 embryos from two litters showed a significant difference between transgenic (mean weight of 434mg, n=17) and non-transgenic (mean weight of 471mg, n=10) E15.5 embryos ($P<0.05$, t-test). A single TgTP6.3 allele therefore resulted in a slight reduction in embryonic weight and a predisposition to postnatal death. It should be emphasised that many TgTP6.3 heterozygotes did reach adulthood and were fertile.

This aspect of the TgTP6.3 transgene has been examined in more detail in collaboration with John Wests' laboratory and the results of this collaboration are presented in Appendix C rather than in this section as this data was not acquired by me. Survival and weight of transgenic and non-transgenic animals were compared at

Figure 2.9

Heterozygotes for the TgTP6.3 transgene exhibit reduced embryonic growth survival to adulthood compared to their non-transgenic littermates, whereas TgTP6.4 heterozygotes do not. (A) Survival of TgTP6.3 and TgTP6.4 animals during embryonic and postnatal development. The graph shows the mean number of tau-GFP$^+$ and tau-GFP$^-$ animals per litter. Animals were counted during embryogenesis (between E14 and E16) and postnatally (between 3 and 6 weeks of age). These litters were generated by mating a TgTP6.3 or TgTP6.4 heterozygote with a non-transgenic animal so half of the progeny should inherit the tau-GFP transgene. Deviation from a 1:1 tau-GFP$^+$:tau-GFP$^-$ ratio therefore implies that the tau-GFP transgene is deleterious (or advantageous) for viability. There was no evidence that there were significantly fewer (or more) tau-GFP$^+$ animals than tau-GFP$^-$ animals per litter for TgTP6.3 E14 to E16 embryos or for postnatal TgTP6.4 animals of 3 to 6 weeks of age (Mann-Whitney Rank Sum Test, $P>0.05$) but significantly fewer (*) TgTP6.3 tau-GFP$^+$ animals survived to 3-6 weeks of age than their tau-GFP$^-$ littermates (Mann-Whitney Rank Sum Test, $P<0.05$). These results show that the TgTP6.3 transgene confers a reduced postnatal viability phenotype in heterozygotes. The litter sizes were not normally distributed so error bars cannot be shown. (B) This graph shows that the mean weight of TgTP6.3 tau-GFP$^+$ E15 embryos is significantly lower (*) than that of their tau-GFP$^-$ littermates (t-test, $P<0.05$).

Figure 2.9

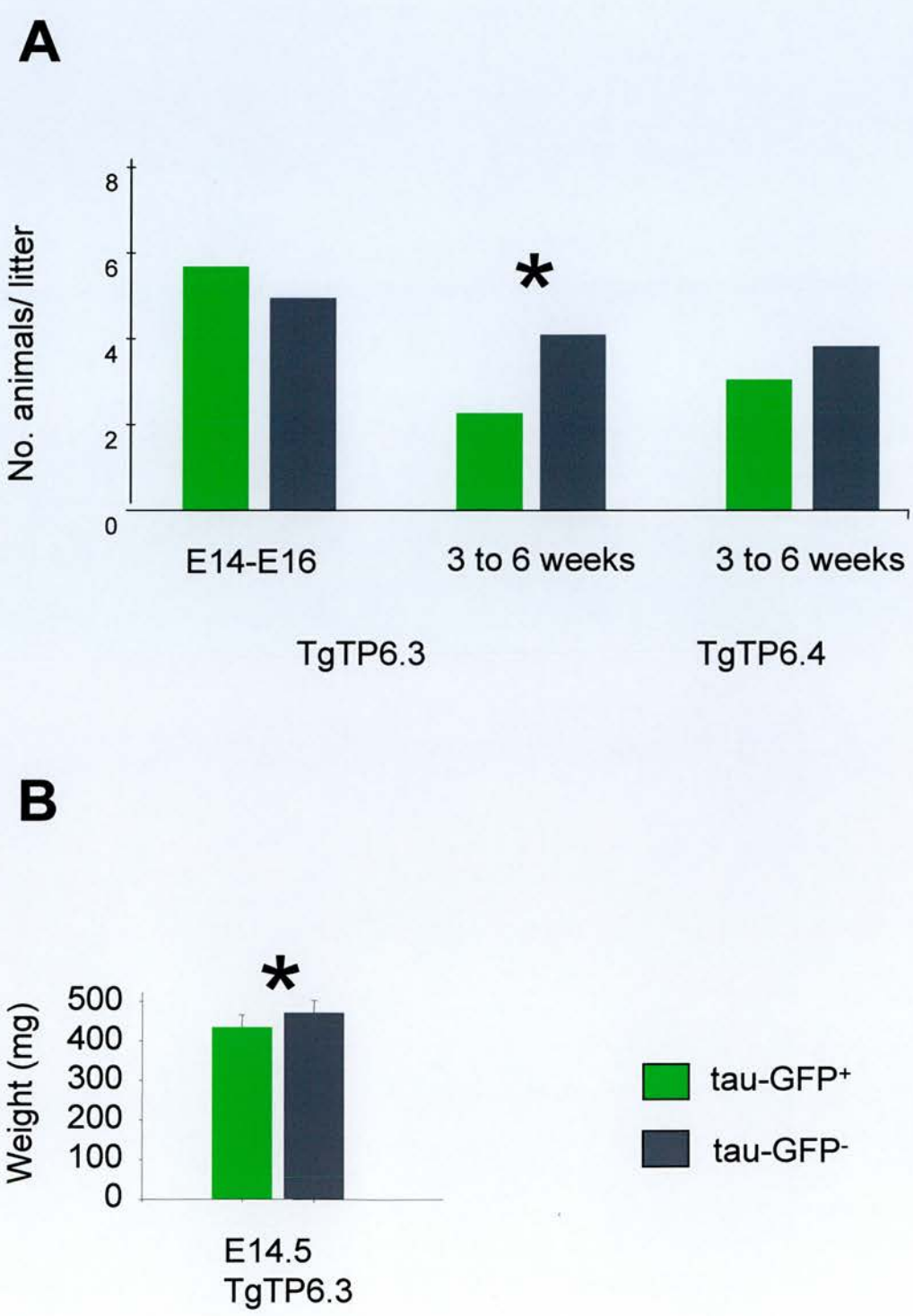
A
No. animals/ litter
8
6
4
2
0
*
E14-E16
3 to 6 weeks
3 to 6 weeks
TgTP6.3
TgTP6.4
B
Weight (mg)
500
400
300
200
100
0
*
E14.5
TgTP6.3
tau-GFP+
tau-GFP-

various ages. These experiments confirmed and expanded on results presented in this Chapter and showed that animals heterozygous for the TgTP6.3 transgene were generally slower to gain weight and more likely to die during postnatal life than their non-transgenic littermates.

TgTP6.3 Homozygotes

One third of fluorescent males resulting from a mating between TgTP6.3 heterozygotes would be predicted to be TgTP6.3 homozygotes (Mendelian ratio *Tg/Tg*: *Tg/*-:-/- of 1:2:1 for a Tg/- x Tg/- cross, with a ratio of 1:2 for Tg/Tg: Tg/-). Mating of homozygous TgTP6.3 males with wild type females should yield only TgTP6.3 heterozygotes (Tg/Tg x -/- cross yields only Tg/- progeny). In collaboration with John West, male and female TgTP6.3 heterozygotes were crossed and 20 fluorescent male progeny from these intercross litters were test crossed to wild-types and their progeny examined. None of these males transmitted the transgene to 100% of their progeny indicating that none of them were homozygous for the TgTP6.3 transgene. The observed frequency of TgTP6.3 homozygotes reaching sexual maturity (0%) was significantly different to the expected frequency (33.3%) indicating that the TgTP6.3 transgene is a homozygous lethal ($\chi^2 = 10$, $P<0.005$). The χ^2 was used to test the null hypothesis that 1 in 3 fertile green fluorescent males were TgTP6.3 homozygotes.

TgTP6.4 Heterozygotes

Unlike the TgTP6.3 line, the differences between the numbers of TgTP6.4 transgenic animals and their non-transgenic littermates in a litter at the time of weaning was not statistically significant (Mann-Whitney Rank Sum Test) with mean numbers of transgenic and non-transgenic in a litter being 3.0 and 3.8 respectively for 22 litters counted. The TgTP6.4 tau-GFP$^+$ and tau-GFP$^-$ animals appeared to survive equally well

to between three and six weeks (67 versus 84, χ^2=2.13, P>0.05). The χ^2 was used to test the null hypothesis that equal numbers of tau-GFP$^+$ and tau-GFP$^-$ animals survived to each time-point. This suggests that the adverse effects on viability of the TgTP6.4 transgene, if any, were more mild than those for the TgTP6.3 transgene.

DISCUSSION

This chapter describes the generation of a panel of expression constructs for evaluating the suitability of tau tagged GFP as a marker in transgenic mice and the production of ES cells and transgenic mice expressing tau-tagged GFP. Tagging GFP with tau at either the C- or N-terminus did not result in a reduction in GFP fluorescence. Both fusion proteins exhibited similar subcellular distributions suggesting that the GFP tag did not disrupt the subcellular localisation of tau. The properties of tau-GFP subcellular localisation is more fully addressed in the next chapter but the results presented in this chapter suggest that tau tagged GFP is a better marker of cellular processes than untagged GFP.

One possible concern in using cells or tissues from these mice is that ectopic expression of tau-GFP might compromise cell function. As discussed in Chapter 1, there is mixed evidence for adverse consequences associated with ectopic expression of tau protein in transgenic mice. Ectopic expression of a tau-GFP fusion protein might disrupt cell function by in some way interfering with microtubule assembly or predisposing transgenic animals to neural pathological disorders resembling Alzheimer's disease. Differences between the methodologies employed to generate different transgenic mice ectopically expressing tau make it difficult to predict the phenotype of novel strains. This thesis reports the generation of two lines of transgenic mice ectopically expressing a tau tagged GFP. These lines do not exhibit the same pattern of tau-GFP expression. As

described more fully in the following chapter, the TgTP6.3 line exhibits apparently ubiquitous tau-GFP expression whereas in the TgTP6.4 line tau-GFP expression is largely absent from large proportions of the CNS while being widely expressed in non-neural tissues. The two lines also differ in the effect that transgene expression has on postnatal growth and viability. The TgTP6.3 allele affects growth and viability in a dosage dependent manner. TgTP6.3 heterozygotes are predisposed to grow more slowly and die before reaching adulthood whereas homozygous animals never reach adulthood. TgTP6.4 heterozygotes do not appear to suffer from reduced viability. The same tau-GFP expression construct therefore participates in two distinct alleles. The TgTP6.3 allele confers a homozygous lethal semi-dominant phenotype whereas the TgTP6.4 allele does not.

As discussed in Chapter 1, examination of existing tau overexpressing transgenic mice suggests that increasing dosage of tau has increasingly adverse consequences. It could be that the higher levels of tau-GFP in the CNS of developing TgTP6.3 mice compared to TgTP6.4 mice accounts for the more severe phenotype. A similar argument could be used to explain why TgTP6.3 homozygotes might have a more severe phenotype than TgTP6.3 heterozygotes. It is also possible that differences between the TgTP6.3 and TgTP6.4 alleles reflects sequence alterations to different genomic loci associated with the two different transgene integration events, with the TgTP6.3 integration event presumably disrupting gene(s) involved in growth and viability. It is not possible to resolve these issues without more detailed information on the nature of the transgene integration event and more data on tau-GFP expression patterns and dosage in these animals. In this context it would be interesting to examine the phenotypes of transgenic mice generated from the other tau-GFP expressing ES cell lines. Adverse effects associated with mutagenic transgene integration events are likely to be highly variable between independent transgenic lines as each line is likely to have

a different transgene integration site. Adverse affects associated with tau-GFP expression might be expected to be less variable between independent tau-GFP expressing transgenic lines although the potential for variability in the patterns of transgene expression in different transgenic lines resulting from position effects would complicate this type of analysis.

It cannot be ruled out that further subtle cell type specific phenotypes will be identified with more detailed analysis. Experiments using these ES cells and animals should be designed with controls for possible effects of the transgene in whatever system is being studied.

These transgenic mice were produced via the generation of ES cells ubiquitously expressing tau-GFP protein. The use of the bicistronic expression vector pCAGiPuro in which tau-GFP expression was linked to puromycin resistance allowed for selection of stably expressing clones with puromycin so obviating screening for fluorescent clones. The similar fluorescence of all clones picked confirms the success of this strategy. It was also possible to screen the ES cells for likely suitability in generating a useful transgenic mouse. In this case I was interested in marking neurons, so took advantage of the potential of ES cells to differentiate into neurons in vitro (Bain *et al.,* 1995, Li *et al.*, 1998). If there were ES clones which switched off tau-GFP during the differentiation, or had for some reason become incompetent to differentiate, then these could be discarded at this stage. In this study, all clones could be induced to differentiate into cells with neuronal morphology that expressed tau-GFP in their processes and three were picked for generation of transgenic mice. Surprisingly, of two lines generated only one (TgTP6.3) exhibited strong tau-GFP expression in the brain although tau-GFP was expressed in other tissues in both. The incomplete success of this screening strategy emphasises the care that must be taken in extrapolating from neurons derived from ES cells to the full repertoire of neuronal subtypes present in the brain.

Because the transgene was introduced as a random integration event, it is unknown how many copies of the transgene were present in the TgTP6.3 and TgTP6.4 lines. As I was primarily concerned with characterisation and exploitation of the transgenic lines, I decided that determination of the transgene copy number was not central to this study and I did not pursue it further.

CHAPTER 3

CHARACTERISATION OF TAU-GFP EXPRESSION

SUMMARY

Chapter 3 describes the characterisation of tau-GFP expression in the TgTP6.3 and TgTP6.4 lines of transgenic mice whose generation was described in Chapter 2. This analysis shows that the TgTP6.3 line does express tau-GFP ubiquitously in neural structures whereas the TgTP6.4 line does not. In the TgTP6.3 line, tau-GFP is expressed in pre-implantation embryos and throughout subsequent development so is suitable as a source of cells for the cell mixing experiments of planned in Chapter 1 and described in Chapters 4 and 5. The subcellular distribution of tau-GFP was investigated by analysing sections of developing brain and cultured cells and tissues. This showed that tau-GFP was excluded from the interphase nucleus and concentrated in cellular processes and axon tracts. During mitosis, tau-GFP labelled the mitotic spindle.

INTRODUCTION

The primary motive behind generating these transgenic lines was to obtain embryonic tau-GFP labelled thalamocortical axons for use in in vitro models of thalamocortical tract formation (see Chapters 1, 4, and 5). A secondary aim was to achieve ubiquitous tau-GFP expression so that the transgenic line could be exploited more generally as a universal source of tau-GFP labelled cells. The characterisation of tau-GFP expression described here therefore concentrates on developmental stages and neural structures relevant to thalamocortical tract formation although other structures and developmental stages are also described.

MATERIALS AND METHODS

Materials used for primary cell culture, tissue processing and imaging are listed in Appendix B. ES culture is described in Chapter 2. Characterisation of pre-implantation development and the adult brain was a joint study with Linda Sharp.

Dissociation of embryonic brain

Tissues were dissected from E14.5 brains (TgTP6.3, TgTP6.4, or their non-transgenic littermates) in ice cold oxygenated EBSS and dissociated with papain solution (containing DNase) at 37°C for 45 minutes followed by triturating with a flame polished glass Pasteur pipette to generate a single cell suspension. Cells were washed twice by centrifugation at 300g for 5 minutes and the cell pellet gently resuspended in EBSS containing 10% ovomucoid inhibitor and DNase. Cells for FACS were then resuspended in PBS containing 1% bovine serum albumin. Cells for primary culture were gently layered over 100% ovomucoid inhibitor solution and centrifuged at 70g for 5 minutes. The upper (cell containing) layer was recovered, centrifuged at 300g for 5 minutes, cells resuspended in EBSS and counted before pelleting at 300g for 5 minutes and resuspension in serum free culture medium at an appropriate concentration.

Quantification of GFP fluorescence by FACS analysis

Embryonic brain tissues from E14.5 TgTP6.3 and TgTP6.4 embryos or their non-transgenic littermates were dissociated. White blood cells were isolated from whole blood by hypotonic lysis of red blood cells in 0.2% NaCl. Blood was centrifuged at 220g for 3 minutes, the cell pellet resuspended in 0.2% NaCl on ice for 30 seconds and an equal volume of 1.67% NaCl added. This process was then repeated to further enrich for white blood cells which can osmoregulate so do not lyse in 0.2% NaCl. Dissociated cells were subject to FACS as described in Chapter 2.

Tissue processing for Vibratome sections.

Embryos or tissues were fixed in ice cold 4% paraformaldehyde in phosphate buffered saline (PBS) overnight and embedded in 4% low melting point agarose. Sections (200μm) were cut on a Vibratome in ice cold PBS or water. Some sections were counterstained with the DNA stain propidium iodide (PI) before mounting in 1:1 glycerol:PBS containing 10% Vectashield.

Primary neural cell culture

Dissociated cells were plated onto poly-D-lysine coated glass coverslips at a density of 2000-4000 cells/mm^2 and cultured in serum free medium at 37°C in a humidified incubator containing 5% CO_2. After 2-3 days in culture the cells were fixed by immersion in ice cold 4% paraformaldehyde in PBS for 30 minutes and transferred to PBS. Some were counterstained with PI before quickly rinsing in water (to prevent salt crystals forming) and mounting in 1:1 glycerol:PBS containing 10% Vectashield.

Confocal microscopy

Cells and tissues were imaged using a Leica TCS NT confocal system and associated software with DMIRBE (inverted) or DMRE (compound) microscope in a confocal facility run by Linda Sharp. Bright field images were collected in the transmitted channel. GFP was detected in the FITC (green) channel. In some cases sections were counterstained with PI which was detected in the TRITC (red) channel. Generally, serial optical sections were collected and combined.

Visualising mitotic machinery in fixed and live tau-GFP ES cells

The tau-GFP expressing ES cell line E14Tg2aSc4TP6.3 from which the TgTP6.3 transgenic line was derived was used for these experiments. For live imaging, ES cells were cultured on poly-D-lysine and gelatine coated Willco thin glass bottomed 35mm dishes in a climate controlled chamber (5% CO_2, 37°C, humidified) on the stage of an inverted microscope. For chromosomal staining, ES cells were grown on gelatin coated plastic, fixed for 15 minutes in 4% paraformaldehyde in PHEM buffer (Schliwa and van Blerkom, 1981) at room temperature, and permeabilised with 0.1% TritonX100. Cells were then stained in a solution of propidium iodide containing 4μg/ml RNase, and mounted in 100% Vectashield. Confocal images were collected using an oil immersion lens.

RESULTS

Tau-GFP labelling in TgTP6.3 and TgTP6.4 heterozygotes

Quantification by FACS analysis

FACS was used to quantify the tau-GFP expression in TgTP6.3 and TgTP6.4 embryonic brain at the time of thalamocortical tract formation. Tissues from non-transgenic littermates were used as controls (Fig. 3.1). Structures dissected from E14.5 brain were dissociated into single cell suspensions for FACS. The protocol used resulted in the removal of cellular processes, so that, these values effectively represent the tau-GFP labelling of the cell body. The structures analysed in isolation were hippocampus, cerebral cortex, ventral telencephalon, and dorsal thalamus. FACS profiles were also obtained for whole brain and mid- and hind- brain combined.

Figure 3.1

(A to K) FACS profiles showing tau-GFP fluorescence in cells isolated from various regions of TgTP6.3 and TgTP6.4 embryonic brain. (A,H) Dissociated whole brain from E14.5 non-transgenic littermates of TgTP6.3 and TgTP6.4 embryos respectively used to establish baseline fluorescence. (B to G) show FACS profiles of E14.5 TgTP6.3 embryonic brain regions. (I to N) show FACS profiles of E14.5 TgTP6.4 embryonic brain regions. The regions examined were: (B,I) whole brain; (C,J) hippocampus; (D,K) cerebral cortex; (E,L) ventral telencephalon; (F,M) dorsal thalamus; and (G,N) mid- and hind-brain combined. Note that A', B' and I' shown above Table 3.1 are the same profiles as A, B, and I respectively with the fluorescent ranges M1, M2, and M3 used to categorise cells into the bins listed in Table 3.1 marked. (O to R) FACS profiles showing tau-GFP fluorescence of white blood cells isolated from (P) TgTP6.3 adult, (R) TgTP6.4 adult compared to non-transgenic littermates (O and Q respectively).

Figure 3.1

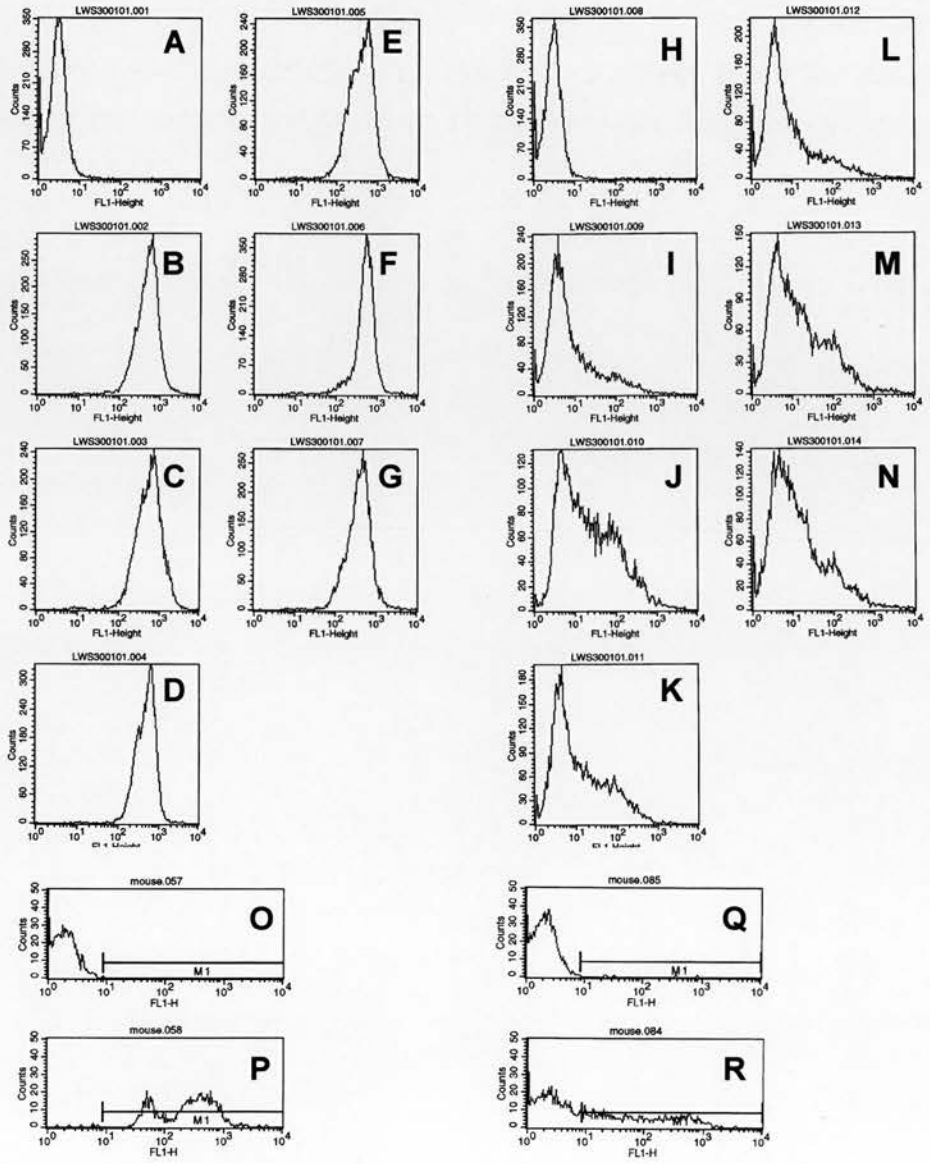
LWS300101.001
A
LWS300101.005
E
LWS300101.008
H
LWS300101.012
L
LWS300101.002
B
LWS300101.006
F
LWS300101.009
I
LWS300101.013
M
LWS300101.003
C
LWS300101.007
G
LWS300101.010
J
LWS300101.014
N
LWS300101.004
D
LWS300101.011
K
mouse.057
O
mouse.085
Q
mouse.058
P
mouse.084
R
Counts
FL1-Height
FL1-H
M1

Table 3.1

Green fluorescence properties of cells dissociated from E14.5 TgTP6.3 and TgTP6.4 embryonic brain (with non-transgenic littermate cells used to define the non-fluorescent baseline). The FACS profiles illustrated in Fig. 3.1 were quantified by assigning cells to one of three bins: M1 comprised of 'all fluorescent cells' defined as having fluorescence greater than the majority of non-transgenic cells; M2 comprised of 'weakly fluorescent cells' defined as having fluorescence intermediate between the majority of non-transgenic (non-fluorescent) cells and the majority of TgTP6.3 (strongly fluorescent) cells; M3 comprising of 'strongly fluorescent cells' defined as the fluorescent range exhibited by the majority of TgTP6.3 cells. M1=M2+M3. The ranges contained within these bins are marked on panels A', B', and I' representing the FACS profiles obtained from non-transgenic, TgTP6.3 and TgTP6.4 whole brain respectively (these profiles are the same as figures A, B, and I in Fig. 3.1). The table shows the % cells within each bin for TgTP6.3, TgTP6.4 and non-transgenic cells extracted from the tissues listed. These figures show that for all tissues examined, the vast majority of TgTP6.3 cells exhibit similar high fluorescence properties and that the TgTP6.4 cells are either 'non-fluorescent' or 'weakly fluorescent'. Note that the proportion of cells within each bin does vary between certain tissues expressing a particular transgene.

Table 3.1

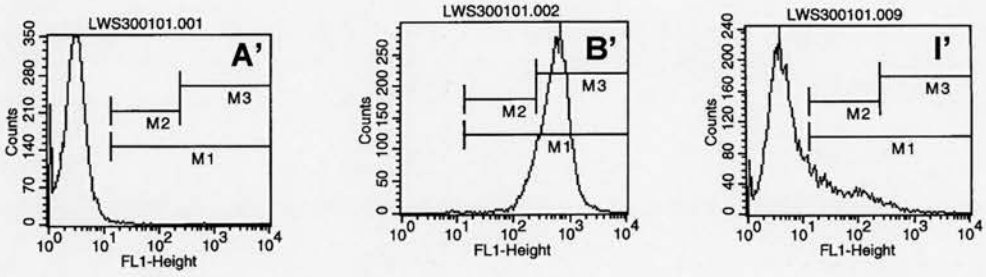

Genotype		% cells in each bin			
	E14.5 tissue	'non-fluorescent'	M1	M2	M3
WT	whole brain	98.8	0.6	0.6	0.0
TgTP6.3	whole brain	0.1	99.9	13.5	87.6
	hippocampus	0.3	99.7	11.9	88.9
	cerebral cortex	0.2	99.8	11.8	89.2
	ventral telencephalon	0.2	99.8	24.5	76.9
	dorsal thalamus	0.4	99.6	8.7	91.5
	midbrain and hindbrain	0.2	99.8	24.0	77.3
WT	whole brain	98.6	0.7	0.6	0.1
TgTP6.4	whole brain	73.9	26.1	23.5	2.7
	hippocampus	46.0	54.0	47.2	7.0
	cerebral cortex	60.3	39.7	36.5	3.5
	ventral telencephalon	72.5	27.5	24.6	3.1
	dorsal thalamus	55.2	44.8	40.1	5.0
	midbrain and hindbrain	58.2	41.8	37.2	4.8

For comparison of tau-GFP expression in developing TgTP6.3 and TgTP6.4 brains, fluorescence was divided into three bins ('M1', 'M2' and 'M3') comprising of cells with fluorescence: (M1) greater than the majority of non-transgenic cells; (M2) greater than the majority of non-transgenic cells and less than the majority of TgTP6.3 cells; (M3) the range seen in the majority of TgTP6.3 cells (M1=M2+M3). Table 3.1 shows the proportions of cells in each category.

Most TgTP6.4 cells from the regions of the developing brain examined exhibit indistinguishable fluorescence as non-transgenic cells. The vast majority of the remaining TgTP6.4 cells were more weakly fluorescent than the equivalent TgTP6.3 cells. Although it cannot be ruled out that some non-neural cells (for example blood vessels and membranes) contaminated the preparations of dissociated cells, it is unlikely that such contamination could account for the intermediate (bin M2) fluorescence seen in the TgTP6.4 FACS profiles judging from the intense tau-GFP labelling seen in these cell types in the TgTP6.4 brain (see Fig. 3.3 B,C).

Although the TgTP6.3 brain cells generated FACS profiles with a single peak, these profiles were not perfect bell-shaped curves. This suggests that each population actually consists of subpopulations of cells with distinct (though similar) fluorescence properties whose individual profiles overlap to generate a composite profile. This may reflect subtle cell type specific differences in the activity of the transgene promoter or in tau-GFP structure or stability. The TgTP6.4 FACS profiles bore even less resemblance to a bell shaped curve than the TgTP6.3 profiles indicating a continuum of fluorescence intensities ranging from non-fluorescent to levels approaching those seen in the TgTP6.3 cells. This suggests that the CAG promoter in the TgTP6.4 line is more sensitive to cell type specific effects than it is in the TgTP6.3 line, presumably this is a position effect reflecting the properties of integration site (as discussed in Chapter 2).

FACS analysis of white blood cells from TgTP6.3 and TgTP6.4 adult heterozygotes showed that TgTP6.3 white blood cells were all fluorescent compared to white blood cells from non-transgenic controls. Unlike in brain tissues, however, there were clearly two distinct populations (see the two fluorescent peaks in Fig. 3.1 P) presumably corresponding to two subpopulations of TgTP6.3 blood cells with distinct fluorescent properties. In contrast, many TgTP6.4 white blood cells exhibited the same fluorescence as non-transgenic controls and the remainder exhibited a range of fluorescence intensities which overlapped with those seen for the TgTP6.3 white blood cells but did not resolve into two distinct subpopulations (see Fig. 3.1 R).

Spatial and temporal labelling pattern

The onset of detectable paternal transgene expression was determined as the stage of development at which GFP fluorescence could be detected in approximately half of the embryos obtained from a cross between heterozygous (*Tg/-*) males and wild-type (-/-) females (Mendelian ratio Tg/-:-/- of 1:1 for a Tg/- x -/- cross). Examination of preimplantation TgTP6.3 embryos showed that transgenic embryos could first be distinguished from their non-transgenic littermates at the 8-cell stage (Fig. 3.2 A to D). All embryos younger than the 4-cell stage had a similar fluorescent appearance indicating that paternal transgene expression was not detectable before the 4-cell stage. The onset of maternal TgTP6.3 expression could not be determined by this method as all eggs and early embryos from TgTP6.3 females were highly fluorescent due to maternally expressed tau-GFP regardless of whether the embryos themselves were transgenic (not shown). Interestingly, sperm from TgTP6.3 heterozygote males were not detectably more fluorescent than sperm from non-transgenic males (not shown).

Examination of Vibratome sections of TgTP6.3 embryos and post-natal animals indicated that tau-GFP was widely expressed throughout the developing brain.

Following the onset of tau-GFP expression in the preimplantation embryo (Fig. 3.2 A to D), expression continues to be widespread in TgTP6.3 blastocysts (Fig. 3.2 E,F), in developing embryos throughout the remainder of gestation (Fig. 3.2 G to K) and in the adult brain (Fig. 3.2 L,M).

TgTP6.4 embryos exhibited strong and widespread tau-GFP expression in many non-neural tissues but tau-GFP was almost undetectable in a large proportion of the CNS. At E10.5 TgTP6.4 heterozygotes do express tau-GFP but the head structures do not appear to be as fluorescent as is seen in TgTP6.3 embryos (compare TgTP6.4 embryo in Fig. 3.3 A to an equivalent TgTP6.3 embryo in Fig. 3.2 G). Examination of coronal sections of E14.5 TgTP6.4 forebrain show that the majority of the fluorescence resided in the membranes surrounding the brain and in blood vessels embedded in neural tissue. Almost no fluorescence was detectable in the neural tissue itself (see figure 3.3 B, C and compare to equivalent sections of TgTP6.3 embryos in Fig. 3.2 I, also see Fig. 3.4 E).

Non-uniform distribution of tau-GFP fluorescence in embryonic brain

Although FACS analysis (Fig. 3.1 and Table 3.1) showed that all TgTP6.3 embryonic brain cells (or at least their cell bodies) expressed similar levels of tau-GFP, the intensity of tau-GFP labelling was not uniform across all regions of the developing brain. Certain regions were more intensely labelled with GFP fluorescence than others (Fig. 3.2). As discussed below, this can at least partly be attributed to the subcellular distribution of tau-GFP. As tau-GFP label is excluded from the interphase nucleus, structures exhibiting a high nuclear packing density appear more weakly labelled than

Figure 3.2

Confocal images showing widespread tau-GFP expression throughout development of TgTP6.3 heterozygotes and in the adult brain. (A) Bright field and (B) green fluorescent images of the same field showing that at the 8-cell stage tau-GFP is expressed throughout two transgenic embryos with no expression detectable in four non-transgenic littermates. (C) Bright field and (D) green fluorescent images of one of these fluorescent 8-cell embryos are also shown. (E) Bright field and (F) green fluorescent images of the same field showing that at the blastocyst stage (E3.5) tau-GFP is expressed throughout two transgenic embryos with no expression detectable in a third non-transgenic littermate. (G) Wholemount of a transgenic E10.5 embryo showing expression throughout head and body. (H,I) E14.5 embryo showing (H) sagittal section through whole embryo (similar orientation to (G)) and (I) coronal section through the head at the level of the forebrain. (J,K) E19.5 brain showing (J) sagittal section and (K) coronal section of forebrain. (L,M) Adult brain showing (L) sagittal section and (M) coronal section of left hemisphere. Note that the posterior end of the embryo in (H) and rostral-most brain region in (L) are missing from these sections. In all cases, tau-GFP expression appears throughout all embryonic tissues. Dorsal thalamus (dt), cerebellum (cb), cerebral cortex (cc) and carotid artery (ca), are indicated in some panels. Bar in (A,B); 100μm, (C,D); 10μm, (E,F), 20μm; (G to M), 500μm.

Figure 3.2

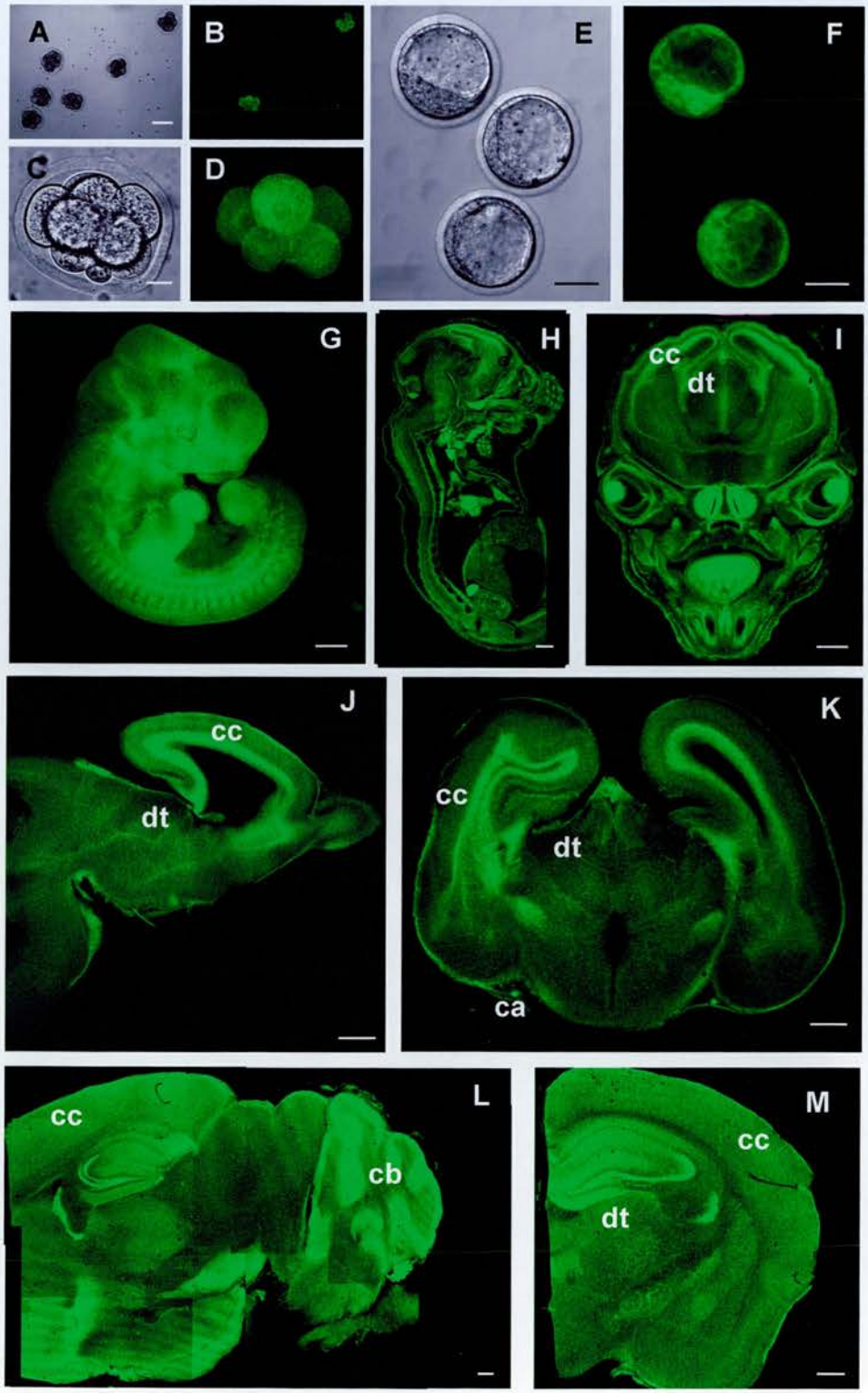

Figure 3.3

Confocal images showing limited tau GFP expression throughout development of TgTP6.4 heterozygotes. (A) E10.5 embryo. (B, C) Coronal sections through head of E14.5 embryo at the level of the forebrain. Note that although eye and brain tissue is weakly labelled, blood vessels are labelled as is surrounding non-neural tissue. Dorsal thalamus (dt), cerebral cortex (cc), and eye (e) are indicated. Bars, 100μm

Figure 3.3

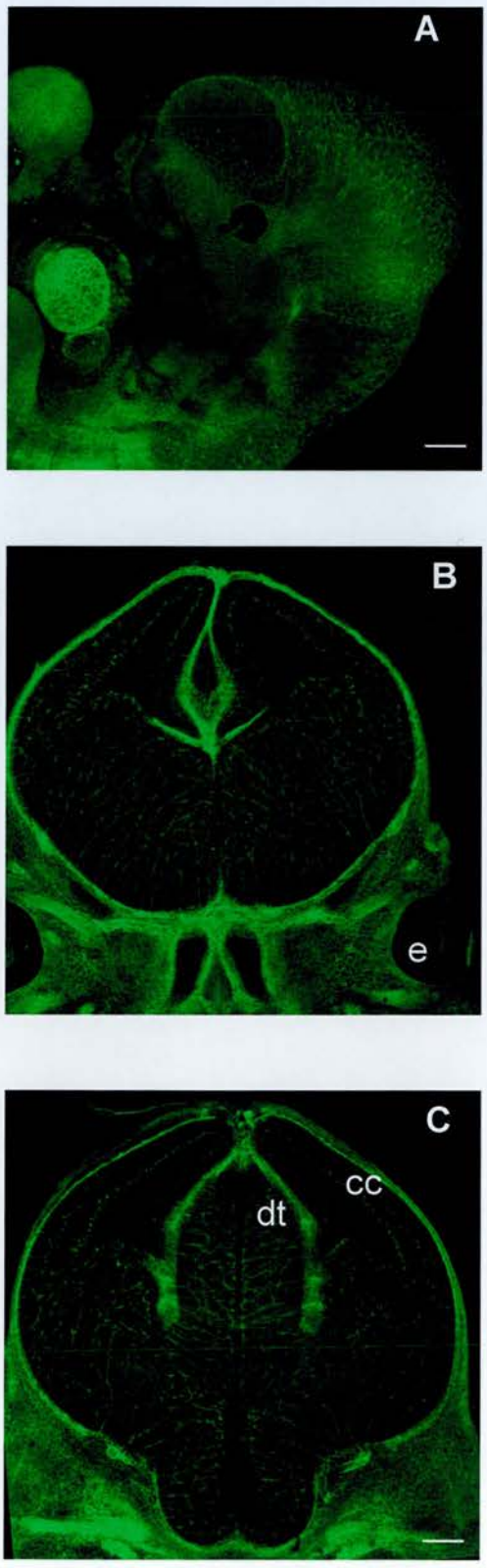

regions with more cytoplasm (including fibre tracts and the lens of the eye). TgTP6.3 tissues whose nuclei have been stained with PI (Fig. 3.4 C,D and F to M) illustrate this.

Tau-GFP efficiently labels long cellular processes

In using a tau-GFP fusion transgene I anticipated labelling microtubule containing structures, notably the long cellular processes which connect cells in the CNS. To test whether this had been successfully accomplished I looked at tau-GFP localisation in cultured cells and in fibre tracts. E16 cortex was dissociated into single cells, plated onto coverslips, and imaged after time in culture. Tau-GFP was present in the cytoplasm where it efficiently filled cellular processes (compare Fig. 3.4 A, B). To evaluate the TgTP6.3 transgene as a marker of fibre tracts I chose the thalamocortical axon tract (Fig. 3.4 E) as an example (Auladell et al., 2000). As described in Chapter 1, the thalamocortical tract consists of axons connecting the dorsal thalamus (dt) with the cerebral cortex (cc). The thalamocortical tract passes ventrally through the ventral thalamus (vt), makes a sharp lateral turn (avoiding the hypothalamus (ht)) and enters the ventral telencephalon (vtel) through the internal capsule (ic), before turning dorsally into the intermediate zone (iz) of the cerebral cortex. The thalamocortical fibre tract is highlighted by tau-GFP label with particularly strong staining seen in the internal capsule and intermediate zone (Fig. 3.4 E). The direction of fibres is apparent although individual fibres are hard to resolve (Fig. 3.4 F,H). There was strikingly reciprocity between the localisation of tau-GFP and cell nuclei (compare Fig. 3.4 C, F, and H to D, G, and I). Apparent 'holes' in tau-GFP labelling correspond to the nuclei of cells stained red with propidium iodide (compare tau-GFP label in Fig. 3.4 C with propidium iodide staining in Fig. 3.4 D, see also Fig. 3.3 J to M).

Figure 3.4

Tau-GFP label reveals neural processes and is excluded from the nucleus in TgTP6.3 transgenic mice. (A) Bright field and (B) green fluorescent images of dissociated E16 cortical cells cultured on coverslips. Tau-GFP efficiently labels all the neural processes which can be detected by bright field microscopy. (C) Green fluorescence and (D) PI stained nuclei in Vibratome sections of E16 cortex. Apparent 'holes' in the tau-GFP labelling correspond to the location of nuclei showing that tau-GFP is excluded from the nucleus. (E) Coronal Vibratome section of transgenic embryonic brain illustrating the thalamocortical axon pathway which connects the dorsal thalamus (dt) and cerebral cortex (cc). Note the intense green fluorescence of the fibre tract in the ventral thalamus (vt), internal capsule (ic), and intermediate zone (iz) of the cerebral cortex indicating that the entire tract is efficiently labelled. (F,H) Green fluorescence and (G,I) PI staining in Vibratome sections of E16 brain showing (F,G) intermediate zone (coronal section) and (H,I) internal capsule(sagittal section). Note the reciprocity of tau-GFP and propidium iodide staining which accounts for the intense labelling in fibre tracts compared to regions of high nuclear packing density. (J to K) Merged tau-GFP and PI fluorescence images of E18.5 brain showing (J) the anterior commissure, (K) the corpus callosum, and (L) the optic nerve (all sections in a coronal plane). Note that these fibre tracts (marked with an 'f') exhibit concentrated green fluorescent label and were of lower nuclear packing density than adjacent tissue. (M) the carotid artery (ca). Note also the extremely intense green fluorescence of the carotid artery wall in M (M is a higher magnification of the carotid artery indicated in Fig. 3.2 K). Bar in (A to D and J to M); 20μm, (E); 500μm, (F to I); 100μm.

Figure 3.4

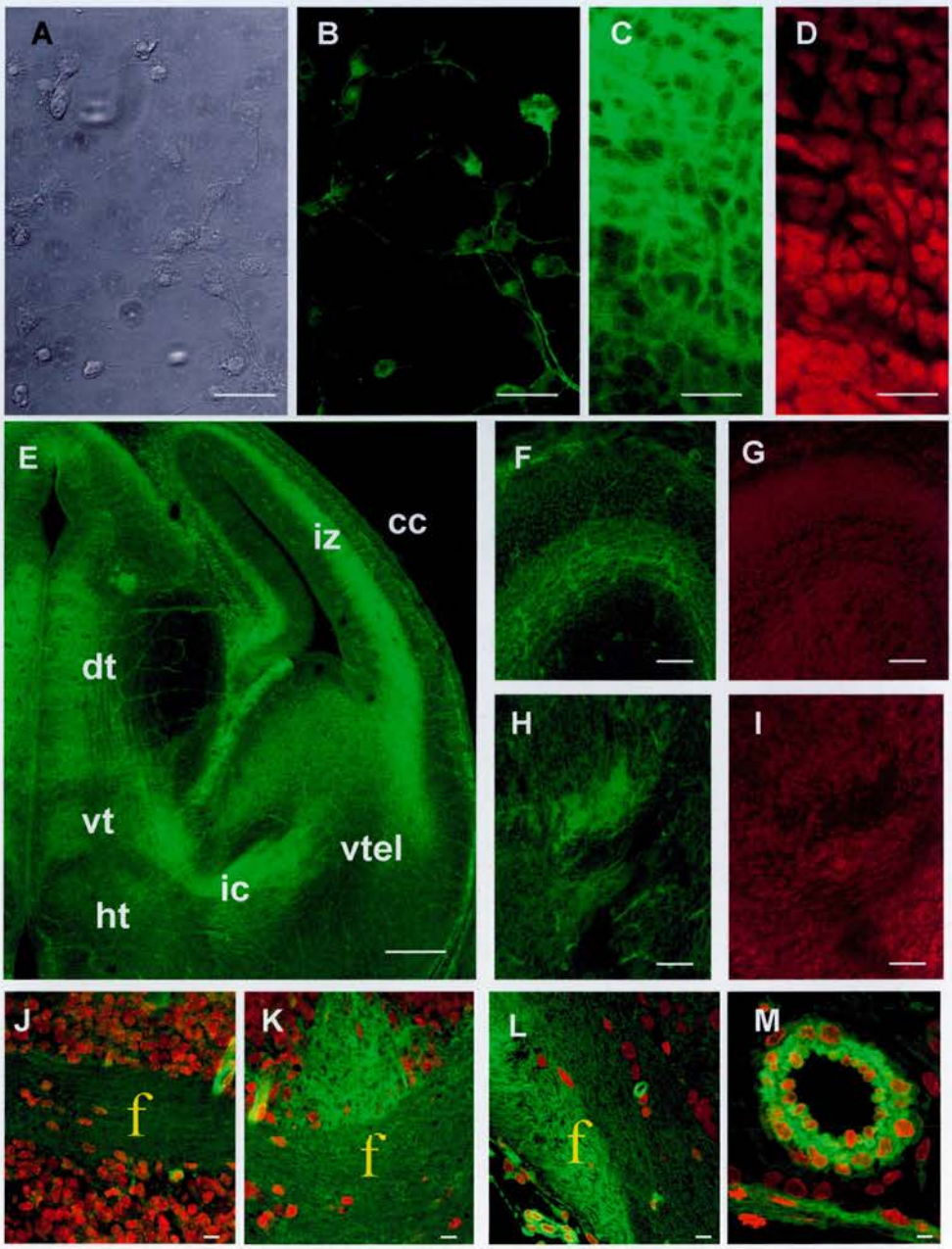

Intense tau-GFP labelling was also apparent in other fibre tracts in TgTP6.3 brain including the anterior commissure, corpus callosum, and optic nerve (see Fig. 3.4 J, K, and L respectively). For unknown reasons, blood vessels were intensely fluorescent (this feature was also seen in the TgTP6.4 line as shown in Fig. 3.2 B,C). Fig. 3.4 M shows a high power magnification of the carotid artery (ca) indicated in Fig. 3.2 K. The artery wall is intensely fluorescent.

Tau-GFP labels mictrotubule-containing structures

As described in Chapter 1, tau is a microtubule binding protein. I expected that the ability of tau-GFP to bind to microtubules would provide a means to visualise the microtubule component of the cytoskeleton. In living cells these subcellular details are otherwise inaccessible.

The microtubule component of the cytoskeleton plays an important role in cell function throughout the cell cycle with microtubules existing in a constant state of dynamic instability. During interphase, microtubules radiating from a single microtubule organising centre (MTOC) fill the cytoplasm and bundle together to form the core of developing processes. At the onset of mitosis, the MTOC replicates to generate two daughters, which migrate to opposing poles of the cell. The microtubules reorganise to generate the mitotic spindle, a structure which co-ordinates the equal segregation of chromosomes to the daughter cells.

To confirm that tau-GFP labels a variety of microtubule containing structures, I examined live preparations of tau-GFP expressing cells from TgTP6.3 transgenic mice and the E14Tg2aSc4TP6.3 ES cell line from which the mice were derived. A single optical section through live ES cells (Fig. 3.5 A) shows a subcellular fibrous tau-GFP labelling pattern in the cytoplasm. Live interphase cells from embryonic heart exhibit

Figure 3.5

Confocal imaging of tau-GFP in living cells allows visualisation of subcellular structures and reveals the filamentous microtubule network. (A to C) Tau-GFP labelling of living interphase cells. (A) Filamentous tau-GFP labelling in live ES cells. (B) Tau-GFP labelling radiates from a single point in embryonic heart cells (see also cell in top left-hand corner of A). (C) Tau-GFP labels growing processes in cultured neurons. (D to K) Tau-GFP labels the mitotic machinery in dividing ES cells. (D to G) In fixed cells representing key stages of mitosis tau-GFP labelling can be seen as green spots that correspond to the expected position occupied by the MTOCs. Chromosomes are stained red. The location of the spots of tau-GFP label relative to the chromosomes matches the location occupied by the MTOCs after they: (D) replicate during prophase to coincide with chromosome condensation and the onset of mitosis; (E) flank the chromosomes as they line up along the plane of division (equator) during metaphase; and (F,G) segregate to the opposite poles of the cell occupied by the MTOCs at anaphase. (H to K) Confocal images selected from time-lapse footage of a live tau-GFP expressing ES cell undergoing mitosis. The position of tau-GFP labelling matches the position occupied by the mitotic spindle as the cell divides. (H,I) Intense tau-GFP labelling can be seen perpendicular to and symmetrically arranged around the plane of cell division as the cell undergoes metaphase. (J,K) The cell proceeds (J) through anaphase and (K) telophase to generate two daughter cells (the lower daughter cell is not included in this optical section). Pairs of yellow bars (H to K) mark the plane of cell division. Note that the mitotic spindle appears much more strongly labelled in live cells (H,I) than in fixed cells at comparable stages of mitosis (E,F). Images in (A, D to G, I to K) are single optical sections chosen to emphasise subcellular detail. Bar in (A, C to K); 5μm, (B); 10μm.

Figure 3.5

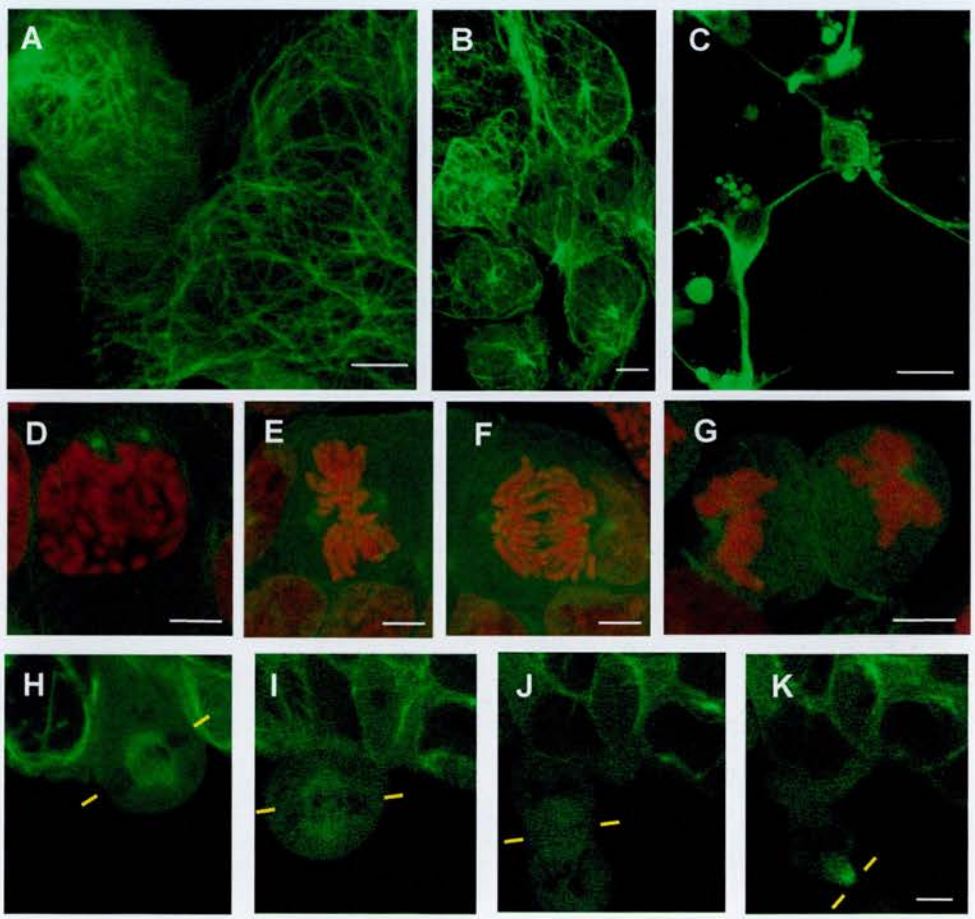

GFP labelling radiating from a single intensely labelled point into the cytoplasm (Fig. 3.5 B). Neural cells which have been dissociated and cultured exhibit long evenly labelled processes, with a particularly strong GFP signal extending from their base (Fig. 3.5 C).

During mitosis tau-GFP labels the mitotic machinery. Representative examples of fixed cells (chromosomes stained red with the DNA stain propidium iodide) are shown (Fig. 3.5 D to G). At the start of mitosis the MTOCs replicate as the chromosomes condense (Fig. 3.5 D). The chromosomes then congregate along the plane of division (equator) to form the metaphase plate which is flanked (at the poles) by the MTOCs between which the mitotic spindle is formed (Fig. 3.5 E) before segregating towards the MTOCs along the mitotic spindle (Fig. 3.5 F). Mitosis concludes as the daughter cells separate each with a complete set of chromosomes associated with a MTOC (Fig. 3.5 G).

The pattern of tau-GFP labelling described above is consistent with tau-GFP labelling microtubules during interphase and mitosis with particularly strong labelling seen at the MTOC. The tau-GFP does not associate with the chromosomes themselves as propidium iodide and tau-GFP label do not co-localise (Fig. 3.5 E to G).

Time-lapse footage of a tau-GFP expressing ES cell undergoing cell division shows that tau-GFP permits visualisation of the mitotic machinery as mitosis proceeds. Images selected from this time-lapse footage are shown (Fig. 3.5 H to K). Tau-GFP labels an oval structure reminiscent of the mitotic spindle (Fig. 3.5 H,I) in a cell, which goes on to divide (Fig. 3.5 J,K). A strong signal corresponds to the microtubule rich midbody which forms at the constriction between daughter cells (Fig. 3.5 K). Tau-GFP label is excluded from the chromosomes, which can therefore be visualised (particularly clear in Fig. 3.5 J but also apparent in Fig. 3.5 H,I).

These patterns of tau-GFP labelling resemble the distribution of microtubules within the cell during different phases of the cell cycle (Waters et al., 1993) and are consistent with the localisation of ectopically expressed tau protein reported by others (Ludin and Matus, 1998, Kaech et al., 1996, Preuss and Mandelkow, 1998, Mills et al., 1998, Rodriguez et al., 1999) where tau decorates the microtubule component of the cytoskeleton.

DISCUSSION

The TgTP6.3 line exhibits widespread tau-GFP expression throughout development and data presented in this Chapter confirm that at E14.5, during the period of thalamocortical tract development, expression is uniform and ubiquitous throughout the brain. This is in marked contrast to the TgTP6.4 line which exhibits much weaker tau-GFP expression in neural structures with most cells being apparently unlabelled. Analysis of white blood cells extracted from TgTP6.3 and TgTP6.4 heterozygous adults showed that the expression properties seen in neural tissue were mirrored in the blood. TgTP6.3 white blood cells were all fluorescent, although two fluorescent populations were discernible, whereas many TgTP6.4 white blood cells appeared to be non-fluorescent. The TgTP6.4 line is therefore unsuitable for my purposes and the remainder of this study concentrates on the evaluation and exploitation of the TgTP6.3 line.

Since transgenic mice ubiquitously expressing untagged GFP are already available (Okabe *et al.,* 1997, Hadjantonakis *et al.*, 1998, Kawamoto et al., 2000), it is important to emphasise the benefits of each labelling system. Untagged GFP diffuses throughout the cell freely so a labelled cell generates a uniform fluorescent signal, although the cell body tends to fluoresce much more strongly than thin processes. Axons of cells transfected with soluble GFP are less easy to detect than those of cells transfected with tau tagged GFP (see Chapter 2, Rohm et al, 2000). Tau tagged GFP

decorates the microtubule component of the cytoskeleton and is excluded from the interphase nucleus (this Chapter, Ludin and Matus, 1998, Kaech et al., 1996, Preuss and Mandelkow, 1998, Mills et al., 1998, Rodriguez et al., 1999). This allows cellular features to be visualised in cells expressing tau-GFP which are less clear in cells expressing soluble GFP. For example, cell division can be tracked by watching the fluorescent signal generated by tau-GFP decorating the mitotic machinery, and alterations in microtubule organisation are also associated with other processes such as cell death (Mills et al., 1998) and migration. A potential benefit of tau tagged GFP over untagged GFP is that the tagged version is anchored to the cytoskeleton so is less likely to diffuse out of cells during tissue processing resulting in loss of signal and increased background. This problem was reported for a line of transgenic mice expressing GFP where live preparations had to be perfused to wash away leaking GFP (Van den Pol and Ghosh, 1998). In my experiments, tau-GFP expressing cells and tissues are cultured in contact with unlabelled tissue without any obvious deterioration of signal caused by GFP leaking (see Chapters 4 and 5) and the tau-GFP label remains detectable in fixed tissue preparations after immunostaining for several other proteins (data not shown). Tau tagged GFP therefore appears to be a more robust label than soluble GFP with the advantage of illuminating the microtubule component of the cytoskeleton.

Fixation of tau-GFP labelled cells using the methods employed in this study does not obviously result in a decrease in GFP fluorescence since labelled and unlabelled cells and their processes could easily be distinguished in live and fixed preparations (see Chapters 4 and 5). Fixation, even when using protocols specifically developed to preserve microtubule structure (Schliwa and van Blerkom, 1981, Waters et al., 1993), does however appear to alter the subcellular distribution of tau-GFP. For example, comparison of tau-GFP labelling of the mitotic machinery in fixed and live cells reveals that whereas in live cells the mitotic spindle is very clearly labelled, in fixed cells it

appeared much fainter and the clearest fluorescent features are the MTOCs between which the spindle forms. In general, fixation appears to cause tau-GFP label to become 'hazy' compared to the sharply defined tau-GFP labelling seen in live cells, but does not result in significant deterioration in the quality of labelling above the subcellular level.

Of particular importance for the exploitation of these mice for the experiments described in Chapters 4 and 5, the tau-GFP is efficiently transported down cellular extensions and therefore labels axons and fibre tracts.

The ability of tau-GFP to decorate microtubules allows the visualisation of the microtubule containing cytoskeleton at a subcellular level. In proliferating cells expressing tau-GFP, I show that the pattern of tau-GFP labelling can be used to identify phases of the cell cycle. The breakdown of the nuclear envelope is indicated by tau-GFP label, excluded from the nucleus during interphase, filling the cell. This alteration in subcellular distribution might also reflect phosphorylation of tau-GFP occuring at the onset of mitosis as phosphorylation reduces the affinity of tau for microtubules (Fig. 1.9, page 62). The MTOCs are strongly labelled allowing their replication and movement to be tracked and the formation and orientation of the mitotic spindle is also apparent. Intense GFP labelling corresponds to the structure separating the daughter cells (the midbody) at the end of mitosis. Although not addressed in such detail as cell division in this study, the indications are that changes in microtubule structure associated with cell differentiation, migration, and death, should also be apparent.

Although the transgene is ubiquitously expressed, the subcellular localisation of tau-GFP causes certain anatomical features to be highlighted. In the brain for example, fibre tracts appear bright, regions of high nuclear density appear dim, and blood vessels and membranes (which are richly supplied with blood vessels) also appear bright. These

features can be used to provide fluorescent anatomical landmarks which are useful when targeting brain regions for dissection or injection.

CHAPTER 4

EVALUATION OF TgTP6.3 CELLS AND TISSUES IN MIXING EXPERIMENTS

SUMMARY

Chapter 4 describes applications of TgTP6.3 mice as a source of cells in a variety of cell mixing paradigms. TgTP6.3↔non-transgenic chimeras are examined at the blastocyst stage and after development into late gestation embryos. In other experiments TgTP6.3 and non-transgenic embryonic neural cells and tissues are combined in culture to evaluate the extent to which neural cell morphology and axons of labelled cells can be distinguished against a background of unlabelled cells and tissues. These experiments demonstrated that TgTP6.3 cells and tissues could readily be detected against a background of unlabelled cells and tissues and that the TgTP6.3 line was suitable as a source of cells for the experiments described in Chapter 5.

INTRODUCTION

As described in Chapter 1, my primary motive for generating transgenic mice ubiquitously expressing a tau-GFP transgene was as a source of cells and tissues for use in an investigation of the genetic control of thalamocortical tract formation. Before embarking on these experiments (described in Chapter 5) I performed some 'proof of concept' cell mixing experiments with cells and tissues derived from the TgTP6.3 line. The aim of these experiments was to establish whether the tau-GFP labelled cells could be readily detected after mixing with un-labelled cells and the extent to which cell morphology and axons of labelled cells was revealed by the tau-GFP label.

TgTP6.3↔non-transgenic chimeras generated by aggregation of 8-cell TgTP6.3 and non-transgenic embryos were examined at various stages of development. In the

developing chimera, TgTP6.3 and non-transgenic cells 'compete' to contribute to various structures (see Rossant and Spence, 1998) and analysis of these chimeras was anticipated to indicate if the tau-GFP expressing cells were differently competent to contribute to various structures compared to non-transgenic cells. This type of analysis has been used to show that cells lacking Pax6 function do not contribute to certain developing eye structures (Quinn et al., 1996, Collinson et al., 2000).

The examination of TgTP6.3 brains described in Chapter 3 established that tau-GFP expression was uniform and ubiquitous at the time of thalamocortical tract formation and that fibre tracts, including the thalamocortical tract, were strongly labelled. These results strongly suggested that tau-GFP labelled the full extent of cell morphology but because all the cells were 'green' it was conceivable that unlabelled tau-GFP expressing fibres might not be detected against a labelled background. Tau-GFP expressing cells and tissues were cultured with non-expressing cells and tissues to test the extent to which fibres were labelled and could be detected against an unlabelled background.

MATERIALS AND METHODS

Materials used for cell culture, tissue processing, and preparation of specimens for microscopy in this Chapter are listed in Appendix B. Chimeras were produced by Margaret Keighren and Gillian MacKay. Vibratome sectioning, dissociated cell culture, and mounting for confocal microscopy were performed as described in Chapter 3. Organotypic explant and seeding co-cultures were performed as described in Chapter 5.

Aggregation chimeras

Chimeras were produced as described by Tarkowski (1961) and reviewed in Rossant and Spence, (1998). 8 cell stage transgenic and non-transgenic embryos were aggregated to produce chimeras. Some of these were allowed to develop in vitro into blastocysts. These were then imaged while still growing in culture medium in a climate controlled chamber (5% CO_2 , 37°C, humidified) on the stage of an inverted confocal microscope. Others were transferred to pseudo-pregnant females and allowed to develop into E14.5 chimeric embryos before harvesting their brains for Vibratome sectioning and imaging.

RESULTS

Tau-GFP labelled cells are detectable in cell mixing experiments

I anticipated that a major application of TgTP6.3 mice is as a universal source of tau-GFP labelled cells. I next assessed their properties in three types of cell mixing paradigm in which transgenic and non-transgenic cells were combined in vivo in chimeras or in vitro in primary neural culture.

Chimeras

The production of chimeras allows analysis of cellular interactions throughout development (Rossant and Spence, 1998). As the onset of tau-GFP expression occurs in the first few days after fertilisation, I wanted to test whether TgTP6.3 and non-transgenic cells could be distinguished in early embryos. TgTP6.3↔non-transgenic chimeras produced by aggregating 8 cell stage transgenic and non-transgenic embryos

Figure 4.1

Tau-GFP labelled cells are easily detected after mixing with non-transgenic cells in TgTP6.3↔non-transgenic chimeras . (A,B) Blastocyst stage aggregation chimeras between transgenic and non-transgenic embryos. These chimeras were generated by G. MacKay and M. Keighren. Fluorescent confocal images show (A) a balanced chimera and (B) an unbalanced chimera in which most of the cells are of transgenic origin. In each case the position of labelled cells can easily be mapped. The nuclear exclusion of tau-GFP facilitates the counting of labelled cells. (C to K) Vibratome sections illustrating tau-GFP fluorescence in E14.5 TgTP6.3↔non-transgenic chimeras. (C to E) shows a chimeric eye at (D) low power and (E) a higher magnification of the retina. Note the sectoring of tau-GFP labelled cells into columns in (D,E). (F to H) shows chimeric dorsal telencephalon (G) at low power and (H) at higher magnification of the ventricular and intermediate zones of the cerebral cortex. Note the sectoring of tau-GFP labelled cells into columns in (G) and tau-GFP labelled axons in the intermediate zone in (H). (I to K) shows (J) the thalamocortical tract in a chimeric embryo (similar section to that shown in Fig 3.4 E on page 118) with (K) a higher power magnification of the dorsal thalamus. (C,F and I) show PI staining of the section shown in (D,G and J) does not reveal gross differences in cytoarchitecture between regions enriched for tau-GFP or non-expressing cells. Bars in (A,B); 20μm, (C, D, F, G, I, J); 100μm, (E, H, K); 25μm.

Figure 4.1

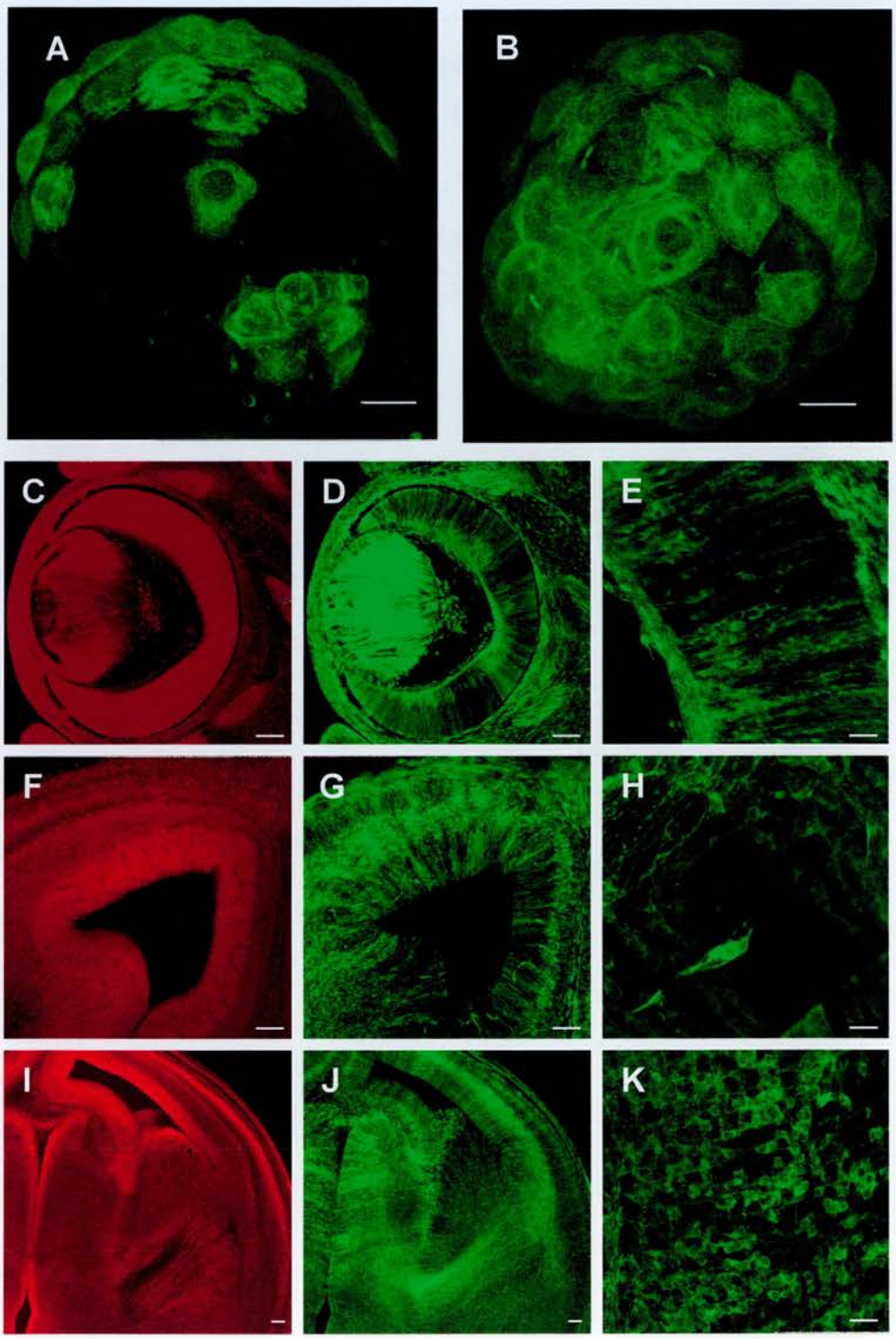

were cultured and imaged while still alive. Fluorescent images of two such chimeras undergoing blastocoel formation, in which labelled and unlabelled cells have become intermingled, are shown in Fig. 4.1. In one chimera (Fig. 4.1A) numbers of transgenic and non-transgenic cells are balanced and in the other (Fig. 4.1B) transgenic cells are more abundant than non-transgenic cells. Note that the tau-GFP label allows the nuclear position of expressing cells within the chimera to be mapped. Non-expressing cells derived from the non-transgenic embryo appear as gaps in the green fluorescence.

TgTP6.3↔non transgenic chimeras allowed to develop into E14.5 embyos show that tau-GFP expressing cells contribute to a variety of developing forebrain structures including the eye (Fig. 4.1 C to E), the cerebral cortex (Fig. 4.1 F to H), and the thalamocortical tract (Fig. 4.1 I to K). This showed that TgTP6.3 cells were not grossly discriminated against (or for) with respect to generation of structures involved in thalamocortical tract formation. This analysis was not performed in sufficient quantitative detail (see Quinn et al, 1996, Collinson et al., 2000) to conclude whether the tau-GFP expressing cells contributed to exactly the same extent as non-transgenic cells.

Dissociated cell co-culture

Co-culture of dissociated cells is often used to investigate how the behaviour of one cell population is influenced by proximity to another. To test the use of my cells in this type of experiment, dissociated cells from transgenic and non-transgenic embryonic cerebral cortex were mixed and cultured after plating onto coverslips. Bright field images of such a co-culture show a tangle of cellular processes where it is very difficult to assign a particular process to a particular cell (Fig. 4.2 A). This is resolved by

Figure 4.2

Tau-GFP labelled cells are easily detected after mixing with non-transgenic cells in brain in primary neural co-culture. (A) Bright field and (B) fluorescent confocal images of a mixed co-culture of dissociated transgenic and non-transgenic cortex. Note that the morphology of cells expressing tau-GFP is clearly marked by green fluorescence, nuclei are stained red with PI to aid comparison of fields. (C to E) Confocal images of organotypic co-culture of tau-GFP expressing thalamus with non-transgenic ventral telencephalon. (C,D) Green fibres can clearly be seen as they enter unlabelled tissue(dotted lines in (C)) with higher magnification in (D). (E,F) Visualisation of tau-GFP labelled cells which have integrated into unlabelled tissue during (E) organotypic co-culture and (F) after seeding of tau-GFP labelled cortical cells onto an unlabelled cortical slice (greyscale of fluorescent image). Bar in (A, B); 10μm, (C), 500μm, (D); 200μm, (E, F); 20μm.

Figure 4.2

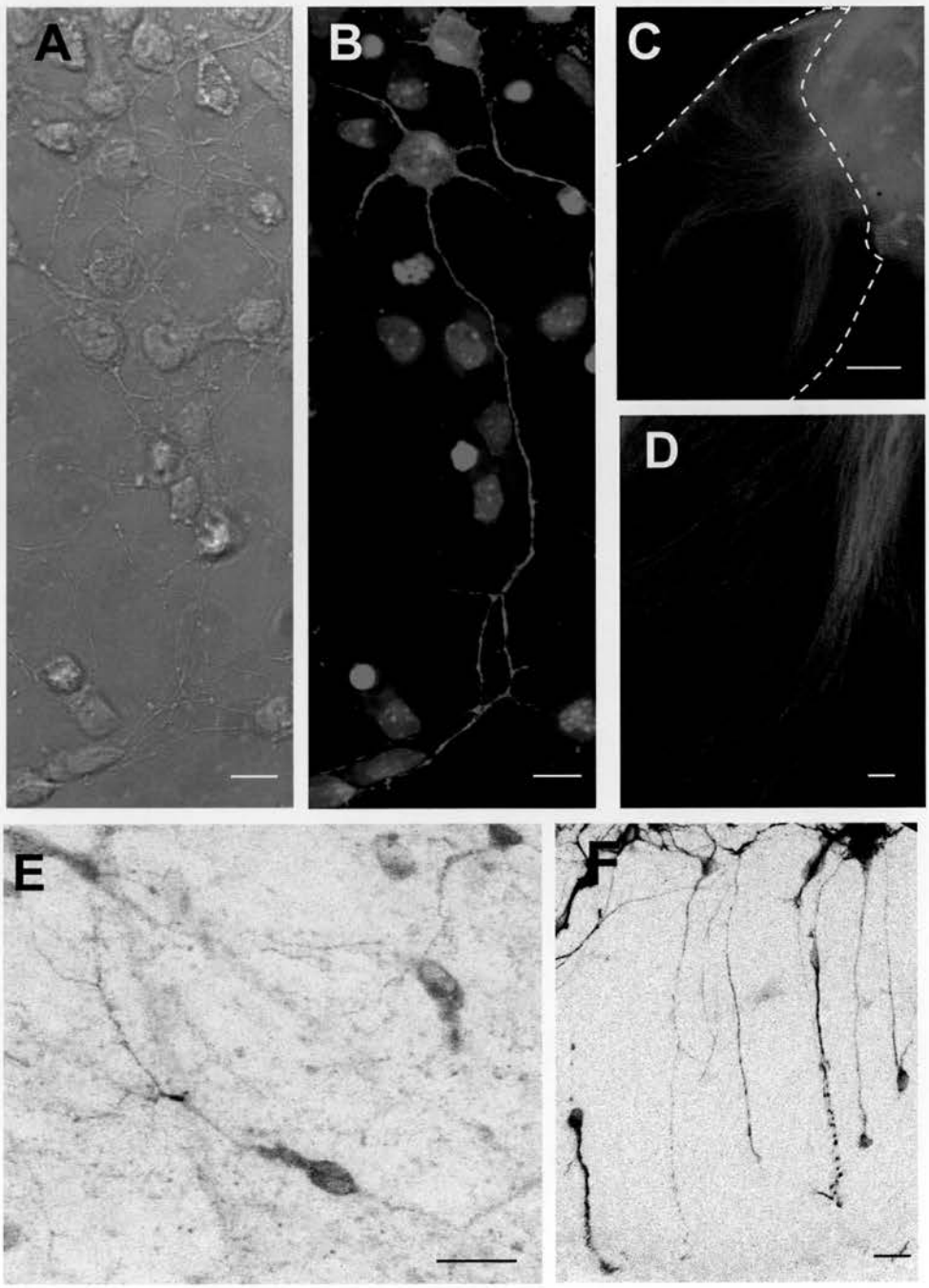

examining the fluorescence image, where tau-GFP clearly marks the morphology of transgenic cells and allows the course of their processes to be traced (Fig. 4.2B, nuclei counterstained red mark positions of cell bodies of both expressing and non-expressing cells).

Organotypic explant and seeding co-cultures

Organotypic co-culture is often used to investigate how axons generated by one tissue respond when challenged with the environment supplied by a second tissue. Axons in organotypic co-culture typically travel longer distances than is seen in cultures of dissociated cells and I wanted to confirm that tau-GFP labelling was efficient over longer distances. In vivo, thalamocortical axons travel from the thalamus to the cortex via the ventral telencephalon. In vitro, thalamic explants innervate explants of ventral telencephalon (see Chapter 5). Explants of transgenic E14.5 thalamus were cultured with explants of non-transgenic ventral telencephalon. After 3 days in culture the explants were fixed and imaged. Tau-GFP labelled fibres, which have grown into the unlabelled explant, were clearly visible (Fig. 4.2C) and at higher power individual fibres could be clearly resolved (Fig. 4.2D). In some of these cultures labelled cells migrated into unlabelled tissues and integrated into them (Fig. 4.2E). Tau-GFP labelled cells are also easily detected after seeding onto slices of non-transgenic cortex and sprouting of processes in culture (Fig. 4.2F).

DISCUSSION

Experiments in which tau-GFP expressing cells and tissues derived from TgTP6.3 heterozygote embryos are cultured with non-expressing cells or tissues demonstrate the experimental potential of these mice in cell mixing experiments.

Labelled cells and their processes can be visualised by fluorescence microscopy in live and fixed preparations and their behaviour mapped.

Long term cell mixing experiments such as transplants and chimeras where labelled cell populations must remain identifiable for weeks or months after the experiment is started demand that the label must be stable. TgTP6.3 cells fit these criteria since tau-GFP expression is ubiquitous both in ES cells before and after differentiation in vitro and in all cells from transgenic mice derived from these ES cells. A cell carrying the transgene and its descendants should therefore be detectable indefinitely.

These tau-GFP expressing ES cells and TgTP6.3 transgenic mice can be used as a source of labelled cells of any cell type for use in short or long term cell mixing experiments or to establish cell lines. Transgenic 'donor' cells and tissues can be visualised in exquisite detail after mixing and culture with non-transgenic 'host' tissues demonstrating the value of my cells in cell mixing applications. These include the development of neural transplantation technologies (Isacson et al., 1995, Scheffler et al., 1999, Svendsen and Smith, 1999, Mezey et al., 2000, Brazelton et al., 2000). Genetic modifications to the labelled cells can be achieved by manipulating the ES cells or by breeding the transgenic mice to place the tau-GFP transgene on different genetic backgrounds (see Chapter 5).

CHAPTER 5

PAX6 IS REQUIRED AUTONOMOUSLY BY THALAMOCORTICAL AXONS

SUMMARY

Chapter 5 describes the identification of an autonomous requirement for Pax6 within the dorsal thalamus for thalamocortical tract projection. To perform these experiments I developed an in vitro assay for thalamocortical tract navigation. By using tau-GFP expressing embryonic dorsal thalamic explants, I was able to see the green fluorescent axons as they navigated through unlabelled tissues.

INTRODUCTION

As described in Chapter 1, the thalamus fails to make appropriate cortical connections in mouse embryos lacking Pax6 function. Thalamic axons become stalled in the ventral telencephalon. Axon tracing studies in rat embryos lacking Pax6 function (*Pax6*$^{rSey/rSey}$) show that rather than growing through the internal capsule towards the cerebral cortex, thalamocortical axons become stalled in the ventral telencephalon forming a characteristic mushroom shaped structure composed of stalled axons (Kawano et al., 1999 and Fig. 1.4 B on page 38). Mouse *Pax6*$^{Sey/Sey}$ embryos exhibit similar thalamocortical defects in the absence of Pax6 function (Pratt et al., 2000b). A comparison of the timetables of Pax6 expression and thalamocortical tract formation reveals several sites at which Pax6 might influence thalamocortical tract projection (Fig. 1.4 A,B,C note that Fig. 1.4 B represents a stage of development after the time Pax6 has become down-regulated in the dorsal thalamus). The failure of the tract to form might reflect an autonomous requirement of thalamocortical axons for Pax6 (source defect), a requirement for Pax6 in cells lining the thalamocortical tract (pathway defect), or a combination of the two.

MATERIALS AND METHODS

Materials used for primary cell culture, tissue processing, and mounting for microscopy are listed in Appendix B. Vibratome sectioning and confocal microscopy were performed as described in Chapter 3.

Primary culture of embryonic neural cells and tissues

Brains from E14.5 wild type or mutant embryos were collected in ice cold oxygenated EBSS prior to processing for slices or dissociation and cultured in serum free medium as described below. The culture strategies are outlined in Fig. 5.2.

Organotypic co-cultures

Explants were prepared from E14.5 embryonic brains using the methods and reagents described by Lotto and Price, (1999a,b) and Pratt et al., (2000a,b). Organotypic explants (300 μm thick) containing the regions of interest (dorsal thalamus, cerebral cortex, ventral telencephalon or hypothalamus) were dissected from coronal slices of E14.5 brains obtained using a tissue chopper (as illustrated in Fig. 5.4 A-D) and arranged on collagen-coated inserts. Dorsal thalamic explants were from *tau-GFP:Pax6*$^{+/+}$ or *tau-GFP:Pax6*$^{Sey/Sey}$ embryos; other tissues were from *Pax6*$^{+/+}$ or *Pax6*$^{Sey/Sey}$ embryos that did not carry the transgene. Dorsal thalamus was recognised under transmitted and epifluorescence illumination, guided by anatomical landmarks known to correspond to gene expression boundaries defining the dorsal thalamus in both wild-types and mutants (Fig. 5.4 A-E; described in Results). The left and right dorsal thalamus were left joined dorsally in culture and their cut edges (red dotted lines in Fig. 5.4 B,D, just anterior to the border between dorsal and ventral thalamus) were placed against different tissues on each side. To recreate the topography of intact brain as much

as possible, these cut edges of dissected thalamus were placed in contact with either the medial edge of dissected ventral telencephalon or the dorsal edge of dissected hypothalamus (Fig. 5.4B,D see also Fig. 5.2). Following culture for 3 days in serum-free medium, cultures were fixed in ice-cold 4% paraformaldehyde in phosphate PBS, stained with the nuclear counterstain TO-PRO3 and mounted in 1:1 glycerol:PBS containing 10% Vectashield. Images of the cultures were obtained by combining serial optical sections acquired with a Leica confocal microscope. The following co-culture combinations were tested: *Pax6*$^{+/+}$ ventral telencephalon with either *tau-GFP:Pax6*$^{+/+}$ thalamus (n=25) or *tau-GFP:Pax6*$^{Sey/Sey}$ thalamus (n=21); *Pax6*$^{+/+}$ cortex with either *tau-GFP:Pax6*$^{+/+}$ thalamus (n=21) or *tau-GFP:Pax6*$^{Sey/Sey}$ thalamus (n=21); *Pax6*$^{+/+}$ hypothalamus with either *tau-GFP:Pax6*$^{+/+}$ thalamus (n=6) or *tau-GFP:Pax6*$^{Sey/Sey}$ thalamus (n=6); *Pax6*$^{Sey/Sey}$ ventral telencephalon with *tau-GFP:Pax6*$^{+/+}$ thalamus (n=4). In some cases cultures were viewed under epifluorescence while still growing or fixed for imaging at various time points to establish the time course of innervation.

Seeding experiments

Seeding was based on the method originally described by Emerling and Lander (1994) for seeding thalamic cells onto slices of cerebral cortex with the modifications described below. Embryonic thalamic cells were dissociated from thalamus using a papain dissociation system. Thalamus was dissected from E14.5 *tau-GFP:Pax6*$^{+/+}$ or *tau-GFP:Pax6*$^{Sey/Sey}$ brains in ice cold oxygenated EBSS and incubated in papain solution (containing DNase) at 37°C for 45 minutes followed by triturating with a flame polished glass Pasteur pipette to generate a single cell suspension. Cells were washed twice by centrifugation at 300g for 5 minutes and gentle resuspension of the cell pellet in EBSS containing 10% ovomucoid inhibitor. The cell suspension was then layered over 100% ovomucoid inhibitor, centrifuged at 70g for 5 minutes, and the upper layer

containing dissociated cells recovered. Cells were then counted and the volume adjusted to give a suspension of $3x10^6$ cells/ml in serum free culture medium.

300 μm thick coronal slices of *Pax6*$^{+/+}$ E14.5 brain were obtained using a tissue chopper and incubated in thalamic cell suspension for 1 hour with occasional agitation. After this time, slices were carefully washed by serial transfer through three changes of culture medium using a wide bore flame polished glass Pasteur pipette. Slices were then arranged on a collagen coated filter and cultured for 3 days prior to fixation, TOPRO3 staining, and imaging on a confocal microscope.

The following seeding combinations were tested: *tau-GFP:Pax6*$^{+/+}$ thalamic cells seeded onto *Pax6*$^{+/+}$ forebrain slice (n=6) or *tau-GFP:Pax6*$^{Sey/Sey}$ thalamic cells seeded onto *Pax6*$^{+/+}$ forebrain slice (n=6). After time in culture the forebrain slices often spread out and became distorted making it difficult to identify structures. The results in Fig 5.6 A to D show results from two cultures of each type in which the dorsal thalamus, hypothalamus, and ventral telencephalon could be readily identified.

Mice

Embryos for these experiments were generated by crossing pigmented mixed background: 129 strain (Hooper et al., 1987)/ C57BL/6 strain (Bantom and Kingman, UK) and/or 'Edinburgh-derived Small eye' background (Kaufman et al., 1995, Roberts, 1967) males to albino Swiss strain females (in house colony). Some of these animals were heterozygous for the loss of function 'Small eye' (*Pax6*$^{Sey/+}$) mutant *Pax6* allele (Hill et al., 1991). This produced embryos with the required *Pax6* genotype with pigmented eyes which facilitated genotyping E14.5 embryos from their eye phenotype.

As described by Kaufman et al. (1995), *Pax6*$^{+/+}$ embryos have a perfectly round iris, Pax6$^{Sey/+}$ embryos have a distorted iris, and *Pax6*$^{Sey/Sey}$ embryos have no eyes

RESULTS

Anatomy of *tau-GFP:Pax6*$^{Sey/Sey}$ embryonic brain

Vibratome sections of TgTP6.3 heterozygotes (*tau-GFP:Pax6*$^{+/+}$) were compared to *tau-GFP:Pax6*$^{Sey/Sey}$ at E13.5. A selection of these are shown in Fig. 5.1. The gross disturbances in forebrain morphology characteristic of small-eye homozygotes are apparent in the *tau-GFP:Pax6*$^{Sey/Sey}$ embryos showing that expression of the tau-GFP transgene does not grossly affect the small-eye phenotype. Fig. 5.1 A and B shows that the thalamocortical tract is clearly visible in transgenic mice expressing tau-GFP on a wild-type background (*tau-GFP:Pax6*$^{+/+}$). Axons originate from the dorsal thalamus, enter the ventral thalamus and turn at the hypothalamus into the ventral telencephalon, which they penetrate to reach the cortex. This tract is not seen in *tau-GFP:Pax6*$^{Sey/Sey}$ embryos (Fig. 5.1 C to F). A mushroom shaped tau-GFP labelled structure resembling the conformation adopted by stalled thalamocortical axons (see Fig. 1.4B on page 38) is however apparent (Fig. 5.1 C and D).

Figure 5.1

(A to G) Green fluorescent images of coronal sections of E14.5 *tau-GFP:Pax6*$^{+/+}$ and *tau-GFP:Pax6*$^{Sey/Sey}$ brains. (A,B) *tau-GFP:Pax6*$^{+/+}$ embryo showing strong tau-GFP labelling of thalamic axons as they turn sharply to avoid the hypothalamus and enter the ventral telencephalon to form the internal capsule (*). (C-G) *tau-GFP:Pax6*$^{Sey/Sey}$ embryos exhibit defective tract formation. C, E, G show a rostral (C) to caudal (G) series. (C,D) mushroom shaped tau-GFP staining structure in rostral *tau-GFP:Pax6*$^{Sey/Sey}$ ventral telencephalon. (E,F) the strong tau-GFP label seen in *tau-GFP:Pax6*$^{+/+}$ embryos is lacking from the position normally occupied by the internal capsule (*). (B, D, F) are magnified views of the boxed areas in (A, C, E) respectively. (H) Composition of litters generated from *tau-GFP:Pax6*$^{+/Sey}$x*Pax6*$^{+/Sey}$ crosses counted at E14.5. Pax6 genotype was assessed by examination of eye phenotype and tau-GFP status by examination under epifluorescence. These results show that the TgTP6.3 transgene does not drastically alter the expected Mendelian ratio (1:2:1) of Pax6$^{+/+}$: Pax6$^{+/Sey}$:Pax6$^{Sey/Sey}$ E14.5 embryos. All bars 500μm.

Figure 5.1

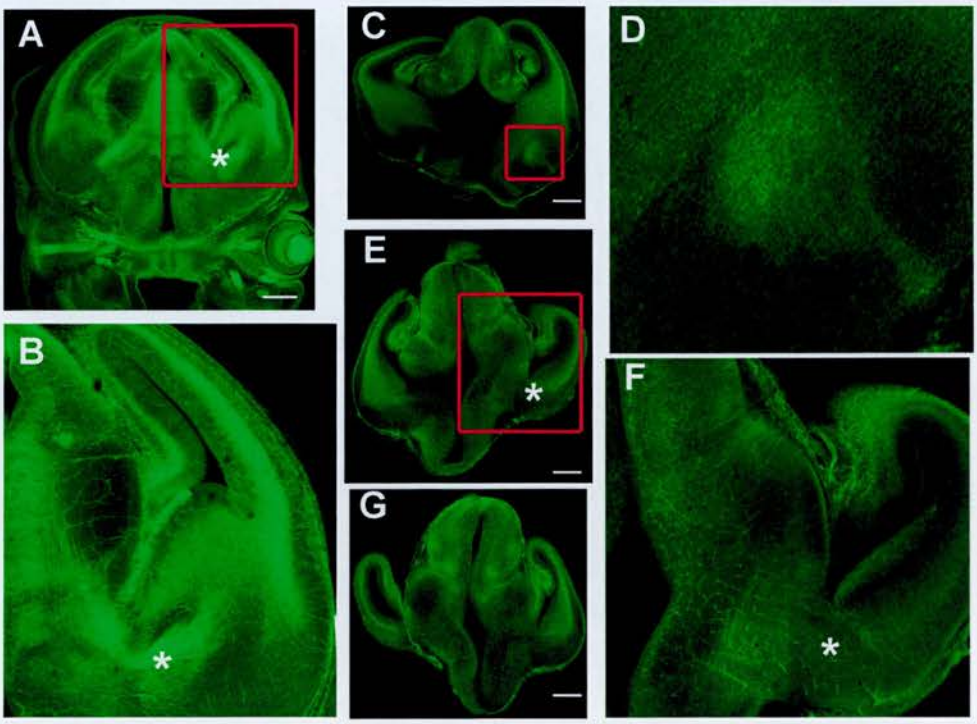

H

E14.5. Embryos with genotype	*Pax6*$^{+/+}$	*Pax6*$^{Sey/+}$	*Pax6*$^{Sey/Sey}$
tau-GFP^{+}	7	21	12
tau-GFP^{-}	4	18	2

Analysis of thalamocortical tract projection in vitro

Time course

In order to determine the time course of thalamic axon outgrowth into target tissues, several explant cultures were set up and observed live at daily intervals using epifluorescence or fixed after 1, 2 or 3 days in culture processed for imaging on a confocal microscope. Typical innervation of a cerebral cortex explant by tau-GFP dorsal thalamic axons is shown in Fig. 5.3 A to F. This experiment shows that between 1 and 2 days in culture were sufficient for extensive axon outgrowth and the establishment of the major features of innervation seen after 3 days.

Pax6$^{+/+}$ versus Pax6$^{Sey/Sey}$

The aim of these experiments was to test whether or not axons from dorsal thalamus in *Pax6$^{Sey/Sey}$* embryos are able to respond to growth and/or guidance signals along their path to the cortex. To test the ability of thalamic axons to innervate tissue encountered along the normal thalamocortical pathway, explants of E14.5 *tau-GFP:Pax6$^{+/+}$* and *tau-GFP:Pax6$^{Sey/Sey}$* thalamus were cultured in contact with wild-type ventral telencephalon, hypothalamus or cerebral cortex (Fig. 5.4 F-M; results are shown on a grey-scale, which makes axons clearer). Dorsal thalamic explants were removed from sections appearing similar to that shown in Fig. 5.4 A,C, as illustrated in Fig. 5.4 B,D. Analysis of *Pax6* (Fig. 5.4 E) and other gene expression patterns (Stoykova et al., 1996, Warren and Price, 1997, Kawano et al., 1999, Pratt et al., 2000b) helped to define tissue landmarks and to make accurate dissections.

Dorsal thalamus from *tau-GFP:Pax6$^{+/+}$* embryos produced prolific outgrowth into wild-type ventral telencephalon, extending well over half-way through the telencephalic explants in 76% of cultures (typical examples are shown in Fig. 5.4 F,G).

Figure 5.2

Schematic showing how tau-GFP labelled and unlabelled tissues are combined in tissue culture for the explant co-culture and seeding experiments described in the text. For explant co-cultures, tau-GFP expressing dorsal thalamus (dt) is combined with non-expressing cerebral cortex (cc), ventral telencephalon (vtel), or hypothalamus (ht) and the extent of innervation of unlabelled explants by tau-GFP labelled fibres is assessed. For seeding cultures, tau-GFP expressing dorsal thalamus is dissociated and seeded onto a slice of unlabelled forebrain and the extent to which labelled cells adhere and grow on particular regions is assessed. Tau-GFP expressing cells and tissues are colored black.

Figure 5.2

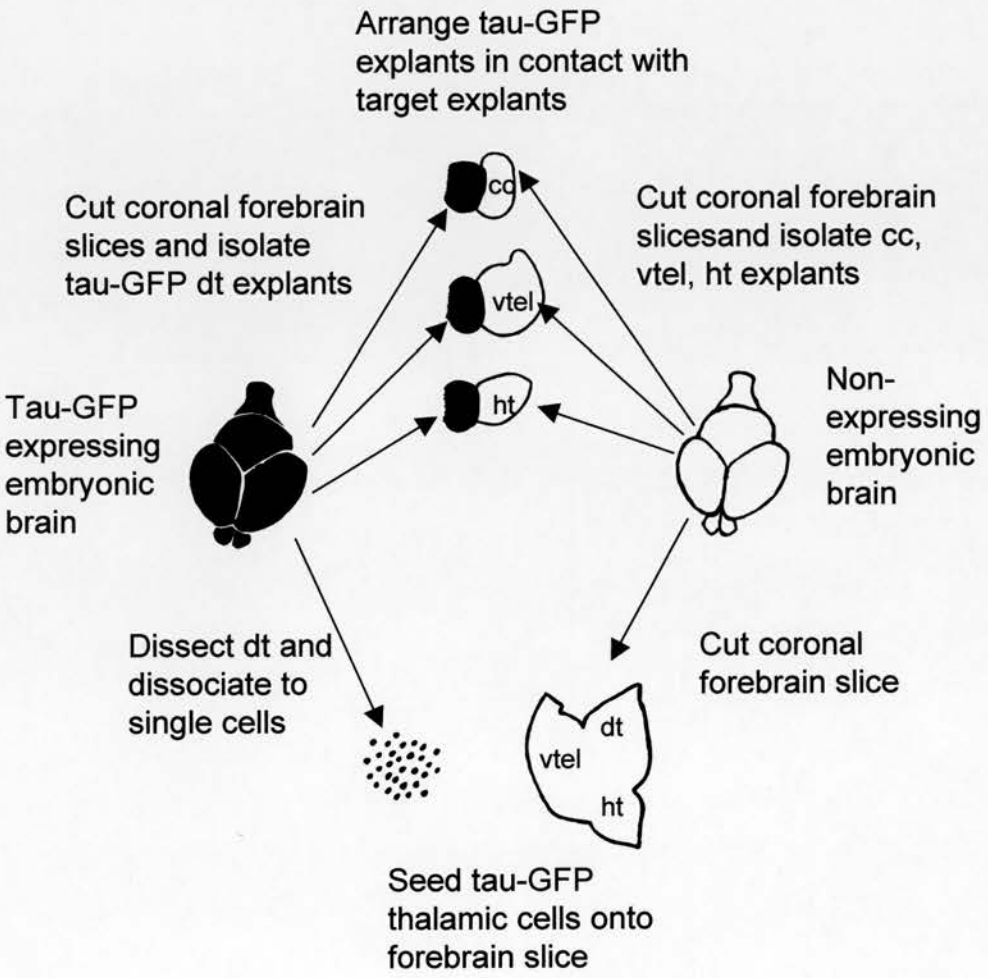
Arrange tau-GFP explants in contact with target explants
Cut coronal forebrain slices and isolate tau-GFP dt explants
Cut coronal forebrain slicesand isolate cc, vtel, ht explants
cc
vtel
ht
Tau-GFP expressing embryonic brain
Non-expressing embryonic brain
Dissect dt and dissociate to single cells
Cut coronal forebrain slice
dt
vtel
ht
Seed tau-GFP thalamic cells onto forebrain slice

In 62% of these cultures large numbers of thalamic axons often curved quite sharply in a dorsal direction. These features, illustrated in figure 5.4 F,G are reminiscent of the in vivo trajectory of thalamic axons as they grow through the internal capsule and turn dorsally towards the neocortex (Fig. 5.4 A, Fig. 1.2 on page 19). In marked contrast, none of the cultures of *tau-GFP:Pax6*$^{Sey/Sey}$ dorsal thalamus with wild-type ventral telencephalon showed these features. In 60% of these cultures, thalamic axons did enter the medial part of the ventral telencephalon, but in almost all these cases (86%) not even a single thalamic axon reached anywhere near halfway through the telencephalic explant. A typical example is shown in Fig. 5.4 H. In none of these cultures, nor in the 14% of cases where longer thalamic axons were seen (Fig. 5.4 I illustrates the culture in which there was most growth), was there any evidence of a consistent turning of the thalamic axons in a dorsal direction. Observations of tau-GFP labelled wild-type and *Pax6*$^{Sey/Sey}$ axons in some of these cultures during their 3 days in vitro revealed that the major features of innervation were established quickly, within 1-2 days of the start of culture, and there was less progression between 2 and 3 days. It is unlikely, therefore, that the defective innervation from the *tau-GFP:Pax6*$^{Sey/Sey}$ thalamic explants can be explained simply by a slowing of development.

In all cultures where *tau-GFP:Pax6*$^{+/+}$ dorsal thalamus was placed next to wild-type hypothalamus, thalamic axons coursed around its edge and failed to innervate it (Fig. 5.4 J), in agreement with previous findings on the repulsive nature of the hypothalamus for dorsal thalamic axons (Braisted et al., 1999). The same result was obtained in all cases where *tau-GFP:Pax6*$^{Sey/Sey}$ dorsal thalamic explants were used (Fig. 5.4 L). When *tau-GFP:Pax6*$^{+/+}$ dorsal thalamus was placed with wild-type cortex, most cultures showed large numbers of thalamic axons wrapping around its edges and upper and lower surfaces (Fig. 5.4 K). This pattern has been described before and is due

Figure 5.3

Time course of thalamic innervation in culture. Panels show green fluorescent images of tau-GFP expressing E14.5 thalamus cultured with cerebral cortex and imaged after (A,B) 1 day , (C,D) 2 days or (E,F) 3 days. (B,D,F) are higher power magnifications of (A, C, E) respectively. The major features of innervation are established between 1 and 2 days in culture. Each time point shows a different culture. Greyscale presentation of fluorescent images are shown with tau-GFP expressing thalamus and axons appearing grey (adjacent tau-GFP$^-$ tissue outlines can be discerned). Bars in (A, C, E); 500μm

Figure 5.3

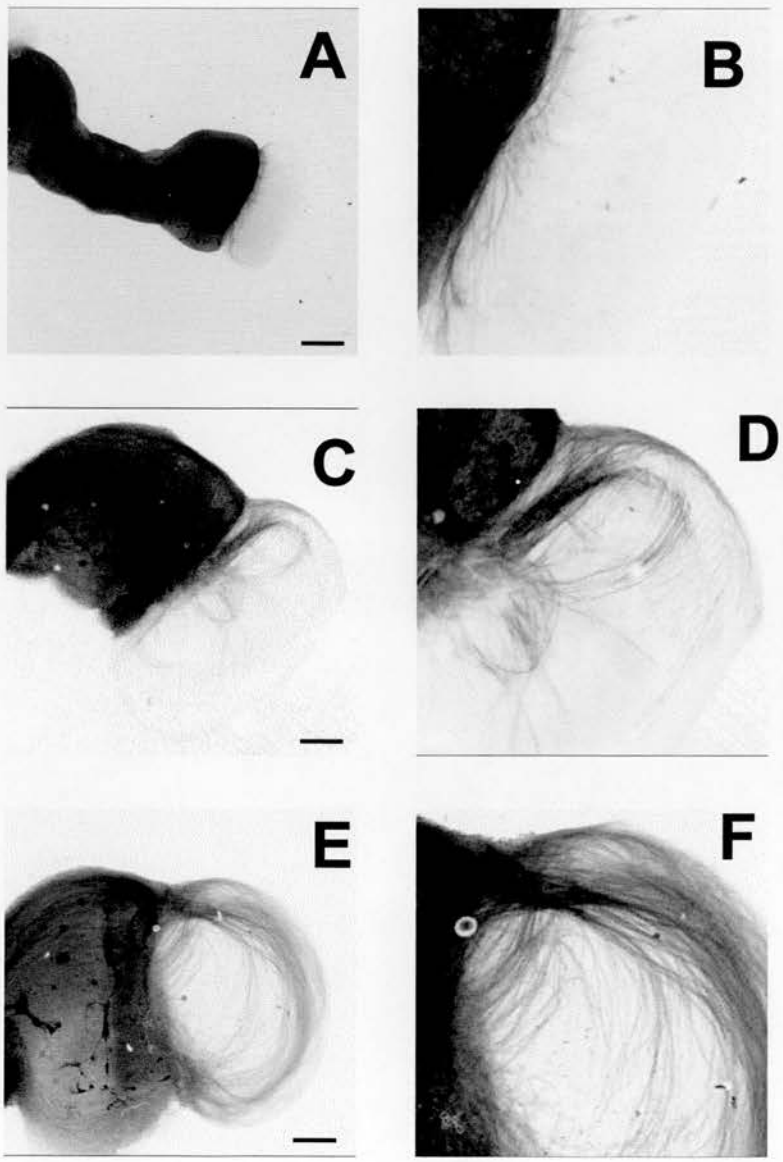

to the inability of the early cortical layers to receive thalamic innervation (Molnar and Blakemore, 1991, Goetz et al., 1992). In 95% of these cultures, thalamic axons extended distances equivalent to at least halfway round the circumference of the cortical explants. When *tau-GFP:Pax6*$^{Sey/Sey}$ dorsal thalamus was cultured with wild-type cortex, the pattern of thalamic axonal growth was similar to that with *tau-GFP:Pax6*$^{+/+}$ dorsal thalamus (Fig. 5.4 M), although in many cases it appeared that there were fewer thalamic axons.. In 92% of these cultures large numbers of axons extended distances equivalent to well over halfway round the circumference of the cortical explants, as occurred with the *tau-GFP:Pax6*$^{+/+}$ dorsal thalamus.

Several observations indicate that the inability of the *Pax6*$^{Sey/Sey}$ dorsal thalamus to generate normal innervation of ventral telencephalon is not caused by a non-specific inability to grow. First, *Pax6*$^{Sey/Sey}$ dorsal thalamic explants are capable of producing many long axons when co-cultured with wild-type cortex, as do *Pax6*$^{+/+}$ thalamic explants (Rennie et al., 1994). The apparent reduction in the numbers of mutant thalamic axons in these co-cultures is compatible with previous observations that mutant dorsal thalamus contains fewer neurons (proliferation in the early mutant diencephalon is reduced: (Warren and Price, 1997) although it could conceivably be due to a defective response by some thalamic neurons to cortex-derived growth-promoting factors. Second, analysis of nuclear morphology with TO-PRO3 showed that under all conditions used here almost all cells remain viable in both *Pax6*$^{+/+}$ and *Pax6*$^{Sey/Sey}$ dorsal thalamic explants. Third, in other experiments in which E14.5 dorsal thalamic explants were dissociated and cultured for 3 days in serum-free medium, *Pax6*$^{+/+}$ and *Pax6*$^{Sey/Sey}$ cells survived and grew neurites equally well (Edgar et al., 1999). Therefore, the inability of the *Pax6*$^{Sey/Sey}$ dorsal thalamus to generate normal ventral telencephalic

Figure 5.4

Pax6$^{Sey/Sey}$ thalamic explants exhibit defective tract formation, as shown by organotypic co-culture of *tau-GFP:Pax6*$^{+/+}$ or *tau-GFP:Pax6*$^{Sey/Sey}$ dorsal thalamic (dt) explants with *Pax6*$^{+/+}$ explants of ventral telencephalon (vtel), hypothalamus (ht), or cerebral cortex (cc). (A,C) Green fluorescent images of coronal sections of E14.5 *tau-GFP:Pax6*$^{+/+}$ and *tau-GFP:Pax6*$^{Sey/Sey}$ brains similar to those from which explants were dissected. (A) *tau-GFP:Pax6*$^{+/+}$ embryo showing strong tau-GFP labelling of thalamic axons as they turn sharply to avoid the hypothalamus and enter the ventral telencephalon to form the internal capsule (*). (C) *tau-GFP:Pax6*$^{Sey/Sey}$ embryo, showing that the strong tau-GFP label seen in *tau-GFP:Pax6*$^{+/+}$ embryos is lacking from the position normally occupied by the internal capsule (*). (B,D) Schematic representations of sections shown in A,C with red dotted lines indicating locations of cuts used to isolate from coronal slices the tissues used in these experiments (dt, vtel, ht and cc). Panels (A-D) show only one side but note that the left and right dorsal thalamus were left joined dorsally in culture and their cut edges, just anterior to the border with ventral thalamus, were placed against different tissues on each side. The border between the ventral and dorsal thalamus, as defined by tissue landmarks and the expression of genes such as *Dlx2* and *Pax6*, is shown with a blue line. (E) In situ hybridisation on a 200 μm-thick Vibratome section (pink counterstain) of a *Pax6*$^{Sey/Sey}$ E14.5 embryo corresponding to the section in C,D, showing expression of *Pax6* (purple) in the thalamus, where it acts as a marker of ventral thalamus even in the mutants (Stoykova et al., 1996; Warren and Price, 1997), and telencephalon. (F-M) Representative examples of co-cultures of (F,G,J,K) *tau-GFP:Pax6*$^{+/+}$ thalamus or (H,I,L,M) *tau-GFP:Pax6*$^{Sey/Sey}$ thalamus with (F-I) *Pax6*$^{+/+}$ ventral telencephalon, (J,L) *Pax6*$^{+/+}$ hypothalamus or (K,M) *Pax6*$^{+/+}$ cerebral cortex. Greyscale presentation of fluorescent images are shown with tau-GFP expressing thalamus and axons appearing grey (adjacent tau-GFP^{-} tissue outlines can be discerned). (N) Schematic showing *Pax6*$^{+/+}$ and *Pax6*$^{Sey/Sey}$ thalamocortical cells. The red **X** indicates an autonomous defect of the *Pax6*$^{Sey/Sey}$ thalamocortical growth cone that prevents it from responding appropriately to growth and guidance cues in the ventral telencephalon. Fig. 5.4 E was taken from Pratt et al., 2000b. All images to same scale with bar in (M); 200μm.

Figure 5.4.

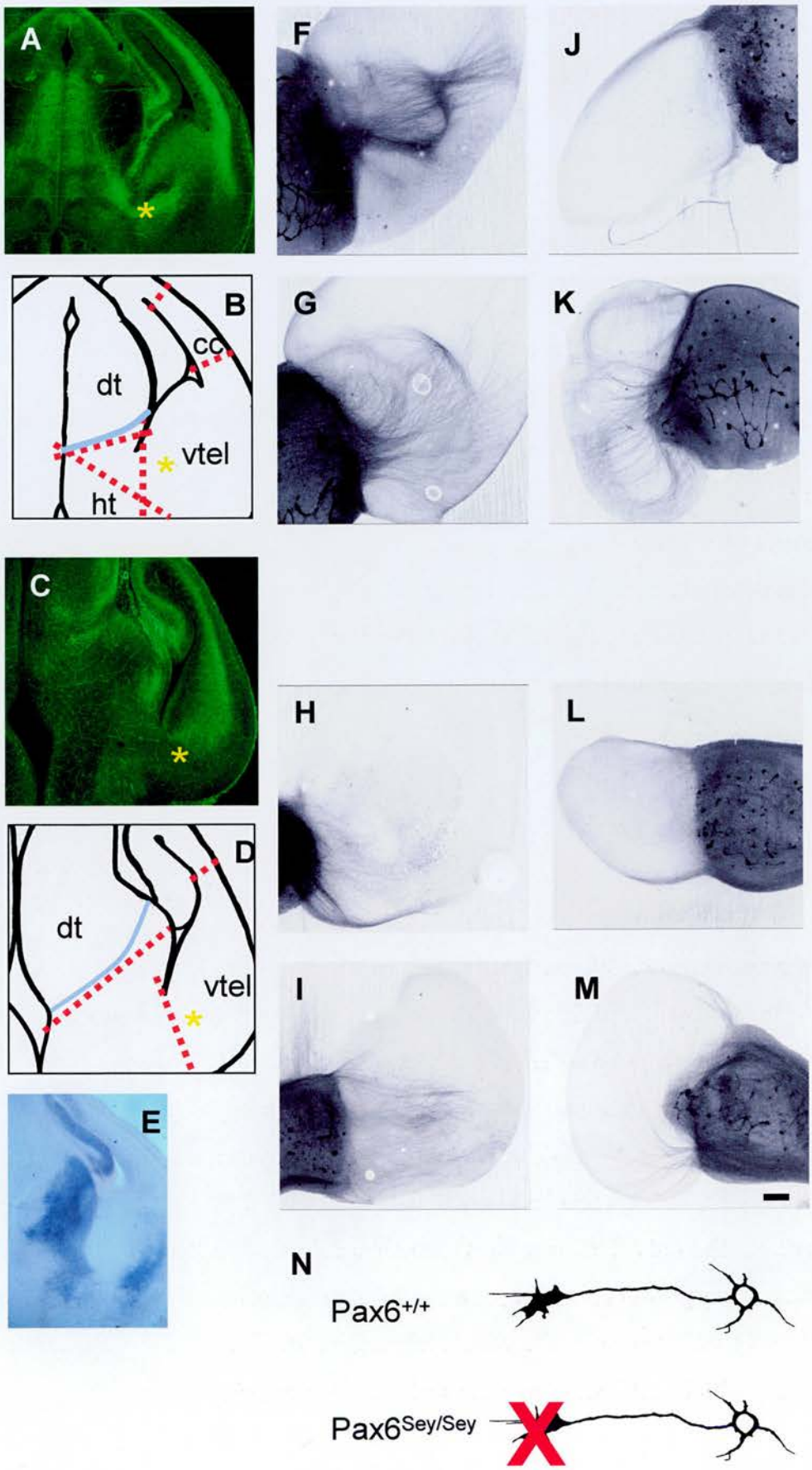

Figure 5.5

The nature of the ventral telencephalon in *Pax6*$^{Sey/Sey}$ embryos. Organotypic co-culture of *tau-GFP:Pax6*$^{+/+}$ dorsal thalamic explant with explant of *Pax6*$^{Sey/Sey}$ ventral telencephalon. Greyscale presentation of fluorescent image shown with tau-GFP expressing thalamus and axons appearing grey (adjacent tau-GFP^{-} tissue outline can be discerned). Note large numbers of thalamic fibres penetrating the ventral telencephalon. Bar, 200μm.

Figure 5.6

Seeding experiment in which dissociated (A, B) *tau-GFP:Pax6*$^{+/+}$ or (C, D) *tau-GFP:Pax6*$^{Sey/Sey}$ thalamic cells were seeded onto *Pax6*$^{+/+}$ forebrain slices and imaged after time in culture. Panels (A-D) are centred on the region occupied by the internal capsule(*). Note that many more *Pax6*$^{+/+}$ cells adhere to the internal capsule than *Pax6*$^{Sey/Sey}$ cells. Panel E shows *tau-GFP:Pax6*$^{Sey/Sey}$ cells adhering to a different forebrain region. F is a cartoon of a forebrain slice showing the position of the internal capsule (*) on which panels (A to D) are centred and the approximate location of the panel shown in E. Greyscale presentation of fluorescent images are shown with tau-GFP expressing thalamic cells appearing grey. Bar; 100μm.

Figure 5.5

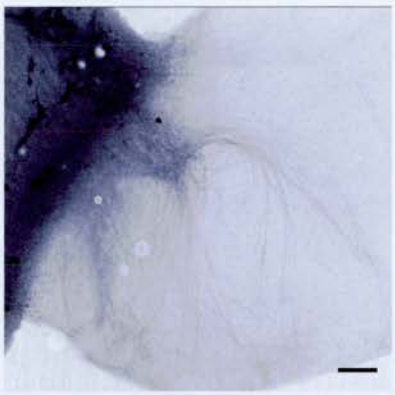

Figure 5.6

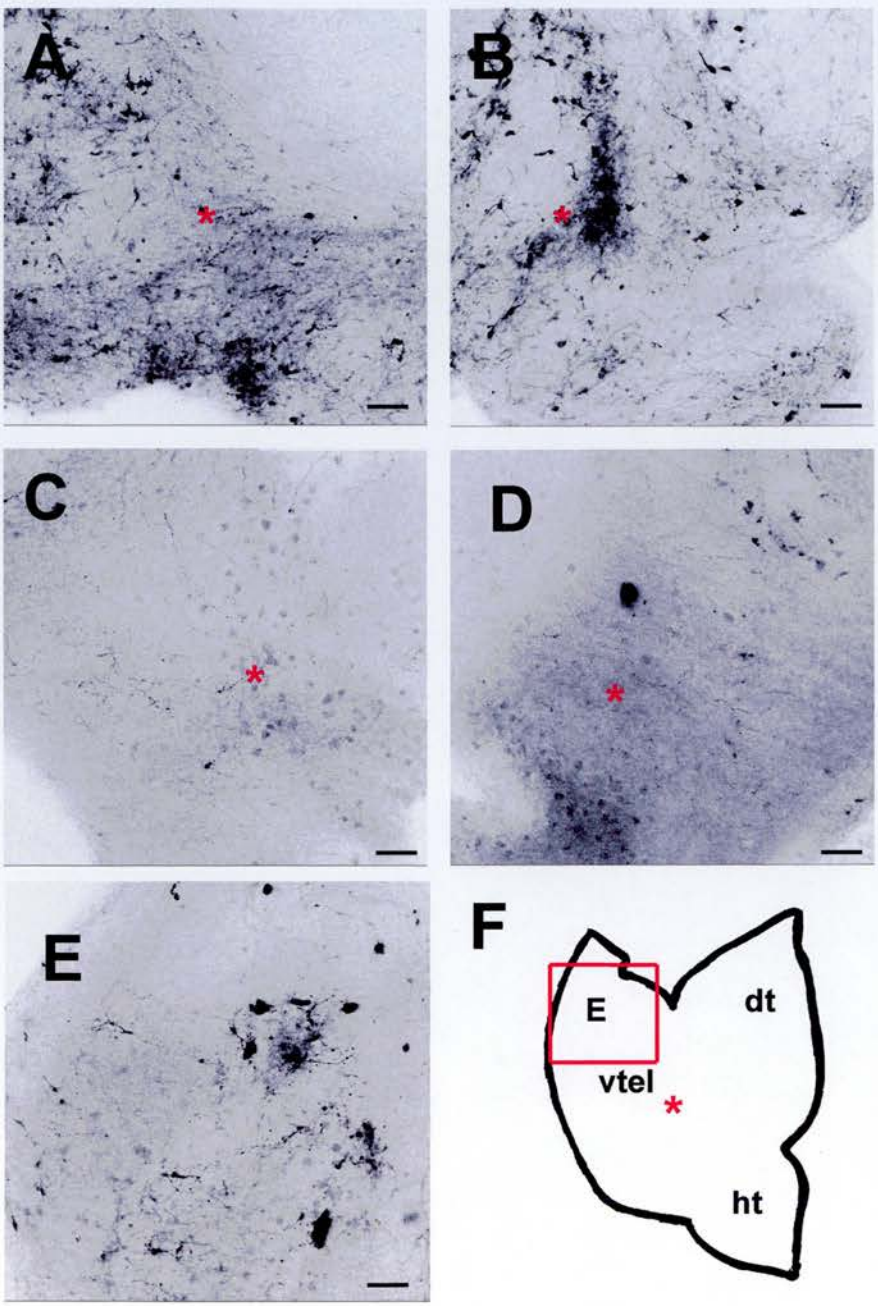

innervation is likely to be due to its inability to respond to growth and guidance cues in that region.

Although the main focus of this work was the dorsal thalamus and its axons, I carried out a few experiments to gain a better idea of the status of the ventral telencephalon in the mutants. In cultures of *tau-GFP:Pax6*$^{+/+}$ dorsal thalamus with *Pax6*$^{Sey/Sey}$ ventral telencephalon I observed prolific innervation by long axons, indicating that the mutant ventral telencephalon does not lack the ability to stimulate and receive dorsal thalamic innervation (Fig. 5.5 A). Innervation did not appear normal, however, and many axons turned in abnormal ways in the mutant ventral telencephalon (compare Fig. 5.5 with Fig. 5.4 F,G). Although the *Pax6*$^{Sey/Sey}$ ventral telencephalon may be permissive for incoming thalamic axons, it is quite possible that defects in this region contribute to the lack of thalamocortical innervation in small eye homozygotes.

When wild-type dorsal thalamic cells were seeded onto coronal wild type brain slices they adhered to the internal capsule (Fig. 5.6 A,B; marked with *). The thalamocortical tract projects through this structure at the junction between ventral thalamus and ventral telencephalon. When the experiment was repeated with mutant thalamic cells, this adhesion was lost (Fig. 5.6 C,D). This result was not due to general lack of viability of the *Pax6*$^{Sey/Sey}$ thalamic cells in my culture as they did adhere to and grow on other regions of the slice (Fig. 5.6 E). This supports the findings from the explant cultures that Pax6 is required in dorsal thalamic cells to program their adhesive properties, specifically their ability to project into the ventral telencephalon.

DISCUSSION

The thalamocortical tract fails to form normally in *Pax6*$^{Sey/Sey}$ mice. In wild type (*Pax6*$^{+/+}$) embryos the tract projects from the dorsal thalamus and travels through the ventral thalamus, avoids the hypothalamus, turns sharply into the ventral telencephalon

(forming the internal capsule) and then reaches its target in the cerebral cortex (Tuttle et al., 1999, Braisted et al., 1999, Auladell et al., 2000). In *Pax6*$^{Sey/Sey}$ mice, the dorsal thalamus does project a tract but it fails to enter the cortex and appears to become stalled en route from the ventral thalamus to the ventral telencephalon (Kawano et al., 1999, Pratt et al., 2000b).

A comparison of timetables for *Pax6* gene expression in developing forebrain (Stoykova et al., 1996, Grindley et al., 1997, Mastick et al., 1997, Warren and Price, 1997, Kawano et al, 1999) and thalamocortical tract formation (Tuttle et al., 1999, Braisted et al, 1999, Auladell et al., 2000) suggests several locations at which *Pax6* could influence the developing thalamocortical tract (Fig. 1.4 on page 38). *Pax6* is expressed at many points along the thalamocortical pathway at times coinciding with critical events in thalamocortical tract formation, including the dorsal thalamus where *Pax6* expression coincides with neurogenesis between E10 and E13 (Angevine, 1970) and the ventral thalamus, the hypothalamus, the ventral telencephalon and the cerebral cortex which also express Pax6. The failure of the thalamocortical tract to form in the absence of *Pax6* could reflect a requirement for *Pax6* at one or more of these locations.

Pax6 and formation of the dorsal thalamus

Previous studies of the embryonic diencephalon in *Pax6*$^{Sey/Sey}$ mice showing relatively normal anterior to posterior (A-P) expression patterns of *Dlx, Otx, Emx,* and *Wnt* genes, *Prox1*, *Gbx2, Mash1* and *Pax6* have indicated that diencephalic A-P patterning is not greatly disturbed (Stoykova et al., 1996, Warren and Price, 1997, Grindley et al., 1997). These gene expression studies have suggested that the embryonic *Pax6*$^{Sey/Sey}$ diencephalon possesses correlates of the histogenetic regions that in wild-types give rise to major diencephalic structures. Despite obvious distortions in the shape of the embryonic *Pax6*$^{Sey/Sey}$ diencephalon (Warren and Price 1997, Stoykova et al., 1996)

which may in part be due to defects of cell proliferation in this region (Warren and Price, 1997) morphological features reminiscent of those that distinguish diencephalic regions in wild-types have been described. Equivalents of prosomeres 1-3 and their main components, the ventral and dorsal thalamus and the pretectum, have been identified on the basis of gene expression and morphology in the mutants and named according to their wild-type counterparts (Stoykova et al., 1996, Mastick et al., 1997, Warren et al., 1997, Kawano et al., 1999, Pratt et al., 2000b).

The alterations in the expression patterns of several genes (*Hbnf*, *VMAT2*, *Lim1/Lhx1*, and *Nkx2.2*) are superimposed on these structures and reflect a failure of the $Pax6^{Sey/Sey}$ dorsal thalamus to differentiate normally in the absence of *Pax6* expression (Pratt et al., 2000b). These molecular patterning defects indicate that the differentiation program of the $Pax6^{Sey/Sey}$ dorsal thalamus is disrupted during the period when it fails to make appropriate connections with the cerebral cortex.

Pax6 and dorsal thalamic tract projection

From observations of the $Pax6^{Sey/Sey}$ brain alone, it is conceivable that the thalamocortical tract defect results from an autonomous defect in the dorsal thalamus itself, or from defects in the environment through which the thalamocortical axons navigate, or a combination of the two. To address this issue, I show that explants of mutant dorsal thalamus are defective in their ability to project a tract capable of correct navigation through wild type ventral telencephalon. This defect may be limited to this specific aspect of thalamocortical growth since $Pax6^{Sey/Sey}$ thalamic axons innervate wild-type cortex and avoid wild-type hypothalamus, as do wild-type thalamic axons. This provides direct evidence that *Pax6* expression is required within the dorsal thalamus itself, regardless of whether *Pax6* expression is also required at other locations. This

experiment could not rule out the possibility that these axon navigation properties were programmed non-autonomously by Pax6 prior to explant preparation.

Because my thalamic explants contained some ventral thalamus and epithalamus as well as dorsal thalamic tissue, it is formally possible that these results could be explained by the lack of essential signalling to axons en passant (Wang and Tessier-Lavigne, 1999). This possibility would demand that adjacent tissues instruct axons leaving the dorsal thalamus in ventral telencephalic navigation. The zli or the ventral thalamus would be possible candidates for this type of interaction (Mastick et al., 1997; Braisted et al., 1999; Tuttle et al., 1999). The evidence, however, is against such a possibility. Wild-type thalamic explants in my cultures exhibit similar features of axon outgrowth to those reported in cultures using dorsal thalamic explants prepared from embryonic brain at similar ages but with surrounding tissues removed. These features include avoidance of the hypothalamus, attraction towards the ventral telencephalon and penetration of the cortex (Molnar and Blakemore, 1991, Goetz et al., 1992, Braisted et al., 1999, Braisted et al., 2000). Since these 'pure' dorsal thalamic explants have been isolated from potential instruction by cells lying outside the dorsal thalamus, such instructions are unlikely to be important for these features of thalamocortical formation.

The design and interpretation of the explant experiments depend on correct identification of the dorsal thalamus in a mutant brain. Given the disturbed anatomy of the *Pax6*$^{Sey/Sey}$ diencephalon, it was critical that in spite of these abnormalities the dorsal thalamic explants isolated from the *Pax6*$^{+/+}$ and *Pax6*$^{Sey/Sey}$ brain were 'equivalent'. The *Pax6*$^{Sey/Sey}$ embryo does possess a structure corresponding to the dorsal thalamus which can be identified by its morphology and gene expression patterns (see above), and which does project axons. The problem of equivalence reduces to choosing explants in which axons projecting from *Pax6*$^{Sey/Sey}$ and *Pax6*$^{+/+}$ dorsal thalamus have equal opportunities to interact with target tissues. The major defect in thalamocortical tract formation in

mutants appears to occur as axons attempt to navigate from the ventral thalamus into the ventral telencephalon (Kawano et al., 1999, Pratt et al., 2000b). There is no evidence that axons originating from the dorsal thalamus become stalled in the ventral thalamus or that they fail to avoid the hypothalamus. I therefore selected explants that centred on the dorsal thalamus but also contained some ventral thalamic and epithalamic tissue. This ensured that dorsal thalamus was present and enabled me to position explants to recreate the topography of the intact brain more accurately than if I had attempted to dissect smaller pieces of tissue with resulting loss of anatomical landmarks. Since the ventral thalamus/ ventral telencephalon transition zone, where thalamocortical defects in the *Pax6*$^{Sey/Sey}$ mice occur, was absent from our thalamic explants, axons from *tau-GFP:Pax6*$^{Sey/Sey}$ or *tau-GFP:Pax6*$^{+/+}$ thalamic explants were able to navigate to the edge of the thalamic explant where they were confronted by the target tissue. The observation that thalamic axons responded to the target tissues in ways reminiscent of their behaviour in vivo supported the accuracy of my culture system.

The explant experiments showed that there is an autonomous requirement for Pax6 within the dorsal thalamus. The dorsal thalamus is a complex structure and it is possible that Pax6 expressing cells not projecting axons to the cortex influence the properties of thalamocortical cells. An analogous role for Pax6 occurs in the tract of the post-optic commissure (Mastick et al., 1997) and en passant interactions (Wang and Tessier-Lavigne, 1999) might influence thalamocortical axons. Dissociation isolates the thalamic cell from non-autonomous signals, which might otherwise be supplied by the dorsal thalamus. When thalamic cells were seeded onto slices of brain the *Pax6*$^{Sey/Sey}$ thalamic cells did not adhere to the internal capsule which was clearly an attractive substrate for *Pax6*$^{+/+}$ thalamic cells. This fitted nicely with the results of the explant co-cultures above, which showed that Pax6 was required within the dorsal thalamus for tract projection into the ventral telencephalon. Pax6 is therefore required to program

these adhesive properties and this requirement is not dependant on continued contact with other cells in the dorsal thalamus. This experiment could not rule out the possibility that these adhesive properties were irreversibly programmed non-autonomously by Pax6 prior to dissociation.

The seeding experiments described here produced a clear result but suffered from several limitations. Firstly, culturing whole forebrain slices resulted in loss of definition due to the culture spreading out and this made identification of structures of interest difficult (the central location of the internal capsule made it the easiest to locate). Secondly, the whole forebrain slice is a complex environment and it would be interesting to assess adhesion of thalamic cells to individual forebrain structures such as internal capsule, hypothalamus and cerebral cortex in isolation. This would minimise problems in subsequent identification of structures. Thirdly, I assessed a mixture of adhesion, growth and survival of seeded cells and it would be interesting to assess adhesion of thalamic cells after shorter periods before they had time to grow and migrate. It would be interesting to perform seeding experiments with cells isolated before the tract starts to project (E10 to E13) while they are still expressing Pax6.

Pax6 and the ventral telencephalon

The *Pax6*$^{Sey/Sey}$ ventral telencephalon maintains normal expression patterns of Netrin1 (Pratt et al., 2000b) a molecule implicated in thalamocortical tract formation (Braisted et al., 2000) and is permissive to wild-type thalamic axons. Therefore, although it is possible that defects in the ventral telencephalon contribute to the lack of thalamocortical innervation in *Pax6*$^{Sey/Sey}$ embryos, I find no evidence that such defects can account for the *Pax6*$^{Sey/Sey}$ thalamocortical phenotype wholly.

Pax6 and regulation of cell surface properties

The cerebral cortex, like the dorsal thalamus, exhibits *Pax6* expression in ventricular zone cells during neurogenesis and downregulates Pax6 expression in postmitotic cells. The expression of Pax6 in proliferating cortical neurons influences their postmitotic gene expression patterns and cell surface properties with the maintenance of this genetic pattern becoming independent of the presence of Pax6 (Warren et al., 1999). Work on the developing cerebral cortex has implicated *Pax6* in regulating members of the cadherin family of cell adhesion molecules (Stoykova et al., 1997) and the trk family of neurotrophin receptors (Warren et al., 1999). In vitro aggregation assays (Stoykova et al., 1997) and transplantation experiments (David Price unpublished observations) have established that the adhesive properties of cortical cells are altered in *Pax6*$^{Sey/Sey}$ embryos. Roles for *Pax6* in regulating adhesive properties have been elegantly demonstrated in the eye by analysis of *Pax6*$^{-/-}$ $\leftrightarrow$ *Pax6*$^{+/+}$ chimeras (Quinn et al., 1996, Collinson et al., 2000). *Pax6* has also been implicated in axon pathfinding in the tract of the postoptic commissure (Mastick et al., 1997) and the spinal cord (Ericson et al., 1997, Osumi et al., 1997) as well as in the thalamocortical tract (Tuttle et al, 1999, Kawano et al., 1999). Consistent with its roles elsewhere in the CNS, Pax6 probably controls thalamocortical tract formation by regulating the cell surface

properties of thalamocortical cells and influencing the navigation choices made by their growth cones.

Clarification of the molecular mechanisms of Pax6 action will be facilitated as the tally of molecules implicated in thalamocortical tract formation increases. At present these include cell surface receptors DCC, Neogenin, Robo1, Robo2, RPTPδ, Sema6A and LAMP, and secreted molecules Netrin1, Slit1 and Slit2 (Ringsted et al., 1999, Braisted et al., 2000, Tuttle et al., 1999, Mann et al., 1998, Leighton et al., 2001). These signalling systems may not act in isolation. For example, Robo1 and DCC (receptors for Slit2 and Netrin1) form a complex which controls commissural axon crossing of the vertebrate midline via a receptor mediated silencing mechanism (Stein and Tessier-Lavigne, 2001) and similar interactions may also operate in thalamocortical axons. A recent study by Braisted et al., (2000) has demonstrated that Netrin1 promotes the growth of thalamocortical axons through the ventral telencephalon and so it is possible that abnormalities in *Pax6*$^{Sey/Sey}$ embryos may be contributed to by defects of receptors mediating its attractant effects, DCC and Neogenin. Both are expressed in the normal dorsal thalamus. Preliminary evidence, however, suggests that DCC is still expressed in the dorsal thalamus of *Pax6*$^{Sey/Sey}$ embryos (Pratt et al., 2000b). As thalamocortical tract defects are less severe in loss-of-function Netrin1 mutants than in *Pax6*$^{Sey/Sey}$ embryos and blocking Netrin1 in vitro does not abolish thalamic axon attraction to ventral telencephalon (Braisted et al., 2000), it is hard to explain the small eye defects on the basis of a loss of Netrin1 responsiveness alone. Other perhaps as yet unidentified signalling systems are likely involved.

Conclusion

The requirement for Pax6 in the dorsal thalamus is lifted by the time its cells become postmitotic. It is possible that *Pax6* has direct effects on the expression of cell surface molecules involved in receptor/ligand interactions, cell adhesion or axon pathfinding before it is downregulated. On the other hand, findings that the defective responses of $Pax6^{Sey/Sey}$ dorsal thalamic axons coincide with persistent changes in the expression patterns of regulatory genes other than *Pax6* from the early stages of dorsal thalamic development (Pratt et al., 2000b) allows the possibility that these defects result indirectly from the early absence of Pax6 in this region. Genes such as *Lim1/Lhx1* or *Nkx2.2* whose expression is influenced by *Pax6* may have more direct effects, for example up- or downregulating the expression of effector molecules. Whether direct or indirect, I conclude that *Pax6* plays an essential role in the development of the dorsal thalamus and the ability of its axons to respond to key growth and guidance cues.

Future work

Presumably Pax6 influences the development of thalamocortical axons by transcriptional regulation of genes involved in axon navigation. Identification of transcriptional targets would show the extent to which Pax6 directly regulates the transcription of cell surface molecules as opposed to controlling the transcription of regulatory molecules (for example other transcription factors) which in turn influence axon navigation properties.

Gene expression profiling provides a means for identifying Pax6 targets by identifying genes whose transcription is sensitive to Pax6 activity. Levels of particular transcripts could be compared between thalamocortical cells isolated from $Pax6^{+/+}$ and $Pax6^{-/-}$ embryos at various stages of thalamocortical development. Pax6 expression could be artificially induced (or inhibited) to identify genes whose transcription is

sensitive to Pax6. These profiling studies could be used to perform selected screens, for example screening the panel of genes recently implicated in axon navigation by a gene trap screen (Leighton et al., 2001) or to search random libraries of mouse transcripts for novel genes. Genes whose expression levels have already been shown to be influenced by Pax6 (or not) could be utilised as controls in such experiments.

A complementary approach to understanding Pax6 function is to catalogue *Pax6*$^{Sey/Sey}$ thalamocortical axon defects at the cellular and subcellular levels. For example it is unknown whether properties such as thalamocortical axon fasciculation and branching or growth cone complexity or collapse are altered in the *Pax6* mutant. The use of in vitro assays including neuron-turning assays, membrane stripe assays and primary co-culture experiments (including the co-culture assays described above) allows the measurement of these properties. In vitro systems can be used to assess the roles of candidate effector molecules by manipulating their availability to the thalamocortical axon and observing its response.

Hopefully these two approaches will be synergistic. The characterisation of genes under the direct and indirect transcriptional control of Pax6 will supply candidates whose roles in *Pax6*$^{Sey/Sey}$ thalamocortical tract phenotype can be tested and identification of Pax6$^{Sey/Sey}$ subcellular phenotypes may suggest classes of molecule for gene expression profiling. This knowledge will be useful in the wider context of understanding brain-wiring mechanisms as well as in the more esoteric field of *Pax6* study.

BIBLIOGRAPHY

Acampora, D., Barone, P. and Simeone, A. (1999). *Otx* genes in corticogenesis and brain development. *Cereb Cortex.* **9**, 533-542.

al-Shawi, R., Kinnaird, J., Burke, J. and Bishop, J. O. (1990). Expression of a foreign gene in a line of transgenic mice is modulated by a chromosomal position effect. *Mol. Cell Biol.* **10**, 1192-1198.

Altman, J. and Bayer, S. A. (1995). Atlas of prenatal rat brain development. CRC Press.

Anderson, S. A., Eisenstat, D. D., Shi, L. and Rubenstein, J. L. (1997). Interneuron migration from basal forebrain to neocortex: dependence on Dlx genes. *Science* **278**, 474-476.

Angevine, J. B. Jr. (1970). Time of neuron origin in the diencephalon of the mouse. An autoradiographic study. *J. Comp. Neurol.* **139**, 129-187.

Aruffo, A. and Seed, B. (1987). Molecular cloning of a CD28 cDNA by a high-efficiency COS cell expression *Proc Natl Acad Sci U S A* **84**, 8573-8577.

Auladell, C., Perez-Sust, P., Super, H. and Soriano, E. (2000) The early development of thalamocortical and corticothalamic projections in the mouse. *Acta Embryol.* **201**, 169-179.

Bain, G., Kitchens, D., Yao, M., Huettner, J. E. and Gottlieb, D. I. (1995). Embryonic stem cells express neuronal properties *in vitro. Dev. Biol.* **168**, 342-357.

Baird, G. S., Zacharias, D. A. and Tsien, R. Y.(2000). Biochemistry, mutagenesis, and oligomerization of DsRed, a red fluorescent protein from coral. *Proc. Natl. Acad. Sci. U.S.A.* **97**, 11984-11989.

Bishop, K. M., Goudreau, G. and O'Leary, D. D. M. (2000). Regulation of area identity in the mammalian neocortex by Emx2 and Pax6. *Science* **288**, 344-349.

Braisted, J. E., Catalano, S. M., Stimac, R., Kennedy, T. E., Tessier-Lavigne, M., Shatz, C. J. and O'Leary, D. D. M. (2000) Netrin1 promotes thalamic growth and is required for proper development of the thalamocortical projection. (2000). *J. Neurosci.* **20,** 5792-5801.

Braisted, J. E., Tuttle, R. and O'Leary, D. D. M. (1999). Thalamocortical axons are influenced by chemorepellent and chemoattractant activities localized to decision points along their path. *Dev. Biol.* **208**, 430-440.

Brazelton, T. R., Rossi, F. M., Keshet, G. I. and Blau, H. M. (2000). From marrow to brain: expression of neuronal phenotypes in adult mice. *Science* **290**, 1775-1779.

Brion, J. P., Tremp, G. and Octave, J. N. (1999). Transgenic expression of the shortest human tau affects its compartmentalization and its phosphorylation as in the pretangle stage of Alzheimer's disease. *Am. J. Pathol.* **154**, 255-270.

Briscoe, J., Sussel, L., Serup, P., Hartigan-O'Connor, D., Jessell, T. M., Rubenstein, J. L. and Ericson, J. (1999). Homeobox gene Nkx2.2 and specification of neuronal identity by graded Sonic hedgehog signalling. *Nature* **398**, 622-627.

Bryan, J. T. and Morasso, M. I.(2000). The Dlx3 protein harbors basic residues required for nuclear localization, transcriptional activity and binding to msx1. *J. Cell Sci.* **113**, 4013-4023.

Buee, L., Bussiere, T., Buee-Scherrer, V., Delacourte, A. and Hof, P. R. (2000). Tau protein isoforms, phosphorylation and role in neurodegenerative disorders. *Brain Res. Brain Res. Rev.* **33**, 95-130.

Bulfone, A., Puelles, L., Porteus, M. H., Frohman, M. A., and Rubenstein, J. L. R. (1993). Spatially restricted expression of Dlx-1, Dlx-2 (Tes-1), Gbx-2 and Wnt-3 in the embryonic day 12.5 mouse forebrain defines potential transverse and longitudinal segmental boundaries. *J. Neurosci.* **13**, 3155-3172.

Butner, K. A., Kirschner, M. W. (1991). Tau protein binds to microtubules through a flexible array of distributed weak sites. *J. Cell Biol.* **115**, 717-730.

Callahan, C. A. and Thomas, J. B. (1994). Tau-β-galactosidase, an axon targeted fusion protein. *Proc. Natl. Acad. Sci. U.S.A* **91**, 5972-5976.

Caric, D., Gooday, D., Hill, R. E., McConnell, S. K. and Price, D. J. (1997). Determination of the migratory capacity of embryonic cortical cells lacking the transcription factor Pax6. *Development* **124**, 5087-5096.

Cecconi, F. and Meyer, B. I. (2000). Gene trap: a way to identify novel genes and unravel their biological function. *F.E.B.S. Lett.* **480**, 63-71.

Chalfie, M., Tu, Y., Euskirchen, G., Ward, W. W. and Prasher, D. C. (1994). Green fluorescent protein as a marker for gene expression. *Science* **263**, 802-805.

Chapouton, P., Gartner, A. and Gotz, M. (1999). The role of Pax6 in restricting cell migration between developing cortex and basal ganglia. *Development* **126**, 5569-5579.

Chen, J., Kanai Y., Cowan, N. J. and Hirokawa, N. (1992). Projection domains of MAP2 and tau determine spacings between microtubules in dendrites and axons. *Nature* **360**, 674-677.

Chiang, C., Litingtung, Y., Lee, E., Young, K. E., Corden, J. L., Westphal, H. and Beachy, P. A. (1996). Cyclopia and defective axial patterning in mice lacking Sonic hedgehog gene function. *Nature* **383**, 407-413.

Chow, R. L., Altmann, C. R., Lang, R. A. and Hemmati-Brivanlou, A. (1999). Pax6 induces ectopic eyes in a vertebrate. *Development* **126**, 4213-4222.

Cohen-Tannoudji, M., Babinet, C. and Wassef, M. (1994). Early determination of a mouse somatosensory cortex marker. *Nature* **368**, 460-463.

Collinson, J. M., Hill, R. E. and West, J. D. (2000). Different roles for Pax6 in the optic vesicle and facial epithelium mediate early morphogenesis of the murine eye. *Development* **127**, 945-956.

Cooke, J. E., Moens, C. B., Roth, L. W. A., Durbin, L., Shiomi, K., Brennan, C., Kimmel, C. B., Wilson, S. W. and Holder, N. (2001). Eph functions downstream of Val to regulatecell sorting and boundary formation in the caudalhindbrain. *Development* **128**, 571-580

Corish, P. and Tyler-Smith, C.(1999). Attenuation of green fluorescent protein half-life in mammalian cells. *Protein Eng.* **12**, 1035-40.

Cormack, B. P., Valdivia, R. H. and Falkow, S. (1996). FACS-optimized mutants of the green fluorescent protein (GFP). *Gene* **173,** 33-8.

Cvekl, A., Sax, C. M., Li, X., McDermott, J. B. and Piatigorsky, J. (1995). Pax-6 and lens-specific transcription of the chicken delta 1-crystallin gene. *Proc. Natl. Acad. Sci. U.S.A.* **92**, 4681-4685.

Dawson, H. N., Ferreira, A., Eyster, M. V.,Ghoshal, N., Binder, L .I. and Vitek, M. P. (2001). Inhibition of neuronal maturation inprimary hippocampal neurons from tau deficient mice. *Journal of Cell Science* **114**, 1179-1187

Deiner, M. S. and Sretavan, D. W. (1999). Altered midline axon pathways and ectopic neurons in the developing hypothalamus of netrin-1- and DCC-deficient mice. *Development* **120**, 2811-2822.

Dopf, J. and Horiagon, T. M. (1996). Deletion mapping of the Aequorea victoria green fluorescent protein. *Gene* **173**, 39-44.

Duncan. M. K., Haynes, J.I., Cvekl, A. and Piatigorsky, J. (1998). Dual roles for Pax-6: a transcriptional repressor of lens fiber cell-specific beta-crystallin genes. *Mol. Cell Biol.* **18**, 5579-5586.

Edgar, J. M., Asavaritikrai, P. and Price, D. J. (1999) Cell death and the neurotrophic theory in developing thalamus. *Soc. Neurosci. Abstr.* **25**, 705.5.

Emerling, D. E. and Lander, A. D. (1996). Inhibitors and promoters of thalamic neuron adhesion and outgrowth in embryonic neocortex: functional association with chondroitin sulfate. *Neuron* **17**, 1089-1100.

Emerling, D. E. and Lander, A. D.(1994). Laminar specific attachment and neurite outgrowth of thalamic neurons on cultured slices of developing cerebral neocortex. *Development* **120**, 2811-2822.

Engelkamp, D., Rashbass, P., Seawright, A. and van Heyningen, V. (1999). Role of Pax6 in development of the cerebellar system. *Development* **126**, 3585-96.

Ericson, J., Morton, S., Kawakami, A., Roelink, H. and Jessell, T. M. (1996). Two critical periods of sonic hedgehog signalling required for the specification of motor neuron identity. *Cell* **87**, 661-673.

Ericson, J., Muhr, J., Placzek, M., Lints, T., Jessell, T. M. and Edlund, T. (1995). Sonic hedgehog induces the differentiation of ventral forebrain neurons: a common signal for ventral patterning along the rostrocaudal axis of the neural tube. *Cell* **81**, 747-756.

Ericson, J., Rashbass, P., Schedl, A., Brenner-Morton, S., Kawakami, A., van Heyningen, V., Jessell, T. M. and Briscoe, J. (1997). Pax6 controls progenitor cell identity and neuronal fate in response to graded Shh signalling. *Cell* **90**, 169-180.

Erskine, L., Williams, S. E., Brose, K., Kidd, T., Rachel, R. A., Goodman, C. S., Tessier-Lavigne, M. and Mason, C. A. (2000). Retinal ganglion cell axon guidance in the mouse optic chiasm: expression and function of robos and slits. *J. Neurosci.* **20**, 4975-4982.

Feng, G., Mellor, R. H., Bernstein, M., Keller-Peck, C., Nguyen, Q. T., Wallace, M., Nerbonne, J. M., Lichtman, J. W. and Sanes, J. R. (2000). Imaging neuronal subsets in transgenic mice expressing multiple spectral variants of GFP. *Neuron* **28**, 41-51.

Figdor, M. C. and Stern, C. D.(1993). Segmental organization of embryonic diencephalon. *Nature* **363**, 630-634.

Fishell, G., Mason, C. A. and Hatten, M. E. (1993). Dispersion of neural progenitors within the germinal zones of the forebrain. *Nature* **362**, 636-638.

Forrester, L. M., Nagy, A., Sam, M., Watt, A., Stevenson, L., Bernstein, A., Joyner A. L. and Wurst, W. (1996). An induction gene trap screen in embryonic stem cells: Identification of genes that respond to retinoic acid in vitro. *Proc. Natl. Acad. Sci. U.S.A.* **93**, 1677-1682.

Forss-Petter, S., Danielson, P. E., Catsicas, S., Battenberg, E., Price, J., Nerenberg, M. and Sutcliffe, J. G. (1990). Transgenic mice expressing beta-galactosidase in mature neurons under neuron-specific enolase promoter control. *Neuron* **5**, 187-97.

Friedman, G. C. and O'Leary, D. D. (1996) Retroviral misexpression of engrailed genes in the chick optic tectum perturbs the topographictargeting of retinal axons. *J. Neurosci.* **16**, 5498-5509.

Friedrich, G. and Soriano, P. (1991). Promoter traps in embryonic stem cells: a genetic screen to identify and mutate developmental genes in mice. *Genes Dev.* **5**, 1513-1523.

Godwin, A. R., Stadler, H. S., Nakamura, K. and Capecchi, M. R. (1998). Detection of targeted GFP-Hox fusions during mouse embryogenesis. *Proc. Natl. Acad. Sci. U.S.A* **95**, 13042-13047.

Goetz, M., Novak, N., Bastmeyer, M. and Bolz, J. (1992). Membrane-bound molecules in rat cerebral cortex regulate thalamic innervation. *Development* **116**, 507-519.

Golden, J. A., Cepko, C. L. (1996). Clones in the chick diencephalon contain multiple cell types and siblings are widely dispersed. *Development* **122**, 65-78.

Gotz, J., Probst, A., Spillantini, M. G., Schafer, T., Jakes, R., Burki, K. and Goedert, M. (1995). Somatodendritic localisation and hyperphosphorylation of tau protein in transgenic mice expressing the longest human brain tau isoform. *The EMBO J.* **14**, 1304-1313.

Gotz, M., Stoykova A. and Gruss, P.(1998). Pax6 controls radial glia differentiation in the cerebral cortex. *Neuron* **21**, 1031-1044.

Gotz, M., Wizenmann, A., Reinhardt, S., Lumsden, A. and Price, J.(1996). Selective adhesion of cells from different telencephalic regions. *Neuron* **16**, 551-564.

Grindley, J. C., Hargett, L., Hill, R. E., Ross, A. and Hogan, B. L. M. (1997). Disruption of Pax6 function in mice homozygous for the Pax6Sey-1NEU mutation produces abnormalities in the early development and regionalization of the diencephalon. *Mech. Dev.* **64**, 111-126.

Hadjantonakis, A., Gertsenstein, M., Ikawa, M., Okabe, M. and Nagy, A. (1998). Generating green fluorescent mice by germline transmission of green fluorescent ES cells. *Mech. Dev.* **76**, 79-90.

Halder, G., Callaerts, P. and Gehring, W. J. (1995). Induction of ectopic eyes by targeted expression of the eyeless gene in Drosophila. *Science* **267**, 1788-92.

Hall, A. C., Lucas, F. R. and Salinas, P. C. (2000). Axonal remodeling and synaptic differentiation in the cerebellum is regulated by WNT-7a signaling. *Cell* **100**, 525-535.

Hanks, M., Wurst, W., Anson-Cartwright, L., Auerbach, A. B. and Joyner, A. L. (1995). Rescue of the En-1 mutant phenotype by replacement of En-1 with En-2. *Science* **269**, 679-682.

Harada, A., Oguchi, K., Okabe, S., Kuna, J., Terada, S., Oshima, T., Sato-Yoshitake, R., Takei, Y., Noda, T. and Hirokawa, N. (1994). Altered microtubule organisation in small-calibre axons of mice lacking tau protein. *Nature* **369**, 488-491.

Heim, R., Tsien, R. Y. (1996). Engineering green fluorescent protein for improved brightness, longer wavelengths and fluorescence resonance energy transfer. *Curr. Biol.* **6**, 178-182.

Hill, R. E., Favor, J., Hogan, B. L. M., Ton, C. C. T., Saunders, G. F., Hanson, I. M., Prosser, J., Jordan, T., Hastie, N. D. and van Heyningen, V. (1991). Mouse Small eye results from mutations in a paired-like homeobox-containing gene. *Nature* **354**, 522-525.

Hirokawa, N., Funakoshi, T., Sato-Harada, R. and Kanai, Y. (1996). Selective stabilization of tau in axons and microtubule-associated protein 2C in cell bodies and dendrites contributes to polarized localization of cytoskeletal proteins in mature neurons. *J. Cell Biol.* **132**, 667-679.

Hogan, B., Beddington, R., Costantini, F. and Lacy, E. (1994). Manipulating the mouse embryo: A laboratory manual. Second edition. Cold Spring Harbour Laboratory Press.

Hooper, M. L., Hardy, K., Handyside, A., Hunter, S. and Monk, M. (1987). HPRT-deficient (Lesch-Nyham) mouse embryos derived from germline colonisation by cultured cells. *Nature* **326**, 292-295.

Hu, H. (1999). Chemorepulsion of neuronal migration by Slit2 in the developing mammalian forebrain. *Neuron* **23**, 703-711.

Ikawa, M., Kominami, K., Yoshimura, Y., Tanaka, K., Nishimune, Y. and Okabe, M. (1995). A rapid and non-invasive selection of transgenic embryos before implantation using green fluorescent protein (GFP). *F.E.B.S. Lett.* **375**, 125-128.

Inoue, T., Tanaka, T., Takeichi, M., Chisaka, O., Nakamura, S. and Osumi, N. (2001). Role ofcadherins in maintaining the compartmentboundary between the cortex and striatum during development. *Development* **128**, 561-569.

Isacson, O., Deacon, T. W., Pakzaban, P., Galpern, W. R., Dinsmore, J. and Burns, L. H. (1995). Transplanted xenogenic neural cells in neurodegenerative disease models exhibit remarkable axonal target specificity and distinct growth patterns of glial and axonal fibres. *Nature Medicine* **1** 1189-1194.

Ishihara, T., Hong, M., Zhang, B., Nakagawa, Y., Lee, M. K., Trojanowski, J. Q. and Lee, V. M. (1999). Age-dependent emergence and progression of a tauopathy in transgenic mice overexpressing the shortest human tau isoform. Neuron. **24**, 751-762.

Jaenisch, R. (1988). Transgenic animals. *Science* **240**, 1468-74.

Kaech, S., Ludin, B. and Matus, A. (1996). Cytoskeletal plasticity in cells expressing neuronal microtubule associated proteins. *Neuron* **17**, 1189-1199.

Kanai, Y. and Hirokawa, N. (1995). Sorting mechanisms of tau and MAP2 in neurons: suppressed axonal transit of MAP2 and locally regulated microtubule binding. *Neuron* **14**, 421-432.

Kandel, E. R., Schwartz, J. H. and Jessell, T. M. (2000) Principles of neural science, New York, 4th edition.

Kaufman, M. H. (1995). The atlas of mouse development (revised edition). Academic Press.

Kaufman, M. H., Chang, H-H. and Shaw, J. P. (1995). Craniofacial abnormalities in homozygous Small eye (Sey/Sey) embryos and newborn mice. *J. Anat.* **186**, 606-617.

Kawamoto, S., Niwa, H., Tashiro, F., Sano, S., Kondoh, G., Takeda, J., Tabayashi, K. and Miyazaki, J.(2000). A novel reporter mouse strain that expresses enhanced green fluorescent protein upon Cre-mediated recombination. *F.E.B.S. Lett.* **470**, 263-268.

Kawano, H., Fukuda, T., Kubo, K., Horie, M., Uyemura, K., Takeuchi, K., Osumi, N., Eto, K. and Kawamura, K. (1999) Pax-6 is required for thalamocortical pathway formation in fetal rats. *J. Comp. Neurol.* **408**, 147-160.

Kinnunen, A, Niemi, M., Kinnunen, T., Kaksonen, M., Nolo, R. and Rauvala, H. (1999). Heparan sulphate and HB-GAM (heparin-binding growth-associated molecule) in the development of the thalamocortical pathway of rat brain. *Eur. J. Neurosci.* **11**, 491-502.

Knoll, B., Zarbalis, K., Wurst, W. and Drescher, U. (2001). A role for the EphA family inthe topographic targeting of vomeronasal axons. *Development* **128**, 895-906

Korn, R ., Schoor, M., Neuhaus, H., Henseling, U., Soininen, R., Zachgo, J. and Gossler, A. (1992). Enhancer trap integrations in mouse embryonic stem cells give rise to staining patterns in chimaeric embryos with a high frequency and detect endogenous genes. *Mech. Dev.* **39**, 95-109.

Lang, T., Wacker, I., Steyer, J., Kaether, C., Wunderlich, I., Soldati, T., Gerdes, H. H. and Almers, W.(1997) Ca2+-triggered peptide secretion in single cells imaged with green fluorescent protein and evanescent-wave microscopy. *Neuron* **18**, 857-863.

Lee, V. M., and Trojanowski, J. Q. (1999). Neurodegenerative tauopathies: Human disease and transgenic models. *Neuron* **24**, 507-510.

Leighton, L. A., Mitchell, K. J., Goodrich, L. V., Lu, X., Pinson, K., Scherz, P., Skarnes, W. C. and Tessier-Lavigne, M. (2001). Defining brain wiring patterns and mechanisms through gene trapping in mice. *Nature* **410**, 174-179.

Li, M., Pevny, L., Lovell-Badge, R. and Smith, A. (1998). Generation of purified neural precursors from embryonic stem cells by lineage selection. *Curr. Biol.* **8**, 971-974.

Li, X., Zhao, X., Fang, Y., Jiang, X., Duong, T., Fan, C., Huang, C. C. and Kain, S. R. (1998). Generation of destabilized green fluorescent protein as a transcription reporter. *J. Biol. Chem.* **273**, 34970-34975.

Litman, P., Barg, J. and Ginzburg, I. (1994). Microtubules are involved in the localization of tau mRNA in primary neuronal cell cultures. *Neuron* **13**, 1463-1474.

Litman, P., Barg, J., Rindzoonski, L. and Ginzburg, I. (1993). Subcellular localization of tau mRNA in differentiating neuronal cell culture: implications for neuronalpolarity. *Neuron* **10**, 627-638.

Lotto, R. B. and Price, D. J. (1999a). Thalamus and cerebral cortex: organotypic culture and co-culture. In 'The neuron in tissue culture' (Ed. Haynes, L. John Wiley and Sons Ltd., Chichester). pp 518-524.

Lotto, R. B. and Price, D. J. (1999b). Thalamus: dispersed neuron culture. In 'The neuron in tissue culture' (Ed. Haynes, L. John Wiley and Sons Ltd., Chichester). pp 525-530.

Lucas, F. R. and Salinas, P. C. (1997). WNT-7a induces axon remodelling and increases synapsin I levels in cerebellar neurons. *Dev. Biol.* **192**, 31-44.

Ludin, B. and Matus, A. (1998). GFP illuminates the cytoskeleton. *Trends Cell Biol.* **8**, 72-77.

Lumsden, A. and Krumlauf, R. (1996). Patterning the vertebrate neuraxis. *Science* **274**, 1109-1115.

Mackarehtschian, K., Lau, C. K., Caras, I. and McConnell, S. K. (1999). Regional differences in the developing cerebral cortex revealed by ephrin-A5 expression. *Cereb. Cortex* **9**, 601-610.

Mandelkow, E. M. and Mandelkow, E. (1998). Tau in Alzheimer's disease. *Trends Cell Biol.* **11**, 425-427.

Mann, F., Zhukareva, V., Pimenta, A., Levitt, P. and Bolz, J. (1998). Membrane associated molecules guide limbic and non-limbic thalamocortical projections. *J. Neurosci.* **18**, 9409-9419.

Mansouri, A., Stoykova, A. and Gruss, P. (1994). Pax genes in development. *J. Cell Sci.* **18**, 35-42.

Marcus, R. C., Matthews, G. A., Gale, N. W., Yancopoulos, G. D. and Mason, C. A. (2000). Axon guidance in the mouse optic chiasm: retinal neurite inhibition by ephrin "A"-expressing hypothalamic cells in vitro. *Dev. Biol.* **221**, 132-147.

Mastick, G. S. and Easter, S. S. (1996). Initial organization of neurons and tracts in the embryonic mouse fore- and midbrain. *Dev. Biol.* **173**, 79-94.

Mastick, G. S., Davis, N. M., Andrews, G. L. and Easter, Jr, S. S. (1997). Pax6 functions in boundary formation and axon guidance in the embryonic mouse forebrain. *Development* **124**, 1985-1997.

Matz, M. V., Fradkov, A. F., Labas, Y. A., Savitsky, A. P., Zaraisky, A. G., Markelov, M.L. and Lukyanov, S. A. (1999). Fluorescent proteins from nonbioluminescent Anthozoa species. *Nat. Biotechnol.* **17**, 969-973.

Mezey, E., Chandross, K. J., Harta, G., Maki, R. A. and McKercher, S. R. (2000). Turning blood into brain: cells bearing neuronal antigens generated in vivo from bone marrow. *Science* **290,** 1779-82.

Mills, J. C., Lee, V. M. Y. and Pittman, R. N. (1998). Activation of a PP2A-like phosphatase and dephosphorylation of tau protein characterise onset of the execution phase of apoptosis. *J. Cell Sci.* **111**, 625-636.

Miyashita-Lin, E. M., Hevner, R., Wassarman, K. M., Martinez, S. and Rubenstein, J. L. (1999). Early neocortical regionalization in the absence of thalamic innervation. *Science* **285**, 906-909.

Molnar, Z. and Blakemore, C. (1991). Lack of regional specificity for connections formed between thalamus and cortex in coculture. *Nature* **351**, 475-477.

Molnar, Z. and Blakemore, C. (1999). Development of signals influencing the growth and termination of thalamocortical axons in organotypic culture. *Exp. Neurol.* **156**, 363-393.

Molnar, Z., Adams, R. and Blakemore, C. (1998). Mechanisms underlying the early establishment of thalamocortical connections in the rat. *J. Neurosci.* **18**, 5723-5745.

Molnar, Z., and Blakemore, C. (1995). How do thalamic axons find their way to the cortex? *Trends Neurosci.* **18**, 389-397.

Mombaerts, P., Wang, F., Dulac, C., Chao, S.K., Nemes, A., Mendelsohn, M., Edmondson, J. and Axel, R. (1996). Visualising an olfactory sensory map. *Cell* **87**, 675-686.

Mountford, P. S. and Smith, A. G. (1995). Internal ribosome entry sites and dicistronic RNAs in mammalian transgenesis. *Trends Genet.* **11**, 179-184.

Mountford, P., Zevnik, B., Duwel, A., Nichols, J., Li, M., Dani, C., Robertson, M., Chambers, I. and Smith, A. (1994). Dicistronic targeting constructs: reporters and modifiers of mammalian gene expression. *Proc. Natl. Acad. Sci. U.S.A.* **91**, 4303-4307.

Nguyen Ba-Charvet, K. T., Brose, K., Marillat, V., Kidd, T., Goodman, C. S., Tessier-Lavigne, M., Sotelo, C. and Chedotal, A. (1999). Slit2-Mediated chemorepulsion and collapse of developing forebrain axons. *Neuron* **22**, 463-473.

Nguyen Ba-Charvet, K. T., von Boxberg, Y., Guazzi, S., Boncinelli, E. and Godement, P. (1998). A potential role for the OTX2 homeoprotein in creating early 'highways' for axon extension in the rostral brain. *Development* **125**, 4273-82.

Niwa, H., Yamamura. K. and Miyazaki, J. (1991). Efficient selection for high-expression transfectants with a novel eukaryotic vector. *Gene* **108**, 193-199.

Okabe, M., Ikawa, M., Kominami, K., Nakanishi, K. and Nishimune, Y. (1997). 'Green mice' as a source of ubiquitous green cells. *F.E.B.S. Lett.* **407**, 313-319.

Olson, K. R., McIntosh, J.R. and Olmsted, J. B. (1995). Analysis of MAP 4 function in living cells using green fluorescent protein (GFP) chimeras. *J. Cell Biol.* **130,** 639-650.

Ormo, M., Cubitt, A. B., Kallio, K., Gross, L. A., Tsien, R. Y. and Remington, S. J. (1996). Crystal structure of the Aequorea victoria green fluorescent protein. *Science* **273**, 1392-1395.

Osumi, N., Hirota, A., Ohuchi, H., Nakafuku, M., Iimura, T., Kuratani, S., Fujiwara, M., Noji, S. and Eto, K. (1997). Pax-6 is involved in the specification of hindbrain motor neuron subtype. *Development* **124**, 2961-2972.

Peterson, K. R., Clegg, C. H., Huxley, C., Josephson, B. M., Haugen, H. S., Furukawa, T. and Stamatoyannopoulos, G. (1993). Transgenic mice containing a 248-kb yeast artificial chromosome carrying the human beta-globin locus display proper developmental control of human globin genes. *Proc. Natl. Acad. Sci. U.S.A.* 1993 **90**, 7593-7597.

Pettit, D. L., Perlman, S. and Malinow, R. (1994). Potentiated transmission and prevention of further LTP by increased CaMKII activity in postsynaptic hippocampal slice neurons. *Science* **266**, 1881-1885.

Polleux, F., Giger, R. J., Ginty, D. D., Kolodkin, A. L. and Ghosh, A. (1998). Patterning of cortical efferent projections by semaphorin-neuropilin interactions. *Science* **282**, 1904-1906

Polleux, F., Morrow, T. and Ghosh, A. (2000). Semaphorin 3A is a chemoattractant for cortical apical dendrites. *Nature* **404**, 567-573.

Prasher, D. C., Eckenrode, V. K., Ward, W. W., Prendergast, F. G. and Cormier, M. J. (1992). Primary structure of the Aequorea victoria green-fluorescent protein. *Gene* **111**, 229-233.

Pratt, T., Sharp, L., Nichols, J., Price, D. J. and Mason, J. O. (2000a). Embryonic stem cells and transgenic mice ubiquitously expressing a tau-tagged green fluorescent protein. *Dev. Biol.* **228**, 19-28.

Pratt, T., Vitalis, T., Warren, N., Edgar, J. M., Mason, J. O. and Price, D. J. (2000b) A role for Pax6 in the normal development of dorsal thalamus and its cortical connections. *Development* **127**, 5167-5178.

Preuss, U. and Mandelkow, E-M. (1998). Mitotic phosphorylation of tau protein in neuronal cell lines resembles phosphorylation in Alzheimers disease.*Eur. J. Cell Biol.* **76**, 176-184.

Probst, A., Gotz, J., Wiederhold, K. H., Tolnay, M., Mistl, C., Jaton, A. L., Hong, M., Ishihara, T., Lee, V. M., Trojanowski, J. Q., Jakes, R., Crowther, R. A., Spillantini, M. G., Burki, K. and Goedert, M. (2000). Axonopathy and amyotrophy in mice transgenic for human four-repeat tau protein. *Acta Neuropathol. (Berl).* **99**, 469-481.

Puelles, L. and Rubenstein, J. L. (1993). Expression patterns of homeobox and other putative regulatory genes in the embryonic mouse forebrain suggest a neuromeric organization. *Trends Neurosci.* **16**, 472-479.

Quinn, J. C., West, J. D. and Hill, R .E. (1996). Multiple functions for *Pax6* in mouse eye and nasal development. *Genes Dev.* **10**, 435-446.

Rennie, S., Lotto, R. B. and Price, D. J. (1994) Growth-promoting interactions between the murine neocortex and thalamus in organotypic co-cultures. *Neuroscience* **61**, 547-564.

Rhinn, M., Dierich, A., Le Meur, M. and Ang, S. (1999) Cell autonomous and non-cell autonomous functions of Otx2 in patterning the rostral brain. *Development* **126**, 4295-4304.

Richardson, J., Cvekl, A. and Wistow, G. (1995). Pax-6 is essential for lens-specific expression of zeta-crystallin. *Proc. Natl. Acad. Sci. U.S.A.* **92**, 4676-4680.

Ringstedt, T., Braisted, J. E., Brose, K., Kidd, T., Goodman, C. S., Tessier-Lavigne, M. and O'Leary, D. D. M. (1999). Slit repulsion influences thalamocortical and retinal axon pathfinding in the diencephalon. *Soc. Neurosci. Abstr.* **25**, 305.4.

Roberts, R. C. (1967). Small eyes- a new dominant eye mutant in the mouse. *Genetical Research* **9**, 121-122.

Rodriguez, I., Feinstein, P. and Mombaerts P. (1999). Variable patterns of axonal projections of sensory neurones in the mouse vomeronasal system. *Cell* **97**, 199-208.

Rohm, B., Ottemeyer, A., Lohrum, M. and Puschel, A. W. (2000). Plexin/neuropilin complexes mediate repulsion by the axonal guidance signal semaphorin 3A. *Mech. Dev.* **93**, 95-104.

Rossant, J. and Spence, J. (1998). Chimeras and mosaics in mouse mutant development. *Trends Genet.***14**, 358-363.

Rubenstein, J. L. R., Martinez, S., Shimamura, K. and Puelles, L. (1994). The embryonic vertebrate forebrain: the prosomeric model. *Science* **266**, 578-580.

Rubenstein, J. L., Shimamura, K., Martinez, S. and Puelles, L. (1998). Regionalization of the prosencephalic neural plate. *Annu. Rev. Neurosci.* **21**, 445-477.

Sakai, N., Sasaki, K., Ikegaki, N., Shirai, Y., Ono, Y. and Saito, N. (1997). Direct visualization of the translocation of the gamma-subspecies of protein kinase C in living cells using fusion proteins with green fluorescent protein. *J. Cell Biol.* **139**, 1465-76.

Sambrook, J., Fritsch, E. F. and Maniatis, T. (1989). Molecular cloning: a laboratory manual 2nd edition. Cold Spring Harbor, N.Y.

Sander, M., Neubuser, A., Kalamaras, J., Ee, H. C., Martin, G. R. and German, M. S. (1997). Genetic analysis reveals that PAX6 is required for normal transcription of pancreatic hormone genes and islet development. *Genes Dev.* **11**, 1662-73.

Schedl, A., Ross, A., Lee, M., Engelkamp, D., Rashbass, P., van Heyningen, V. and Hastie, N. D. (1996). Influence of PAX6 gene dosage on development: overexpression causes severe eye abnormalities. *Cell* **86**, 71-82.

Scheffler, B., Horn, M., Blumcke, I., Laywell, E. D., Coomes, D., Kukekov, V. G. and Steindler, D. A. (1999). Marrow-mindedness: a perspective on neuropoisis. *Trends Neurosci.* **22**, 348-356.

Schliwa, M. and van Blerkom, J. (1981). Structural interaction of cytoskeletal components. *J. Cell Biol.* **90,** 222-235.

Schmahl, W., Knoediseder, M., Favor, J. and Davidson, D. (1993). Defects of neuronal migration and the pathogenesis of cortical malformations are associated with small eye (sey) in the mouse, a point mutation at the Pax-6 locus. *Acta Neuropathol.* **86**, 126-135.

Schwarz, M., Cecconi, F., Bernier, G., Andrejewski, N., Kammandel, B., Wagner, M. and Gruss, P. (2000). Spatial specification of mammalian eye territories by reciprocal transcriptional repression of Pax2 and Pax6. *Development* **127**, 4325-34.

Serafini, T., Colamarino, S. A., Leonardo, E. D., Wang, H., Beddington, R., Skarnes, W. C. and Tessier-Lavigne, M. (1996). Netrin1 is required for commissural axon guidance in the developing vertebrate nervous system. *Cell* **87**, 1001-14.

Shields, J. M. and Yang, V. W. (1997). Two potent nuclear localization signals in the gut-enriched Kruppel-like factor define a subfamily of closely related Kruppel proteins. *J. Biol. Chem.* **272**, 18504-18507.

Shimamura, K. and Rubenstein, J. L. (1997). Inductive interactions direct early regionalization of the mouse forebrain. *Development* **124**, 2709-2718.

Shimamura, K., Hartigan, D. J., Martinez, S., Puelles, L. and Rubenstein, J. L. R. (1995). Longitudinal organisation of the anterior neural plate and neural tube. *Development* **121**, 3923-3933.

Siegel, M. S. and Isacoff, E. Y. (1997). A genetically encoded optical probe of membrane voltage. *Neuron* **19**, 735-741.

Siemering, K. R., Golbik, R., Sever, R. and Haseloff J.(1996) Mutations that suppress the thermosensitivity of green fluorescent protein. *Curr. Biol.* **6**, 1653-1663.

Smith, A. G. (1991). Culture and differentiation of embryonic stem cells. *J. Tissue Culture Methods* **13**, 89-94.

Spillantini, M. G. and Goedert, M.(1998). Tau protein pathology in neurodegenerative diseases. *Trends Neurosci.* **21**, 428-33.

Spittaels, K., Van den Haute, C., Van Dorpe, J., Bruynseels, K., Vandezande, K., Laenen, I., Geerts, H., Mercken, M., Sciot, R., Van Lommel, A., Loos, R. and Van Leuven, F. (1999). Prominent axonopathy in the brain and spinal cord of transgenic mice overexpressing four-repeat human tau protein. *Am. J. Pathol.* **155**, 2153-2165.

Stein, E. and Tessier-Lavigne (2001). Hierarchical organisation of guidance receptors: silencing of Netrin attraction by Slit through a Robo/DCC receptor complex. *Science* **291**, 1928-1935.

Stephens, D. J. and Pepperkok, R. (2001). Illuminating the secretory pathway: when do we need vesicles? *J. Cell Sci.* **114**, 1053-1059

St-Onge, L., Sosa-Pineda, B., Chowdhury, K., Mansouri, A. and Gruss, P. (1997). Pax6 is required for differentiation of glucagon-producing alpha-cells in mouse pancreas. *Nature* **387**, 406-409.

Stoykova, A. and Gruss, P. (1994). Roles of Pax-genes in developing and adult brain as suggested by expression patterns. *J. Neurosci.* **14**, 1395-1412.

Stoykova, A., Fritsch, R., Walther, C. and Gruss, P. (1996). Forebrain patterning defects in Small eye mutant mice. *Development* **122**, 3453-3465.

Stoykova, A., Gotz, M. and Price, J. (1997). Pax6-dependent regulation of adhesive patterning, R-cadherin expression and boundary formation in developing forebrain. *Development* **124**, 3765-3777.

Studer, M., Lumsden, A., Ariza-McNaughton, L., Bradley, A. and Krumlauf, R. (1996). Altered segmental identity and abnormal migration of motor neurons in mice lacking Hoxb-1. *Nature* **384**, 630-634.

Svendsen, C. N. and Smith, A. G. (1999). New prospects for human stem-cell therapy in the nervous system. *Trends Neurosci.* **22**, 357-364.

Takeuchi, T., Yamazaki, Y., Katoh-Fukui, Y., Tsuchiya, R., Kondo, S., Motoyama, J. and Higashinakagawa. T. (1995). Gene trap capture of a novel mouse gene, jumonji, required for neural tube formation. *Genes Dev.* **9**, 1211-1222.

Tanabe, Y. and Jessell, T. M. (1996). Diversity and pattern in the developing spinal cord. *Science* **274**, 1115-1123.

Tarkowski, A. K. (1961). Mouse chimeras developed from fused eggs. *Nature* **190**, 857-860.

Tessier-Lavigne, M. and Goodman, C. S. (1996). The molecular biology of axon guidance. *Science* **274**, 1123-1133.

Toresson, H., Potter, S. S. and Campbell, K. (2000). Genetic control of dorsal-ventral identity in the telencephalon: opposing roles for Pax6 and Gsh2. *Development* **127,** 4361-4371.

Tsien, R. Y. (1998). The green fluorescent protein. *Annu. Rev. Biochem.* **67**, 509-544.

Tuttle, R., Nakagawa, Y., Johnson, J. E. and O'Leary, D. D. M. (1999). Defects in thalamocortical axon pathfinding correlate with altered cell domains in Mash-1-deficient mice. *Development* **126**, 1903-1916.

Van den Pol, A. N. and Ghosh, P. K. (1998). Selective neuronal expression of green fluorescent protein with cytomegalovirus promoter reveals entire neuronal arbor in transgenic mice. *J. Neurosci.* **18**, 10640-10651.

Van der Loos, H. and Woolsey, T. A. (1973). Somatosensory cortex: structural alterations following early injury to sense organs. *Science* **179**, 395-398.

Vanderhaeghen, P., Lu, Q., Prakash, N., Frisen, J., Walsh, C. A., Frostig, R. D. and Flanagan, J. G. (2000). A mapping label required for normal scale of body representation in the cortex. *Nat. Neurosci.* **3**, 358-365.

Vitalis, T., Cases, O., Engelkamp, D., Verney, C. and Price, D. J. (2000). Defect of tyrosine hydroxylase-immunoreactive neurons in the brains of mice lacking the transcription factor Pax6. *J. Neurosci.* **20**, 6501-16.

Walther, C. and Gruss, P. (1991). *Pax6,* a murine paired box gene, is expressed in the developing CNS. *Development* **113**, 1435-1449.

Wang, H. and Tessier-Lavigne, M. (1999). En passant neurotrophic action of an intermediate axonal target in the developing mammalian CNS. *Nature* **401**, 765-769.

Warren, N. and Price, D. J. (1997). Roles of Pax6 in murine diencephalic development. *Development* **124**, 1573-1582.

Warren, N., Caric, C., Pratt, T., Clausen, J. A., Asavaritikrai, P., Mason, J. O., Hill, R. E. and Price D. J. (1999). The transcription factor, Pax6, is required for cell proliferation and differentiation in the cerebral cortex. *Cerebral Cortex* **9**, 627-635.

Waters, J. C., Cole, R. W. and Reider, C. L. (1993). The force-producing mechanism for centrosome separation during spindle formation in vertebrates is intrinsic to each aster. *J. Cell Biol.* **122**, 361-372.

Westerfield, M., Wegner, J., Jegalian, B. G., DeRobertis, E. M. and Puschel, A. W. (1992). Specific activation of mammalian Hox promoters in mosaic transgenic zebrafish. *Genes Dev.* **4,** 591-598.

Woolsey, T. A. and Van der Loos, H. (1970). The structural organization of layer IV in the somatosensory region (SI) of mouse cerebral cortex. The description of a cortical field composed of discrete cytoarchitectonic units. *Brain Res.* **17**, 205-42.

Yang, F., Moss, L. G. and Phillips, G. N. (1996). The molecular structure of green fluorescent protein. *Nat. Biotechnol.* **14**, 1247-1251.

Ye, W., Shimamura, K., Rubenstein, J. L., Hynes, M. A. and Rosenthal, A. (1998). FGF and Shh signals control dopaminergic and serotonergic cell fate in the anterior neural plate. *Cell* **93**, 755-66.

Yuan, W., Zhou, L., Chen, J. H., Wu, J. Y., Rao, Y. and Ornitz, D. M. (1999). The mouse SLIT family: secreted ligands for ROBO expressed in patterns that suggest a role in morphogenesis and axon guidance. *Dev. Biol.* **212**, 290-306.

Zambrowicz, B. P., Imamoto, A., Fiering, S., Herzenberg, L. A., Kerr, W. G. and Soriano, P. (1997). Disruption of overlapping transcripts in the ROSA beta geo 26 gene trap strain leads to widespread expression of beta-galactosidase in mouse embryos and hematopoietic cells. *Proc. Natl. Acad. Sci. U.S.A.* **94**, 3789-3794.

Zernicka-Goetz, M., Pines, J., McLean-Hunter, S., Dixon, J. P., Siemering, K.R., Haseloff, J. and Evans, M. J.(1997) Following cell fate in the living mouse embryo. *Development* **124**, 1133-1137.

Zernicka-Goetz, M., Pines, J., Ryan, K., Siemering, K. R., Haseloff, J., Evans, M. J. and Gurdon, J. B. (1996) An indelible lineage marker for Xenopus using a mutated green fluorescent protein. *Development* **122**, 3719-3724.

Zhang, G., Gurtu, V. and Kain, S. R. (1996). An enhanced green fluorescent protein allows sensitive detection of gene transfer in mammalian cells. *Biochem. Biophys. Res. Commun.* **227**, 707-711.

Zhu, G., Mehler, M. F., Zhao, J., Yu Yung, S. and Kessler, J. A. (1999). Sonic hedgehog and BMP2 exert opposing actions on proliferation and differentiation of embryonic neural progenitor cells. *Dev. Biol.* **215**, 118-129.

Zhuo, L., Sun, B., Zhang, C., Fine, A., Chiu, S. and Messing, A. (1997). Live astrocytes visualised by green fluorescent protein in transgenic mice. *Dev. Biol.* **187**, 36-42.

APPENDIX A:

MOLECULAR BIOLOGY MATERIALS AND REAGENTS

General-purpose molecular biology reagents were purchased from Sigma UK, Fisher UK, and BDH/Merck, UK.

Agarose for gel electrophoresis

Seakem LE Agarose (Flowgen: 50000)

Bacterial culture media and antibiotics

LB tablets (Sigma: L-7275)

1 tablet dissolved in 50ml water and sterilised by autoclaving.

LB-Agar (Sigma: L-2897)

35g added to 1l water and dissolved and sterilised by autoclaving.

Competent cell freezing mix (CCFM)

100mM KCl, 50mM $CaCl_2$, 10% Glycerol, 10mM potassium acetate pH7.5

Ampicillin (Roche: 835 242):

50mg/ml stock dissolved in 50% ethanol stored at –20°C and diluted 1000-fold to working concentration of 50μg/ml in LB or LB-Agar at temperatures not exceeding 50°C.

Enzymes for molecular biology

DNA Restriction enzymes.

These were purchased from Roche or Amersham Pharmacia Biotech and used according to manufacturers guidelines.

DNA modifying enzymes

Cloned Pfu polymerase (Stratagene: 600153)

Sequenase v2.0: (Amersham Pharmacia Biotech: US70770)

T4 DNA ligase (Roche: 481 220)

Polynucleotide Kinase (Roche: 174 645)

Calf intestinal alkaline phosphatase (Roche: 713 023)

Other enzymes

Proteinase K (Roche:745 723)

Lysozyme (Roche: 107 255)

Molecular Biology Kits

DNA extraction & purification

Ultraclean mini plasmid prep kit (Mo Bio Laboratories: 12300-100)

Plasmid midi kit (Qiagen: 12143)

Qiaex II gel extraction system (Qiagen: 20021)

Manual DNA sequencing

Sequenase v 2.0 (Amersham Pharmacia Biotech: US70770).

^{35}S-ATP for manual sequencing was purchased from ICN.

DNA labelling

High Prime DNA labelling kit (Roche:1585584)

Oligonucleotides

Purchased from Genosys, MWG-Biotech, or Oswel.

'Adapters'

Used to convert Asp718 to Bgl2 'ASP718/BGL2': GTACTAGATCTA

Used to convert Sac1 site to EcoR1 site 'SAC1/ECOR1': GAATTCAGCT

Site directed mutagenesis

Used to introduce BspH1 site into pMGFP6

'GFPBSPH1.1': TTACACATGTCATGAATGAACTAT

'GFPBSPH1.2': ATAGTTCATTCATGACATGTGTAA

Adapters used to ligate Kpn1 and Sac1 cut ends into BstX1 cut pPHCAGGS-BstX1(+SVori)

'BSTX1CAG': AACCCACA

'KPN1CAG': GGTTGTAC

'SAC1CAG': GGTTAGCT

BstX1 linkers

Used to ligate to blunt ended fragments for insertion into BstX1 digested pCAGGS.

'BST-P1': GGCCGCACTGGCCAGCACA

'BST-P2': CTGGCCAGTGCGGCC

DNA Sequencing

'MGFP6.91-74': TGCCCATTAACATCACC

'MGFP6.462-478': ACGTATACATCATGGCC

'MGFP6.647-655': CCAACGAAAAGAGAGACC

'MGFP6.271-255': CTTGAAGAAGTCGTGCC

'HTAU.1200-1217': GGGGACACGTCTCCACGG

'-40 M13': GTTTTCCCAGTCACGAC

'T7': GTAATACGACTCACTATAGGGC

'T3': AATTAACCCTCACTAAAGGG

Mouse genomic DNA

Mouse genomic DNA extraction

Tail tip lysis buffer (TTLB)

200mM Tris pH8, 200mM NaCl, 5mM EDTA, 0.2% SDS

Southern Blotting and hybridisation

^{32}P-α-dCTP for radiolabeled probe preparation was purchased from ICN.

Southern denaturing solution: 0.5M NaOH

Southern neutralising solution: 0.5M Tris, 3M NaCl, pH7.0

20xSSC: 3M NaCl, 0.3M sodium citrate

Church Solution: 0.5M $NaPO_4$, 7% SDS, 1mM EDTA, 1% BSA, pH7.2

Church Wash: 40mM $NaPO_4$, 1% SDS, 1mM EDTA, pH7.2

Nylon membrane (positively charged): Roche: 1 417 240

APPENDIX B

ES AND PRIMARY CULTURE, TISSUE PROCESSING AND IMAGING.

Tissue culture plasticware

Flasks

25cm^2 culture area (T25) flasks (Iwaki:3100-025)

75cm^2 culture area (T75) flasks (Iwaki:3110-075)

175cm^2 culture area (T175) flasks (Iwaki: 3120-150)

Plates

0.32 cm^2 culture area (96 well) plate (Iwaki:3860-096)

1.9 cm^2 culture area/well (4 well) plate (Nunc:176740A)

2.0 cm^2 culture area/well (24 well) plate (Iwaki: 3820-024)

3.8 cm^2 culture area/well (12 well) plate (Iwaki: 3815-012)

9.4 cm^2 culture area/well (6 well) plate (Iwaki: 3810-006)

Dishes

79 cm^2 tissue culture (10 cm diameter) dish (Iwaki: 3020-100)

Bacterial grade (9 cm diameter) dish (Sterilin: 101VR20)

Sterile plastic pipettes

5ml pipette (Iwaki: LX5ML)

10ml pipette (Iwaki: LX10ML)

25ml pipette (Iwaki: LX25ML)

Solutions and reagents for ES culture

Starting materials

All solutions and reagents were prepared and used under sterile conditions.

10x GMEM (BHK21 Medium (10x) Glasgow MEM) (Gibco BRL: 12541-025)

L-Glutamine 200mM (Gibco BRL: 25030-032)

MEM non-essential amino acids 100x (Gibco BRL: 11140-035)

Sodium Pyruvate MEM 100mM (11360-039)

Sodium Bicarbonate (BDH/Merck: 10247)

Gelatin (Type A from porcine skin) (Sigma: G-1890)

Foetal calf serum (FCS) (Globepharm: Batch F16784).

FCS batches were tested in CGR for ability to support ES cell culture.

TVP 0.025% trypsin solution prepared by diluting 2.5% Trypsin (Gibco BRL: 25090-028) in PBS.

β-Mercaptoethanol (Sigma: M-7522)

Puromycin (Calbiochem: 540222)

DMSO Analar (BDH/Merck: 103234L)

PBS tablets (Oxoid: BR14) 1 tablet dissolved in 100ml water.

Leukemia Inhibitory Factor (LIF): Produced in house by Centre for Genome Research, Edinburgh University. Aliquots (0.5ml) stored at –20°C at 1000x working strength.

Preparation of GMEM+FCS (400ml)

Sterile water: 340ml

10xGMEM: 40ml

Sodium Bicarbonate (7.5%): 13.2ml

MEM non-essential Amino Acids: 4ml

L-Glutamine (200mM): 4ml

Sodium Pyruvate (100mM): 4ml

β-Mercaptoethanol (0.014% v/v): 400µl

Serum: 40ml

Preparation of GMEMβ+FCS+LIF

GMEMβ+FCS: 400ml

LIF x1000: 400µl

ES neuron culture media and reagents

all-trans Retinoic Acid (Sigma: R2625)

10mM Stock prepared in DMSO and stored in the dark at –20°C until use.

DMEM/F12 without L-Glutamine (Gibco BRL: 21331-046)

Neurobasal medium (Gibco BRL: 21103-049)

N2 supplement (Gibco BRL: 17502-048)

B27 supplement (Gibco BRL: 17504-044)

Electroporation of ES cells

GenePulser II (Biorad, USA)

0.4cm Electroporation cuvette (Biorad: 1652088)

The cells and DNA were electroporated as close as possible to 4°C.

Primary neural culture

Stock solutions for serum free culture medium*

Antibiotics: Gentamycin (100mg) Kanamycin (200mg) added to 20ml sterile double deionised water, filter sterilised and stored in 1ml aliquots at –20°C.

Putrescene: 100µM stock (161.1mg/100ml in sterile double deionised water, filter sterilised and stored in 4ml aliquots at –70°C).

Progesterone: 20µM stock (6.29mg/100ml ethanol stored in 1ml and then 50µl aliquots at –70°C).

Na_2SeO_3: 30μM stock (5.2mg/100ml in sterile double deionised water, filter sterilised and stored in 50μl aliquots at –70°C).

$_L$-glutamine: 0.2M stock (6.344g/100ml in sterile double deionised water, filter sterilised and store in 2ml and then 50μl aliquots at –70°C).

Preparation of serum free culture medium

Prepared by mixing the following reagents together under sterile conditions and stored for not more than two weeks at 4°C until use. Medium was warmed and equilibrated in a 37°C humidified incubator containing 5% CO_2 for at least one hour prior to use.

100ml F12 (Hams) (Sigma: N4888)

100ml Dulbecco's modified Eagles' medium (DMEM) (Sigma: D5671)

1mg Insulin (Sigma: I6634. Final concentration 5μg/ml)

2mg apo-transferrin (Sigma: T1147. Final concentration 10μg/ml)

3ml HEPES buffer (Sigma: H0887)

0.24g Na_2HCO_3 (Sigma: S5761. Final concentration 0.12mg/ml)

3ml antibiotics stock* (Gentamycin + Kanamycin) (Sigma: G1264 + K1377)

2ml putrescene stock* (Sigma: P5780. Final concentration 16.11μg/ml)

20μl progesterone stock* (Sigma: P8783. Final concentration 6.29ng/ml)

20μl Na_2SeO_3 stock* (Sigma: S5261. Final concentration 5.2ng/ml)

2ml $_L$-glutamine stock* (Sigma: G2128. Final concentration 25μg/ml)

'EBSS' medium used during embryonic brain dissection

Prepared by mixing the following reagents together under sterile conditions and stored for not more than two weeks at 4°C until use.

100ml Earle's balanced salt solution 10x (EBSS) (Sigma: E-7510)

0.22g Na_2HCO_3 (Sigma: S5761. Final concentration 22mg/ml)

0.065g Glucose (Sigma: G-7021. Final concentration 6.5mg/ml)

900ml double deionised water.

EBSS was oxygenated by bubbling with 95% O_2 and chilled on ice prior to use.

Dissociation of cells from embryonic brain

Tissue was dissected and subjected to dissociation using the Papain Dissociation System (Worthington Biochemical Corporation: LK003160) exactly as described by the manufacturer unless otherwise stated in the text.

Dissociated cell culture substrate

Laminin 1mg/ml (Sigma: L2020)

Poly-D-Lysine 1mg/ml (Sigma: P7280)

Preparation of slices of embryonic brain for organotypic culture

Slices were cut on a McIlwain Tissue Chopper (The Mickle Laboratory Engineering Company). Brains were transferred from ice cold oxygenated EBSS to a small piece of sterile filter paper on the Teflon stage and sliced. Slices were then separated from one another and manipulated in ice cold oxygenated EBSS.

Organotypic culture substrate

The explants were grown in 6-well plates on collagen coated inserts (Costar: 3492) in about 2.2 ml serum free culture medium, this volume was carefully adjusted so that the slices were just covered by the meniscus before cultures were returned to the incubator.

Preparing specimens for imaging

Vibratome (Technical Products International Inc, USA; Vibratome Series 1000).

Embryonic brains were fixed, agarose (4%) embedded, and sectioned at 4°C with Vibratome settings; Amplitude = 8 and Speed = 4.

Fixation

Cells and tissues were routinely fixed at 4°C in PBS containing 4% paraformaldehyde (pH7.0). For improved preservation of microtubule structure cells were fixed at room temperature in PHEM buffer (Schliwa and Blerkom, 1981) containing 4% paraformaldehyde (pH6.9).

PHEM buffer: 60mM PIPES (Merck: 441204M), 25mM HEPES (Sigma: H9136), 10mM EGTA (Aldrich: 23,453-2), 2mM $MgCl_2$ (Fisher: M/0600/53), pH6.9.

Glassware

Glass slides and coverslips were purchased from BDH/ Merck

Thin 'glass bottomed' 35mm dishes (Willco Wells B.V., The Netherlands: HBSt-3522) used for imaging live cultures on an inverted confocal microscope.

Staining and mounting

Vectashield (Vector laboratories: H-1000)

TOPRO3 (Molecular probes, 642/661)

Propidium Iodide (Sigma, P4170)

Fixed preparations were mounted in 1:1 glycerol:PBS containing 10% Vectashield (or in 100% Vectashield). Coverslips were sealed with Aquamount (BDH: 362262H). Thin strips of plastic were placed between the slide and the coverslip when mounting explant cultures to protect the specimen from being squashed.

APPENDIX C

POSTNATAL DEVELOPMENT OF TAU-GFP TRANSGENIC MICE

SUMMARY

As described in Chapter 2, postnatal TgTP6.3 heterozygotes were more likely to die between P21 and P42 than their non-transgenic littermates and a small but significant reduction in embryo weight was evident during late prenatal development in TgTP6.3 embryos (Fig. 2.9 on page 100). The data presented in Appendix C was gathered by Margaret Keighren and Jean Flockhart in collaboration with John West and provides a more detailed picture of weight gain and viability during postnatal development.

RESULTS

Weight gain of transgenic male and female TgTP6.3 heterozygotes compared to their non-transgenic littermates is shown in Fig. C1.

Viability of transgenic male and female TgTP6.3 heterozygotes compared to their non-transgenic littermates is shown in Table C1.

CONCLUSION

Male and female TgTP6.3 heterozygotes are slower to put on weight than their non-transgenic male and female littermates respectively. Although similar numbers of transgenic and non-transgenic animals survive to P21 (time of weaning) there is significantly greater mortality suffered by TgTP6.3 animals before they reach P42 (adulthood). The significance of these findings is discussed in Chapter 2.

Figure C.1

Weight gain of TgTP6.3 heterozygotes (*tau-GFP*$^{+}$) compared to their non-transgenic (*tau-GFP*$^{-}$) littermates. The progeny of Tg/- x -/- crosses were categorised according to tau-GFP status and sex and weighed at 7 day intervals. The graphs show mean animal mass (grams) plotted against postnatal age (days) for each category. Females (upper panel) and males (lower panel). Males and females were treated separately as males put on weight more rapidly and are larger than females. Tau-GFP^{+} and tau-GFP^{-} results are plotted in green and black respectively. These results show that both male and female TgTP6.3 heterozygotes put on weight more slowly than their tau-GFP^{-} littermates although the trajectory of weight gain is similar in both cases.

Figure C.1

Postnatal growth of TgTP6.3 females and their non-transgenic littermates

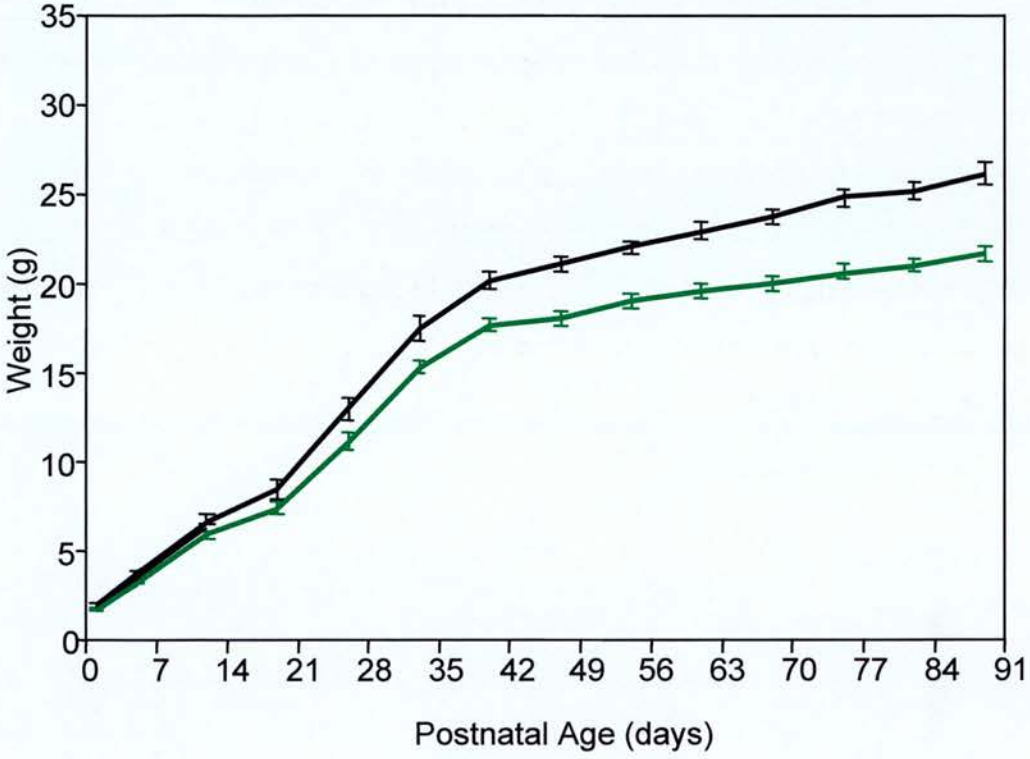

Postnatal growth of TgTP6.3 males and their non-transgenic littermates

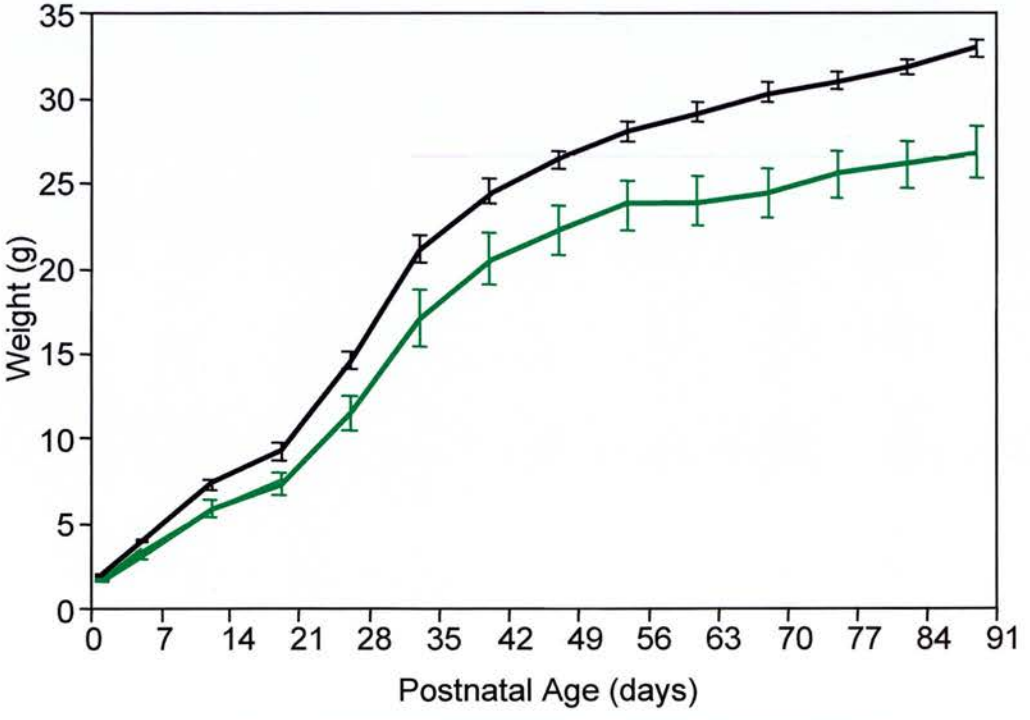

Table C.1

Postnatal viability of TgTP6.3 heterozygotes (*tau-GFP*$^+$) compared to their non-transgenic (*tau-GFP*$^-$) littermates. The progeny of Tg/- x -/- crosses were categorised according to tau-GFP status and the sex and number of animals in each category surviving to P21 (time of weaning) and P42 (adulthood) were tabulated.

There was no significant difference between the numbers of tau-GFP$^+$ and tau-GFP$^-$ animals surviving to P21 (121 and 133 respectively, $\chi^2 = 0.57$, $P > 0.05$).

There was a significant difference between the numbers of tau-GFP$^+$ and tau-GFP$^-$ animals which had died before reaching P42 (15/106 and 3/130 respectively, $\chi^2 = 4.42$, $P < 0.05$).

No significant differences in viability were seen between males and females.

The χ^2 was used to test the null hypothesis that there was no difference between tau-GFP$^+$ and tau-GFP$^-$ populations at each time point.

Table C.1

Viability of heterozygous TgTP6.3 (tau-GFP$^+$) animals compared to their non-transgenic (tau-GFP$^-$) littermates.

Genotype	Sex Male or Female	P0	P21		P42	
			Dead	Alive	Dead	Alive
tau-GFP$^-$	M	ND	ND	77	1	76
tau-GFP$^+$	M	ND	ND	55	6	49
tau-GFP$^-$	F	ND	ND	56	2	54
tau-GFP$^+$	F	ND	ND	66	9	57
tau-GFP$^-$	M+F	ND	ND	133	3	130
tau-GFP$^+$	M+F	ND	ND	121	15	106
Grand Total		266	12	254	18	236

The numbers of tau-GFP$^+$ and tau-GFP$^-$ animals surviving to P21 (weaning) and P42 (adulthood) were counted (ND=not determined).

Development 127, 5167-5178 (2000)
Printed in Great Britain © The Company of Biologists Limited 2000
DEV1583

A role for *Pax6* in the normal development of dorsal thalamus and its cortical connections

Thomas Pratt*, Tania Vitalis*, Natasha Warren*, Julia M. Edgar, John O. Mason and David J. Price‡

Department of Biomedical Sciences, University of Edinburgh, Hugh Robson Building, George Square, Edinburgh EH8 9XD, UK
*These authors contributed equally to the work
‡Author for correspondence (e-mail: dprice@ed.ac.uk)

Accepted 13 September; published on WWW 2 November 2000

SUMMARY

The transcription factor *Pax6* is widely expressed throughout the developing nervous system, including most alar regions of the newly formed murine diencephalon. Later in embryogenesis its diencephalic expression becomes more restricted. It persists in the developing anterior thalamus (conventionally termed "ventral" thalamus) and pretectum but is downregulated in the body of the posterior (dorsal) thalamus. At the time of this downregulation, the dorsal thalamus forms its major axonal efferent pathway via the ventral telencephalon to the cerebral cortex. This pathway is absent in mice lacking functional Pax6 (small eye homozygotes: *Sey/Sey*). We tested whether the mechanism underlying this defect includes abnormalities of the dorsal thalamus itself. We exploited a new transgenic mouse ubiquitously expressing green fluorescent protein tagged with tau, in which axonal tracts are clearly visible, and co-cultured dorsal thalamic explants from *Pax6*$^{+/+}$ or *Pax6*$^{Sey/Sey}$ embryos carrying the transgene with wild-type tissues from other regions of the forebrain. Whereas *Pax6*$^{+/+}$ thalamic explants produced strong innervation of wild-type ventral telencephalic explants in a pattern that mimicked the thalamocortical tract in vivo, *Pax6*$^{Sey/Sey}$ explants did not, indicating a defect in the ability of mutant dorsal thalamic cells to respond to signals normally present in ventral telencephalon. *Pax6*$^{Sey/Sey}$ embryos also showed early alterations in the expression of regulatory genes in the region destined to become dorsal thalamus. Whereas in normal mice *Nkx2.2* and *Lim1/Lhx1* are expressed ventral to this region, in the mutants their expression domains are throughout it, suggesting that a primary action of *Pax6* is to generate correct dorsoventral patterning in the diencephalon. Our results suggest that normal thalamocortical development requires the actions of *Pax6* within the dorsal thalamus itself.

Key words: Confocal microscopy, Diencephalon, Dorsoventral patterning, Green fluorescent protein; *Lim1/Lhx1*, *Nkx2.2*, Organotypic co-cultures, Small eye mice, Tau, Thalamocortical axons, Transgenic mice

INTRODUCTION

The forebrain (prosencephalon) develops from the anterior-most region of the neural tube. Recent studies have revealed that the underlying organisation of the prosencephalon and of more caudal segmented regions of the neural tube may share common properties. On the basis of tissue morphology and patterns of gene expression, the Prosomeric Model (Puelles and Rubenstein, 1993; Rubenstein et al., 1994) was generated to provide a framework for understanding the morphological development of the prosencephalon. The Prosomeric Model subdivides the forebrain into six transverse domains called prosomeres, lying perpendicular to the anteroposterior (AP) axis of the neural tube, and four longitudinal histogenic domains, lying parallel to the AP axis of the neural tube (from dorsal to ventral: roofplate, alar plate, basal plate and floorplate). The diencephalon develops in prosomeres 1-3 (p1-p3; p1 is the most posterior), which are identified by morphological constrictions in the tissue and the expression domains of regulatory genes including *Pax6*, *Dlx2* and *Wnt3* (Bulfone et al., 1993; Puelles and Rubenstein, 1993; Stoykova and Gruss, 1994). The pretectum forms in p1, the dorsal thalamus in p2 and the ventral thalamus in p3. In relation to the AP axis of the CNS, which bends sharply in the brain, the dorsal thalamus develops posterior to the ventral thalamus. In this report, we retain the conventional nomenclature of "ventral thalamus" and "dorsal thalamus" wherever possible, although we sometimes apply the synonymous terms "anterior thalamus" and "posterior thalamus" (e.g. where the terms are embedded in a discussion of the ventral and dorsal longitudinal domains in the neural tube). The dorsal thalamus is a pivotal forebrain structure, receiving sensory inputs from the periphery and communicating via thalamocortical axons with the cerebral cortex.

The mechanisms that pattern the diencephalon and control the later development of structures such as the dorsal thalamus and its thalamocortical connections are poorly understood. In this study, we tested the role of the transcription factor, *Pax6*, in these processes. Pax6 contains two DNA-binding motifs, a paired domain and a paired-like homeodomain. The

spatiotemporal pattern of its expression, extending from embryonic day 8.5 (E8.5) until adulthood in many structures including the diencephalon, suggests that it plays a role in key stages of forebrain development (Walther and Gruss, 1991; Mansouri et al., 1994; Stoykova and Gruss, 1994). Mutations of *Pax6* result in the small eye (*Sey*) phenotype (Hill et al., 1991). Homozygotes (*Pax6*$^{Sey/Sey}$) show defects in numerous forebrain structures, including the diencephalon, and die shortly after birth (Hogan et al., 1986; Schmahl et al., 1993; Quinn et al., 1996; Stoykova et al., 1996; Caric et al., 1997; Grindley et al., 1997; Mastick et al., 1997; Warren and Price, 1997). Previous studies of the expression domains of regulatory genes have indicated that AP patterning of the diencephalon is relatively normal and that the dorsal thalamus is present in *Pax6*$^{Sey/Sey}$ embryos (Stoykova et al., 1996; Grindley et al., 1997; Mastick et al., 1997; Warren and Price, 1997). Kawano et al. (1999) have shown that, despite the presence of the dorsal thalamus in homozygous small eye rat embryos, thalamocortical connections do not form. Dorsal thalamic axons normally traverse the ventral thalamus and ventral telencephalon to reach the cerebral cortex whereas in the mutants they traverse the ventral thalamus but not the ventral telencephalon.

It has been suggested that the absence of thalamocortical axons in *Pax6*$^{Sey/Sey}$ embryos is due to abnormalities of *Pax6*-expressing cell clusters that lie along their path and would normally guide them (Kawano et al., 1999). The full extent of dorsal thalamic abnormalities in the absence of Pax6 has never been clearly defined, however, and it is equally possible that *Pax6*$^{Sey/Sey}$ dorsal thalamic axons have an intrinsic inability to respond to appropriate growth and guidance factors. We tested this hypothesis by taking dorsal thalamic explants from *Pax6*$^{Sey/Sey}$ embryos in which all the cells were marked with green fluorescent protein (GFP) tagged with tau and confronting them with wild-type ventral telencephalon, the region through which thalamocortical axons normally grow. The results indicated autonomous defects in the responses of dorsal thalamic axons to ventral telencephalic factors. Normal dorsal thalamus downregulates *Pax6* expression at the time when thalamocortical axons start to form (Puelles and Rubenstein, 1993; Stoykova and Gruss, 1994; Stoykova et al., 1996; Mastick et al., 1997; Warren and Price, 1997; Kawano et al., 1999; Auladell et al., 2000; our unpublished observations), and we went on to examine whether other regulatory genes might act as intermediates between Pax6 and the responsiveness of the dorsal thalamus. We describe an early abnormality in dorsoventral (DV) patterning of the *Pax6*$^{Sey/Sey}$ thalamus that may underlie defects in the responses of thalamocortical axons.

MATERIALS AND METHODS

Generation of transgenic mice expressing tau-GFP

Transgenic mice carrying a ubiquitously expressed GFP tagged with tau were generated. The GFP variant mmgfp6 cDNA (a gift from J. Haseloff; Siemering et al., 1996; Zernika-Goetz et al., 1997) was fused at its 5′ end to the 3′ end of a cDNA encoding bovine tau (Callahan and Thomas, 1994). The fusion cDNA was inserted into the mammalian expression vector, pCAGiP (a gift from I. Chambers), allowing the CAG promoter to drive expression of tau-GFP and puromycin resistance (Niwa et al., 1991). This construct was introduced into embryonic stem cells and the transgenic mouse line TgTP6.3 was derived by germline transmission. In these animals tau-GFP is expressed throughout the developing CNS including thalamus (Pratt et al., 2000). The tau tag tethers GFP to the microtubule-containing cytoskeleton, resulting in clear labelling of axons including those of the thalamocortical pathway (Fig. 2A).

Breeding

Embryonic development was assumed to have begun at midnight on the night of mating. Experiments were carried out on E10.5, E11.5, E12.5, E13.5, E14.5 E15.5, E17.5 and E19.5 embryos from matings between *Pax6*$^{Sey/+}$ mice, some of which carried the *tau-GFP* transgene (generating *tau-GFP:Pax6*$^{+/+}$ or *tau-GFP:Pax6*$^{Sey/Sey}$ embryos). *Pax6*$^{Sey/Sey}$ embryos were easily distinguished by their absence of eyes and shortened snout (Hill et al., 1991). Age-matched controls were *Pax6*$^{+/+}$ littermates from these matings and embryos from matings between *Pax6*$^{+/+}$ mice, some of which carried the *tau-GFP* transgene.

Organotypic cocultures

Cultures were carried out following methods in Lotto and Price (1999). Organotypic explants (300 μm thick) containing the regions of interest (dorsal thalamus, cerebral cortex, ventral telencephalon or hypothalamus) were dissected from coronal slices of E14.5 brains (as illustrated in Fig. 2A-D) and arranged on collagen-coated inserts (Costar, UK). Dorsal thalamic explants were from *tau-GFP:Pax6*$^{+/+}$ or *tau-GFP:Pax6*$^{Sey/Sey}$ embryos; other tissues were from *Pax6*$^{+/+}$ or *Pax6*$^{Sey/Sey}$ embryos that did not carry the transgene. Dorsal thalamus was recognized under transmitted and epifluorescence illumination, guided by anatomical landmarks known to correspond to gene expression boundaries defining the dorsal thalamus in both wild-type and mutants (Fig. 2A-E; described in Results). The left and right dorsal thalamus were left joined dorsally in culture and their cut edges (red dotted lines in Fig. 2B,D, just anterior to the border between dorsal and ventral thalamus) were placed against different tissues on each side. To recreate the topography of intact brain as much as possible, these cut edges of dissected thalamus were placed in contact with either the medial edge of dissected ventral telencephalon or the dorsal edge of dissected hypothalamus (Fig. 2B,D). Three days after being placed in serum-free medium, cultures were fixed in ice-cold 4% paraformaldehyde in phosphate-buffered saline (PBS), stained with the nuclear counterstain TO-PRO3 (Molecular Probes, USA) and mounted in 1:1 glycerol:PBS containing 10% Vectashield (Vector Laboratories, UK). Images of the cultures were obtained by combining serial optical sections acquired with a Leica confocal microscope. The following co-culture combinations were tested: *Pax6*$^{+/+}$ ventral telencephalon with either *tau-GFP:Pax6*$^{+/+}$ thalamus (n=25) or *tau-GFP:Pax6*$^{Sey/Sey}$ thalamus (n=21); *Pax6*$^{+/+}$ cortex with either *tau-GFP:Pax6*$^{+/+}$ thalamus (n=21) or *tau-GFP:Pax6*$^{Sey/Sey}$ thalamus (n=21); *Pax6*$^{+/+}$ hypothalamus with either *tau-GFP:Pax6*$^{+/+}$ thalamus (n=6) or *tau-GFP:Pax6*$^{Sey/Sey}$ thalamus (n=6); *Pax6*$^{Sey/Sey}$ ventral telencephalon with *tau-GFP:Pax6*$^{+/+}$ thalamus (n=4).

In situ hybridisation

RNA probes were labelled with digoxigenin, as described by the manufacturer (Roche Diagnostics, UK). The *Sonic hedgehog (Shh), Pax6, Lim1/Lhx1, Nkx2.2* and *Dlx2* plasmids were provided by J. Rubenstein, the *Netrin 1* plasmid by M. Tessier-Lavigne, the *Hbnf* plasmid by T. Vogt and L. Amet and the *VMAT2* plasmid by R. Edwards. Sense probes were synthesised for controls. Embryos were dissected from anaesthetised mothers (0.3 ml of 25% urethane in sterile saline, i.p.) in phosphate-buffered saline (PBS) at 4°C and fixed for 3-12 hours in 4% paraformaldehyde + 0.2 mM egtazic acid (EGTA) at 4°C. The embryos were washed in PBS, dehydrated in ethanol and cleared in xylene for 3 hours. The embryos were then wax embedded, coronally sectioned at 6 μm and collected on TESPA-coated slides. In situ hybridisations were performed as described by Wilkinson (1992). Whole-mount in situ hybridisations (for *Pax6*,

Nkx2.2 and *Netrin 1*) were performed on whole embryos or on 150-200 μm-thick sections, as described by Shimamura et al. (1994).

Pharmacological treatments

Clorgyline (NBI, 30 mg/kg), a specific inhibitor of monoamine oxidase A activity, was administered intraperitoneally to pregnant dams at E17.5. Embryos were sacrificed 3 hours following injection.

Immunocytochemistry for serotonin, calretinin and Nkx2.2

5-HT immunocytochemistry was performed using a rat monoclonal anti-5-HT antibody (1:50; Harlan-SeraLab). Calretinin immunocytochemistry was performed using rabbit polyclonal antibodies (1:10,000; Swant). Embryos were transcardially perfused with saline followed by 4% paraformaldehyde in 0.1 M phosphate buffer (PB) pH 7.4. Brains were removed and postfixed 2-5 days in the same fixative and cryoprotected in 30% sucrose in PB. Serial coronal sections (50 μm) were cut on a freezing microtome and processed as described previously (Cases et al., 1996). Nkx2.2 immunocytochemistry was performed on paraffin-embedded sections. Sections were dewaxed and rehydrated, transferred to a glass container containing 10 mM sodium citrate pH 5.5 and antigens were retrieved by boiling the sections in a microwave (med-high for 15 min). Tissue sections were then transferred to PBS. Non-specific binding sites were blocked by using 2% (v:v) normal sheep serum and 2% (w:v) bovine serum albumin (BSA) in PBS. The excess blocking solution was carefully removed and tissue sections were incubated overnight at room temperature with a 1:30 dilution of mouse monoclonal anti-Nkx2.2 antibody (74.5A5, Developmental Studies Hybridoma Bank, USA). Tissue sections were washed three times in PBS, then incubated for 2 hours with a 1:200 dilution of biotinylated secondary sheep anti-mouse IgG (Amersham, UK). After washing with PBS, tissue sections were incubated with a streptavidin-biotin complex (Amersham, UK) for 2 hours, washed again in PBS and developed as described previously (Cases et al., 1996).

Anatomical analyses

E15.5, E17.5 and E19.5 embryos were processed for wax sectioning as described above and counterstained with Haematoxylin and Eosin or Nissl-stained. We used the nomenclature for anatomical structures described by Paxinos et al. (1991). To reveal the thalamocortical tract with dioctadecyl tetramethylindocarbocyanine perchlorate (DiI; Molecular Probes, USA), E13.5, E15.5. and E17.5 embryos were fixed with paraformaldehyde, small crystals of DiI were placed in the dorsal thalamus and, after diffusion, sections were cut with a vibratome.

RESULTS

Lack of thalamocortical projections in *Pax6$^{Sey/Sey}$* embryos

Kawano et al. (1999) described a failure of thalamocortical axonal development in homozygous small eye rat embryos and, as illustrated in Fig. 1, we found a similar defect in *Pax6$^{Sey/Sey}$* mouse embryos. We labelled dorsal thalamic neurons and their projections with antibodies to 5-HT following treatment with clorgyline, a specific inhibitor of the degradative enzyme monoamine oxidase A, as described by Cases et al. (1998) and Vitalis et al. (1998). In E17.5 clorgyline-treated wild-type embryos, we observed immunolabelled thalamocortical sensory neurons and their axons running from the dorsal thalamus to the cortical subplate (Fig. 1A) through the internal capsule (Fig. 1B). In E17.5 clorgyline-treated *Pax6$^{Sey/Sey}$* embryos, we were unable to detect 5HT-immunolabelled axons in the subplate and internal capsule (Fig. 1C,D). Fig. 1E,F shows staining for calretinin in sections of E17.5 wild-type and *Pax6$^{Sey/Sey}$* embryos. In wild-type embryos, staining was detected in the cell bodies and axonal processes of discrete dorsal thalamic nuclei and in the thalamocortical tract (Arai et al., 1994; Frassoni et al., 1998). In *Pax6$^{Sey/Sey}$* embryos, staining was greatly decreased in the dorsal thalamus, labelled cells were absent from the thalamic midline and there was a loss of immunolabelled thalamocortical axons. We also demonstrated absence of thalamocortical projections in *Pax6$^{Sey/Sey}$* embryos using DiI. As shown in Fig. 1G,H, from E15.5 onwards DiI placed in the dorsal thalamus diffused to the cerebral cortex in wild type (Fig. 1G) but did not get further than the medial part of the ventral telencephalon in the mutants (Fig. 1H shows at high magnification, an area in a mutant equivalent to that indicated by an asterisk in Fig. 2C).

Analysis of thalamocortical growth in culture

The aim of these experiments was to test whether or not axons from dorsal thalamus in *Pax6$^{Sey/Sey}$* embryos are able to respond to growth and/or guidance signals along their path to the cortex. Fig. 2A shows that the thalamocortical tract is clearly visible in our transgenic mice expressing tau-GFP on a wild-type background (*tau-GFP:Pax6$^{+/+}$*). Axons originate from the dorsal thalamus, enter the ventral thalamus and turn at the hypothalamus into the ventral telencephalon, which they penetrate to reach the cortex (Fig. 2A). This tract is not seen in *tau-GFP:Pax6$^{Sey/Sey}$* embryos (Fig. 2C). To test the ability of thalamic axons to innervate tissue encountered along the normal thalamocortical pathway, we cultured explants of *tau-GFP:Pax6$^{+/+}$* and *tau-GFP:Pax6$^{Sey/Sey}$* thalamus in contact with wild-type ventral telencaphalon, hypothalamus or cerebral cortex (Fig. 2F-M; results are shown on a grey tint, which makes axons clearer). Dorsal thalamic explants were removed from sections appearing similar to that shown in Fig. 2A,C, as illustrated in Fig. 2B,D. Analysis of *Dlx2*, *Hbnf* and *Pax6* expression patterns (Figs 2E, 4C-F) and previous descriptions of gene expression patterns (Stoykova et al., 1996; Warren and Price, 1997; Kawano et al., 1999), helped us to define tissue landmarks and to make accurate dissections.

Dorsal thalamus from *tau-GFP:Pax6$^{+/+}$* embryos produced prolific outgrowth into wild-type ventral telencephalon, extending well over half-way through the telencephalic explants, in 76% of cultures (typical examples are shown in Fig. 2F,G). In 62% of these cultures large numbers of thalamic axons curved often quite sharply in a dorsal direction. These features, illustrated in Fig. 2F,G are reminiscent of the in vivo trajectory of thalamic axons as they grow through the internal capsule and turn dorsally towards the neocortex (Fig. 2A). In marked contrast, none of the cultures of *tau-GFP:Pax6$^{Sey/Sey}$* dorsal thalamus with wild-type ventral telencephalon showed these features. In 60% of these cultures thalamic axons did enter the medial part of the ventral telencephalon, but in almost all these cases (86%) not even a single thalamic axon reached anywhere near half-way through the telencephalic explant. A typical example is shown in Fig. 2H. In none of these cultures, nor in the 14% of cases where longer thalamic axons were seen (Fig. 2I illustrates the culture in which there was most growth), was there any evidence of a consistent turning of the thalamic axons in a dorsal direction. Repeated observations of tau-GFP-labelled wild-type and *Pax6$^{Sey/Sey}$* axons in some of the cultures during their 3 days in vitro revealed that the major features of

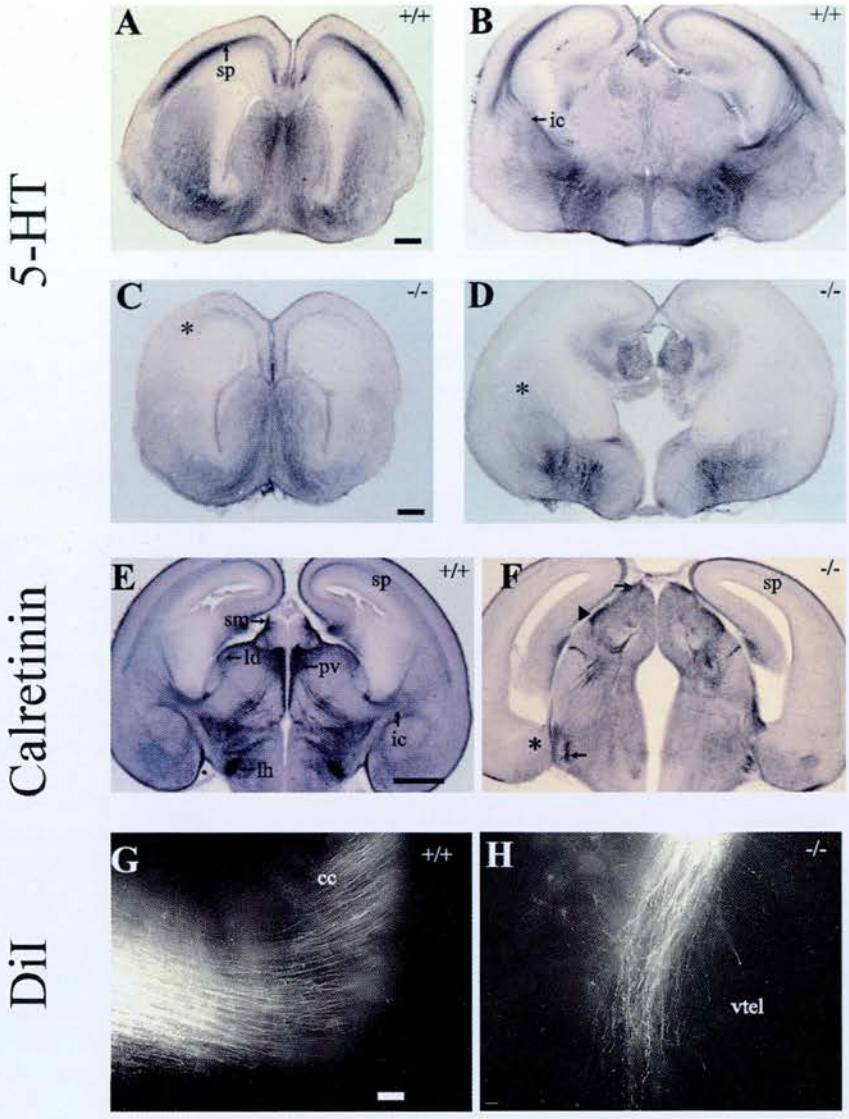

Fig. 1. Thalamocortical defects in *Pax6*$^{Sey/Sey}$ embryos. (A-D) 5-HT immunolabeling in clorgyline-treated E17.5 *Pax6*$^{+/+}$ and *Pax6*$^{Sey/Sey}$ embryos. (A,B) *Pax6*$^{+/+}$ embryos: 5-HT immunolabelled sensory thalamocortical axons at the level of (A) the subplate (sp), and (B) the internal capsule (ic). (C,D) *Pax6*$^{Sey/Sey}$ embryos: loss of 5-HT-immunolabelled sensory axons at the level of (C) the subplate and (D) the internal capsule (* marks expected position of axons in C and D). (E,F) Calretinin immunolabelling in E17.5 *Pax6*$^{+/+}$ and *Pax6*$^{Sey/Sey}$ embryos. (E) *Pax6*$^{+/+}$ embryo: calretinin labelling in the stria medullaris (sm) of the epithalamus, the laterodorsal (ld), paraventricular (pv) and other midline nuclei of the dorsal thalamus and in the lateral hypothalamus (lh). Note calretinin immunopositive fibres extending to/from the pv and ld through the internal capsule (ic) into the subplate (sp) of the developing cortex. (F) *Pax6*$^{Sey/Sey}$ embryo: residual calretinin labelling in lateral regions of the epithalamus (upper arrow), dorsal thalamus (arrowhead) and hypothalamus (lower arrow) and loss of labelling in the midline nuclei. Note loss of calretinin immunopositive fibres at the level of the internal capsule (*marks expected position of fibres). (G,H) High-power views showing the furthest extent of DiI labelling from the dorsal thalamus at E15.5 in (G) *Pax6*$^{+/+}$ and (H) *Pax6*$^{Sey/Sey}$ embryos. Label is in the cerebral cortex (cc) in wild type but has got no further than the medial part of the ventral telencephalon (vtel) in mutants; the mutant axons are more disorganised than those in the wild type. The area in H corresponds to that marked by an asterisk in Fig. 2C. Scale bars, A-F, 500 μm; G,H, 50 μm.

innervation were established quickly, within 1-2 days of the start of culture, and there was less progression between 2 and 3 days. It is unlikely, therefore, that the defective innervation from the *tau-GFP:Pax6*$^{Sey/Sey}$ thalamic explants can be explained simply by a slowing of development.

In all cultures where *tau-GFP:Pax6*$^{+/+}$ dorsal thalamus was placed next to wild-type hypothalamus, thalamic axons coursed around its edge and failed to innervate it (Fig. 2J), in agreement with previous findings on the repulsive nature of the hypothalamus for dorsal thalamic axons (Braisted et al., 1999). The same result was obtained in all cases where *tau-GFP:Pax6*$^{Sey/Sey}$ dorsal thalamic explants were used (Fig. 2L). When *tau-GFP:Pax6*$^{+/+}$ dorsal thalamus was placed with wild-type cortex, most cultures showed large numbers of thalamic axons wrapping around its edges and upper and lower surfaces (Fig. 2K). This pattern has been described before and is due to the inability of the early cortical layers to receive thalamic innervation (Molnar and Blakemore, 1991; Goetz et al., 1992). In 95% of these cultures, thalamic axons extended distances equivalent to at least half-way round the circumference of the cortical explants. When *tau-GFP:Pax6*$^{Sey/Sey}$ dorsal thalamus was cultured with wild-type cortex, the pattern of thalamic axonal growth was similar to that with *tau-GFP:Pax6*$^{+/+}$ dorsal thalamus (Fig. 2M), although in many cases it appeared that there were fewer thalamic axons. In 92% of these cultures large numbers of axons extended distances equivalent to well over half-way round the circumference of the cortical explants, as occurred with *tau-GFP:Pax6*$^{+/+}$ dorsal thalamus.

Several observations indicate that the inability of the *Pax6*$^{Sey/Sey}$ dorsal thalamus to generate normal innervation of ventral telencephalon is not caused by a non-specific inability to grow. First, *Pax6*$^{Sey/Sey}$ dorsal thalamic explants are capable of producing many long axons when co-cultured with wild-type cortex, as do *Pax6*$^{+/+}$ thalamic explants (Rennie et al., 1994). The apparent reduction in the numbers of mutant thalamic axons in these co-cultures is compatible with previous observations that mutant dorsal thalamus contains fewer neurons (proliferation in the early mutant diencephalon is reduced; Warren and Price, 1997), although it could conceivably be due to a defective response by some thalamic neurons to cortex-derived growth-promoting factors. Second, analysis of nuclear morphology with TO-PRO3 showed that

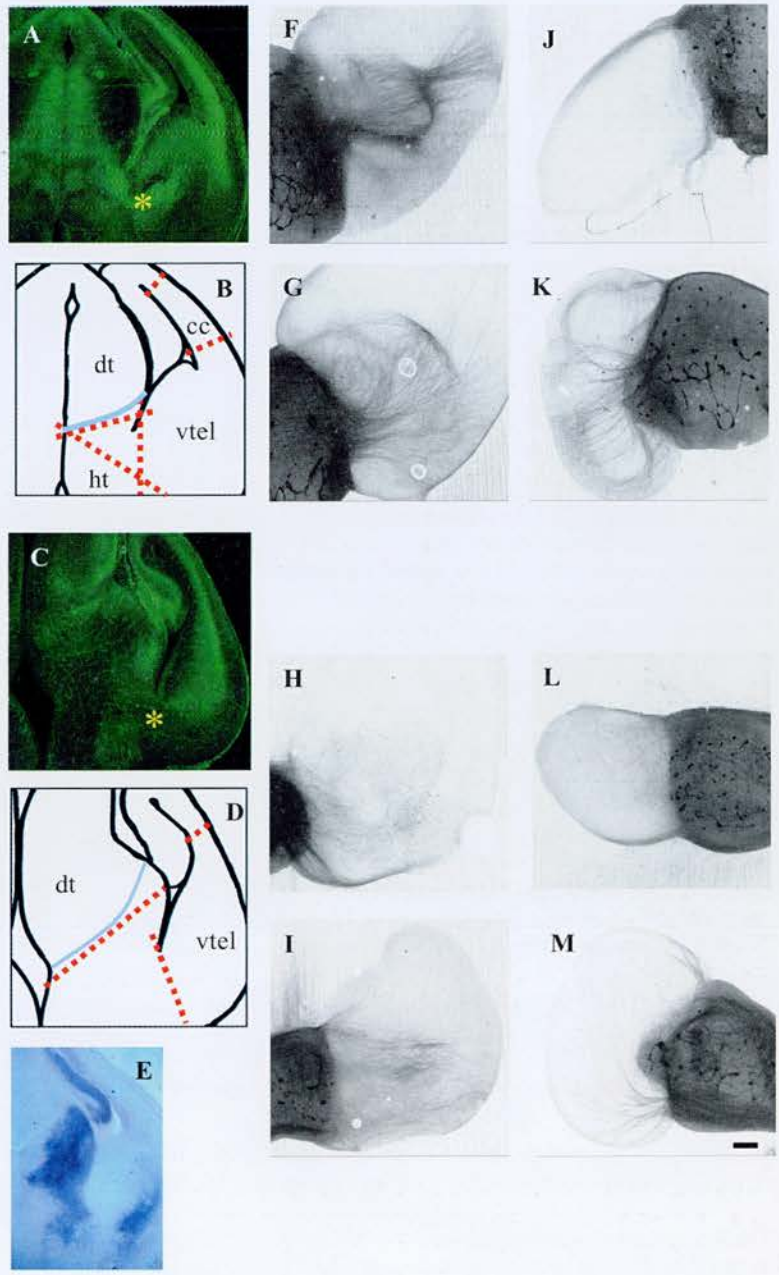

Fig. 2. *Pax6*$^{Sey/Sey}$ thalamic explants exhibit defective tract formation, as shown by organotypic co-culture of *tau-GFP:Pax6*$^{+/+}$ or *tau-GFP:Pax6*$^{Sey/Sey}$ dorsal thalamic (dt) explants with wild-type explants of ventral telencephalon (vtel), hypothalamus (ht), or cerebral cortex (cc). (A,C) Fluorescence images of coronal sections of E14.5 *tau-GFP:Pax6*$^{+/+}$ and *tau-GFP:Pax6*$^{Sey/Sey}$ brains similar to those from which explants were dissected. (A) *tau-GFP:Pax6*$^{+/+}$ embryo showing strong tau-GFP labelling of thalamic axons as they turn sharply to avoid the hypothalamus and enter the ventral telencephalon to form the internal capsule (*). (C) *tau-GFP:Pax6*$^{Sey/Sey}$ embryo, showing that the strong tau-GFP label seen in *tau-GFP:Pax6*$^{+/+}$ embryos is lacking from the position normally occupied by the internal capsule (*). (B,D) Schematic representations of sections shown in A,C with red dotted lines indicating locations of cuts used to isolate the tissues used in these experiments (dt, vtel, ht, and cc) from coronal slices. Panels A-D show only one side but note that the left and right dorsal thalamus were left joined dorsally in culture and their cut edges, just anterior to the border with ventral thalamus, were placed against different tissues on each side. The border between the ventral and dorsal thalamus, as defined by tissue landmarks and the expression of genes such as *Dlx2* and *Pax6*, is shown with a blue line. (E) In situ hybridization on a 200 μm-thick vibratome section (pink counterstain) of a *Pax6*$^{Sey/Sey}$ E14.5 embryo corresponding to the section in C,D, showing expression of *Pax6* (purple) in the thalamus, where it acts as a marker of ventral thalamus even in the mutants (Stoykova et al., 1996; Warren and Price, 1997), and telencephalon. (F-M) Grey tint presentation of fluorescence images showing representative examples of co-cultures of (F,G,J,K) *tau-GFP:Pax6*$^{+/+}$ thalamus or (H,I,L,M) *tau-GFP:Pax6*$^{Sey/Sey}$ thalamus with (F-I) wild-type ventral telencephalon, (J,L) wild-type hypothalamus or (K,M) wild-type cerebral cortex. Scale bar, 200 μm.

under all conditions used here almost all cells in both *Pax6*$^{+/+}$ and *Pax6*$^{Sey/Sey}$ dorsal thalamic explants remain viable. Third, in other experiments in which E14.5 dorsal thalamic explants were dissociated and cultured for 3 days in serum-free medium, *Pax6*$^{+/+}$ and *Pax6*$^{Sey/Sey}$ cells survived and grew neurites equally well (reported in preliminary form by Edgar et al., 1999). Therefore, the inability of the *Pax6*$^{Sey/Sey}$ dorsal thalamus to generate normal ventral telencephalic innervation is likely to be due to its inability to respond to growth and guidance cues in that region.

Although the main focus of this work was the dorsal thalamus and its axons, we carried out a few experiments to gain a better idea of the status of the ventral telencephalon in the mutants. In cultures of *tau-GFP:Pax6*$^{+/+}$ dorsal thalamus with *Pax6*$^{Sey/Sey}$ ventral telencephalon we observed prolific innervation by long axons, indicating that the mutant ventral telencephalon does not lack the ability to stimulate and receive dorsal thalamic innervation (Fig. 3A). Innervation did not appear normal, however, and many axons turned in abnormal ways in the mutant ventral telencephalon (compare Fig. 3A with Fig. 2F,G). We probed the *Pax6*$^{Sey/Sey}$ ventral telencephalon for expression of *Netrin 1*, a potential candidate for a chemoattractant of thalamocortical axons (Braisted et al., 1999, 2000), and found similar expression as in wild-types (Fig. 3B,C). Although the *Pax6*$^{Sey/Sey}$ ventral telencephalon may be permissive for incoming thalamic axons, it is quite possible that defects in this region contribute to the lack of thalamocortical innervation in small eye homozygotes.

Altered expression of dorsal thalamic markers in *Pax6*$^{Sey/Sey}$ embryos

Previous studies of the major subdivisions of the diencephalon in small eye homozygotes, using molecular markers other than those applied here, all identified a region equivalent to dorsal thalamus in the mutants (Stoykova et al., 1996; Grindley et al., 1997; Warren and Price, 1997; Kawano et al., 1999). Major molecular defects of this region were not described. By probing *Pax6*$^{Sey/Sey}$ embryos for expression of two mRNAs that normally mark dorsal thalamus, we obtained evidence of such defects. The mRNAs examined encode the vesicular monoamine transporter type 2 (*VMAT2*; Lebrand et al., 1999)

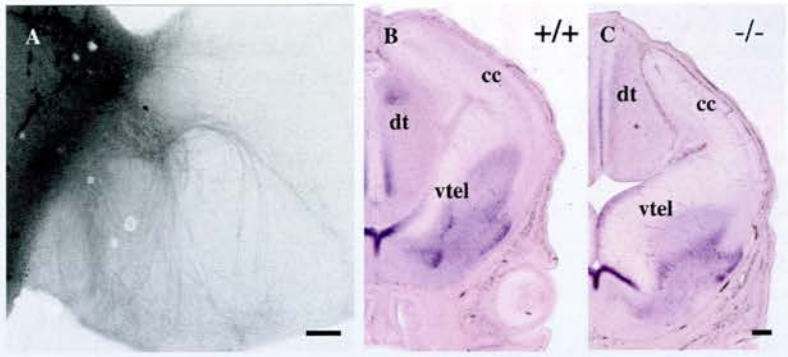

Fig. 3. The nature of the ventral telencephalon in *Pax6*$^{Sey/Sey}$ embryos. (A) Organotypic co-culture of *tau-GFP:Pax6*$^{+/+}$ dorsal thalamic explant with explant of *Pax6*$^{Sey/Sey}$ ventral telencephalon. (B,C) In situ hybridizations showing *Netrin 1* expression in the ventral telencephalon of *Pax6*$^{+/+}$ and *Pax6*$^{Sey/Sey}$ E14.5 embryos. Abbreviations as in Fig. 2. Scale bar, 200 μm.

and the secreted molecule heparin binding neurotrophic factor (*Hbnf*; Bloch et al., 1992; Rauvala et al., 1994). In E15.5 and E17.5 *Pax6*$^{+/+}$ embryos, *VMAT2* was expressed in dorsal thalamic nuclei (Fig. 4A; Lebrand et al., 1999). In age-matched *Pax6*$^{Sey/Sey}$ embryos there was a severe loss of *VMAT2* expression in the body of the dorsal thalamus, with only very faint residual expression barely detectable posterodorsally (arrow in Fig. 4B). In *Pax6*$^{+/+}$ embryos aged E13.5 or more, *Hbnf* was expressed throughout the entire body of the dorsal thalamus, with a sharp anterior boundary at the border with the ventral thalamus, the zona limitans intrathalamica (zli; arrow in Fig. 4C), and in the epithalamus. In *Pax6*$^{Sey/Sey}$ embryos aged E13.5 or more there was a loss of *Hbnf* expression in the dorsal thalamus (Fig. 4D). Expression was retained posterodorsally in the epithalamus (arrow in Fig. 4D). In these experiments we used *Dlx2* expression to mark the posterior ventral thalamic border at the zli, which it does even in *Pax6*$^{Sey/Sey}$ mice (Fig. 4E,F; Warren and Price, 1997), and showed that this boundary is well-separated from residual *Hbnf* expression in *Pax6*$^{Sey/Sey}$ epithalamus (Fig. 4D). The tissue between the posterior boundary of *Dlx2* expression and the epithalamus is labelled dorsal thalamus (dt) in Fig. 4C-F.

Ectopic expression of *Lim1/Lhx1* in the *Pax6*$^{Sey/Sey}$ dorsal thalamus

Since *Pax6* is downregulated in the dorsal thalamus as thalamocortical axons begin to form (around E12.5-E13.5; Auladell et al., 2000), it is possible that the incompetence of *Pax6*$^{Sey/Sey}$ dorsal thalamic axons to navigate the ventral telencephalon is an indirect defect caused via more persistent changes in other regulatory genes. In *Pax6*$^{Sey/Sey}$ embryos aged E13.5 or more, we found a striking abnormality of *Lim1/Lhx1* expression in the thalamus (Fig. 5). In wild-type embryos, *Lim1/Lhx1* was expressed in ventral thalamic nuclei but was excluded from the dorsal thalamus (Fig. 5A,C,D), whereas in mutants it was expressed throughout both the ventral and the dorsal thalamus (Figs 5B,E,F). In these experiments, we confirmed the location of the zli by staining adjacent sections for expression of *Dlx2*. As described before by Mastick et al. (1997), *Lim1/Lhx1* expression was lost from the pretectum in mutants (Fig. 5D,F).

Altered expression of *Shh* and *Nkx2.2* in *Pax6*$^{Sey/Sey}$ diencephalon

We examined expression of two genes, *Shh* and *Nkx2.2*,

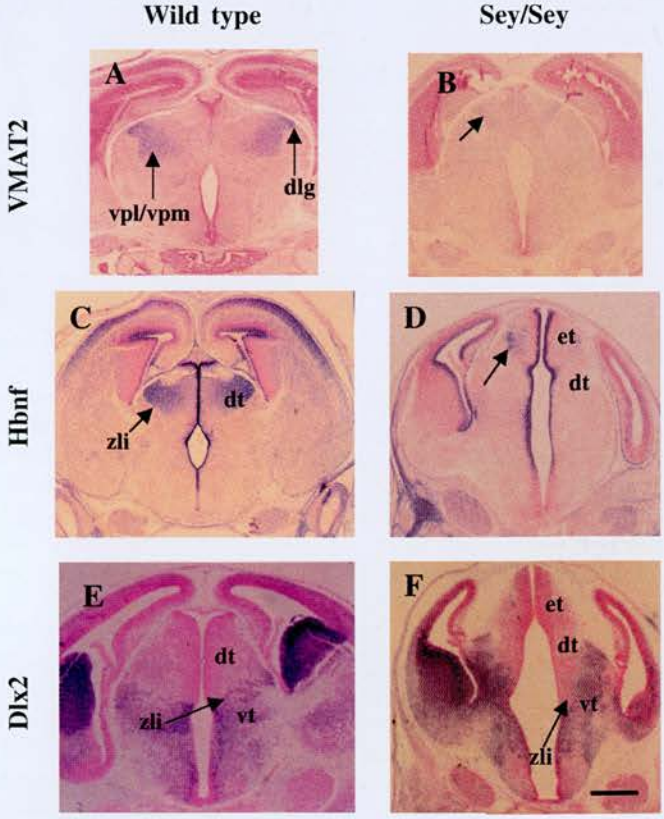

Fig. 4. Expression of dorsal thalamic markers in *Pax6*$^{Sey/Sey}$ embryos. In situ hybridisation on coronal sections of (A,B) E17.5 and (C-F) E15.5 *Pax6*$^{+/+}$ and *Pax6*$^{Sey/Sey}$ embryos for (A,B) *VMAT2* expression, (C,D) *Hbnf* expression and (E,F) *Dlx2* expression. (A) *Pax6*$^{+/+}$ embryo: *VMAT2* expression in dorsal thalamic nuclei including the ventral posteromedial (vpm) and ventral posterolateral (vpl) and dorsolateral geniculate (dlg). (B) *Pax6*$^{Sey/Sey}$ embryo: loss of *VMAT2* expression in the dorsal thalamus, with only very faint residual expression (arrow). (C) *Hbnf* expression in *Pax6*$^{+/+}$ embryo: there is strong expression in the dorsal thalamus as well as at other sites including the epithalamus, cells lining the 3rd and lateral ventricles, the basal telencephalon and developing cortical plate. (D) *Hbnf* expression in *Pax6*$^{Sey/Sey}$ embryos: there is a severe loss of Hbnf expression in the body of the dorsal thalamus with only slight residual expression in the epithalamus (arrow). (E,F) *Dlx2* expression in sections corresponding to those in C and D respectively. Even in *Pax6*$^{Sey/Sey}$ embryos, expression is restricted to ventral thalamus (Stoykova et al., 1996; Warren and Price, 1997), making this a useful marker of the border between dorsal and ventral thalamus. zli, zona limitans intrathalamica; dt, dorsal thalamus; et, epithalamus; vt, ventral thalamus. Scale bar, 500 μm.

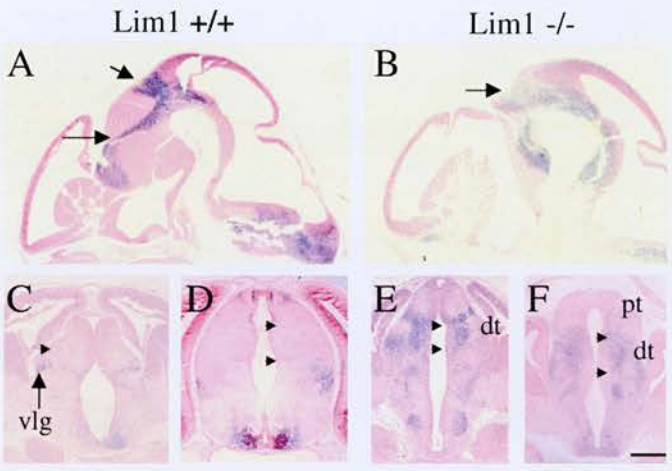

Fig. 5. *Lim1/Lhx1* expression in *Pax6*$^{Sey/Sey}$ embryos. In situ hybridisation on (A,B) sagittal and (C-F) coronal sections of (A,B) E13.5 and (C-F) E15.5 *Pax6*$^{+/+}$ and *Pax6*$^{Sey/Sey}$ embryos. (A) In wild type, *Lim1/Lhx1* is expressed in the pretectum (top arrow), ventral to the dorsal thalamus and around the zli (bottom arrow). (B) In mutants, *Lim1/Lhx1* expression extends over the body of the dorsal thalamus (arrow). (C) Rostral and (D) caudal sections of wild type embryos: *Lim1/Lhx1* expression is restricted to specific nuclei in the ventral thalamus, including the ventrolateral geniculate nucleus (vlg) rostrally. (E) Rostral and (F) caudal sections of mutant embryos: a large band of ectopic *Lim1/Lhx1* expression is visible within the body of the dorsal thalamus (dt) at all rostrocaudal levels. Note the absence of label in the pretectum (pt). In the ventral thalamus, *Lim1/Lhx1* expression is distorted and no longer restricted to discrete areas. The borders of the dorsal thalamus are marked with arrowheads; the position of the border between dorsal and ventral thalamus was confirmed by probing for *Dlx2* expression in nearby sections. Scale bar, 500 μm.

implicated in DV patterning of the central nervous system. The expression of *Shh* in *Pax6*$^{+/+}$ and *Pax6*$^{Sey/Sey}$ embryos, in whole-mount (Fig. 6A,B) and sectioned embryos (not shown), confirmed the findings of others (Barth et al., 1995; Shimamura et al., 1995; Grindley et al., 1997). In both wild-type and mutant embryos at all ages studied (E10.5, E13.5 and E15.5), *Shh* was expressed along the AP axis of the ventral neural tube with a dorsal deflection at the zli (Fig. 6A,B). As reported by Grindley et al. (1997), the domain of expression at the ventral end of the zli (the region between the short lines in Fig. 6A,B) was slightly broader in age-matched mutants, extending a little further into the presumptive dorsal thalamus.

In situ hybridizations for *Nkx2.2* in E10.5 *Pax6*$^{+/+}$ embryos showed expression along the AP axis in a longitudinal band adjacent to *Shh* expression (not shown; described before by Shimamura et al., 1995; summarized in Fig. 8). In E13.5 *Pax6*$^{+/+}$ embryos, the domain of *Nkx2.2* expression remained tightly restricted around the zli and did not encroach on the body of the dorsal (posterior) thalamus (Fig. 6C; Shimamura et al., 1995; Kitamura et al., 1997). In age-matched *Pax6*$^{Sey/Sey}$ embryos, *Nkx2.2* expression extended to include the body of the dorsal thalamus (Fig. 6D).

Immunocytochemical analysis of Nkx2.2 expression confirmed these findings. At E10.5, diencephalic expression of Nkx2.2 was restricted to a band of cells adjacent to *Shh* expression in both *Pax6*$^{+/+}$ and *Pax6*$^{Sey/Sey}$ embryos. A difference between diencephalic expression in *Pax6*$^{+/+}$ and *Pax6*$^{Sey/Sey}$ embryos emerged between E11.5 and E12.5, with cells labelled for Nkx2.2 dispersed in the body of the presumptive dorsal thalamus in the mutants but not in the wild-type embryos. This difference persisted at older ages. At E17.5 (Fig. 7), many cells expressing Nkx2.2 in the mutants were present throughout the dorsal thalamus and the pretectum, right up to their dorsal edge (between the arrows in Fig. 7B), whereas Nkx2.2-positive cells were confined to the ventral edge of these regions in wild type (Fig. 7A). The density of ectopic labelled cells in the mutants was greatest in the anterior and ventral parts of the dorsal thalamus.

The results of our work are summarized in Fig. 8. Our gene expression studies indicate a respecification of the presumptive posterior (dorsal) thalamus in prosomere 2 in *Pax6*$^{Sey/Sey}$ embryos. In this respecification the dorsal thalamus takes on molecular characteristics normally restricted to tissue ventral and anterior to it, changes that are indicated by arrows in Fig.

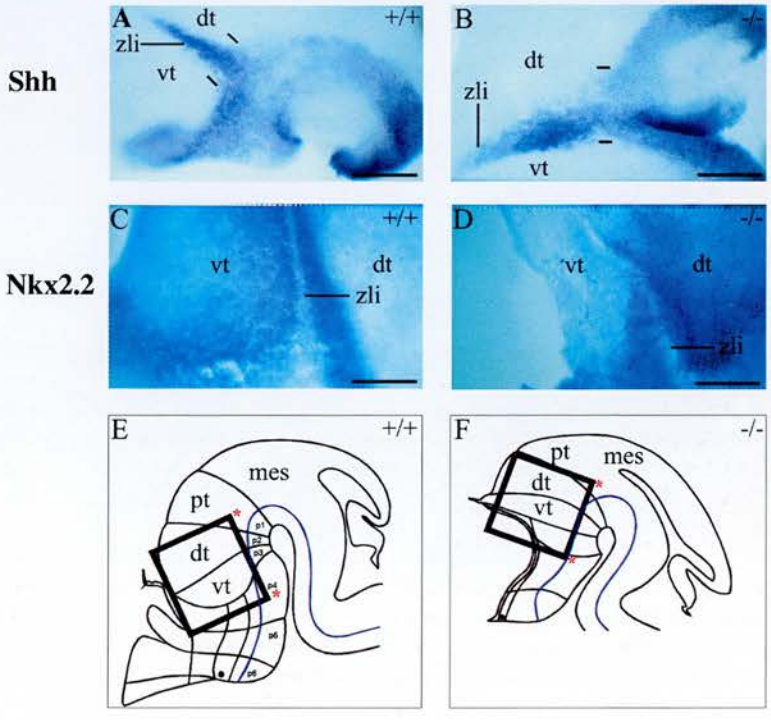

Fig. 6. In situ hybridisations on dissected embryos at E13.5. (A) *Pax6*$^{+/+}$ embryo: *Shh* expression along the AP axis of the ventral neural tube and along the zli. (B) *Pax6*$^{Sey/Sey}$ embryo: a similar pattern is seen, but note slight expansion of the domain of *Shh* expression around the zli (described by Grindley et al., 1997; compare distance between black bars in A and B). (C) *Pax6*$^{+/+}$ embryo: *Nkx2.2* expression flanks the zli and is confined to a narrow strip along its posterior edge. (D) *Pax6*$^{Sey/Sey}$ embryo: abnormal *Nkx2.2* expression is seen throughout the body of the dorsal thalamus. The black boxes in the schematics shown in E and F indicate where panels C and D were taken from; the bases of the panels are indicated by red asterisks in E and F. Abbreviations as in Fig. 4; mes, mesencephalon. Scale bars A,B, 500 μm; C,D, 250 μm.

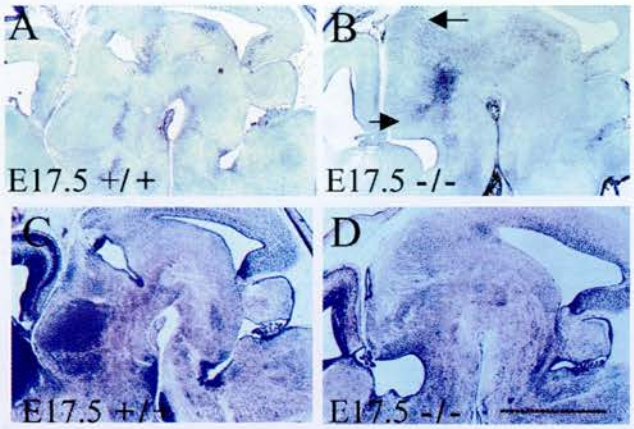

Fig. 7. Illustrates the results of immunocytochemistry for Nkx-2.2 in parasagittal sections of E17.5 *Pax6*$^{+/+}$ and *Pax6*$^{Sey/Sey}$ embryos. (A,B) Immunochemistry and (C,D) corresponding Nissl sections. In mutants labelled cells are found throughout the dorsoventral extent of the diencephalon, even along its dorsal edge (between the arrows in B). In wild type embryos they are confined in a strip running ventral to the posterior thalamus and its surrounding structures. Scale bar, 1 mm.

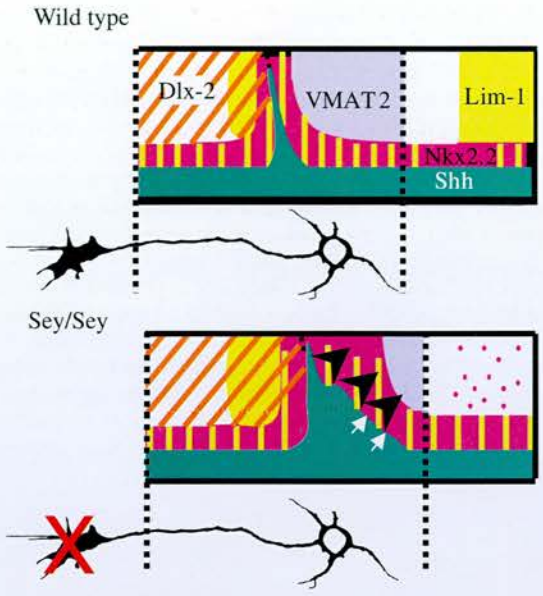

Fig. 8. Summary diagram of our main findings. Gene expression: dark blue, *Shh*; red (areas and dots, the latter indicating less dense label), *Nkx2.2*; yellow (areas and vertical bars, the latter used where there is overlap), *Lim1/Lhx1*; light blue, *VMAT2*; orange cross-hatching, *Dlx2*. Arrows and arrowheads indicate the main changes that form the focus of this study. For clarity, the schematics provide a qualitative summary only, they do not reflect the shape of the diencephalon nor are they to scale. The neuron below each schematic represents a thalamocortical axon, the red cross indicating incompetence to respond to ventral telencephalic growth and guidance factors.

8. For comparison with work in other regions of the central nervous system, this respecification may be more easily described as a ventralization than an anteroventralization, since elsewhere *Shh* and *Nkx2.2* are expressed ventrally and not, as is the case at and around the zli, in alar regions.

DISCUSSION

The thalamocortical tract fails to form normally in *Pax6*$^{Sey/Sey}$ mice. In the wild type, the tract projects from the dorsal thalamus and travels through the ventral thalamus, avoids the hypothalamus, turns sharply into the ventral telencephalon (forming the internal capsule), and then reaches its target in the cerebral cortex (Tuttle et al., 1999; Braisted et al., 1999; Auladell et al., 2000). In *Pax6*$^{Sey/Sey}$ mice, the dorsal thalamus does project a tract but it fails to enter the cortex and appears to become stalled en route from the ventral thalamus to the ventral telencephalon (Kawano et al., 1999; present study).

A comparison of timetables for *Pax6* gene expression in developing forebrain (Stoykova et al., 1996; Grindley et al., 1997; Mastick et al., 1997; Warren and Price, 1997; Kawano et al., 1999) and thalamocortical tract formation (Tuttle et al., 1999; Braisted et al., 1999; Auladell et al., 2000) suggests several locations at which *Pax6* could influence the developing thalamocortical tract. *Pax6* is expressed at many points along the thalamocortical pathway at times coinciding with critical events in thalamocortical tract formation including the dorsal thalamus, where *Pax6* expression coincides with neurogenesis between E10 and E13 (Angevine, 1970), the ventral thalamus, the hypothalamus, the ventral telencephalon and the cerebral cortex. The failure of the thalamocortical tract to form in the absence of *Pax6* function could reflect a requirement for *Pax6* at one or more of these locations.

We present new evidence that supports the hypothesis that a structure equivalent to the dorsal thalamus emerges in the absence of *Pax6* but that its subsequent differentiation and ability to project a thalamocortical tract does require *Pax6* function.

Pax6 is not required for formation of the dorsal thalamus but is required for its correct differentiation

Previous studies of the embryonic diencephalon in *Pax6*$^{Sey/Sey}$ mice showing relatively normal AP expression patterns of *Dlx, Otx, Emx Wnt* genes, *Prox1*, *Gbx2, Mash1* and *Pax6* have indicated that diencephalic AP patterning is not greatly disturbed (Stoykova et al., 1996; Warren and Price, 1997; Grindley et al., 1997). These gene expression studies have suggested that the embryonic *Pax6*$^{Sey/Sey}$ diencephalon possesses correlates of the histogenetic regions that in the wild type give rise to major diencephalic structures. Despite obvious distortions in the shape of the embryonic *Pax6*$^{Sey/Sey}$ diencephalon (Stoykova et al., 1996), which may in part be due to defects of cell proliferation in this region (Warren and Price, 1997), morphological features reminiscent of those that distinguish diencephalic regions in the wild type have been described. Equivalents of prosomeres 1-3 and their main components, the ventral and dorsal thalamus and the pretectum, have been identified on the basis of gene expression and morphology in the mutants and named according to their wild-type counterparts (Stoykova et al., 1996; Mastick et al., 1997; Warren et al., 1997; Kawano et al., 1999; present study).

The alterations we observe in the expression patterns of several genes (*Hbnf*, *VMAT2*, *Lim1/Lhx1*, and *Nkx2.2*) are

superimposed on these structures and reflect a failure of the *Pax6*$^{Sey/Sey}$ dorsal thalamus to differentiate normally in the absence of *Pax6* expression. These molecular patterning defects indicate that the differentiation program of the *Pax6*$^{Sey/Sey}$ dorsal thalamus is disrupted during the period when it fails to make appropriate connections with the central cortex.

Pax6 is required within the dorsal thalamus for thalamocortical tract formation

Pax6 and dorsal thalamic tract projection

From observations of the *Pax6*$^{Sey/Sey}$ brain alone, it is conceivable that the thalamocortical tract defect results from an autonomous defect in the dorsal thalamus itself, or from defects in the environment through which the thalamocortical axons navigate, or a combination of the two. To address this issue, we show that explants of mutant dorsal thalamus are defective in their ability to project a tract capable of correct navigation through wild-type ventral telencephalon. This defect may be limited to this specific aspect of thalamocortical growth since *Pax6*$^{Sey/Sey}$ thalamic axons innervate wild-type cortex and avoid wild-type hypothalamus, as do wild-type thalamic axons. These new data provide direct evidence that *Pax6* expression is required within the dorsal thalamus itself, regardless of whether *Pax6* expression is also required at other locations.

Because our thalamic explants contained some ventral thalamus and epithalamus as well as dorsal thalamic tissue, it is formally possible that our results could be explained by the lack of essential signalling to axons *en passant* (Wang and Tessier-Lavigne, 1999). This possibility would demand that adjacent tissues instruct axons leaving the dorsal thalamus in ventral telencephalic navigation. The zli or the ventral thalamus would be possible candidates for this type of interaction (Mastick et al., 1997; Braisted et al., 1999; Tuttle et al., 1999). The evidence, however, is against such a possibility. Wild-type thalamic explants in our cultures exhibit similar features of axon outgrowth to cultures using dorsal thalamic explants prepared from embryonic brain at similar ages but with surrounding tissues removed. These features include avoidance of the hypothalamus, attraction towards the ventral telencephalon and penetration of the cortex (Molnar and Blakemore, 1991, Goetz et al., 1992; Braisted et al., 1999, 2000). Since these 'pure' dorsal thalamic explants have been isolated from potential instruction by cells lying outside the dorsal thalamus, such instructions are unlikely to be important for these features of thalamocortical tract formation.

The design and interpretation of the explant experiments depends on correct identification of dorsal thalamus in mutant brain for explant isolation. Given the disturbed anatomy of the mutant diencephalon, it was critical that in spite of these abnormalities the dorsal thalamic explants isolated from wild-type and mutant brain were equivalent. We argue above that the *Pax6*$^{Sey/Sey}$ embryo does possess a structure corresponding to the dorsal thalamus which can be identified by its morphology and gene expression patterns. The problem of equivalence reduces to choosing explants in which axons projecting from *Pax6*$^{Sey/Sey}$ and wild-type dorsal thalamus have equal opportunities to interact with target tissues. The major defect in thalamocortical tract formation in mutants appears to occur as axons attempt to navigate from the ventral thalamus into the ventral telencephalon (Kawano et al., 1999; present study). There is no evidence that axons originating from the dorsal thalamus become stalled in the ventral thalamus or that they fail to avoid the hypothalamus. We therefore selected explants that centered on the dorsal thalamus but also contained some ventral thalamic and epithalamic tissue. This ensured that dorsal thalamus was present and enabled us to position our explants to recreate the topography of intact brain more accurately than if we had attempted to dissect smaller pieces of tissue with resulting loss of anatomical landmarks. Since the ventral thalamus/ventral telencephalon transition zone, where thalamocortical defects in the *Pax6*$^{Sey/Sey}$ mice occur, was absent from our thalamic explants, axons from *Pax6*$^{Sey/Sey}$ or wild-type were able to navigate to the edge of the thalamic explant where they were confronted by the target tissue. The observation that thalamic axons responded to the target tissues in ways reminiscent of their behavior in vivo supported the accuracy of our culture system.

Pax6 and the ventral telencephalon

We also show that *Pax6*$^{Sey/Sey}$ ventral telencephalon maintains normal expression patterns of netrin 1, a molecule implicated in thalamocortical tract formation (Braisted et al., 2000), and is permissive to wild-type thalamic axons. Therefore although we cannot rule out the possibility that defects in the ventral telencephalon contribute to the lack of thalamocortical innervation in *Pax6*$^{Sey/Sey}$ embryos, we find no evidence that such defects can account for the *Pax6*$^{Sey/Sey}$ thalamocortical phenotype wholly.

Roles of *Pax6* in the genetic cascade which programs the development of dorsal thalamus

Regulation of transcription factors and secreted morphogens by *Pax6*

Work on the developing spinal cord and hindbrain has implicated Pax6, together with the secreted morphogen Shh, the transcription factor Nkx2.2 and members of the LIM/LHX family of homeodomain proteins in DV patterning and neuronal fate determination in these posterior regions (Echelard et al., 1993; Krauss et al., 1993; Roelink et al., 1994, 1995; Appel et al., 1995; Marti et al., 1995; Tanabe et al., 1995; Ericson et al., 1995, 1996, 1997; Osumi et al., 1997; Briscoe et al., 1999). *Pax6* may play a similar role in the developing diencephalon. It is possible that *Nkx2.2* expression ventral and anterior (at the zli) to the posterior thalamus of normal embryos is induced by Shh, which diffuses from ventral territory and from the zli, and directly or indirectly repressed by Pax6 in dorsal territory. The accumulation of *Nkx2.2*-positive cells in the posterior thalamus in *Pax6*$^{Sey/Sey}$ embryos older than E10.5 could result from Shh induction in the absence of a constraining influence from Pax6. Our observation that densities of ectopic labelling for *Nkx2.2* in the mutants were highest at the ventral and anterior parts of the posterior thalamus could be explained because these are the parts closest to the expression domain of *Shh*. Another likely contributing factor is that, as first reported by Grindley et al. (1997), the domain of *Shh* expression is slightly expanded at the ventral end of the zli. It is interesting that the normal downregulation of *Pax6* in the developing wild-type posterior thalamus is not followed by upregulation of expression of *Nkx2.2* in this region. This argues against the persistence of a simple reciprocal relationship between levels of *Pax6* and *Nkx2.2*

expression throughout the period of posterior thalamic development. While such a relationship may play an important role in early patterning of this region, other factors such as the levels of Shh protein or repressive molecules in the posterior thalamus may constrain the dorsal edge of the domain of *Nkx2.2* later on in normal development. It is possible that ectopic expression of *Nkx2.2* in the posterior thalamus in *Pax6*$^{Sey/Sey}$ embryos contributes to generating ectopic expression of *Lim1/Lhx1* in this region, as in more caudal regions of the neural tube (Ericson et al., 1997; Briscoe et al., 1999).

Regulation of cell surface properties by *Pax6*

The cerebral cortex, like the dorsal thalamus, exhibits *Pax6* expression in ventricular zone cells during neurogenesis and downregulates *Pax6* expression in postmitotic cells. The expression of Pax6 in proliferating cortical neurons influences their postmitotic gene expression patterns and cell surface properties with the maintenance of this genetic pattern becoming independent of the presence of Pax6 (Warren et al., 1999). Work on the developing cerebral cortex has implicated *Pax6* in regulating members of the cadherin family of cell adhesion molecules (Stoykova et al., 1997) and the trk family of neurotrophin receptors (Warren et al., 1999). In vitro aggregation assays (Stoykova et al., 1997) and transplantation experiments (our unpublished results) have established that the adhesive properties of cortical cells are altered in *Pax6*$^{Sey/Sey}$ embryos. Roles for *Pax6* in regulating adhesive properties have been elegantly demonstrated in the eye by analysis of *Pax6*$^{Sey/Sey}$ $\leftrightarrow$ wild-type chimeras (Quinn et al., 1996; Collinson et al., 2000). *Pax6* has also been implicated in axon pathfinding in the tract of the postoptic commissure (Mastick et al., 1997) and spinal cord (Ericson et al., 1997) as well as in the thalamocortical tract (Tuttle et al, 1999; Kawano et al., 1999; present study). Consistent with its roles elsewhere in the CNS, Pax6 probably controls thalamocortical tract formation by regulating the cell surface properties of dorsal thalamic cells and influencing the navigation choices made by their growth cones.

Clarification of the molecular mechanisms of Pax6 action will be facilitated as the tally of molecules implicated in thalamocortical tract formation increases. At present these include cell surface receptors DCC, Neogenin, Robo1, Robo2, RPTPδ, and LAMP, and secreted molecules Netrin 1, Slit1 and Slit2 (Ringsted et al., 1999; Braisted et al., 2000; Tuttle et al., 1999; Mann et al., 1998). A recent study by Braisted et al. (2000) has demonstrated that Netrin 1 promotes the growth of thalamocortical axons through the ventral telencephalon and so it is possible that abnormalities in *Pax6*$^{Sey/Sey}$ embryos may be contributed to by defects of receptors mediating its attractant effects, DCC and Neogenin. Both are expressed in the normal dorsal thalamus. Our preliminary evidence, however, suggests that DCC is still expressed in the dorsal thalamus of *Pax6*$^{Sey/Sey}$ embryos (T. V., unpublished observations). Given that defects of thalamocortical axons are less severe in loss-of-function mutation of Netrin 1 than in *Pax6*$^{Sey/Sey}$ embryos and that blocking Netrin 1 in vitro does not abolish thalamic axon attraction to ventral telencephalon (Braisted et al., 2000), it is hard to explain the small eye defects on the basis of a loss of Netrin 1 responsiveness alone. Other perhaps as yet unidentified signalling systems are likely involved.

Conclusion

The requirement for Pax6 in the dorsal thalamus is lifted by the time its cells become postmitotic. It is possible that *Pax6* has direct effects on the expression of cell surface molecules involved in receptor/ligand interactions, cell adhesion or axon pathfinding before it is downregulated. However, our findings that the defective responses of *Pax6*$^{Sey/Sey}$ dorsal thalamic axons coincide with persistent changes in the expression patterns of regulatory genes other than *Pax6* from the early stages of dorsal thalamic development allows that these defects may result indirectly from the early absence of Pax6 from this region. Genes such as *Lim1/Lhx1* or *Nkx2.2* whose expression is influenced by *Pax6* may have more direct effects, for example up- or downregulating the expression of effector molecules. Whether direct or indirect, we conclude that *Pax6* plays an essential role in the development of the dorsal thalamus and the ability of its axons to respond to key growth and guidance cues.

We thank J. Rubenstein, T. Vogt, L. Amet, M. Kaufman, E. McLean, M. Canning, H. Pearson, P. Gaspar, R. Edwards, M. Tessier-Lavigne, I. Chambers, J. Haseloff and O. Cases for their help throughout this study, and the Medical Research Council, EC Biomed and The Wellcome Trust for financial support.

REFERENCES

Angevine, J. B. Jr. (1970) Time of neuron origin in the diencephalon of the mouse. An autoradiographic study. *J. Comp. Neurol.* **139**, 129-187.

Appel, B., Korzh, V., Glasgow, E., Thor, S., Edlund, T., Dawid, I. B. and Eisen, J. S. (1995). Motoneuron fate specification revealed by patterned LIM homeobox gene expression in embryonic zebrafish. *Development* **121**, 4117-4125.

Arai, R., Jacobowitz, D. M. and Deura, S. (1994). Distribution of calretinin, calbindin-D28k and parvalbumin in the the rat thalamus. *Brain Research Bulletin* **33**, 595-615.

Auladell, C., Perez-Sust, P., Super, H. and Soriano, E. (2000) The early development of thalamocortical and corticothalamic projections in the mouse. *Acta Embryol.* **201**, 169-179.

Barth, K. A. and Wilson, S. W. (1995). Expression of zebrafish *nk2.2* is influenced by *sonic hedgehog/vertebrate hedgehog-1* and demarcates a zone of neuronal differentiation in the embryonic forebrain. *Development* **121**, 1755-1768.

Bloch, B., Normand, E., Kovesdi, I. and Bohlen, P. (1992). Expression of HBNF gene in the brain of fetal, neonatal and adult rat: an in situ hybridisation study. *Dev. Brain Res.* **70**, 267-278.

Braisted, J. E., Tuttle, R. and O'Leary, D. D. M. (1999). Thalamocortical axons are influenced by chemorepellent and chemoattractant activities localized to decision points along their path. *Dev. Biol.* **208**, 430-440.

Braisted, J. E., Catalano, S. M., Stimac, R., Kennedy, T. E., Tessier-Lavigne, M., Shatz, C. J. and O'Leary, D. D. M. (2000) Netrin-1 promotes thalamic growth and is required for proper development of the thalamocortical projection. (2000). *J. Neurosci.* **20,** 5792-5801.

Briscoe, J., Sussel, L., Serup, P., Hartigan-O'Connor, D., Jessell, T. M., Rubenstein, J. L. and Ericson J. (1999). Homeobox gene Nkx2.2 and specification of neuronal identity by graded Sonic hedgehog signalling. *Nature* **398**, 622-627.

Bulfone, A., Puelles, L., Porteus, M. H., Frohman, M. A. and Rubenstein, J. L. R. (1993). Spatially restricted expression of Dlx-1, Dlx-2 (Tes-1), Gbx-2 and Wnt-3 in the embryonic day 12.5 mouse forebrain defines potential transverse and longitudinal segmental boundaries. *J. Neurosci.* **13**, 3155-3172.

Callahan, C. A. and Thomas, J. B. (1994). Tau-β-galactosidase, an axon targeted fusion protein. *Proc. Natl. Acad. Sci. USA* **91**, 5972-5976.

Caric, D., Gooday, D., Hill, R. E., McConnell, S. K. and Price, D. J. (1997). Determination of the migratory capacity of embryonic cortical cells lacking the transcription factor Pax6. *Development* **124**, 5087-5096.

Cases, O., Vitalis, T., Seif, I., De Maeyer, E., Sotelo, C. and Gaspar, P.

(1996). Lack of barrels in the somatosensory cortex of monoamine oxidase A-deficient mice: a role of a serotonin excess during the critical period. *Neuron* **16**, 297-307.

Cases, O., Lebrand, C., Giros, B., Vitalis, T., De Mayer, E., Caron, M. G., Price, D. J., Gaspar, P. and Seif, I. (1998). Plasma membrane transporters of serotonin, dopamine and norepinephrine mediate serotonin accumulation in atypical locations in the developing brain of monoamine oxidase A knock-outs. *J. Neuorosci.* **18**, 6914-6927.

Collinson, J. M., Hill, R. E. and West, J. D. (2000). Different roles for Pax6 in the optic vesicle and facial epithelium mediate early morphogenesis of the murine eye. *Development* **127**, 945-956.

Echelard, Y., Epstein, D. J., St-Jacques, B., Shen, L., Mphler, J., McMaho, J. A. and McMahon, A. P. (1993). Sonic hedgehog, a member of a family of putative signalling molecules, is implicated in the regulation of CNS polarity. *Cell* **75**, 1417-1430.

Edgar, J. M., Asavaritikrai, P. and Price, D. J. (1999). Cell death and the neurotrophic theory in developing thalamus. *Soc. Neurosci. Abstr.* **25**, 705.5.

Ericson, J., Muhr, J., Placzek, M., Lints, T., Jessell, T. M. and Edlund, T. (1995). Sonic hedgehog induces the differentiation of ventral forebrain neurons: a common signal for ventral patterning along the rostrocaudal axis of the neural tube. *Cell* **81**, 747-756.

Ericson, J., Morton, S., Kawakami, A., Roelink, H. and Jessell, T. M. (1996). Two critical periods of sonic hedgehog signalling required for the specification of motor neuron identity. *Cell* **87**, 661-673.

Ericson, J., Rashbass, P., Schedl, A., Brenner-Morton, S., Kawakami, A., van Heyningen, V., Jessell, T. M. and Briscoe, J. (1997). Pax6 controls progenitor cell identity and neuronal fate in response to graded Shh signalling. *Cell* **90**, 169-180.

Frassoni, C., Arcelli, P., Selvaggio, M. and Spreafico, R. (1998). Calretinin immunoreactivity in the developing thalamus of the rat: A marker of early generated thalamic cells. *Neuroscience* **83**,1203-1214.

Goetz, M., Novak, N., Bastmeyer, M. and Bolz, J. (1992). Membrane-bound molecules in rat cerebral cortex regulate thalamic innervation. *Development* **116**, 507-519.

Grindley, J. C., Hargett, L., Hill, R. E., Ross, A. and Hogan, B. L. M. (1997). Disruption of Pax6 function in mice homozygous for the Pax6Sey-1NEU mutation produces abnormalities in the early development and regionalization of the diencephalon. *Mech. Dev.* **64**, 111-126.

Hill, R. E., Favor, J., Hogan, B. L. M., Ton, C. C. T., Saunders, G. F., Hanson, I. M., Prosser, J., Jordan, T., Hastie, N. D. and van Heyningen, V. (1991). Mouse small eye results from mutations in a paired-like homeobox-containing gene. *Nature* **354**, 522-525.

Hogan, B. L. M., Horsburgh, G., Cohen, J., Hetherington, C. M., Fischer, G. and Lyon, M. F. (1986). Small eye (Sey): a homozygous lethal mutation on chromosome 2 which affects the differentiation of both lens and nasal placodes in the mouse. *J. Embryol. Exp. Morph.* **97**, 95-110.

Kawano, H., Fukuda, T., Kubo, K., Horie, M., Uyemura, K., Takeuchi, K., Osumi, N., Eto, K. and Kawamura, K. (1999) Pax-6 is required for thalamocortical pathway formation in fetal rats. *J. Comp. Neurol.* **408**, 147-160.

Kitamura, K., Miura, H., Yanazawa, M., Miyashita, T. and Kato, K. (1997) Expression patterns of *Brx1* (*Rieg* gene), *Sonic hedgehog*, *Nkx2.2*, *Dlx1* and *Arx* during zona limitans intrathalamica and embryonic ventral lateral geniculate nuclear formation. *Mech. Dev.* **67**, 83-96.

Krauss, S., Concordet, J. P. and Ingham, P. W. (1993). A functionally conserved homolog of the Drosophila segment polarity gene hh is expressed in tissues with polarizing activity in zebrafish embryos. *Cell* **75**, 1431-1444.

Lebrand, C., Cases, O., Werhle, R., Blakely, R., Edwards, J. and Gaspar, P. (1999). Transient developmental expression of monoamine transporters in the rodent brain. *J. Comp Neurol* **401**, 506-524.

Lotto, R. B. and Price, D. J. (1999). Thalamus and cerebral cortex: organotypic culture and co-culture. In *The neuron in tissue culture. Ed. Haynes, L.* John Wiley and Sons Ltd., Chichester. pp. 518-524.

Mann, F., Zhukareva, V., Pimenta, A., Levitt, P. and Bolz, J. (1998). Membrane associated molecules guide limbic and non-limbic thalamocortical projections. *J. Neurosci.* **18**, 9409-9419.

Mansouri, A., Stoykova, A. and Gruss, P. (1994). Pax genes in development. *J. Cell Sci.* **18**, 35-42.

Marti, E., Bumcrot, D. A., Takada, T. and McMahon, A. P. (1995). Requirement of 19K form of Sonic hedgehog for induction of distinct ventral cell types. *Nature* **375**, 322-325.

Mastick, G. S., Davis, N. M., Andrews, G. L. and Easter, Jr, S. S. (1997). Pax6 functions in boundary formation and axon guidance in the embryonic mouse forebrain. *Development.* **124**, 1985-1997.

Molnar, Z. and Blakemore, C. (1991). Lack of regional specificity for connections formed between thalamus and cortex in co-culture. *Nature* **351**, 475-477.

Niwa, H., Yamamura, K. and Miyazaki, J. (1991). Efficient selection for high-expression transfectants with a novel eukaryotic vector. *Gene* **108**, 193-199.

Osumi, N., Hirota, A., Ohuchi, H., Nakafuku, M., Iimura, T., Kuratani, S., Fujiwara, M., Noji, S. and Eto, K. (1997). Pax6 is involved in specification of the hindbrain motor neuron subtype. *Development,* **124**, 2961-2972.

Paxinos, G., Tork, E., Tecott, L. H. and Valentino, K. L. (1991). *Atlas of the Developing Rat Brain.* Academic Press.

Pratt, T., Sharp, L., Nichols, J., Price, D. J. and Mason, J. O. (2000). Embryonic stem cells and transgenic mice ubiquitously expressing a tau tagged green fluorescent protein. *Dev. Biol.* (in press).

Puelles, L. and Rubenstein, J. L. (1993). Expression patterns of homeobox and other putative regulatory genes in the embryonic mouse forebrain suggest a neuromeric organization. *Trends Neurosci* **16**, 472-479.

Quinn, J. C., West, J. D. and Hill, R. E. (1996). Multiple functions for *Pax6* in mouse eye and nasal development. *Genes. Dev.* **10**, 435-446.

Rauvala, H., Vanhala, A., Castren, E., Nolo, R., Raulo, E., Merenmies, J. and Panula, P. (1994). Expression of HB-GAM (heparin-binding growth-associated molecules) in the pathways of developing axonal processes in vivo and neurite outgrowth in vitro induced by HB-GAM. *Dev. Brain Res.* **79**, 157-176.

Rennie, S., Lotto, R. B. and Price, D. J. (1994) Growth-promoting interactions between the murine neocortex and thalamus in organotypic co-cultures. *Neuroscience* **61**, 547-564.

Ringstedt, T., Braisted, J. E., Brose, K., Kidd, T., Goodman, C. S., Tessier-Lavigne, M. and O'Leary, D. D. M. (1999). Slit repulsion influences thalamocortical and retinal axon pathfinding in the diencephalon. *Society for Neuroscience Abstract* **25**, 305. 4.

Roelink, H., Augsburger, A., Heemskerk, J., Korzh, V., Norlin, S., Ruiz i Altaba, A., Tanabe, Y., Placzek, M., Edlund, T., Jessell, T. M., et al. (1994) Floor plate and motor neuron induction by vhh-1, a vertebrate homolog of hedgehog expressed by the notochord. *Cell* **76**, 761-775

Roelink, H., Porter, J. A., Chiang, C., Tanabe, Y., Chang, D. T., Beachy, P. A. and Jessell, T. M. (1995). Floor plate and motor neuron induction by different concentrations of the amino-terminal cleavage product of Sonic hedgehog autoproteolysis. *Cell* **81**, 445-455.

Rubenstein, J. L. R., Martinez, S., Shimamura, K. and Puelles, L. (1994). The embryonic vertebrate forebrain: the prosomeric model. *Science* **266**, 578-580.

Schmahl, W., Knoediseder, M., Favor, J. and Davidson, D. (1993). Defects of neuronal migration and the pathogenesis of cortical malformations are associated with small eye (sey) in the mouse, a point mutation at the Pax-6 locus. *Acta Neuropathol* **86**, 126-135.

Shimamura, K., Hirano, S., McMahon, A. P. and Takeichi, M. (1994). *Wnt1*-dependent regulation of local E-cadherin and αN-catenin expression in the embryonic mouse brain. *Development* **120**, 2225-2234.

Shimamura, K., Hartigan, D. J., Martinez, S., Puelles, L. and Rubenstein, J. L. R. (1995). Longitudinal organisation of the anterior neural plate and neural tube. *Development.* **121**, 3923-3933.

Siemering, K. R., Golbik, R., Sever, R. and Haseloff, J. (1996). Mutations that suppress the thermosensitivity of green fluorescent protein. *Curr. Biol.* **6**, 1653-1663.

Stoykova, A. and Gruss, P. (1994). Roles of Pax-genes in developing and adult brain as suggested by expression patterns. *J. Neurosci.* **14**, 1395-1412.

Stoykova, A., Fritsch, R., Walther, C. and Gruss, P. (1996). Forebrain patterning defects in Small eye mutant mice. *Development* **122**, 3453-3465.

Stoykova, A., Gotz, M. and Price, J. (1997). Pax6-dependent regulation of adhesive patterning, R-cadherin expression and boundary formation in developing forebrain. *Development* **124**, 3765-3777.

Tanabe, Y., Roelink, H. and Jessell, T. M. (1995). Induction of motor neurons by sonic hedgehog is independent of floor plate differentiation. *Curr. Biol.* **5**, 651-658.

Tuttle, R., Nakagawa, Y., Johnson, J. E. and O'Leary, D. D. M. (1999). Defects in thalamocortical axon pathfinding correlate with altered cell domains in Mash-1-deficient mice. *Development* **126**, 1903-1916.

Vitalis, T., Cases. O., Callebert, J., Lanay, G. M., Price, D. J., Seif, I. and

Gaspar, P. (1998). Effects of monoamine oxidase A inhibition on barrel formation in the mouse somatosensory cortex. *J. Comp. Neurol.* **393**, 169-184.

Walther, C. and Gruss, P. (1991). *Pax6,* a murine paired box gene, is expressed in the developing CNS. *Development* **113**, 1435-1449.

Wang, H. and Tessier-Lavigne, M. (1999). En passant neurotrophic action of an intermediate axonal target in the developing mammalian CNS. *Nature* **401**, 765-769.

Warren, N. and Price, D. J. (1997). Roles of Pax6 in murine diencephalic development. *Development* **124**, 1573-1582.

Warren, N., Caric, C., Pratt, T., Clausen, J. A., Asavaritikrai, P., Mason, J. O., Hill, R. E. and Price D. J. (1999). The transcription factor, Pax6, is required for cell proliferation and differentiation in the cerebral cortex. *Cerebral Cortex* **9**, 627-635.

Wilkinson, D. G. (1992). In Situ Hybridization. A Practical Approach. *The Practical Approach Series.* Senior Editors: D. Rickwood and B. D. Hames. Oxford: IRL Press.

Zernika-Goetz, M., Pines, J., McLean hunter, S., Dixon, J. P. C., Siemering, K. R. and Haseloff, J. (1997). Following cell fate in the living mouse embryo. *Development* **124**, 1133-1137.

Developmental Biology 228, 19–28 (2000)
doi:10.1006/dbio.2000.9935, available online at http://www.idealibrary.com on IDEAL®

Embryonic Stem Cells and Transgenic Mice Ubiquitously Expressing a Tau-Tagged Green Fluorescent Protein

Thomas Pratt,* Linda Sharp,* Jenny Nichols,† David J. Price,* and John O. Mason*

**Department of Biomedical Sciences and Centre for Developmental Biology, The University of Edinburgh, Hugh Robson Building, George Square, Edinburgh, EH8 9XD, United Kingdom; and* †*Centre for Genome Research, The University of Edinburgh, King's Buildings, West Mains Road, Edinburgh EH9 3JQ, United Kingdom*

We have generated embryonic stem (ES) cells and transgenic mice carrying a tau-tagged green fluorescent protein (GFP) transgene under the control of a powerful promoter active in all cell types including those of the central nervous system. GFP requires no substrate and can be detected in fixed or living cells so is an attractive genetic marker. Tau-tagged GFP labels subcellular structures, including axons and the mitotic machinery, by binding the GFP to microtubules. This allows cell morphology to be visualized in exquisite detail. We test the application of cells derived from these mice in several types of cell-mixing experiments and demonstrate that the morphology of tau–GFP-expressing cells can be readily visualized after they have integrated into unlabeled host cells or tissues. We anticipate that these ES cells and transgenic mice will prove a novel and powerful tool for a wide variety of applications including the development of neural transplantation technologies in animal models and fundamental research into axon pathfinding mechanisms. A major advantage of the tau–GFP label is that it can be detected in living cells and labeled cells and their processes can be identified and subjected to a variety of manipulations such as electrophysiological cell recording. © 2000 Academic Press

Key Words: **axon; coculture; confocal microscopy; cytoskeleton; GFP; ES cells; microtubules; mitosis; tau; transgenic mice.**

INTRODUCTION

In many biological experiments it is necessary to distinguish between two populations of cells. It is often useful to mark one population of cells genetically so that the cell and its descendants can be identified indefinitely. An animal expressing the marker in every cell would provide a universal source of labeled cells without the need to generate new lines for each subset of labeled cells required.

Green fluorescent protein (GFP), originally extracted from jellyfish *Aequorea victoria*, requires no substrate for detection and can be detected in fixed or living cells by fluorescent microscopy (Chalfie *et al.*, 1994). Over recent years the gene encoding GFP has undergone directed evolution in the hands of biologists anxious to exploit its experimental potential. Alterations of the GFP-coding sequence have produced variants with improved expression and detection properties in transgenic mice (Siemering *et al.*, 1996; Zernika-Goetz *et al.*, 1997). By imposing different genetic controls, transgenic mice have been produced which express GFP either ubiquitously (Okabe *et al.*, 1997; Hadjantonakis *et al.*, 1998) or in a more restricted number of cell types (Godwin *et al.*, 1998; Van den Pol and Ghosh, 1998; Zhuo *et al.*, 1997). We combined the use of a strong promoter (Niwa *et al.*, 1991) which drives ubiquitous expression of a GFP transgene in mice (Okabe *et al.*, 1997; Hadjantonakis *et al.*, 1998) and tau tagging (Rodriguez *et al.*, 1999) which we anticipated would improve our ability to visualize cell morphology, particularly long processes such as axons and other cytoskeletal features (Callahan and Thomas, 1994; Ludin and Matus, 1998; Kaech *et al.*, 1996; Preuss and Mandelkow, 1998; Mills *et al.*, 1998; Rodriguez *et al.*, 1999).

We report the generation and characterization of ES cells and transgenic mice ubiquitously expressing a tau–GFP fusion protein. Tau–GFP labeling reveals specific subcellular features such as the mitotic machinery by illuminating the microtubule component of the cytoskeleton. Detection

0012-1606/00 $35.00

of tau–GFP in living preparations will provide a powerful tool for studying microtubule dynamics in a variety of cell types and cellular processes including axon pathfinding, cell division, differentiation, migration, and death. Experiments in which tau–GFP-expressing cells and tissues are cultured with nonexpressing cells or tissues demonstrate the experimental potential of these mice in cell-mixing experiments. Labeled cells and their processes can be visualized by fluorescence microscopy in live and fixed preparations and their behavior can be mapped.

MATERIALS AND METHODS

Construction of Tau–GFP Expression Vector pTP6

The GFP variant mmgfp6 cDNA (Siemering *et al.*, 1996; Zernika-Goetz *et al.*, 1997) was fused at its 5′ end to the 3′ end of a cDNA-encoding bovine tau (Callahan and Thomas, 1994) to generate an in-frame fusion. The fusion cDNA was inserted into the mammalian expression vector pCAGiP (a kind gift from I. Chambers) which uses the CAG promoter (Niwa *et al.*, 1991) to drive expression of the tau–GFP fusion and puromycin resistance (Fig. 1a). Similar constructs containing GFP alone or GFP fused in frame at its 3′ end to the 5′ end of a human tau cDNA were also constructed.

Generation of Tau–GFP-Expressing ES Cells and Transgenic Mice

ES cell line E14Tg2a (Hooper *et al.*, 1987) were maintained in the presence of leukemia inhibitory factor (LIF) without a feeder layer (Smith, 1991). pTP6 was linearized with *Sca*I and introduced into embryonic stem (ES) cells by electroporation. Ten puromycin-resistant clones were selected and expanded for analysis. ES cells were induced to differentiate into neurons by aggregation into embryoid bodies (EBs) for 8 days with inclusion of retinoic acid for the final 4 days. EBs were then dissociated and cultured in serum-free medium on poly-D-lysine- and laminin-coated plastic (Bain *et al.*, 1995; Li *et al.*, 1998). Injection of three ES clones into blastocysts resulted in germline transmission in two lines of transgenic mice designated TgTP6.3 and TgTP6.4. These lines were maintained as heterozygotes for the tau–GFP transgene.

Visualizing Mitotic Machinery in Fixed and Live Tau–GFP ES Cells

The tau–GFP-expressing ES cell line E14Tg2aSc4TP6.3 from which the TgTP6.3 transgenic line was derived was used for these experiments. For live imaging, ES cells were cultured on poly-D-lysine- and gelatin-coated glass coverslip bottomed dishes (Wilco Wells B.V., The Netherlands) in a climate-controlled chamber (5% CO_2, 37°C, humidified) on the stage of an inverted confocal microscope. For chromosomal staining, ES cells were grown on gelatin-coated plastic, fixed for 15 min in 4% paraformaldehyde in PHEM buffer (Schliwa and van Blerkom, 1981) at room temperature, permeabilized with 0.1% Triton X-100, stained in a solution of propidium iodide containing 4 μg/ml RNase, and mounted in Vectashield (Vector Laboratories, Burlingame, CA). Images were collected using an oil immersion lens.

FACS Analysis

Dissociated ES cells or cortical cells were sorted for green fluorescence using a fluorescence activated cell sorter (FACS) (Becton Dickinson, Rutherford, NJ) to generate histograms of green fluorescence intensity (FL1 channel) versus cell number.

Confocal Microscopy

Cells and tissues were visualized using a Leica TCS NT confocal microscope (Leica Microsystems, Germany). Bright-field images were collected in the transmitted channel. GFP was detected in the FITC (green) channel. In some cases sections were counterstained with the nuclear dye propidium iodide which was detected in the TRITC (red) channel. Unless otherwise stated, serial optical sections were collected and combined. Time-lapse footage was acquired using Leica TCS NT software.

Tissue Processing for Vibratome Sections

Embryos were fixed in ice cold 4% paraformaldehyde in phosphate-buffered saline (PBS) overnight prior to embedding in 4% low-melting-point agarose and sectioning with a Vibratome (Technical Products International, St. Louis, MO) to produce 200-μm sections. Some preparations were counterstained with propidium iodide before mounting in 1:1 glycerol:PBS containing 10% Vectashield (Vector Laboratories).

Primary Culture of Neural Cells and Tissues

Cultures were carried out essentially as described by Lotto and Price (1999a,b). Embryonic cortical cells were dissociated from cortex using a papain dissociation system (Worthington Biochemical Corporation, Freehold, NJ) and cultured on poly-D-lysine-coated coverslips for 1 to 3 days. Organotypic slices were obtained from embryonic brains dissected in ice-cold oxygenated Earle's balanced salt solution and sliced into 300-μm slices with a tissue chopper. The regions of interest (thalamus and ventral telencephalon) were dissected from the slices and arranged on collagen coated inserts (Costar, UK) prior to culture for 3 days using an air interface protocol. Slices were then fixed and imaged. For both dissociated and organotypic culture, a defined serum-free medium was used and cultures were fixed for between 20 and 60 min in ice cold 4% paraformaldehyde in PBS. Some cultures were counterstained with propidium iodide before mounting in 1:1 glycerol:PBS containing 10% Vectashield (Vector Laboratories).

Production of Chimeras

Chimeras were produced as described by Tarkowski (1961) (reviewed in Rossant and Spence, 1998). Eight-cell-stage transgenic and nontransgenic embryos were aggregated to produce chimeras, which were allowed to develop *in vitro* into blastocysts. These were then imaged while still growing in culture medium in a climate-controlled chamber (5% CO_2, 37°C, humidified) on the stage of an inverted confocal microscope.

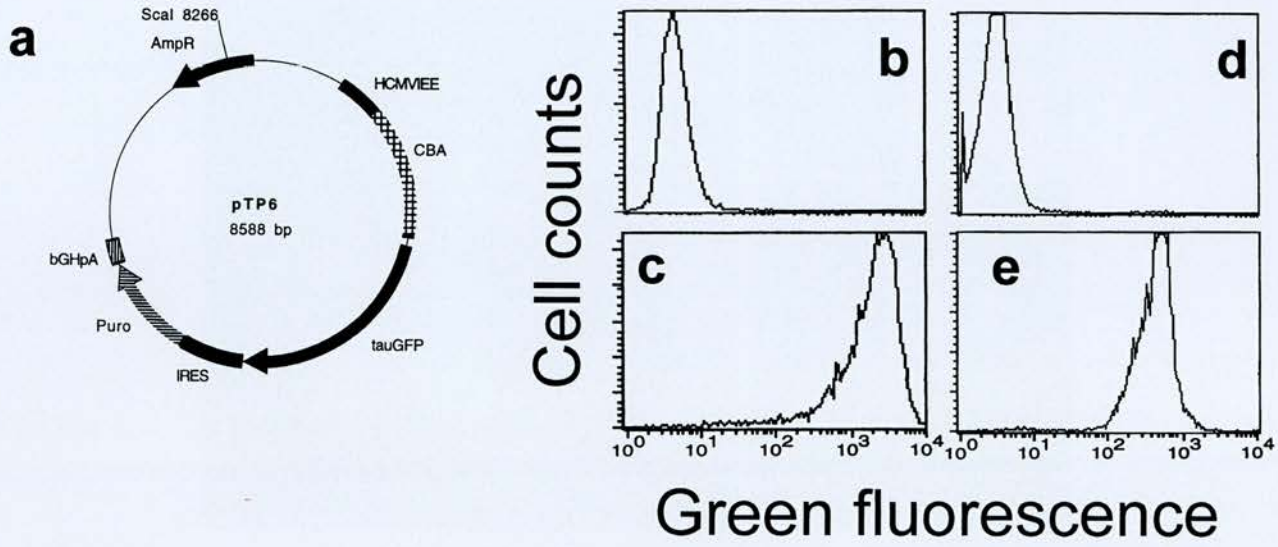

FIG. 1. Expression of a tau–GFP fusion transgene in murine embryonic stem (ES) cells and TgTP6.3 transgenic mice. (a) Structure of tau–GFP transgene. In pTP6 the tau–GFP fusion (tau–GFP) and puromycin resistance (Puro) genes are linked by an internal ribosome entry site (IRES) and expression of both is driven by a human cytomegalovirus immediate early enhancer (HCMVIEE) coupled to the chicken β-actin promoter and first intron (CBA) and a bovine growth hormone polyadenylation signal (bGHpA). The plasmid was linearized with *Sca*I (which cuts within the ampicillin resistance (AmpR) gene) prior to introduction into ES cells by electroporation. (b–e) FACS profiles of ES cells and cells from embryonic neocortex of TgTP6.3 transgenic mice. Histograms show green fluorescence plotted against cell number. (c) ES cells stably transfected with pTP6 exhibit a single green fluorescent peak indicating that all cells express tau–GFP at similar levels. (e) Cells from the E16 cerebral cortex of transgenic mice derived from these ES cells exhibit comparable green fluorescence. Profiles of (b) untransfected ES cells and (d) embryonic neocortical cells from nontransgenic littermates indicate background levels of green fluorescence exhibited by nonexpressing cells.

RESULTS

Generation of Tau–GFP-Expressing ES Cells and Transgenic Mice

Linearized tau–GFP expression construct pTP6 (Fig. 1a) was introduced into ES cells by electroporation. In this construct the tau–GFP fusion protein and puromycin resistance genes are linked by an internal ribosome entry site and expression of both is driven by a cytomegalovirus immediate early enhancer coupled to the chicken β-actin promoter and first intron (Niwa *et al.*, 1991). Ten puromycin-resistant clones were picked at random and expanded for analysis of tau–GFP expression. FACS analysis of tau–GFP ES cells grown in the presence of LIF showed that all clones exhibited broadly similar green fluorescence intensity with the vast majority of cells being green (compare Fig. 1c to untransfected control in Fig. 1b). Similar FACS profiles were also seen in ES cells stably transfected with constructs analogous to pTP6 but which expressed untagged GFP or an alternative GFP–tau fusion (data not shown). Tau should cause the tau–GFP to be localized in cellular processes including axons. To test the tau–GFP transgene expression in neurons, tau–GFP ES cells were differentiated into neurons by aggregating them into EBs and growing them in the absence of LIF for 8 days with retinoic acid included for the final 4 days. EBs were then dissociated and cultured in serum-free medium. Comparison of bright-field and fluorescence images showed that cells with neuronal morphology continued to express the transgene and that the tau–GFP label was distributed evenly throughout cellular processes while being excluded from the nucleus. All tau–GFP ES clones analyzed were of similar appearance in this respect. This contrasted with cells expressing untagged GFP where although the cell body was fluorescent, the fluorescence in processes was less easy to detect (data not shown). Three tau–GFP-expressing ES cell clones were injected into blastocysts which were reimplanted and allowed to develop. Germline transmission was established for two lines. Transgenic pups could easily be distinguished from nontransgenic littermates by examination of ear clippings under a microscope equipped for GFP fluorescence. Southern blot analysis (not shown) confirmed that all animals carrying the transgene exhibited green fluorescence.

Tau–GFP transgene expression has been maintained in both lines over several generations. Preliminary analysis of the TgTP6.3 line indicated that widespread tau–GFP expression could be detected in all tissues throughout development. The other line, TgTP6.4, exhibited strong and widespread tau–GFP expression in many nonneural tissues but tau–GFP was al-

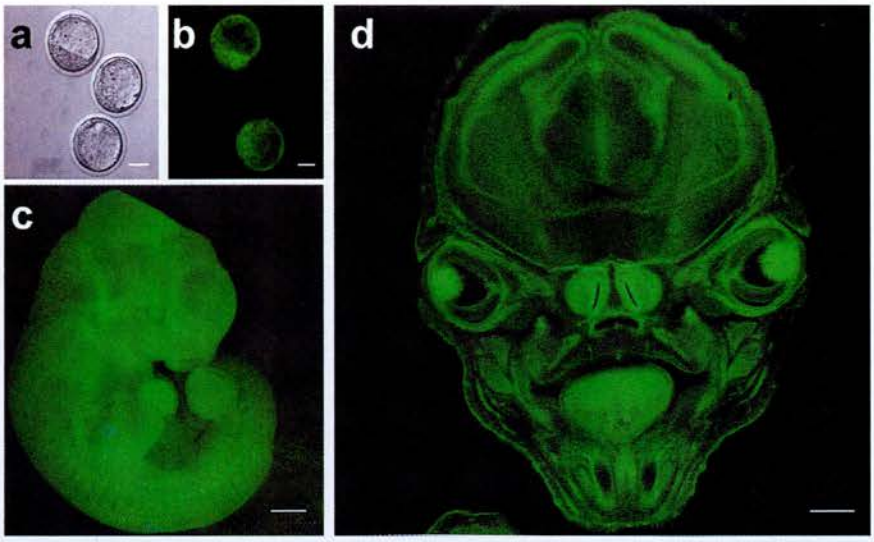

FIG. 2. Confocal images showing widespread tau–GFP expression throughout development of TgTP6.3 heterozygotes. (a) Bright-field and (b) green fluorescent images of the same field showing that at the blastocyst stage (E3.5) tau–GFP is expressed throughout two transgenic embryos with no expression detectable in a third nontransgenic littermate. (c) Whole mount of transgenic E10.5 embryo showing expression throughout head and body. (d) Coronal Vibratome section through head of E16 embryo showing green fluorescence throughout brain and nonneural tissues. Bar in a, b, 20 μm; c, d, 500 μm.

most undetectable in a large proportion of the central nervous system (CNS). Interestingly in both lines, the blood vessels exhibited high levels of expression resulting in an unexpectedly clear view of the vascular supply to the brain which was particularly apparent in the TgTP6.4 line. The remainder of this study focuses on the TgTP6.3 line.

In order to establish whether the tau–GFP transgene was expressed in all cells in the CNS we examined whole mounts and serial sections at a variety of embryonic stages (Fig. 2 and data not shown). This suggested that expression was indeed ubiquitous, although we would not have detected small subsets of unlabeled cells intermingled with labeled cells with this method. When whole embryonic brain was dissociated and plated onto coverslips we found that all cells were indeed labeled (data not shown). To quantify tau–GFP expression in more detail we chose embryonic cerebral cortex which contains cells at various stages of development including proliferating cells in the ventricular and subventricular zones, postmitotic cells migrating through the intermediate zone, and more differentiated cells in the cortical plate. Dissociated E16 cortical cells were subjected to FACS analysis. A single green fluorescent peak indicated that all cortical cell types express similar levels of tau–GFP protein and that there are no subsets of nonexpressing cells (compare Fig. 1e to nontransgenic littermate in Fig. 1d).

Tau–GFP Expression Profile during Embryonic Development

Embryos heterozygous for a paternally derived tau–GFP transgene were taken at various stages of development for examination of tau–GFP expression in whole-mount preparations. Tau–GFP-expressing embryos can first be distinguished from nontransgenic littermates at the four-cell stage indicating the onset of detectable expression (not shown). Transgene expression becomes detectable in all cells simultaneously. At E3.5 (blastocyst stage) the embryo consists of several distinct cell lineages: epiblast (inner cell mass), polar trophectoderm, and mural trophectoderm, all of which express at similar levels (Figs. 2a and 2b). By E10.5 the embryo has undergone substantial differentiation with head, limbs and internal organs being recognizable (Fig. 2c). Tau–GFP expression remains widespread at this stage and at all other ages examined throughout postnatal life (Fig. 2d and data not shown).

Tau–GFP Efficiently Labels Long Cellular Processes

In using a tau–GFP fusion transgene we anticipated labeling microtubule containing structures, notably the long cellular processes which connect cells in the CNS. To test whether this had been successfully accomplished we looked at tau–GFP localization in cultured cells and in fiber tracts. E16 cortex was dissociated into single cells, plated onto coverslips, and imaged after time in culture. Tau–GFP was present in the cytoplasm where it efficiently filled cellular processes (compare Fig. 3b to Fig. 3a). To evaluate our transgene as a marker of fiber tracts we chose the thalamocortical axon (TCA) pathway (Fig. 3e) as an example (Auladell *et al.*, 2000). The TCA pathway consists of axons connecting the dorsal thalamus with the cerebral cortex. The TCA tract passes ventrally through the ventral thala-

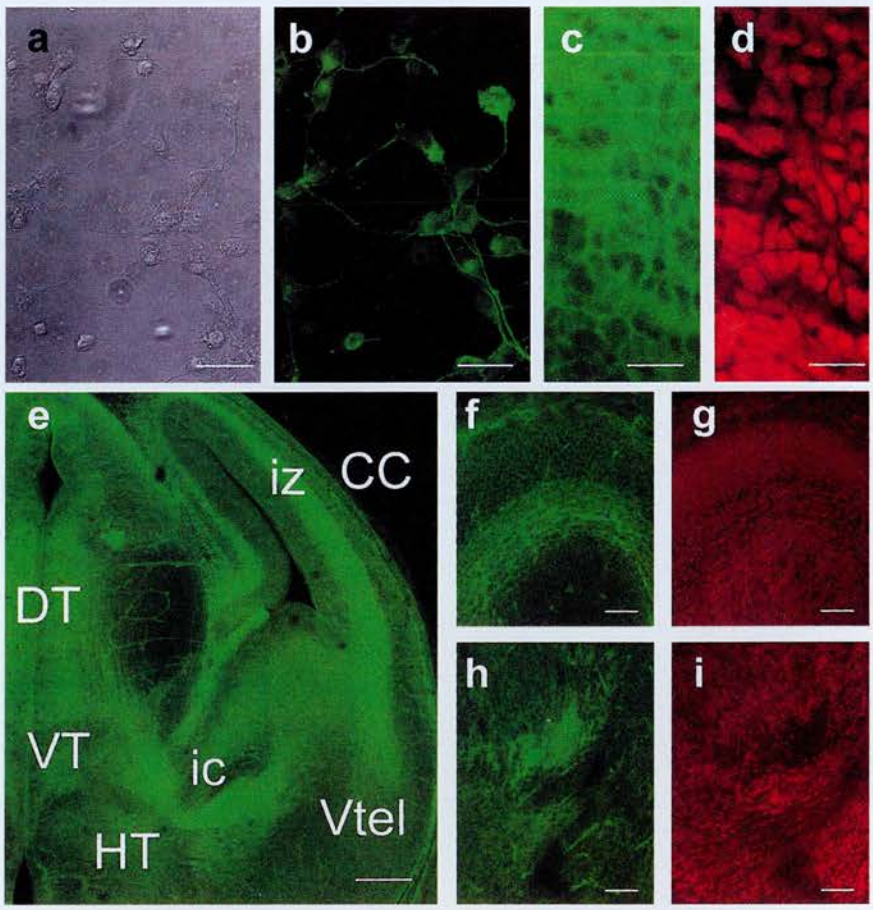

3

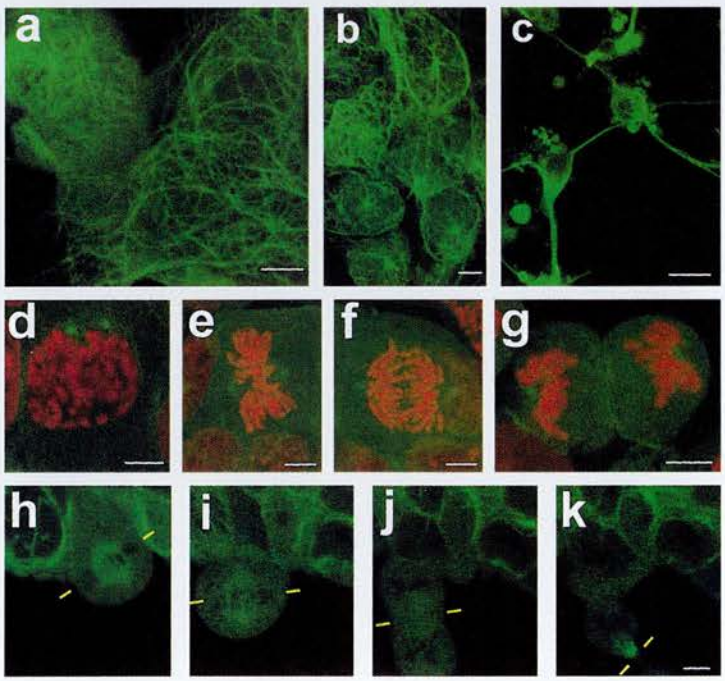

4

mus, makes a sharp lateral turn at the hypothalamus, and enters the ventral telencephalon through the internal capsule, before turning dorsally into the intermediate zone of the cerebral cortex. The TCA fiber tract is highlighted by tau–GFP label with particularly strong staining seen in the internal capsule and intermediate zone (Fig. 3e). The direction of fibers is apparent although individual fibers are hard to resolve (Figs. 3f and 3h). There was strikingly reciprocity between the localization of tau–GFP and cell nuclei (Figs. 3g and 3i). Apparent "holes" in tau–GFP labeling correspond to the nuclei of cells stained red with propidium iodide (compare tau–GFP label in Fig. 3c with propidium iodide staining in Fig. 3d).

Subcellular Localization of Tau–GFP in Living Cells Reveals Mictrotubule-Containing Structures

We expected that the ability of tau–GFP to bind to microtubules would provide a means to visualize the microtubule component of the cytoskeleton. In living cells these subcellular details are otherwise inaccessible.

The microtubule component of the cytoskeleton plays an important role in cell function throughout the cell cycle with microtubules existing in a constant state of dynamic instability. During interphase, microtubules radiating from a single microtubule organizing center (MTOC) fill the cytoplasm and bundle together to form the core of developing processes. At the onset of mitosis, the MTOC replicates to generate two daughters, which migrate to opposing poles of the cell. The microtubules reorganize to generate the mitotic spindle, a structure which coordinates the equal segregation of chromosomes to the daughter cells.

To confirm that tau–GFP labels a variety of microtubule-containing structures we examined live preparations of tau–GFP-expressing cells from TgTP6.3 transgenic mice and the E14Tg2aSc4TP6.3 ES cell line from which the mice were derived. A single optical section through live ES cells (Fig. 4a) shows a subcellular fibrous tau–GFP labeling pattern in the cytoplasm. Live interphase cells from embryonic heart exhibit tau–GFP label radiating from a single intensely labeled point into the cytoplasm (Fig. 4b). Neural cells which have been dissociated and cultured exhibit long evenly labeled processes, with a particularly strong GFP signal extending from their base (Fig. 4c).

During mitosis tau–GFP labels the mitotic machinery. Representative examples of fixed cells (chromosomes stained red with the DNA stain propidium iodide) are shown (Figs. 4d–4g). At the start of mitosis the MTOCs replicate as the chromosomes condense (Fig. 4d). The chromosomes then congregate along the plane of division (equator) to form the metaphase plate which is flanked (at the poles) by the MTOCs between which the mitotic spindle is formed (Fig. 4e) before segregating toward the MTOCs along the mitotic spindle (Fig. 4f). Mitosis concludes as the daughter cells separate each with a complete set of chromosomes associated with a MTOC (Fig. 4g).

The pattern of tau–GFP labeling described above is consistent with tau–GFP labeling microtubules during interphase and mitosis with particularly strong labeling seen at the MTOC. The tau–GFP does not associate with the

FIG. 3. Tau–GFP label reveals neural processes and is excluded from the nucleus in TgTP6.3 transgenic mice. (a) Bright-field and (b) green fluorescent images of dissociated E16 cortical cells cultured on coverslips. Tau–GFP efficiently labels all the neural processes which can be detected by bright field microscopy. (c) Green fluorescence- and (d) propidium iodide-stained nuclei in Vibratome sections of E16 cortex. Apparent "holes" in the tau–GFP labeling correspond to the location of nuclei showing that tau–GFP is excluded from the nucleus. (e) Coronal Vibratome section of transgenic embryonic brain illustrating the thalamocortical axon pathway which connects the dorsal thalamus (DT) and cerebral cortex (CC). Note the intense green fluorescence of the fiber tract in the ventral thalamus (VT), internal capsule (ic), and intermediate zone (iz) of the cerebral cortex indicating that the entire tract is efficiently labeled. (f, h) Green fluorescence and (g, i) propidium iodide staining in Vibratome sections of E16 brain showing (f, g) intermediate zone and (h, i) internal capsule. Note the reciprocity of tau–GFP and propidium iodide staining which accounts for the intense labeling in fiber tracts compared to regions of high nuclear packing density. Bar in a–d, 20 μm; e, 500 μm; f–i, 100 μm.

FIG. 4. Confocal imaging of tau–GFP in living cells allows visualization of subcellular structures and reveals the filamentous microtubule network. (a–c) Tau–GFP labeling of living interphase cells. (a) Filamentous tau–GFP labeling in live ES cells. (b) Tau–GFP labeling radiates from a single point in embryonic heart cells (see also cell in top left-hand corner of a). (c) Tau–GFP labels growing processes in cultured neurons. (d–k) Tau–GFP labels the mitotic machinery in dividing ES cells. (d–g) In fixed cells representing key stages of mitosis tau–GFP labeling can be seen as green spots that correspond to the expected position occupied by the MTOCs. Chromosomes are stained red. The location of the spots of tau–GFP label relative to the chromosomes matches the location occupied by the MTOCs after they: (d) replicate during prophase to coincide with chromosome condensation and the onset of mitosis; (e) flank the chromosomes as they line up along the plane of division (equator) during metaphase; and (f, g) segregate to the opposite poles of the cell occupied by the MTOCs at anaphase. (h–k) Confocal images selected from time-lapse footage of a live tau–GFP-expressing ES cell undergoing mitosis. The position of tau–GFP labeling matches the position occupied by the mitotic spindle as the cell divides. (h, i) Intense tau–GFP labeling can be seen perpendicular to and symmetrically arranged around the plane of cell division as the cell undergoes metaphase. (j, k) The cell proceeds (j) through anaphase and (k) telophase to generate two daughter cells (the lower daughter cell is not included in this optical section). Pairs of yellow bars in (h–k) mark the plane of cell division. Note that the mitotic spindle appears much more strongly labeled in live cells (h, i) than in fixed cells at comparable stages of mitosis (e, f). Images in (a, d–g, i–k) are single optical sections chosen to emphasize subcellular detail. Bar in a, c–k, 5 μm; b, 10 μm.

chromosomes themselves as propidium iodide and tau–GFP label do not colocalize (Figs. 4e–4g).

Time-lapse footage of a tau–GFP-expressing ES cell undergoing cell division shows that tau–GFP permits visualization of the mitotic machinery as mitosis proceeds. Images selected from this time-lapse footage are shown (Figs. 4h–4k). Tau–GFP labels an oval structure reminiscent of the mitotic spindle (Figs. 4h–4i) in a cell, which goes on to divide (Figs. 4j–k). A strong signal corresponds to the microtubule-rich midbody which forms at the constriction between daughter cells (Fig. 4k). Tau–GFP label is excluded from the chromosomes, which can therefore be visualized (particularly clear in Fig. 4j but also apparent in Figs. 4h–4i).

These patterns of tau–GFP labeling resemble the distribution of microtubules within the cell during different phases of the cell cycle (Waters *et al.*, 1993) and are consistent with the localization of ectopically expressed tau protein reported by others (Ludin and Matus, 1998; Kaech *et al.*, 1996; Preuss and Mandelkow, 1998; Mills *et al.*, 1998; Rodriguez *et al.*, 1999) where tau decorates the microtubule component of the cytoskeleton.

Tau–GFP-Labeled Cells Are Readily Detected in a Variety of Cell-Mixing Experiments

We anticipate that a major application of these mice is as a universal source of tau–GFP-labeled cells for cell-mixing experiments. Therefore, we next assessed the properties of our cells in three types of cell-mixing paradigm.

The production of chimeras allows analysis of cellular interactions throughout development (Rossant and Spence, 1998). As the onset of transgene expression occurs in the first few days after fertilization, we wanted to test whether we could distinguish between transgenic and nontransgenic cells in early embryos. We generated chimeras by aggregating eight-cell-stage transgenic and nontransgenic embryos. These chimeras were cultured and imaged while still alive. Fluorescent images of two such chimeras undergoing blastocoel formation, in which labeled and unlabeled cells have become intermingled, are shown in Fig. 5. In one chimera (Fig. 5a) numbers of transgenic and nontransgenic cells are balanced and in the other (Fig. 5b) transgenic cells are more abundant than nontransgenic cells. Note that the tau–GFP label allows the nuclear position of expressing cells within the chimera to be mapped. Nonexpressing cells derived from the nontransgenic embryo appear as gaps in the green fluorescence.

Coculture of dissociated cells is often used to investigate how the behavior of one cell population is influenced by proximity to another. To test the use of our cells in this type of experiment, dissociated cells from transgenic and nontransgenic E16 cortex were mixed and cultured after plating onto coverslips. Bright-field images of such a coculture show a tangle of cellular processes where it is very difficult to assign a particular process to a particular cell (Fig. 5c). This is resolved by examining the fluorescence image, where tau–GFP clearly marks the morphology of transgenic cells and allows the course of their processes to be traced (Fig. 5d, nuclei counterstained red mark positions of cell bodies of both expressing and nonexpressing cells).

Organotypic coculture is often used to investigate how axons generated by one tissue respond when challenged with the environment supplied by a second tissue. Axons in organotypic coculture typically travel longer distances than is seen in cultures of dissociated cells and we wanted to confirm that tau–GFP labeling was efficient over longer distances. *In vivo*, TCAs travel from the thalamus to the cortex via the ventral telencephalon. *In vitro*, thalamic explants innervate explants of ventral telencephalon. Explants of transgenic E16 thalamus were cultured with explants of nontransgenic ventral telencephalon. After 3 days in culture the explants were fixed and imaged. Tau–GFP-labeled fibers, which have grown into the unlabeled explant, were clearly visible (Fig. 5e) and at higher power individual fibers could be clearly resolved (Fig. 5f). In some of these cultures labeled cells migrated into unlabeled tissues and integrated into them. Examples of such cells are shown in Fig. 5g.

DISCUSSION

We have produced a line of transgenic mice which ubiquitously express a tau-tagged GFP protein. Since transgenic mice ubiquitously expressing untagged GFP are already available (Okabe *et al.*, 1997; Hadjantonakis *et al.*, 1998), it is important to emphasize the benefits of each labeling system. Untagged GFP diffuses throughout the cell freely so a labeled cell generates a uniform fluorescent signal, although the cell body tends to fluoresce much more strongly than thin processes. Axons of cells transfected with soluble GFP are less easy to detect than those of cells transfected with tau-tagged GFP (this study; Rohm *et al.*, 2000). Tau-tagged GFP decorates the microtubule component of the cytoskeleton and is excluded from the interphase nucleus (this study; Ludin and Matus, 1998; Kaech *et al.*, 1996; Preuss and Mandelkow, 1998; Mills *et al.*, 1998; Rodriguez *et al.*, 1999). This allows cellular features to be visualized in cells expressing tau–GFP which are less clear in cells expressing soluble GFP. For example, cell division can be tracked by watching the fluorescent signal generated by tau–GFP decorating the mitotic machinery, and alterations in microtubule organization are also associated with other processes such as cell death and migration. A potential benefit of tau-tagged GFP over untagged GFP is that the tagged version is anchored to the cytoskeleton so is less likely to diffuse out of cells during tissue processing resulting in loss of signal and increased background. This problem was reported for a line of transgenic mice expressing GFP where live preparations had to be perfused to wash away leaking GFP (Van den Pol and Ghosh, 1998). In the present study, slices of tau–GFP-expressing tissue can be cultured in contact with unlabeled tissue without any obvious deterioration of signal caused by GFP leaking from

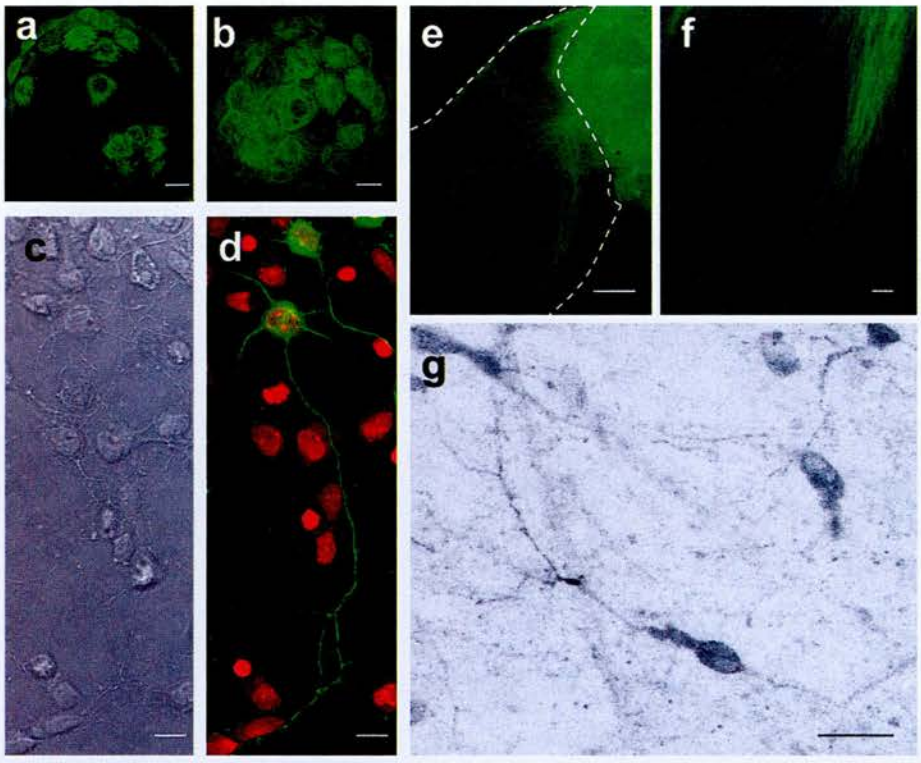

FIG. 5. Tau–GFP-labeled cells are easily detected in a variety of cell mixing paradigms. (a, b) Blastocyst stage aggregation chimeras between transgenic and nontransgenic embryos. These chimeras were generated by G. MacKay. Fluorescent confocal images show (a) a balanced chimera and (b) an unbalanced chimera in which most of the cells are of transgenic origin. In each case the position of labeled cells can easily be mapped. The nuclear exclusion of tau–GFP facilitates the counting of labeled cells. (c) Bright-field and (d) fluorescent confocal images of a mixed coculture of dissociated transgenic and nontransgenic cortex. Note that the morphology of cells expressing tau–GFP is clearly marked by green fluorescence; nuclei are stained red to aid comparison of fields. (e–g) Confocal images of organotypic coculture of tau–GFP-expressing thalamus with nontransgenic ventral telencephalon. (e, f) Green fibers can clearly be seen as they enter unlabeled tissue (demarcated by dotted lines in (e)) with higher magnification in (f). (g) Visualization of tau–GFP-labeled cells which have integrated into unlabeled tissue (gray scale of fluorescent image). Bar in a, b, g, 20 μm; c, d, 10 μm; e, 500 μm; f, 200 μm.

the explant and the tau–GFP label remains detectable in fixed tissue preparations after immunostaining for several other proteins (data not shown). Tau-tagged GFP therefore appears to be a more robust label than soluble GFP with the advantage of illuminating the microtubule component of the cytoskeleton.

Fixation of tau–GFP-labeled cells using the methods employed in this study does not obviously result in a decrease in GFP fluorescence since labeled and unlabeled cells and their processes could easily be distinguished in live and fixed preparations. Fixation, even when using protocols specifically developed to preserve microtubule structure (Schliwa and van Blerkom, 1981; Waters *et al.*, 1993), does however appear to alter the subcellular distribution of tau–GFP. For example, comparison of tau–GFP labeling of the mitotic machinery in fixed and live cells reveals that whereas in live cells the mitotic spindle is very clearly labeled, in fixed cells it appeared much fainter and the clearest fluorescent features are the MTOCs between which the spindle forms. In general, fixation appears to cause tau–GFP label to become "hazy" compared to the sharply defined tau–GFP labeling seen in live cells, but does not result in significant deterioration in the quality of labeling above the subcellular level.

Of particular interest to us is that the tau–GFP is efficiently transported down cellular extensions and therefore labels axons and fiber tracts. These can easily be detected when growing in among unlabeled cells so providing a useful tool for investigating axon pathfinding, in identifying neural connections for use in electrophysiological recordings, and in assessing the success with which transplanted cells integrate into host tissues and form appropriate connections. In cell-mixing experiments, it was possible to view the GFP fluorescence of cultures while they were growing so providing a dynamic view of axon navigation. Without this label the cells of interest are obscured by the cells or tissues providing the host environment. The use of tau–GFP obviates the need for tissue processing before the

signal can be revealed. This is not generally the case with carbocyanine dye labeling or immunostaining, which can take days or weeks and complicates the option of observing or manipulating identified cells while they are still alive.

The ability of tau–GFP to decorate microtubules allows the visualization of the microtubule containing cytoskeleton at a subcellular level. In proliferating cells expressing tau–GFP, we show that the pattern of tau–GFP labeling can be used to identify phases of the cell cycle. The breakdown of the nuclear envelope is indicated as tau–GFP, excluded from the nucleus during interphase, fills the cell. The MTOCs are strongly labeled allowing their replication and movement to be tracked and the formation and orientation of the mitotic spindle is also apparent. Intense GFP labeling corresponding to the point at which the daughter cells separate signals the end of mitosis. Although not addressed in such detail as cell division in this study, the indications are that changes in microtubule structure associated with cell differentiation, migration, and death should also be apparent.

Although the transgene is ubiquitously expressed, the subcellular localization of tau–GFP causes certain anatomical features to be highlighted. In the brain, for example, fiber tracts appear bright, regions of high nuclear packing density appear dim, and blood vessels and membranes (which are richly supplied with blood vessels) also appear bright. These features can be used to provide fluorescent anatomical landmarks which are useful when targeting brain regions for dissection or injection.

One possible concern in using cells or tissues from these mice is that ectopic expression of tau–GFP might compromise cell function. Tau is a microtubule-binding protein, which is usually only found in axons. Furthermore, disruption of normal tau function is associated with neurodegenerative disorders such as Alzheimer's disease (reviewed in Lee and Trojanowski, 1999) although transgenic mice lacking tau protein appeared to develop relatively normally (Harada *et al.*, 1994) and neurodegenerative pathology was not reported in transgenic mice ectopically expressing a tau isoform similar to the one we used to tag GFP (Gotz *et al.*, 1995). Ectopic expression of a tau–GFP fusion protein might disrupt cell function by in some way interfering with microtubule assembly or predisposing transgenic animals to neural pathological disorders resembling Alzheimer's disease. A second concern is that as the transgene was introduced as a random integration event, it is possible that this insertion event mutagenized an unknown genomic locus.

In this study, expression of our transgene has no obvious deleterious consequences. Ubiquitously expressing ES cells can proliferate and contribute to the germline and ubiquitously expressing mice heterozygous for the transgene appear to develop normally and are fertile. In addition, transgenic mouse lines expressing tau-tagged GFP (Rodriguez *et al.*, 1999) and *LacZ* (Mombaerts *et al.*, 1996) in subsets of postmitotic neurons have been produced with no report of altered behavior. It cannot be ruled out that more subtle cell-type-specific phenotypes will be identified with more detailed analysis. Experiments using these ES cells and animals should be designed with controls for possible effects of the transgene in whatever system is being studied.

These transgenic mice were produced via the generation of ES cells ubiquitously expressing tau–GFP protein. The use of a bicistronic expression vector in which tau–GFP expression was linked to puromycin resistance allowed for selection of stably expressing clones with puromycin so obviating screening for fluorescent clones. The similar fluorescence of all clones picked confirms the success of this strategy. It was also possible to screen the ES cells for likely suitability in generating a useful transgenic mouse. In this case we were interested in marking neurons so we took advantage of the potential of ES cells to differentiate into neurons *in vitro* (Bain *et al.*, 1995; Li *et al.*, 1998). If there were ES clones which switched off tau–GFP during the differentiation, or had for some reason become incompetent to differentiate, then these could be discarded at this stage. In this study, all clones could be induced to differentiate into cells with neuronal morphology which expressed tau–GFP in their processes and three were picked for generation of transgenic mice. Surprisingly, of two lines generated only one (TgTP6.3) exhibited strong tau–GFP expression in the brain although tau–GFP was expressed in other tissues in both. The incomplete success of this screening strategy emphasizes the care that must be taken in extrapolating from neurons derived from ES cells to the full repertoire of neuronal subtypes present in the brain.

Long-term cell-mixing experiments such as transplants and chimeras where labeled cell populations must remain identifiable for weeks or months after the experiment is started demand that the label must be stable. Our cells fit these criteria since tau–GFP expression is ubiquitous both in ES cells before and after differentiation *in vitro* and in all cells from transgenic mice derived from these ES cells. A cell carrying our transgene and its descendants should therefore be detectable indefinitely.

These tau–GFP-expressing ES cells and TgTP6.3 transgenic mice can be used as a source of labeled cells of any cell type for use in short- or long-term cell-mixing experiments or to establish cell lines. Transgenic "donor" cells and tissues can be visualized in exquisite detail after mixing and culture with nontransgenic host tissues demonstrating the value of our cells in cell mixing applications such as those involved in the development of neural transplantation technologies (Isacson *et al.*, 1995; Scheffler *et al.*, 1999; Svendsen and Smith, 1999). Genetic modifications to the labeled cells can be achieved by manipulating the ES cells or by breeding the transgenic mice to place the tau–GFP transgene on different genetic backgrounds.

ACKNOWLEDGMENTS

We thank Jim Haseloff for the GFP clone mgfp6; Chris Callahan for the bovine tau clone pTLacZ; Gloria Lee for the human tau clone htau40; Ian Chambers for the pCAGiP expression vector; Ian Cham-

bers and Austin Smith for advice and discussion; Meng Li for advice on neuronal differentiation of ES cells; the excellent transgenic facilities provided by the Centre for Genome Research for enabling our work with ES cells and transgenic mice; Andrew Sanderson for assistance with FACS analysis; Gillian Mackay and John West for producing chimeras; Tania Vitalis for helpful discussions about brain anatomy; and Sophie Brown for preparing some of the primary cultures as part of her undergraduate project. This work was funded by grants from the MRC and European Commission.

REFERENCES

Auladell, C., Perez-Sust, P., Super, H., and Soriano, E. (2000). The early development of thalamocortical and corticothalamic projections in the mouse. *Acta Embryol.* **201,** 169–179.

Bain, G., Kitchens, D., Yao, M., Huettner, J. E., and Gottlieb, D. I. (1995). Embryonic stem cells express neuronal properties *in vitro*. *Dev. Biol.* **168,** 342–357.

Callahan, C. A., and Thomas, J. B. (1994). Tau-β-galacosidase, an axon targetted fusion protein. *Proc. Natl. Acad. Sci. USA* **91,** 5972–5976.

Chalfie, M., Tu, Y., Euskirchen, G., Ward, W. W., and Prasher, D. C. (1994). Green fluorescent protein as a marker for gene expression. *Science* **263,** 802–805.

Godwin, A. R., Stadler, H. S., Nakamura, K., and Capecchi, M. R. (1998). Detection of targeted GFP-Hox fusions during mouse embryogenesis. *Proc. Natl. Acad. Sci. USA* **95,** 13042–13047.

Gotz, J., Probst, A., Spillantini, M. G., Schafer, T., Jakes, R., Burki, K., and Goedert, M. (1995). Somatodendritic localisation and hyperphosphorylation of tau protein in transgenic mice expressing the longest human brain tau isoform. *EMBO J.* **14,** 1304–1313.

Hadjantonakis, A., Gertsenstein, M., Ikawa, M., Okabe, M., and Nagy, A. (1998). Generating green fluorescent mice by germline transmission of green fluorescent ES cells. *Mech. Dev.* **76,** 79–90.

Harada, A., Oguchi, K., Okabe, S., Kuna, J., Terada, S., Oshima, T., Sato-Yoshitake, R., Takei, Y., Noda, T., and Hirokawa, N. (1994). Altered microtubule organisation in small-calibre axons of mice lacking tau protein. *Nature* **369,** 488–491.

Hooper, M. L., Hardy, K., Handyside, A., Hunter, S., and Monk, M. (1987). HPRT-deficient (Lesch-Nyham) mouse embryos derived from germline colonisation by cultured cells. *Nature* **326,** 292–295.

Isacson, O., Deacon, T. W., Pakzaban, P., Galpern, W. R., Dinsmore, J., and Burns, L. H. (1995). Transplanted xenogenic neural cells in neurodegenerative disease models exhibit remarkable axonal target specificity and distinct growth patterns of glial and axonal fibres. *Nature Med.* **1,** 1189–1194.

Kaech, S., Ludin, B., and Matus, A. (1996). Cytoskeletal plasticity in cells expressing neuronal microtubule associated proteins. *Neuron* **17,** 1189–1199.

Lee, V. M. Y., and Trojanowski. (1999). Neurodegenerative tauopathies: Human disease and transgenic models. *Neuron* **24,** 507–510.

Li, M., Pevny, L., Lovell-Badge, R., and Smith, A. (1998). Generation of purified neural precursors from embryonic stem cells by lineage selection. *Curr. Biol.* **8,** 971–974.

Lotto, R. B., and Price, D. J. (1999a). Thalamus and cerebral cortex: Organotypic culture and co-culture. *In* "The Neuron in Tissue Culture" (L. Haynes, Ed.), pp. 518–524. Wiley, Chichester.

Lotto, R. B., and Price, D. J. (1999b). Thalamus: dispersed neuron culture. *In* "The Neuron in Tissue Culture" (L. Haynes, Ed.), pp. 525–530. Wiley, Chichester.

Ludin, B., and Matus, A. (1998). GFP illuminates the cytoskeleton. *Trends Cell Biol.* **8,** 72–77.

Mills, J. C., Lee, V. M.-Y, and Pittman, R. N. (1998). Activation of a PP2A-like phosphatase and dephosphorylation of tau protein characterise onset of the execution phase of apoptosis. *J. Cell Sci.* **111,** 625–636.

Mombaerts, P., Wang, F., Dulac, C., Chao, S. K., Nemes, A., Mendelsohn, M., Edmondson, J., and Axel, R. (1996). Visualising an olfactory sensory map. *Cell* **87,** 675–686.

Niwa, H., Yamamura. K., and Miyazaki, J. (1991). Efficient selection for high-expression transfectants with a novel eukaryotic vector. *Gene* **108,** 193–199.

Okabe, M., Ikawa, M., Kominami, K., Nakanishi, K., and Nishimune, Y. (1997). 'Green mice' as a source of ubiquitous green cells. *FEBS Lett.* **407,** 313–319.

Preuss, U., and Mandelkow, E-M. (1998). Mitotic phosphorylation of tau protein in neuronal cell lines resembles phosphorylation in Alzheimers disease. *Eur. J. Cell Biol.* **76,** 176–184.

Rodriguez, I., Feinstein, P., and Mombaerts, P. (1999). Variable patterns of axonal projections of sensory neurones in the mouse vomeronasal system. *Cell* **97,** 199–208.

Rohm, B., Ottemeyer, A., Lohrum, M., and Puschel, A. W. (2000). Plexin/neuropilin complexes mediate repulsion by the axonal guidance signal semaphorin 3A. *Mech. Dev.* **93,** 95–104.

Rossant, J., and Spence, J. (1998). Chimeras and mosaics in mouse mutant development. *Trends Genet.* **14,** 358–363.

Scheffler, B., Horn, M., Blumcke, I., Laywell, E. D., Coomes, D., Kukekov, V. G., and Steindler, D. A. (1999). Marrow-mindedness: A perspective on neuropoisis. *Trends Neurosci.* **22,** 348–356.

Schliwa, M., and van Blerkom, J. (1981). Structural interaction of cytoskeletal components. *J. Cell Biol.* **90,** 222–235.

Siemering, K. R., Golbik, R., Sever, R., and Haseloff, J. (1996). Mutations that suppress the thermosensitivity of green fluorescent protein. *Curr. Biol.* **6,** 1653–1663.

Smith, A. G. (1991). Culture and differentiation of embryonic stem cells. *J. Tissue Cult. Methods* **13,** 89–94.

Svendsen, C. N., and Smith, A. G. (1999). New prospects for human stem-cell therapy in the nervous system. *Trends Neurosci.* **22,** 357–364.

Tarkowski, A. K. (1961). Mouse chimeras developed from fused eggs. *Nature* **190,** 857–860.

Van den Pol, A. N., and Ghosh, P. K. (1998). Selective neuronal expression of green fluorescent protein with cytomegalovirus promoter reveals entire neuronal arbor in transgenic mice. *J. Neurosci.* **18,** 10640–10651.

Waters, J. C., Cole, R. W., and Reider, C. L. (1993). The force-producing mechanism for centrosome separation during spindle formation in vertebrates is intrinsic to each aster. *J. Cell Biol.* **122,** 361–372.

Zernika-Goetz, M., Pines, J., McLean Hunter, S., Dixon, J. P. C., Siemering, K. R., Haseloff, J. (1997). Following cell fate in the living mouse embryo. *Development* **124,** 1133–1137.

Zhuo, L., Sun, B., Zhang, C., Fine, A., Chiu, S., and Messing, A. (1997). Live astrocytes visualised by green fluorescent protein in transgenic mice. *Dev. Biol.* **187,** 36–42.

Received for publication June 13, 2000
Revised August 29, 2000
Accepted August 30, 2000
Published online November 2, 2000

The Transcription Factor, *Pax6*, is Required for Cell Proliferation and Differentiation in the Developing Cerebral Cortex

Natasha Warren, Damira Caric[1], Thomas Pratt, Julia A. Clausen, Pundit Asavaritikrai, John O. Mason, Robert E. Hill[1] and David J. Price

Department of Biomedical Sciences (Centre for Developmental Biology), University Medical School, Teviot Place, Edinburgh EH8 9AG and [1]Medical Research Council Human Genetics Unit, Western General Hospital, Crewe Road, Edinburgh EH4 2XU, UK

The cerebral cortex develops from the dorsal telencephalon, at the anterior end of the neural tube. Neurons are generated by cell division at the inner surface of the telencephalic wall (in the ventricular zone) and migrate towards its outer surface, where they complete their differentiation. Recent studies have suggested that the transcription factor Pax6 is important for regulation of cell proliferation, migration and differentiation at various sites in the CNS. This gene is widely expressed from neural plate stage in the developing CNS, including the embryonic cerebral cortex, where it is required for radial glial cell development and neuronal migration. We report new findings indicating that, in the absence of *Pax6*, proliferative rates in the early embryonic cortex are increased and the differentiation of many cortical cells is defective. A major question concerns the degree to which cortical defects in the absence of *Pax6* are a direct consequence of losing the gene function from defective cells themselves, rather than being secondary to abnormalities in other cells. Cortical defects in the absence of *Pax6* become much more pronounced later in cortical development, and we propose that many result from a compounding of abnormalities in proliferation and differentiation that first appear at the onset of corticogenesis.

Introduction

The cerebral cortex arises from a sheet of undifferentiated neuroepithelial cells that line the lateral ventricle of the dorsal telencephalon. During development, cells proliferate in the ventricular zone and, following their final cell division, migrate along radial glia through the overlying intermediate zone to the cortical plate (Angevine and Sidman, 1961; Rakic, 1974, 1988). On arrival in the cortical plate, cells assume progressively more superficial positions to form the six layers of the adult cortex in an inside-first, outside-last sequence. The laminar identity of deep layer neurons is determined by cues in the ventricular zone, just prior to final mitotic division (McConnell and Kaznowski, 1991). The laminar identity of superficial layer neurons is probably determined by restriction of the developmental potential of progenitor cells (Frantz and McConnell, 1996).

The transcription factor *Pax6* encodes two DNA-binding motifs, a paired domain (Bopp *et al.*, 1986; Treisman *et al.*, 1991) and a paired-like homeodomain (Frigerio *et al.*, 1986). In mice, it is first expressed on embryonic day 8.5 (E8.5) in the developing eyes, nasal structures, spinal cord and forebrain, including the telencephalon (Walther and Gruss, 1991; Stoykova and Gruss, 1994; Grindley *et al.*, 1995, 1997; Mastick *et al.*, 1997; Warren and Price, 1997). Within the telencephalon, *Pax6* expression is restricted to the ventricular zone (where neurogenesis primarily occurs) and to the subventricular zone (where gliogenesis primarily occurs) of the dorsal telencephalon (Caric *et al.*, 1997; Gotz *et al.*, 1998). *Pax6* expression persists in both these regions throughout neurogenesis and gliogenesis, suggesting that it may play a role in these processes. Mutations in the mouse *Pax6* gene result in the small eye phenotype (Hill *et al.*, 1991). Homozygotes have severe defects of the eyes, face and central nervous system (CNS), including the cerebral cortex, and die at birth (Hogan *et al.*, 1986; Schmahl *et al.*, 1993; Quinn *et al.*, 1996; Stoykova *et al.*, 1996; Caric *et al.*, 1997; Grindley *et al.*, 1997; Warren and Price, 1997; Gotz *et al.*, 1998).

Earlier studies of the small eye cerebral cortex have shown that the ventricular and subventricular zones are enlarged, the cortical plate is thinner than normal and within the intermediate zone there are clusters of cells characteristic of the subventricular zone (Schmahl *et al.*, 1993; Caric *et al.*, 1997). It has been shown that reduced migration of late-born cortical precursors contributes to this phenotype, whereas early-born cortical precursors appear to migrate relatively normally (Caric *et al.*, 1997). The cells that fail to migrate in the absence of *Pax6* accumulate in the subventricular and intermediate zones, forming progressively more obvious cell-dense masses that show no overt signs of differentiation as the *Sey/Sey* embryo approaches term (Schmahl *et al.*, 1993; Caric *et al.*, 1997). In fact, these collections of cells do express the early neuronal marker TuJ1 (Caric *et al.*, 1997), but in other respects their state of differentiation has not been characterized. Here we report new findings indicating that many of these cells become specified to a neuronal fate but that they are defective in the expression of molecules characteristic of normal mature cortical neurons. The first part of this conclusion was drawn from studies of the expression of the *Sox11* gene in the cortex of *Sey/Sey* embryos. *Sox11* is a member of the *Sox* family of transcription factors containing a DNA-binding motif termed the HMG box. It is expressed in the developing CNS from E8.5 and is thought to play a role in early stages of neuronal differentiation (Hargrave *et al.*, 1997). The second part of this conclusion was drawn from studies of the expression of the genes encoding the high affinity receptors for the neurotrophins, *trkB* (Klein *et al.*, 1989, 1990) and *trkC* (Lamballe *et al.*, 1994), and the low affinity neurotrophin receptor, p75 (Chao and Hempstead, 1995). These receptors are expressed during normal neuronal differentiation, usually in association with sites of innervation (reviewed by Barbacid, 1994). They are expressed in developing embryonic cortical neurons, including those relatively mature neurons that have migrated into the cortical plate. Expression of these receptors was lacking in the cells that accumulated beneath the cortical plate in the *Sey/Sey* cortex. Since the neurotrophins and their receptors have been implicated in the regulation of cell survival (Barde, 1989; Lewin and Barde, 1996), we examined rates of cell death in the cortex of normal and *Sey/Sey* embryos, but found no differences.

The primary cause of the cortical defects in *Sey/Sey* mice remains unclear. It is important to discover this, since it will indicate more clearly what the direct actions of *Pax6* are in the control of cortical development. To test the hypothesis that the defect in late migration is due to a cell-autonomous defect in the

Sey/Sey precursors, these cells were labelled and transplanted into wild-type embryonic rat brains to follow their migration and developmental potential into postnatal life (Caric *et al.*, 1997). *Sey/Sey* cortical precursors showed similar integrative, migrational and differentiative abilities to those of transplanted wild-type mouse precursors. These results suggested that late-born cells in the mutants have a non-autonomous defect of migration that results from an abnormality in their environment. Subsequently, it has been reported that radial glial cells (which are present in *Sey/Sey* cortex) (Caric *et al.*, 1997) require *Pax6* for their normal development and that at least some aspects of this requirement may be cell-autonomous (Gotz *et al.*, 1998). Thus, it is likely that defects of the glial environment of migrating neuronal precursors make a contribution to the late migratory defects observed in the cortex of *Sey/Sey* mice. The question remains of whether a glial cell defect can explain all the abnormalities of the small eye cortex.

All these recent studies have focused on the later stages of cortical development in *Sey/Sey* mice, when secondary defects are likely to be numerous (Caric *et al.*, 1997; Gotz *et al.*, 1998). In addition to defects of cortical radial glial cells (Gotz *et al.*, 1998), it is possible that the numerous extracortical defects present in the *Sey/Sey* embryo contribute to the late embryonic cortical phenotype. For example, diencephalic afferents grow to the cortex about midway through cortical neurogenesis in the mouse (Ferrer *et al.*, 1992; Lotto and Price, 1995) and normal diencephalic afferent innervation has been suggested to influence the migration of cells in the cerebral cortex (Price and Lotto, 1996). In *Sey/Sey* embryos, the diencephalon is reduced in size and is not normally differentiated (Stoykova *et al.*, 1996; Warren and Price, 1997). Using molecular markers of different regions of the diencephalon including *Dlx1* and *Dlx2*, *Gbx2* and *Wnt3*, it has been shown (Stoykova *et al.*, 1996; Warren *et al.*, 1997) that the major subdivisions of the diencephalon are still present in the *Sey/Sey* forebrain, although specification of discrete nuclei is disrupted. Our more recent work (unpublished observations) has indicated that the dorsal thalamus, which is normally the source of thalamocortical axons, may be re-specified in the mutants, expressing ventral markers and failing to innervate the cerebral cortex.

Here we considered the possibility that *Pax6* may be playing a crucial role much earlier in corticogenesis, well before thalamocortical innervation. Given that *Pax6* is required for the correct regulation of diencephalic precursor proliferation (Warren and Price, 1997) and is expressed in the cortical ventricular zone, we tested whether *Pax6* regulates cell proliferation in the cortex by pulse-labelling with bromodeoxyuridine. We observed changes in the proliferation of cortical progenitors as early as E10.5. We then considered whether these might be due to changes in the expression of *BF1*, another transcription factor that is known to regulate cortical proliferation (Xuan *et al.*, 1995). *BF1* is a member of the winged-helix family of transcription factors, expressed in the telencephalon and nasal half of the optic stalk from E8 (Tao and Lai, 1992; Hatini *et al.*, 1994). Expression of *BF1* was not altered in the mutants.

Taking our new results together with published and preliminary data suggesting that *Pax6* regulates cell–cell adhesion (see Discussion), we suggest that *Pax6* plays an important primary role in regulating the proliferation and adhesiveness of cortical progenitors from a very early stage of corticogenesis. Loss of the gene may result in the overproduction of cortical cells that are more adhesive that normal. This may lead to problems with migration that become more severe as more and more cortical cells accumulate below the cortical plate. Further primary and secondary defects appearing later in corticogenesis may compound this problem and lead to the striking phenotype seen late in corticogenesis in *Sey/Sey* mice. This proposal is expanded in the Discussion.

Materials and Methods

Animals

Adult *Sey/+* mice (on a Swiss background) are distinguished by their abnormally small eyes. *Sey/Sey* mice die at birth and *Sey/Sey* embryos were derived from *Sey/+* × *Sey/+* matings. The morning of a vaginal plug was designated E0.5. Homozygotes were recognized by the absence of eyes and a shortened snout (Hogan *et al.*, 1986; Hill *et al.*, 1991). Wild-type embryos were derived from +/+ × +/+ matings (Swiss outbred strain).

Precursor Proliferation

Pregnant mothers were injected with bromodeoxyuridine (BrdU; 70 μg/g in sterile saline i.p.) on E10.5, E12.5 and E15.5 and killed by cervical dislocation after 30 min. Fetuses were fixed in 4% paraformaldehyde and embedded in wax. E10.5 embryos were sectioned coronally at 10 μm. E12.5 and E15.5 embryos were sectioned parasagittally at 10 μm. The sections were reacted to reveal BrdU as described (Gillies and Price, 1993). Sections were lightly counterstained with cresyl violet.

To estimate proliferative rates in E10.5 embryos, average labelling indices (LIs) in the proliferative zone of the dorsal telencephalon were obtained (LI: labelled cells as a proportion of total cells; Takahashi *et al.*, 1993). LIs were calculated from three equally spaced sections through the dorsal telencephalon. Care was taken to ensure that the LIs were not obtained from the ganglionic eminence, a region that does not express *Pax6*.

In older embryos (E12. 5–E15.5), proliferating cells were counted in parasagittal sections of the neocortex. Quantified sections were from medial, lateral and intermediate (one-third of the distance from the medial to the lateral edge of the brain) positions. The densities of BrdU positive cells in the proliferative zone were estimated in 150 μm wide bins through its entire depth (three equally spaced bins per section). For each embryo, the average density of BrdU labelled cells in the proliferative zone was calculated and then multiplied by the volume of the proliferative zone in that hemisphere to give an estimate of the total numbers of proliferating cells. The volume of the proliferative zone was estimated from a series of sections (1-in-9) using a computer image analysis system (NIH Image).

In Situ Hybridizations

Digoxigenin-labelled RNA antisense probes were prepared as described previously (Warren and Price, 1997). *Pax6* and *BF1* plasmids were provided by J. Rubenstein; *Sox11* plasmid was provided by M. Hargrave; *trkB* and *trkC* plasmids were provided by Bristol-Myers Squibb. Sense probes were synthesized for controls. E10.5, E12.5, E14.5, E16.5 and E19.5 embryos were dissected from anaesthetized mothers (0.3 ml urethane in sterile saline, i.p.) in phosphate buffered saline (PBS) at 4°C and fixed for 3–12 h in 4% paraformaldehyde + 0.2 mM egtazic acid (EGTA) at 4°C.The embryos were embedded in wax, sectioned coronally at 6 μm and collected on TESPA-coated slides. *In situ* hybridizations were performed as described (Wilkinson, 1992).

Immunohistochemistry

E17.5 *Sey/Sey* and +/+ cortices were dissected and sectioned at 5 μm. Immunohistochemistry was carried out with an antibody against the low affinity neurotrophin receptor, p75 (Chemicon), using standard methods. The primary antibody was detected with a biotinylated secondary antibody and FITC-avidin (Vector Laboratories).

RNAse Protection Assay

Total RNA was extracted from dissected cortices (cortical plate and proliferative zone, but not striatum) of E19.5 wild-type or *Sey/Sey* embryos using the RNeasy kit (Qiagen). Ribonuclease protection assay (RPA) was carried out (using the RPAII kit; Ambion) with

digoxigenin-labelled RNA probes to *trkB* (pFRK16, Klein *et al.*, 1990; probe detects both full-length and truncated versions), *trkC* (pFL25, Lamballe *et al.*, 1994; probe detects both full-length and truncated versions) or β-*actin* (supplied with kit). Protected RNA products (*trkC*, 520 nucleotides; *trkB*, 500 nucleotides; β-*actin*, 250 nucleotides) were separated on a 4% polyacrylamide/urea gel, transferred to a nylon membrane and detected by exposure to film after using the digoxigenin detection system (Boehringer Mannheim) with CDP-Star (Tropix) as a chemiluminescent substrate. Autoradiographs were scanned using a Biorad densitometer and band intensity quantified using Molecular Analyst software. Levels of β-*actin* were used to normalize *trkB* and *trkC* mRNA levels.

Cell Death

E17.5 *Sey/Sey* and +/+ cortices (four of each) were dissected, embedded in wax and sectioned at 5 μm. TdT-mediated dUTP nick ending labelling (TUNEL) was performed as described (Gavrieli *et al.*, 1992). Positive controls were done by preincubating sections with 10 μg/ml DNaseI; for negative controls, TdT was omitted. Sections at regular intervals (25, 50 and 75% of the distance between the anterior and posterior poles of the cortex) were quantified by superimposing grids spanning the full depth of the cortical wall and counting the numbers of TUNEL-positive cells and the total numbers of cells within them. The proportions of cells that were TUNEL positive were averaged across all mutant and wild-type brains and compared with Student's *t*-test.

Results

Early Defect in Cell Proliferation

To study the proliferation of cells in the developing dorsal telencephalon at E10.5, we measured the proportions of cells labelled by a 30 min pulse of BrdU (the labelling indices, LIs). As illustrated in Figure 1, there was a significant increase in the LI in *Sey/Sey* embryos (n = 3) compared to +/+ embryos (n = 3) (Student's *t*-test; $P < 0.01$). LIs were also measured in the mesencephalon, where *Pax6* is not expressed, and we found no significant differences between normal and mutant embryos (Warren and Price, 1997).

In addition to these quantitative observations, we also noticed that the pattern of BrdU labelling was altered in the mutants. In E10.5 +/+ embryos, BrdU-labelled nuclei were present at the ventricular surface of the telencephalon (arrow in Fig. 1*A*). By contrast there were very few BrdU-labelled nuclei at this surface in the telencephalon of *Sey/Sey* embryos (arrowhead in Fig. 1*B*). During normal neurogenesis, S-phase occurs in nuclei deep to the ventricular surface that then move to undergo M-phase at this surface (Takahashi *et al.*, 1993). In +/+ embryos, the labelled nuclei at the ventricular edge often had fragmented BrdU rather than presenting a smooth nuclear profile as in the overlying neuroepithelium; it is likely that these cells were undergoing M phase. The absence of these nuclei in *Sey/Sey* telencephalon suggests that interkinetic nuclear movement may be disrupted. M-phase may be occurring ectopically in the middle of the neuroepithelium or M-phase may be delayed due to elongated S-phase or G2-phase. The shape of the BrdU-labelled nuclei was also altered in *Sey/Sey* embryos, being more rounded and less elongated than in +/+ embryos (Fig. 1), also suggestive of disrupted interkinetic nuclear movement.

Our conclusion from these analyses of E10.5 embryos was that, in the absence of *Pax6*, cell proliferation is disrupted in several ways, including a loss of normal interkinetic movements of progenitors and an overall increase in the proliferative rate.

Studies of older embryos indicated compatible changes in proliferation at later embryonic ages. We have described previously how, at E12.5, the organization of proliferating cells in the cortex, as visualized with a 30 min pulse of BrdU shortly before

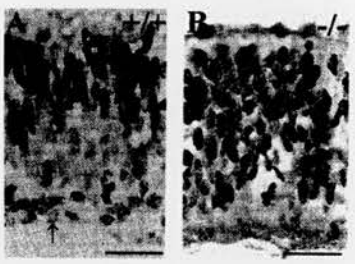

Figure 1. High magnification views of coronal sections through the dorsal telencephalon of *A* an E10.5 +/+ and *B* an E10.5 *Sey/Sey* (–/–) embryo showing BrdU labelling. Note an increase in the proportion of BrdU-labelled cells in the *Sey/Sey* dorsal telencephalon compared to +/+. Arrow in *A* indicates cells with fragmented BrdU labelling; note the absence of such labelled cells at the ventricular surface in *Sey/Sey* embryos (arrowhead in *B*). Scale bars: 25 μm.

death, is disrupted in *Sey/Sey* embryos in a manner similar to that shown in Figure 1 (Caric *et al.*, 1997). At E12.5, a 30 min pulse of BrdU labelled significantly higher numbers of cells in *Sey/Sey* embryos (57 742 ± 5291 SEM; n = 3) than in wild-type embryos (35 043 ± 2232; n = 3; $P < 0.02$). These results indicate that, during a 30 min period, more cells in the ventricular zone are in S-phase in the mutants. The possible reasons for this include the following: S-phase may be elongated relative to the overall length of the cell cycle, there may be an increase in the total number of proliferating cells, or there may be a combination of both. By E15.5, this difference was reduced and was not significant. The numbers of labelled cells were 127 277 ± 17 945 (n = 3) in mutant embryos and 103 683 ± 15 168 (n = 3; $P < 0.37$) in wild-type embryos.

Pax6 and BF1 Expression

In E10.5 +/+ embryos, *Pax6* expression was detected in the dorsal telencephalon and at other more caudal sites, as described previously (Walther and Gruss, 1991; Stoykova and Gruss, 1994; Grindley *et al.*, 1995, 1997; Mastick *et al.*, 1997; Warren and Price, 1997). There was variation in the intensity of staining throughout the cortex, with labelling strongest anteriorly and posteriorly (arrows in Fig. 2*A*). No expression was seen in the ganglionic eminence (ge) of the ventral telencephalon (Fig. 2*A*). By E14.5, *Pax6* expression was detected uniformly thoroughout the anterior–posterior extent of the dorsal telencephalon. Within the proliferative zone, labelling for *Pax6* expression was more intense in the subventricular zone than in the ventricular zone (Fig. 2*B*). By E16.5, staining for *Pax6* expression was less intense and was restricted to the ventricular zone (Fig. 2*C*).

In E10.5 +/+ embryos, *BF1* expression was detected in the ventral telencephalon (Fig. 2*D*). Labelling was strongest in the ganglionic eminence, decreased dorsally towards the developing neocortex and was weakest at the posterior end of the cortex (Fig. 2*D*). These observations suggest that different positions in the E10.5 cortex express different relative levels of *Pax6* and *BF1* (compare Fig. 2*A*, *D*). In E14.5 +/+ embryos, staining for BF1 expression was more uniform anterior–posteriorly and was more intense in the subventricular zone than in the ventricular zone (Fig. 2*E*). These observations were similar to those for *Pax6* expression: unlike *Pax6* expression, *BF1* expression was also detected at the pial edge of the telencephalic wall, in the cortical plate (Fig. 2*E*). In E16.5 +/+ embryos, *BF1* expression

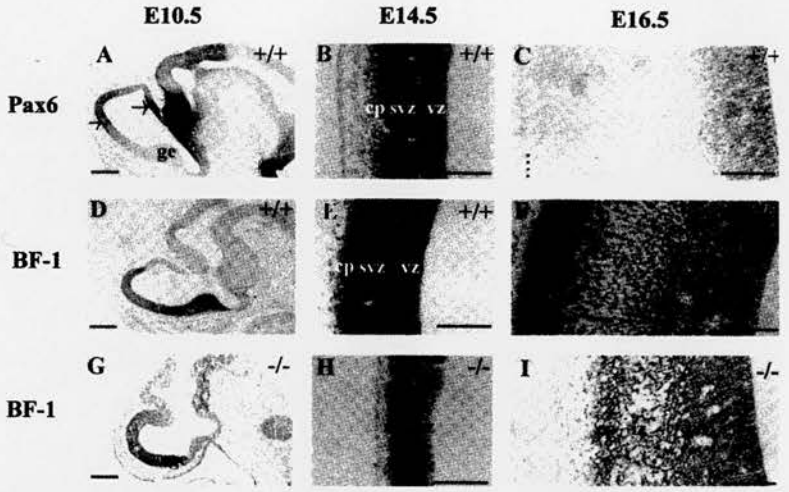

Figure 2. *In situ* hybridizations on sections of E10.5, E14.5 and E16.5 +/+ and *Sey/Sey* (–/–) embryos. *A, B, C Pax6* expression in +/+ embryos. *A* Expression is in the cortex of the dorsal telencephalon from E10.5 (staining is particularly strong rostroventrally and caudodorsally, arrows). *B, C* Expression is in the proliferative zones (the subventricular and ventricular zones, svz and vz) of the cortical wall at E14.5 and E16.5. Dotted line in *C* marks the pial edge of the cortical wall; ge, ganglionic eminence. *D, E, F* BF1 expression in +/+ embryos. *D* E10.5: note expression in the ganglionic eminence of the ventral telencephalon, decreasing into the dorsal telencephalon. *E* E14.5: note strong expression throughout the cortical wall, involving the proliferative zones and extending to the pial surface. *F* E16.5: note strong expression throughout the cortical wall, in the cortical plate (cp), intermediate zone (iz) and proliferative zones. *G, H, I BF1* expression in *Sey/Sey* embryos. There is relatively normal expression of *BF1* in the cortical wall of *G* E10.5, *H* E14.5 and *I* E16.5 mutant embryos compared to +/+ embryos of the same age. Scale bars, *A, D* and *G*, 200 μm; rest, 100 μm.

was detected throughout the ventricular, subventricular and intermediate zones and cortical plate, with strongest staining in the developing cortical plate (Fig. 2*F*). In E10.5, E14.5 and E16.5 *Sey/Sey* embryos, after making allowances for morphological abnormalities, we could detect no differences in these patterns of *BF1* expression (Fig. 2*G, H, I*).

In conclusion, these finding suggest that there are variations in the expression of *Pax6* and *BF1* in E10.5 embryos that are often reciprocal. Different cortical regions may have different relative levels of expression of these two genes. These differences appear to be lost over the following days. It appears that *Pax6* expression is not required for *BF1* expression.

Sox11 Expression

In E10.5 and E12.5 +/+ embryos, *Sox11* expression was detected predominantly in the ventral telencephalon in the mantle layers of the ganglionic eminence with only a few scattered cells stained in the proliferative zone (data not shown). Expression was also detected in a few cells in the neocortex (Fig. 3*A*). By E14.5, staining for *Sox11* expression was much more intense in the developing cortical plate (Fig. 3*B*). It was very strong in the superficial half of the dorsal telencephalic wall, coinciding with the cortical plate and the upper part of the subventricular zone (regions that would contain the most highly differentiated postmitotic neurons). It was very weak in the deeper layers (the ventricular zone and deeper part of the subventricular zone). In the ventral telencephalon, *Sox11* expression was detected in the mantle layers of the ganglionic eminence but not in the ventricular zone (data not shown). In the region of the archicortex that will form the hippocampus, *Sox11* expression was again detected mainly among cells in the hippocampal cortical plate and not in the ventricular zone (Fig. 3*C*). A similar distribution of *Sox11* expression was detected at E17.5 in wild-type embryos (data not shown).

In E10.5 and E12.5 *Sey/Sey* embryos, *Sox11* expression appeared normal in the ganglionic eminence, an area that does not express *Pax6* (data not shown). As in wild-type embryos, staining for *Sox11* was weak in the dorsal telencephalon at these ages (Fig. 3*D*). In E14.5 *Sey/Sey* embryos, strong *Sox11* expression was detected in the superficial half of the dorsal telencephalic wall, as in wild-type cortex, but there was also intense labelling of the underlying proliferative layers (Fig. 3*E*).

Figure 3. *In situ* hybridizations for *Sox11* on sections of *A–C* +/+ and *D–F Sey/Sey* (–/–) embryos. *A* E12.5 +/+ dorsal telencephalon: there is weak expression in the developing neocortex (nc). *B* E14.5 +/+ dorsal telencephalon: there is strong expression in the cortical plate (cp) and upper subventricular zone (svz) but little in the ventricular zone (vz). *C* E14.5 archicortex (hippocampal primordium): there is strong expression in the hippocampal cortical plate (hc) but not in the underlying proliferative zone. *D* E12.5 *Sey/Sey* dorsal telencephalon: expression was similar to that in +/+ cortex. *E* E14.5 *Sey/Sey* dorsal telencephalon: as in +/+ cortex, staining was strongest in the superficial half of the cortical wall but there was much more than normal in the proliferative zones. *F* E14.5 *Sey/Sey* hippocampal primordium: as in the neocortex (E), expression was present throughout the depth of the cortical wall, including the ventricular zone, where it is normally lacking. *A* and *D* are parasagittal sections; *B, C, E* and *F* are coronal sections. Scale bars, 100 μm.

Figure 5. Localization of *trkB* mRNA in coronal sections of E19.5 (*A*) +/+ and (*B, C*) *Sey/Sey* (–/–) cortices as assessed by in-situ hybridization. Purple stain indicates the presence of transcripts. Note the lack of *trkB* expression in the enlarged cell dense proliferative zone of the mutant cortex (large, pink counterstained area). Abbreviations: cp, cortical plate; iz, intermediate zone; svz, subventricular zone; vz, ventricular zone. Scale bar, 100 μm.

Figure 3

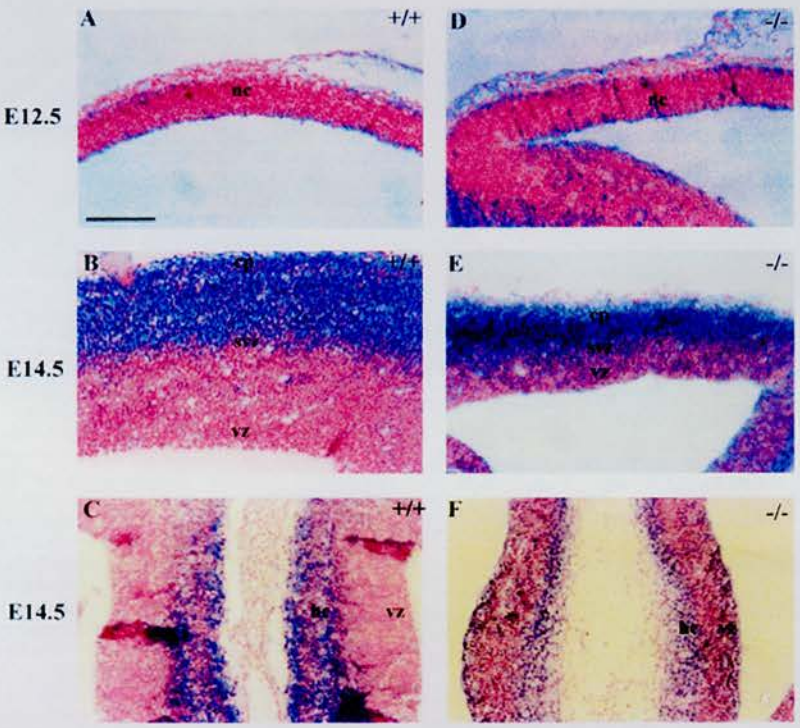

Figure 5

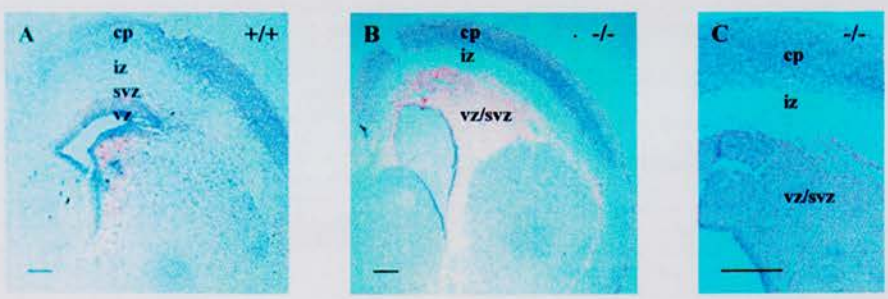

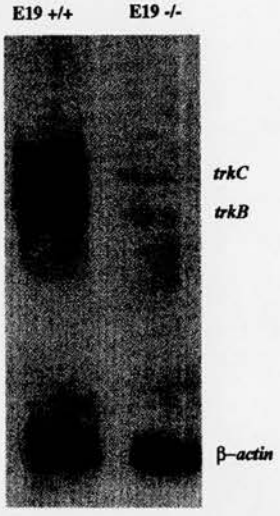

Figure 4. RNase protection assay for *trkB*, *trkC* and β-*actin* mRNA in total RNA extracted from E19.5 +/+ and *Sey/Sey* (–/–) cortices . Protected bands: *trkC*, 520 nucleotides; *trkB*, 500 nucleotides; β-*actin*, 250 nucleotides. Faint bands corresponding to transcription start site and splicing variants of *trkB* mRNA (Klein *et al.*, 1990) and *trkC* mRNA (Lamballe *et al.*, 1994) did not overlap with protected bands used for quantification.

A similar abnormality was seen in the hippocampal primordium (Fig. 3*F*). Similarly, by E17.5, *Sox11* expression was detected throughout all layers of the mutant cortex, including the ventricular zone (data not shown).

In summary, our results indicate that, in both +/+ and *Sey/Sey* cortex, the period of strong *Sox11* expression begins at a similar time to the onset of the major phase of cortical neuronal differentiation. In +/+ cortex, *Sox11* is expressed predominantly by cells in the superficial differentiating layers, whereas in *Sey/Sey* cortex it is also strongly expressed by cells in the deeper layers, where neurons do not normally differentiate. Given that these deeper regions contain many cells that should have migrated into the cortical plate and that these cells express the early neuronal marker TuJ1 (Caric *et al.*, 1997), the most parsimonious explanation of this finding is that *Sox11* is being expressed by cells that are stuck below the cortical plate but are nonetheless specified to a neuronal fate.

Loss of Neurotrophin Receptor Expression Late in Corticogenesis

To characterize further the cortical phenotype in small eye mice, the expression of the genes for the high-affinity neurotrophin receptors TrkB and TrkC was compared in *Sey/Sey* and wild-type E19.5 embryos. A RPA was used to quantify the overall levels of *trkB* and *trkC* transcripts in RNA extracted from these tissues. Levels of ubiquitously expressed β-*actin* mRNA were determined simultaneously and used to correct for differences in RNA yield from the two types of tissue. The RPA was repeated three times and each was quantified densitometrically; all three repeats gave results similar to that in Figure 4, showing a large reduction in

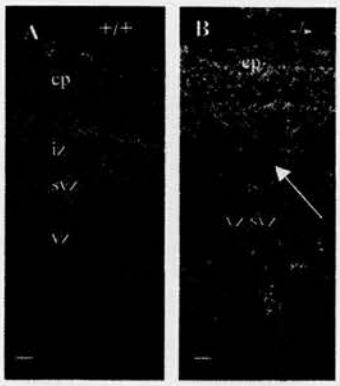

Figure 6. Localization of p75 protein in E17.5 (*A*) +/+ and (*B*) *Sey/Sey* (–/–) cortices as assessed by immunohistochemistry. Note that p75 is lacking in the cell dense clusters in the intermediate zone/proliferative zone of the mutant cortex (arrow). Abbreviations as in Figure 5. Scale bar, 25 μm.

the amounts of *trkB* and *trkC* transcripts relative to changes in β-*actin* mRNA in *Sey/Sey* cortex. In-situ hybridizations indicated that the reduction in *trkB* and *trkC* transcript levels could be accounted for by a reduced proportion of expressing cells in the mutants rather than a global down-regulation in expression. Figure 5 shows expression of *trkB*; expression of *trkC* was similar (not shown). In wild-type cortex, staining for *trkB* and *trkC* was present in most layers (purple staining in Fig. 5*A*). It was most intense in cells of the cortical plate; it was also present in cells of the ventricular zone, and, at low levels, in cells in the intermediate zone. In *Sey/Sey* cortex, *trkB* and *trkC* were expressed in the cortical plate and at the ventricular edge of the proliferative zone (purple staining in Fig. 5*B*, *C*), but expression was lacking among the cells that had accumulated between the ventricular zone and cortical plate (counterstained pink in Fig. 5*B*, *C*). This result suggests that the failure of cells to reach the cortical plate coincides with their failure to express receptors characteristic of cortical plate neurons. While many of these cells appear to express early markers of neuronal diffrentiation [TuJ1 (Caric *et al.*, 1997) and *Sox11*, see above], it seems that they do not express other molecules found in more mature neurons.

The neurotrophins also bind with low affinity to a receptor called p75 (Chao and Hempstead, 1995). Staining with an antibody against p75 gave a broadly similar result to the *in situ* hybridizations for *trkB* and *trkC* (Fig. 6). In wild-type cortex, staining for p75 was strongest in the cortical plate, intermediate zone and upper part of the subventricular zone. In *Sey/Sey* cortex, staining for p75 was also strongest in the cortical plate and intermediate zone, but it was low or absent in the dense clusters of cells that had accumulated in the intermediate and subventricular zones. As can be seen in Figure 6, staining in the intermediate zone outlined these clusters. This indicates that, as for the expression of *trkB* and *trkC*, these accumulations of cells that had failed to migrate into the cortical plate lacked expression of receptors appropriate for their developmental age.

Cell Death

Programmed cell death during normal development is caused

when cells activate intracellular biochemical pathways that lead to their systematic self-destruction. This process is known as apoptosis. Apoptosis involves fragmentation of nuclear DNA and this can be detected by the TUNEL method used here. Neurotrophins regulate this process; in general, the presence of neurotrophins prevents apoptosis. In view of the results on the expression of neurotrophin receptors, we measured rates of apoptosis through the full depth of the cortical wall, from ventricular edge to pia, in wild-type and *Sey/Sey* cortices (E17.5, $n = 4$ of each). We found no significant difference (Student's *t*-test); rates were similarly low in wild-type (0.090 ± 0.016% SEM) and *Sey/Sey* (0.087 ± 0.022% SEM) cortices.

Discussion

Present Results and their Relationship to Previously Published Work

Here, we report new findings suggesting increased proliferation in the early *Sey/Sey* dorsal telencephalon. In broad agreement with our results, it has also been noted (Gotz *et al.*, 1998) that short pulses of BrdU given to mice aged E13.5–E16.5 appeared to label more cells in *Pax6*-deficient cortex than in wild type cortex. Their study of acutely dissociated cells from wild-type and *Pax6*-deficient cortex suggested that this increase was due to an alteration of the cell cycle characteristics of the cortical cells. As yet, it is not possible to conclude how the various components of the cell cycle are altered. Our results may be explained by a lengthening of S-phase relative to the length of the cell cycle, although it is not clear how the absolute lengths of the different components may be altered.

In further agreement with our results, Gotz *et al.* (1998) also suggested that the proliferative defect in the mutants was less apparent at the later stages of cortical neurogenesis. There is a slight discrepancy in that their quantitative analysis of dissociated cells suggested persistent defects to an older age than our *in vivo* quantification, which showed no defects at E15.5 (this may be accounted for by the methodological difference).

These results contrast with those from our previous analysis of proliferation in the embryonic diencephalon. In this region, a lack of *Pax6* leads to a 50% reduction in proliferative rates from E10.5 (Warren and Price, 1997). The telencephalon and diencephalon are both extremely complex structures and, although adjacent in the forebrain, they differ in many ways, both morphological and molecular. Each expresses a large number of regulatory genes from the earliest stages of their development, often in subregions that have specific fates (Rubenstein and Beachy, 1998). Thus, each telencephalic and diencephalic region expresses a characteristic cocktail of transcription factors to which *Pax6* contributes at some places and not others. It is possible that the action of *Pax6* in regulating proliferative rates depends on what other regulatory factors that region expresses. For example, *BF1* is expressed in the developing telencephalon and its loss severely reduces telencephalic proliferation (Xuan *et al.*, 1995). *BF1* expression overlaps that of *Pax6* in the cerebral cortex, where its expression is maintained in the absence of *Pax6*, but *BF1* is not expressed in the developing diencephalon. There are many possible ways in which *Pax6* may interact with other factors to influence proliferation. For example, *Pax6* may play a modulatory role, perhaps dampening the effects of other factors that may tend to increase proliferation rates in the cortex (e.g. *BF1* or Lhx2) (Porter *et al.*, 1997) or decrease proliferation rates in the diencephalon. Whether such a role is cell-autonomous remains to be tested; there is evidence (Gotz *et al.*, 1998) that the numbers of at least some cortical progenitors (those detected with radial glial markers) are affected by *Pax6* on proliferation and mediated by secreted factors.

Another of our new findings using a probe for *Sox11*, which is expressed in neurons from an early stage of their development, is compatible with our previous findings that cells that accumulate beneath the cortical plate in the absence of *Pax6* show signs of early neuronal differentiation (Caric *et al.*, 1997). Previous work has shown that these accumulations in the late *Sey/Sey* embryo comprise cells that would, in normal mice, have become incorporated into the cortical plate (Caric *et al.*, 1997). However, we found that these cells lack expression of neuro- trophin receptors that are characteristic of cortical plate cells. This suggests that the differentiation of these cells is retarded or prevented compared to that of cells that have entered the cortical plate. Since these receptors are still expressed in the cortical plate of *Sey/Sey* mice, *Pax6* is not an absolute requirement for their expression; rather, it may modulate neurotrophin receptor expression. It is possible that the loss of neurotrophin receptors in *Sey/Sey* mice is related to the defects of proliferation, since neurotrophin receptors are expressed in the ventricular zone where their activation may influence proliferative rates (Ghosh and Greenberg, 1995). Whether the effects of loss of Pax6 on the expression of neurotrophin receptors are cell-autonomous or whether they are indirect (perhaps resulting from a lack of cortical innervation; Schmahl *et al.*, 1993; our unpublished observations) are all open questions.

Neurotrophins and their receptors are associated with the regulation of cell death (Barde, 1989; Lewin and Barde, 1996). We found no evidence for an increase in cell death in the *Sey/Sey* cortex (in agreement with findings of Gotz *et al.*, 1998). Similarly, in previous work we observed no difference from normal in rates of cell death in the *Sey/Sey* embryonic diencephalon (Warren and Price, 1997). Mice with deletions of the neurotrophin receptors do not show a marked increase in cell death in the cerebral cortex, perhaps because many neurotrophic factors are expressed in the developing cortex and there may be redundancy of action among them (Silos-Santiago *et al.*, 1997).

Speculations on the Primary Functions of Pax6 in the Developing Cerebral Cortex

The preceding discussion indicates that, despite a catalogue of abnormalities in the cortex of *Sey/Sey* mice, we still have very little information on the primary, cell-autonomous actions of *Pax6* in the regulation of cortical development. A strong possibility is that one of the primary functions of *Pax6* is to regulate the adhesiveness of cells in which it is expressed. If true, this might go a long way towards explaining the cortical phenotype of the *Sey/Sey* embryo.

There are several lines of evidence suggesting that *Pax6* may have a cell-autonomous effect on cell-cell adhesion. *In vitro* experiments have indicated that transcription factors encoded by the *Pax* genes, including *Pax6*, bind to specific sequences in the neural cell adhesion molecule and L1 adhesion molecule promoters (Chalepakis *et al.*, 1994; Edelman and Jones, 1995; Holst *et al.*, 1997). *In vivo*, it has been shown (Stoykova *et al.*, 1996) that loss of *Pax6* leads to disruption of the boundary between the neocortex and the lateral ganglionic eminence, which is thought to be maintained by differential cell adhesion (Gotz *et al.*, 1996). They observed *Dlx1*-positive cells, that are normally mainly confined to the medial and lateral ganglionic eminences, in large numbers in the *Sey/Sey* neocortex. They

suggested that this ectopic cortical expression of *Dlx1* in the mutants results from abnormal migration of cells across the border between the lateral ganglionic eminence and the cortex, due to a loss of adhesive differences between these regions. In later work, alterations were reported in the expression of the homophilic adhesion molecule, R-cadherin, in the developing cortex (Stoykova *et al.*, 1997). By carrying out *in vitro* aggregation studies on dissociated embryonic cortical cells, we have found evidence that those lacking *Pax6* are more adhesive than normal (shown by our own preliminary results, D. Gooday and D.J. Price, unpublished). In the developing eye, where the study of *Sey/Sey* ↔ +/+ chimeras has given a clearer picture of the cell-autonomous roles of *Pax6* (Quinn *et al.*, 1996), it has been proposed that the regulation of cell sorting by Pax6 is mediated by effects on the expression of cell adhesion molecules.

The fact that migratory defects in the cortex of mice lacking *Pax6* become obvious from about midway through corticogenesis onwards (Schmahl *et al.*, 1993; Caric *et al.*, 1997) has focused attention on the possibility that *Pax6* plays its most important primary roles in the cortex at relatively late stages, during radial glial cell guided migration (Caric *et al.*, 1997; Gotz *et al.*, 1998). Indeed, there is some evidence of cell autonomous defects in radial glial cells at these stages (Gotz *et al.*, 1998). However, current evidence is against a primary role for *Pax6* in the migratory capacity of late-born cortical precursors themselves; if such cells are taken from *Sey/Sey* embryos they can migrate apparently normally when placed into a wild-type environment (Caric *et al.*, 1997). Since our new data, presented here, indicate defects of proliferation in the cortical primordium of the *Sey/Sey* embryo from as early as E10.5, it is important to consider the possibility that the abnormalities in the cortex of *Sey/Sey* mice originate from primary defects at the earliest stages of corticogenesis. It is possible that defects of cell–cell adhesion are also present from this early time, although we have not yet tested this; indeed, it is conceivable that adhesive defects might account for the changes in proliferation. In the following discussion, we consider (i) whether the various abnormalities and their reported times of appearance in the *Sey/Sey* cortex could be explained by changes in cell–cell adhesion and (ii) what this might tell us about the actions of *Pax6* in normal cortical development.

One clue to a potentially important role for Pax6 in cortical development comes from close analysis of data on the expression of *Pax6* in the embryonic cortex. Whereas in-situ hybridizations from about E12.5 onwards indicate that *Pax6* mRNA is expressed by most cells in the cortical proliferative zone (Caric *et al.*, 1997; present results), antibody studies have suggested that Pax6 protein levels are very variable in this region. It appears that only some cells contain the protein at high level, others contain low levels or none at all (Gotz *et al.*, 1998; our unpublished observations). The identity of the cells that express Pax6 protein strongly is not entirely clear, although there is evidence that some are radial glial cells (Gotz *et al.*, 1998). Neither *Pax6* mRNA nor Pax6 protein is present in cells that have migrated out of the proliferating zones.

These observations indicate that Pax6 protein may be absent from some proliferative zone cells that express *Pax6* transcripts, raising the possibility of post-transcriptional regulation of *Pax6* expression in this region. One suggestion is that changes in the levels of Pax6 protein occur as cells undergo mitosis, with the protein being expressed at specific points in the cell cycle. Pax6 may regulate the adhesive properties of cortical precursors and progenitors, allowing them to undergo their movements within the ventricular zone and then migrate away from it. As a rule, Pax6 may lower the adhesiveness of cells or alter the nature of their adhesive interactions, allowing newborn cortical cells to escape from the ventricular zone and/or to develop new adhesive interactions with cells outside the proliferative zone. Absence of *Pax-6* may disturb the normal proliferative processes in the ventricular zone and may lower the probability that precursors can escape to the cortical plate. This may underlie the progressive accumulation of cells in the proliferative zones as corticogenesis continues. The build-up of these cells with increased adhesiveness to each other may continue to lower the chances of new precursors migrating away to the cortical plate. This problem may be compounded by the raised proliferative rates (the precursor cells would not only be more adhesive than normal but there would be more of them), a lack of innervation from subcortical structures (this innervation may normally assist migration; Price and Lotto, 1996) and other late-acting defects such as those in radial glia cells (Gotz *et al.*, 1998). The additive effects of these problems may lead to a progressive worsening of the abnormalities seen in the *Sey/Sey* cortex as corticogenesis advances, which would explain why defects of overall cortical structure and cell migration become obvious later in corticogenesis (Caric *et al.*, 1997).

In this hypothesis, the fact that *Sey/Sey* precursor cells migrate normally when placed in the wild-type environment (Caric *et al.*, 1997) could be explained on the grounds that dilution by wild-type cells might increase to near normal levels the probability of mutant precursor cells being able to escape from the ventricular zone. The normal glial environment of the wild-type host could also allow better migration than is possible in the *Sey/Sey* cortex. It is worth noting that the defects of radial glial cells in cortex lacking *Pax6*, as well as the defective differentiation of cortical precursors, could both arise as a consequence of earlier abnormalities. In conclusion, we suggest that, while the absence of *Pax6* gives rise to cortical abnormalities that appear late in embryogenesis, the primary defects that generate these abnormalities occur at the onset of corticogenesis. We propose that the key roles of Pax6 in cortical development are in the regulation of cell proliferation and/or cell–cell adhesion.

Notes

We thank Katherine Giles for help with the *in situ* hybridizations, Stephen Gauldie for help with the cell counts, Katy Gillies and Grace Grant for help with histology, John Verth for care of the mice and members of the Edinburgh 'Pax6 Group' for numerous discussions. This work was supported by the Medical Research Council, The Wellcome Trust and European Union Commission (BMH4-CT-96-1604).

Address correspondence to David J. Price, Department of Biomedical Sciences (Centre for Developmental Biology), University Medical School, Teviot Place, Edinburgh EH8 9AG, UK. Email: dprice@ed.ac.uk.

References

Angevine JB Jr, Sidman RL (1961) Autoradiographic study of cell migration during histogenesis of cerebral cortex in the mouse. Nature 192:766–768.

Barbacid M (1994) The Trk family of neurotrophin receptors. J Neurobiol 25:1386–1403.

Barde Y-A (1989) Trophic factors and neuronal survival. Neuron 2:1525–1534.

Bopp D, Burri M, Baumgartner S, Frigerio G, Noll M (1986) Conservation of a large protein domain in the segmentation gene paired and in functionally related genes of Drosophila. Cell 47:1033–1040.

Caric D, Gooday D, Hill RE, McConnell SK, Price DJ (1997) Determination of the migratory capacity of embryonic cortical cells lacking the transcription factor Pax6. Development 124:5087–5096.

Chalepakis G, Wijnholds J, Giese P, Schachner M, Gruss P (1994) Characterization of Pax6 and Hoxa-1 binding to the promoter region of the neural cell adhesion molecule L1. DNA Cell Biol 13:891–900.

Chao MV, Hempstead BL (1995) p75 and Trk: a two-receptor system. Trends Neurosci 18:321–326.

Edelman GM, Jones FS (1995) Developmental control of NCAM expression by Hox and Pax gene products. Philos Trans R Soc Lond B Biol Sci 349:305–312.

Ferrer I, Soriano E, Del Rio JA, Auladell C (1992) Cell death and removal in the cerebral cortex during development. Prog Neurobiol 39:1–43.

Frantz GD, McConnell SK (1996) Restriction of late cerebral cortical progenitors to an upper-layer fate. Neuron 17:55–61.

Frigerio G, Burri M, Bopp D, Baumgartner S, Noll M (1986) Structure of the segmentation gene paired and the Drosophila PRD gene set as part of a gene network. Cell 47:735–746.

Gavrieli Y, Sherman Y, Ben-Sasson SA (1992) Identification of programmed cell death in situ via specific labeling of nuclear DNA fragmentation J Cell Biol 119:493–501.

Ghosh A, Greenberg ME (1995) Distinct roles for bFGF and NT-3 in the regulation of cortical neurogenesis. Neuron 15:89–103.

Gillies K, Price DJ (1993) The fates of cells in the developing cerebral cortex of normal and methylazoxymethanol acetate-lesioned mice. Eur J Neurosci 5:73–84.

Gotz M, Wizenmann A, Reinhard S, Lumsden A, Price J (1996) Selective adhesion of cells from different telencephalic regions. Neuron 16: 551–564.

Gotz M, Stoykova A, Gruss P (1998) Pax6 controls radial glia differentiation in the cerebral cortex. Neuron 21:1031–1044.

Grindley JC, Davidson DR, Hill RE (1995) The role of Pax6 in eye and nasal development. Development 121:1433–1442.

Grindley JC, Hargett L, Hill RE, Ross A, Hogan BLM (1997) Disruption of Pax6 function in mice homozygous for the Pax6$^{Sey\text{-}1NEU}$ mutation produces abnormalities in the early development and regionalization of the diencephalon. Mech Dev 64:111–126.

Hargrave M, Wright E, Kun J, Emery J, Cooper L, Koopman P (1997) Expression of the Sox11 gene in mouse embryos suggests roles in neuronal maturation and epithelio-mesenchymal induction. Dev Dynamics 210:79–86.

Hatini V, Tao W, Lai E (1994) Expression of winged helix genes, BF-1 and BF-2, define adjacent domains within the developing forebrain and retina. J Neurobiol 25:1293–1309.

Hill RE, Favor J, Hogan BLM, Ton CCT, Saunders GF, Hanson IM, Prosser J, Jordan T, Hastie ND, van Heningen V (1991) Mouse small eye results from mutations in a paired-like homeobox-containing gene. Nature 354:522–525.

Hogan BLM, Horsnurgh G, Cohen J, Hetherington CM, Fischer G, Lyon MF (1986) Small eye (Sey): a homozygous lethal mutation on chromosome 2 which affects the differentiation of both lens and nasal placodes in the mouse. J Embryol Exp Morphol 97:95–110.

Holst BD, Wang Y, Jones FS, Edelman GM (1997) A binding site for Pax proteins regulates expression of the gene for the neural cell adhesion molecule in the embryonic spinal cord. Proc Natl Acad Sci USA 94: 1465–1470.

Klein R, Parada LF, Coulier F, Barbacid M (1989) trkB, a novel tyrosine protein kinase receptor expressed during mouse neural development. EMBO J 8:3701–3709.

Klein R, Conway D, Parada LF, Barbacid M (1990) The trkB tyrosine protein kinase gene codes for a second neurogenic receptor that lacks the catalytic kinase domain. Cell 61:647–656.

Lamballe F, Smeyne RJ, Barbacid M (1994) Developmental expression of trkC, the neurotrophin-3 receptor, in the mammalian nervous system. J Neurosci 14:14–28.

Lewin GR, Barde Y-A (1996) Physiology of the neurotrophins. Annu Rev Neurosci 19:289–317.

Lotto RB, Price DJ (1995) The stimulation of thalamic neurite outgrowth by cortex-derived growth factors in vitro: the influence of cortical age and activity. Eur J Neurosci 7:318–328.

Mastick GS, Davis NM, Andrews GL, Easter Jr SS (1997) Pax6 functions in boundary formation and axon guidance in the embryonic mouse forebrain. Development 124:1985–1997.

McConnell SK, Kaznowski CE (1991) Cell cycle dependence of laminar determination in developing neocortex. Science 254:292–285.

Porter FD, Drago J, Xu Y, Cheema SS, Wassif C, Huang S-P, Lee E, Grinberg A, Massalas JS, Bodine D, Alt F, Westphal H (1997) *Lhx2*, a LIM homeobox gene, is required for eye, forebrain, and definitive erythrocyte development. Development 124:2935–2944.

Price DJ, Lotto RB (1996) Influences of the thalamus on the survival of subplate and cortical plate cell sin cultured embryonic mouse brain. J Neurosci 16:3247–3255.

Quinn JC, West JD, Hill RE (1996) Multiple functions for Pax6 in mouse eye and nasal development. Genes Dev 10:435–446.

Rakic P (1974) Neurons in the rhesus monkey visual cortex: systematic relationship between time of origin and eventual disposition. Science 183:425–427.

Rakic P (1988) Specification of cerebral cortical areas. Science 241: 170–176.

Rubenstein JLR, Beachy PA (1998) Patterning of the embryonic forebrain. Curr Opin Neurobiol 8:18–26.

Schmahl W, Knoediseder M, Favor J, Davidson D (1993) Defects of neuronal migration and the pathogenesis of cortical malformations are associated with small eye (sey) in the mouse, a point mutation at the Pax-6 locus. Acta Neuropathol 86:126–135.

Silos-Santiago I, Fagan A, Garber M, Fritzsch B, Barbacid M (1997) Severe sensory deficits but normal CNS development in newborn mice lacking TrkB and TrkC tyrosine protein kinase receptors. Eur J Neurosci 9:2045–2056.

Stoykova A, Gruss P (1994) Roles of Pax-genes in developing and adult brain as suggested by expression patterns. J Neurosci 14:1395–1412.

Stoykova A, Fritsch R, Walther C, Gruss P (1996) Forebrain patterning defects in Small eye mutant mice. Development 122:3453–3465.

Stoykova A, Gotz M, Gruss P, Price J (1997) Pax6-dependent regulation of adhesive patterning, R-cadherin expression and boundary formation in developing forebrain. Development 124:3765–3777.

Takahashi T, Nowakowski RS, Caviness VS (1993) Cell cycle parameters and patterns of nuclear movement in the neocortical proliferative zone of the fetal mouse. J Neurosci 13:820–833.

Tao W, Lai E (1992) Telencephalic-restricted expression of BF1, a new member of the HNF-3/fork head gene family, in the developing rat brain. Neuron 8:957–966.

Treisman F, Harris E, Desplan C (1991) The paired box encodes a second DNA-binding domain in the paired homeodomain protein. Genes Dev 5:594–604.

Walther C, Gruss P (1991) Pax6, a murine paired box gene, is expressed in the developing CNS. Development 113:1435–1449.

Warren N, Price D (1997) Roles of Pax6 in murine diencephalic development. Development 124:1573–1582.

Wilkinson DG (1992) In: In situ hybridization. A practical approach (Rickwood D, Hames BD, eds). Oxford: IRL Press.

Xuan S, Baptista CA, Balas G, Tao W, Soares VC, Lai E (1995) Winged helix transcription factor BF1 is essential for the development of the cerebral hemispheres. Neuron 14:1141–1152.